Supporting Material

Final report of the coordinated research project

On

Accelerator-based Alternatives to Non-HEU Production of Mo-99 /Tc-99m

Table of Contents

SUMMARY

1. INTRODUCTION

A number of IAEA Member States have embarked on research programs to investigate the use of accelerators for the production of Mo-99 or Tc-99m directly. These approaches make use of the ^{100}Mo(γ,n)^{99}Mo and ^{100}Mo(p,2n)^{99m}Tc reactions, respectively. While the photo transmutation of Mo-100 is based on solid scientific evidence, the actual implementation of this approach will involve development in the area of high power electron machines of suitable energy (25-40 MeV) and technological advances in the electron converter.

In ^{100}Mo(p,2n)^{99m}Tc reaction approach, there is an issue on the purity of the final Tc-99m product both from the isotopic ratio of the molybdenum starting material and the proton energy and the ΔE for the particular target. In addition, the isotopic composition for an enriched target will affect the radionuclidic composition of the target matrix.

There are several approaches to isolating and purifying the Tc-99m extracted from the target material. A more complete understanding regarding reproducibility, purity and efficiency for these approaches is needed using prescribed metrics for direct comparisons. The impact of specific activity (Tc-99m/all Tc isotopes including Tc-99g) has to be determined in order to define the shelf-life of the accelerator produced Tc-99m in comparison to generator produced Tc-99m in the formulation of radiopharmaceutical *kits*. The stability of the isolated Tc-99m pertechnetate solution as a function of time and the stability of the prepared radiopharmaceutical will affect the shelf life of the product. The path to recovery of the enriched Mo-100 target material involves tracking the isotopic composition and chemical/radionuclidic impurities.

1.1. Potential areas proposed for Coordinated Research

Potential areas of further investigations were:

- The impact of Tc-99g and other Tc-isotopes on radiopharmaceutical labelling efficiency and consequence on image quality. How much Tc-99g and other Tc-isotopes will be produced, and how can these impurities be minimized if necessary?
- Measurement of still missing data which need to be determined for the large-scale accelerator-based production of ^{99m}Tc.
- Procedures for preparation of an isotopically enriched molybdenum accelerator target.
- Methods to recover pertechnetate from molybdenum accelerator targets post-irradiation.
- Quality Control (QC) parameters required for evaluation of radiopharmaceuticals prepared with cyclotron-produced pertechnetate.
- Recycling methods to recover enriched Mo from irradiated targets, as well as the impact of recycling enriched Mo on the quality of Tc-99m.

2. CRP OVERALL OBJECTIVE

The overall objective of this CRP is the development of procedures on accelerator based production of Molybdenum-99/Technetium-99m with emphasis on development and optimization of production methods of Tc-99m via the (p,2n) reaction.

2.1. Specific Research Objective

To determine:

- Radionuclide production profiles at various beam energies and intervals.
- Manufacturing of robust ^{100}Mo accelerator target.
- Automated Mo/Tc separation system and chemical impurity profile.
- Labelling efficiency and image quality of Tc-radiopharmaceuticals using cyclotron-produced ^{99m}Tc.
- Dosimetry and its impact on shelf life
- Recycling of ^{100}Mo and assessment of the effects of isotopic composition.

2.2. Salient Aspects of the CRP

The participants of the CRP concluded that the project has helped to exchange valuable information and to become acquainted with other laboratories' approaches and procedures and has stimulated cooperation between participating institutions as well as with relevant national counterparts. The specific objectives pursued by the CRP participants varied from country to country subject to the research priorities defined by the national teams, but the overall objectives of the CRP are well addressed.

3. SUMMARY OF THE WORK DONE IN CRP PARTICIPATING INSTITUTIONS

3.1. ARMENIA: National Science Laboratory (Yerevan Physics Institute) Foundation

The activities of target preparation technology, target module cryogenic cooling system design, chemical separation and recovery of target material have been performed. A new technology of molybdenum target preparation using solid state laser focusing beam processing to the front of tablet has been created and tested. The molybdenum powder is melted in trace of laser, creating a solid strip of molybdenum with a width of a few hundred micrometers.

The laser beam applying to press-fitted Mo tablet increased the mechanical strength and its thermal conductivity. For ^{99m}Tc extraction from the irradiated Mo a centrifuge extractor with **M**ethyl **E**thyl **K**etone (**MEK**) solvent technology was chosen. The irradiated Mo oxidized in H_2O_2 peroxide, then dissolved in KOH alkali and then MEK liquid is added to that solution. The irradiated Mo dissolves in KOH while ^{99m}Tc dissolves in MEK so that we have mixture of two solutions with very different densities. The centrifuge extractor allows the separation of these two solutions with high purity, followed by the separation of the ^{99m}Tc from MEK by evaporation. The complete semi-automated system was installed in a "hot" cell, tested by MoO_3 irradiated under electron beam from LUE20 showing good results. It will be used also for extraction of ^{99m}Tc from Mo irradiated under proton beam from C18 is under commissioning and suggested first beam on September 2015.

The system of target cryogenic cooling has been designed, fabricated and preliminary tested using liquid nitrogen. Test shows good result and should be continue under CO_2 laser higher intensity of beam and under real proton beam.

The system of Mo recycling has been designed, mounted and tested. Final test is in progress. It is based on the H_2S hydrogen sulfide use on the first step of recovery - transformation of K_2MoO_4 solution to molybdenum sulfide MoS_3. The second step – transformation of MoS_3 to MoO_3, and on third step – recovery of metallic Mo from MoO_3 – also are performed. The test of recovery efficiency is in progress.

The lead container for irradiated material transportation form cyclotron to "hot" cell is fabricated. And 2 different types of remotely controlled robot-manipulator have been fabricated providing safely remove irradiated target and its installation to the "hot" cell.

3.2. CANADA: University of Alberta, Faculty of Medicine and Dentistry

The consortium led by University of Alberta has completed two new cyclotron facilities, the Medical Isotope and Cyclotron Facility (MICF, Edmonton, AB) and the Centre d'imagerie moléculaire de Sherbrooke (CIMS, Centre Hospitalier Universitaire de Sherbrooke, QC), to help address the expected problems in the supply of ^{99}Mo/^{99m}Tc generators from aging nuclear reactors. In order to best evaluate the potential of cyclotron-produced ^{99m}Tc, our consortium set a series of objectives; the successful completion of each was necessary to prove that a safe and efficacious product, [^{99m}Tc]TcO_4^- could be economically produced in sufficient quantities to meet the needs of a local/regional nuclear medicine community. These objectives can be broadly classified into cyclotron targetry, target processing, and the development of GMP facilities and all regulatory procedures required to incorporate cyclotron-produced [^{99m}Tc]TcO_4^- into the radiopharmacy. Although initially developed for a 19 MeV cyclotron (100 μA), we have recently successfully translated our processes to use a higher power cyclotron (TR24, p=24 MeV @ 500 μA) in order to meet the needs of a larger patient population (EOB ^{99m}Tc ≈ 1.5 TBq). Based on our enhanced production output, we took into account the economic impact for all steps leading to the final product, including the recycling of ^{100}Mo. The resulting financial model is still under development but indicates that a cyclotron can be used to produce clinically useful quantities of [^{99m}Tc]TcO_4^- at a price similar to that for reactor-produced [^{99m}Tc]TcO_4^-.

Completed projects during the term of this CRP have led to the creation and validation of a comprehensive GMP-based program to produce cyclotron derived [^{99m}Tc]TcO_4^-. This resulted in completing a clinical trial (University of Alberta) showing equivalence with reactor-based ^{99m}Tc; a second clinical trial at Centre Hospitalier Universitaire de Sherbrooke is currently underway.

3.3. CANADA: TRIUMF

The production of ^{99m}Tc via the ^{100}Mo(p,2n) reaction has been developed to the point of going into Clinical Trials with the ultimate goal of using the cyclotron produced ^{99m}Tc (CPTc) in clinical practice as an adjunct to generator ^{99m}Tc. The entire cycle of target production, irradiation, chemical separation, recovery of target material and preparation of targets using the recycled ^{100}Mo have been performed. In addition theoretical calculations for the excitation functions for (p,n), (p,2n) and (p,3n) reactions were performed covering the energy range from 6 MeV up to 24 MeV. Based on these results the production of the various Tc-isotopes was performed using standard commercially available ^{100}Mo enrichments including the distributions of accompanying Mo-isotopes. These results were used to estimate the radiation dosimetry for several radiopharmaceuticals using commercial kits in comparison to generator produced ^{99m}Tc.These results have been published in peer reviewed papers.

In addition, the impact on image quality was determined as a function of the quantity of the various Tc-isotopes in the final product. These results have been presented as conferences and will be the subject of a separate publication.

During the development program a number of systems were established including a process for manufacturing a Mo-metal target, a transfer system for sending the target to the cyclotron and retrieving it. Target dissolution and an automated chemical separation system were constructed. A recovery protocol was initiated whereby ^{100}Mo from previously irradiated targets could be recovered at greater than 93%.

This process approach was established for two types of cyclotrons, the 16.5 MeV PETtrace from GE Healthcare and an ACSI 19 MeV TR19 cyclotron. A TR30 cyclotron operating at 24 MeV has been used to measure yields of ^{99m}Tc at this higher energy as well as co-produced Tc-isotopes that may contribute to increased radiation dosimetry to the patient depending upon the Mo target composition and irradiation conditions.

To date we have produced greater than 9 Ci of ^{99m}Tc on the TR19 cyclotron multiple times as well as 4.7 Ci at 16.5 MeV and >32 Ci at 24 MeV.

Based on our results with preparing radiopharmaceutical kits for anionic, cationic and neutral radiopharmaceuticals ^{99g}Tc does not interfere with labeling for freshly prepared ^{99m}Tc. In addition Labeled kits passed all QC tests for standard kits.

The separation chemistry based on the Cross-linked polyethylene glycol resins (ChemMatrix) provides pure Tc-isotopes. There is no evidence of any radionuclidic impurities.

From our theoretical calculations the percent enrichment of Mo-100 affects yield of ^{99m}Tc that is the amount of Mo-100 present in the target is proportional to the yield of ^{99m}Tc. However the percent abundance of other Mo-isotopes determines the quantity of other Tc-isotopes produced which in the end determines the impact of any radiation dosimetry increase and image quality.

Depending upon the proton beam energy and irradiation time the mix of Tc-isotopes produced impact radiation dosimetry and thus the shelf-life which appears to be at least 12 hours with the aim of determining whether a shelf life of 18 hours is possible. The actual shelf-life will have to be determined with further experimentation.

We have developed a simple ion-chamber based quality control protocol that will provide a *go/no-go* that will enable the producer/end user to decide on the use of the ^{99m}Tc radiopharmaceutical based on potential increases in radiation dose due to contributing Tc-isotopes.

3.4. HUNGARY: Institute for Nuclear Research, Hungarian Academy of Sciences

A Reaction Network Calculation Tool (RNCT) was developed with calculating capabilities to estimate the yields of the different reactions for direct and indirect production of Tc, Mo, Nb and Zr isotopes. The available experimental excitation functions were collected and compared with data from the TENDL data library based on TALYS calculation for the reactions included in the calculation. Technetium isotopes have primary importance. They are produced in (p,xn) reactions on Mo target. In general the (p,xn) reactions are well represented in the TENDL library, therefore in those cases for which experimental data were not available data of the TENDL library were used.

The Reaction Network Calculation Tool capable to predict by calculation the amount of ^{99m}Tc and the amount of co-produced unwanted Tc isotopes as well as other stable and radioactive isotopes of Ru, Mo, Nb and Zr. The calculation can be done as function of target composition, bombarding energy and irradiation time. The decay and decay production of the investigated radioisotopes are also included. The RNCT applies numerical integration of the cross sections to estimate the thick target yield. The reaction cross sections are taken from experimental works and from the TENDL-2013 data library based on TALYS version 1.6 calculations. The upper bombarding energy was limited at 30 MeV in order to limit the number of reactions included. The number of reactions having reaction threshold energy less than 30 MeV is around 200. The RNCT can be used to model most of the aspects of the accelerator production of ^{99m}Tc for variety of possible cyclotron infrastructure.

New experiments were performed to determine the excitation functions of the two main reactions ^{100}Mo(p,2n)^{99m}Tc and ^{100}Mo(p,x)^{99}Mo, and one of the earlier experiments was re-evaluated by using up to date nuclear decay data with the aim to improve the quality of experimental data. The experimental work was done to clear the discrepancy of the reported cross section data of the ^{100}Mo(p,2n)^{99m}Tc and ^{100}Mo(p,pn)^{99}Mo main reactions. Cross section values were measured in three independent experiments using the latest evaluated decay data for the radionuclides involved relative to the ^{nat}Ti(p,x)^{48}V monitor reaction. The resulted three data sets are in very good agreement with each other indicating sound results of the cross section of ^{100}Mo(p,2n)^{99m}Tc reaction.

A benchmark experiment was also carried out to check the validity of the deduced cross section data. In this experiment thick target yield of the ^{100}Mo(p,2n)^{99m}Tc and ^{100}Mo(p,pn)^{99}Mo reactions were determined by irradiating a thick Mo target and by measuring the produced activity. The activity change of the irradiated Mo target was followed for several days and about 100 measured activity points were compared with values deduced by calculation based on the latest experimental cross section data measured for both ^{100}Mo(p,2n)^{99m}Tc and ^{100}Mo(p,pn)^{99}Mo reactions. An excellent agreement was found among the experimental and calculated values confirming the validity of the measured cross section data of the ^{100}Mo(p,2n)^{99m}Tc and ^{100}Mo(p,pn)^{99}Mo reactions. The coinciding results of the three independent experiments can provide a strong base for selecting and deselecting the available experimental data sets and narrow the list of experimental works with accepted results.

To estimate the yields of ^{99m}Tc and the amount of the additional unwanted radionuclides co-produced on enriched molybdenum during irradiation and produced after the end of bombardment by decay in the target both direct and indirect production were considered. The range of the possible isotopes produced during irradiation was extended for production of Ru, Mo, Nb and Zr isotopes.

A target thickness which corresponds to the proton range from bombarding energy down to 7.8 MeV, to the threshold of the ^{100}Mo(p,2n)^{99}Tc reaction is considered to minimize the amount of unwanted activity. Change of isotopic composition of the original enriched target material and its chemical impurities can also be followed by estimating the production and decay of the amount of Ru, Mo, Nb and Zr radionuclides.

^{100}Mo enrichment levels at least as high as 99% are required for good quality production of accelerator ^{99m}Tc.

Presence of the long lived Tc isotopes such as ^{99g}Tc, ^{98}Tc and ^{97g}Tc is important only regarding the achievable specific activity of ^{99m}Tc.

The shorter lived Tc contaminants influence the specific activity as well as contribute to the patient dose.

Due to the decay characteristics of the contaminating technetium radionuclides, half lives, type and energy of the emitted radiations, the ^{93g}Tc, ^{94m}Tc, ^{94g}Tc, ^{95m}Tc, ^{95g}Tc, ^{96m}Tc and ^{96g}Tc could give rise most of the additional patient dose.

The bombarding proton energy should not exceed 25 MeV. To minimize the amount of the shorter lived contaminating Tc isotopes the composition of the enriched target material should be chosen carefully and the amount of ^{94}Mo, ^{95}Mo and ^{96}Mo impurities of the target should be minimized.

The actual value of the additional dose depends on the bombarding energy, target thickness, irradiation and cooling time.

3.5. INDIA: Radiopharmaceuticals Laboratory, Variable Energy Cyclotron Centre (VECC), Kolkata

The direct production of ^{99m}Tc through (p, 2n) reaction on a natural molybdenum target was investigated. Extrapolated thick target yield for 1h, 3h and 6h irradiation as a function of incident proton energy (up to 20 MeV) was calculated from the irradiated natural molybdenum targets. Separation of technetium radionuclide from the irradiated ^{100}Mo target by a new method using Dowex-1 ion exchange resin as well as well as by the standard solvent extraction (with methyl ethyl ketone) method was studied. The quality of the final pertechnetate solution was assessed. Recovery of target material as molybdenum trioxide has been achieved and preliminary experiment on reduction of ammonium molybdate to metallic Mo with hydrogen at high temperature was carried out.

3.6. ITALY: INFN, Legnaro National Laboratories, Legnaro

The contribution of the Italian group in the framework of this CRP has been spread over different research areas. The first one has been a comprehensive theoretical investigation related to the accelerator-produced ^{99m}Tc via ^{100}Mo(p,x) reaction. The theoretical studies aimed at the assessment of the optimal proton irradiation condition for the accelerator-produced Tc (i.e. beam energy, irradiation time, optimal layer thickness), as well as the estimation of in-target yields expected for all Tc nuclides from $^{100-9x}$Mo(p,x) reactions. Moreover, a careful post EOB evolution analyses of the most important parameters, namely the Isotopic Purity IP(t) and the Radionuclidic Purity RNP(t) of the final accelerator-Tc, taking into account the real isotopic composition of ^{100}Mo-enriched (>99 %) metallic molybdenum as target material. The excitation functions measurements for the direct ^{99m}Tc ^{99}Mo (p,x) productions, as well as the main side reactions, was instead a parallel experimental activity aimed at the xs verification. That in order to shed light on the unusual ^{99m}Tc(p,2n) spread of excitation functions data available some years ago on world databases. The new measurements performed have covered the range from threshold up to 21 MeV. Efforts have been done in extending the energy range of the excitation function measurements on the almost pure beta emitter ^{99g}Tc isomer as well. In addition, both theoretical and experimental investigations have also been performed on the other possible ^{96}Zr(α,n)^{99}Mo reaction route for the production of very high specific activity ^{99}Mo. In order to mimic the higher ^{99g}Tc/^{99m}Tc isomer ratios expected from accelerator produced ^{99m}Tc, pharmaceuticals studies have been performed first with a set of most used kits, labelled with ^{99m}Tc eluted from standard Mo/Tc generators at 24 h and longer time intervals, About the correlated chemistry activity, after some preliminary tests, a successful accelerator Tc chemical separation procedure at relatively high yields (up to ~4 GBq) has been achieved, with a fully remote-controlled and operated system and an improved Methyl-Ethyl-Ketone (MEK) based solvent extraction method. In all test performed, a yield larger than 90% has been achieved with a radionuclidic purity basically larger than 99%. Impurities present in the pertechnetate solution have been determined to be always below 0.5%. Accelerator-Tc imaging in-vivo studies have been carried out as well. Preliminary SPECT-CT imaging study confirmed that the biodistribution of radiopharmaceuticals labelled with ^{99m}Tc (generator- or cyclotron-produced) is basically comparable. Because of the additional ^{9x}Tc impurities in the accelerator Tc with respect to generator Tc, it has however been noticed that the effect of scattered high-energy γ-rays from impurities strongly depends on the imaging system used. In this connection, the absorbed dose computational studies with OLINDA/EXM tool have been also performed well taking into account four pharmaceutical products commonly used for diagnostic procedure. The cumulated activity in the source organs was calculated for the cyclotron produced Tc isotopes found in our experiments. The main result was that the small activities by other technetium impurities contribute to a slight increase (basically 10-15% larger than generator Tc) 20 hours after EOB, thus suggesting the possibility to replace generator Tc with the new production method in case of future shortages.

At last, first successful results have been achieved on Mo deposition as multilayered films on backing material using the physical evaporative deposition technique at UHV at the super conductivity and surface treatments lab at LNL. Most of the results obtained have been published in peer-reviewed journals.

3.7. ITALY: Laboratorio Energia Nucleare Applicata (L.E.N.A.) of the University of Pavia

The University of Pavia, with Laboratory of Nuclear Energy Applied (LENA) and Radiochemistry Area, tested the ^{99m}Tc production using enriched ^{100}Mo as target in a protons accelerator. The research involves the radiochemical purity of the ^{99m}Tc product adopting different techniques, the evaluation of ^{99g}Tc production and studies on recycling of the enriched Molybdenum after separation. The activity of LENA was focused at the beginning on the ^{99m}Tc production with (n,γ) reaction on ^{98}Mo together with study on the ^{99}Mo production via the ^{100}Mo (n,2n) ^{99}Mo reaction through fast neutrons facility (14.2 MeV D-T). Finally Pavia developed a ^{99m}Tc alternative production by cyclotron. The facilities involve in collaboration with Pavia are the Laboratories of the University of Pavia and Radiochemistry Area, The Cyclotron of the European Commission Joint Research Centre for protons irradiation (Scanditronix MC40), the Laboratory of Accelerator and Applied Superconductivity – L.A.S.A. (associated to INFN sez. Mi), , the LNL (Legnaro National Laboratories), the University of Ferrara (INFN sez. Fe) and the University of Milano-Bicocca. The study starts from the preparation of the target (LNL) and arrive at the recycle of enriched Mo, considering also the automation (University of Ferrara). The targets for test were prepared at LNL using several enriched ^{100}Mo foils of 25 micron separated by aluminum foils. The protons energy chosen, 18MeV, take into account the diffusion of cyclotron in Italy with such protons energy that it is also the same of LENA cyclotron. This allows to foreseen a local production for local needing. After the irradiation, Mo foils were dissolved fast only with H_2O_2 and heat (50°C). Finally, best results, were obtained with Methyl ethyl ketone (MEK). One automatic system was developed at the University of Ferrara based on this separation method. Evaluation of ^{99g}Tc was made with two methods, NAA (LENA) and ICP/MS (MI-BI) and a complete excitation curve is ongoing. Final product is really free from radiochemistry point of view apart from the presence of other Tc and Nb isotopes. Nb contamination can be removed properly along the process in the real production. Precipitation of ammonium isopolymolibdate at pH 2-4 is the method chosen for recovery the enriched Mo. After filtration (trapped on the filter), it is easy recover Mo targets in oxide form at 500°C.

Reduction of Molybdenum by Hydrogen studies is still ongoing in order to close the cycle process.

3.8. JAPAN: Molecular Imaging Centre, National Institute of Radiological Sciences

There are considerable numbers of medical cyclotrons in operation that are mainly dedicated to produce PET nuclides routinely. Owing to these infrastructures, a concept of small-scale direct ^{99m}Tc production at multiple facilities can be proposed to enhance their potential that will contribute domestic ^{99m}Tc supply as a reliable alternative.

The automated production scheme was developed by using ^{100}Mo oxide ($^{100}MoO_3$) or elemental ^{100}Mo powder as a target material, respectively. Briefly, ^{100}Mo oxide target was remotely prepared by a spray-dry method, where ^{100}Mo dissolved in H_2O_2 was sprayed onto a heated target vessel; then, a precipitated ^{100}Mo oxide with its thickness of 3–5 mm was obtained at the appropriate position on the beam trajectory remotely. And in case of elemental target, a weighed ^{100}Mo powder as purchased was prepared into a target vessel that was designed for a vertical irradiation system. Owing to the gravity, even powdery target can be set and hold on the beam position without using any other supports.

In the recovery step following irradiation, both targets were dissolved at respective target vessel in-situ by directly introducing of H_2O_2 and NH_3 aq step-by-step. The liquefied crude target solution was roughly purified and then transferred to a hot cell through a tube without using any robotic devices.

The recovered ^{99m}Tc crude solution was finely purified by using commercially available chelating-resin on an automated apparatus developed in this study. Approximately 3.7 GBq/6.3 GBq (100 mCi/170 mCi, decay uncorrected) of $Na^{99m}TcO_4$ with high radionuclidic- and radiochemical-purity was obtained from oxide/elemental target, respectively, within 2 h of processing via irradiation with 18 MeV protons at 10 μA for 3 h.

Owing to the low stress involved in this production method including target preparation and target recovery, a regional/in-house production could be performed with less effort. Moreover, if 100 or more cyclotrons connected to a sophisticated logistical network are available, a multi-centre production concept would work successfully at the level of 370 GBq (10 kCi) per day throughout Japan.

3.9. POLAND: National Centre for Nuclear Research,, Radioisotope Centre POLATOM

The project was carried out in collaboration of National Centre for Nuclear Research Radioisotope Centre POLATOM, the Heavy Ion Laboratory, University of Warsaw (HIL UW) and The Institute of Nuclear Chemistry and Technology in Warsaw (INCT).

HIL UW: The external target station for commercial PETtrace cyclotron was designed, manufactured and assembled as a standalone system. The thin (down to 250 nm) and thick (400-600 μm) foils were produced by rolling the metal bead preceded by flattening the Mo droplets at a high temperature. The nat and enriched Mo was irradiated with p of 23-8 MeV energy. The p of 23 MeV were used for natMo only. The p in range of 16-8 MeV from the PETtrace was used to produce ^{99m}Tc with ^{100}Mo of 99.05% and 99.815% enrichment. The γ-ray energies and intensities of irradiated samples were measured and the radionuclidic purity of the produced ^{99m}Tc was deduced as a function of time and sample enrichment. The experimental Thick Target Yield (TTY) was compared with values calculated using the published reaction cross sections and the theoretically calculated ones (EMPIRE evaporation code).

POLATOM: Pressed and sintered ^{100}Mo pellets with sufficient hardness, density and mechanical strength adequate for irradiation in cyclotrons have been reproducibly produced. Chemical and electrochemical dissolution of target in 15 to 20 mL of 30% H_2O_2 and 19 mL of 5M KOH has been achieved in 45 and 70 minutes, respectively. About 90% recovery of ^{99m}Tc in less than 100 minutes with 99.6% radiochemical purity has been achieved using AnaLig resin for separation. It was superior to ion exchange and PEG and gave the product of sufficient radiochemical purity. Two production batches were processed resulting with ^{99m}Tc pertechnetate solution quality meeting the developed specification.

The INCT proposed method of molybdenum separation in the form of a solid AMP was fast and efficient. In this method low co-precipitation of $^{99m}TcO_4^-$ and good recovery of Mo was achieved. To obtain pure $^{99m}TcO_4^-$ product in the next step, pertechnetate anions were separated from the excess of molybdate ions on a C18 column coated with PEG-2000 and finally $^{99m}TcO_4^-$ was concentrated on alumina column. Labelling Hynic-Substance P and NS_3-CN-Substance P conjugates with ^{99m}Tc in presence of molybdenum in solution were performed with a high yield. The separation and labeling processes will be confirmed on real solutions obtained from dissolution of irradiated ^{100}Mo target.

3.10. SAUDIA ARABIA: Cyclotron and radiopharmaceuticals department, King Faisal Specialist Hospital and Research Centre

The production of technetium radioisotope is reported in this study including production through natural and enriched *Molybdenum (*^{100}*Mo)*. In this study the Mo target was bombard with different beam current and energies in order to study the stability of the pressed target.

High activity of ^{99m}Tc was successfully produced using the ^{100}Tc (p, 2n) ^{99m}Tc reaction and processed through pressing technique. Extraction of Tc and prepared in the form of $TcO4^-$ was done through MEK and Alumina column.

Moreover we have successfully labeled the Pertechnetate with MDP. A maximum total activity of ^{99m}Tc was 1100 mCi was obtained when the target was bombarded with 15 uA.

3.11. SYRIA: Atomic Energy Commission of Syria, Radioisotopes Department, Cyclotron Division

Multiple methods and experiences have been carried out to perform a suitable target for high current proton beam for ^{99m}Tc production. Different electroplating bathes have been used for target support electroplating.

The quality of the different electroplated Mo layer on copper substrate was not suitable for high current proton beam and high activity Tc-99m production.

The thickness obtained by different electroplating procedure do not exceed 2-3 micrometer having a total surface of 10 cm^2.

After these non satisfied electroplating experiences, testes on pressed then sintered of molybdenum oxide method in order to prepare a molybdenum target had been achieved. Again in an attempt on molybdenum oxide sintering was not successful due to the appearance of crystals on the surface of the prepared pellets.

Another method for the production of ^{99m}Tc based on liquid target has been explored. A related method for the separation of ^{99m}Tc and recovery of enriched molybdenum has been tested.

At the final period of the project a new production method of ^{99m}Tc was tested using a high current solid target. This method can meet cost-effective production and quality of the produced ^{99m}Tc criteria. The separation and purification setup was elaborated to produce high quantity and high specific activity of ^{99m}TcO4^{-} suitable for labeling different ligands in order to be used in nuclear medicine imaging. A semi-automated target dissolution and separation system has been developed and achieved for ^{99m}TcO4^{-} production. The separation chemistry is based on a chromatographic column system. Chemical and radiochemical purity was found to be in accordance with the USP and EP specifications. 99% of radioisotopes in the final product were attributed to the presence of ^{99m}Tc. The labeling efficiency results of the produced Na^{99m}TcO$_4$ show that less than 1% of ^{99m}Tc activity was not labeled with MDP kit. Biodistribution of labeled kits results and their application for in vivo SPECT images demonstrate that the quality of the produced ^{99m}Tc-pertechnetate is identical to that produced from^{99}Mo/^{99m}Tc generators.

3.12. USA: Mallinckrodt Institute of Radiology, Washington University School of Medicine, St. Louis

During the course of the CRP, we have conducted studies of the ^{100}Mo(p,2n)^{99m}Tc reaction on a medical cyclotron using ^{100}Mo$_2$C and ^{100}Mo metal targets. This was the first report of ^{100}Mo$_2$C being used as a target for this reaction. ^{100}Mo$_2$C, refractory carbide with high thermal conductivity, properties which underscore its use on a cyclotron, was synthesized using ^{100}MoO$_3$. Its ease of oxidation back to ^{100}MoO$_3$ under air at elevated temperatures facilitates the use of thermo-chromatography, a high temperature gas phase separation technique for the separation and isolation of ^{99m}Tc. Using a similar technique, we also conducted experiments using enriched ^{100}Mo metal targets. These experiments illustrated that Mo metal was also amenable to the thermo-chromatographic method of separation and that Mo metal can be efficiently recycled under low reducing conditions. Tc was recovered by rinsing the glassware with 0.1mM NaOH. Radio-ITLC analysis of the recovered ^{99m}Tc revealed that a small amount of ^{99m}TcO$_3$ (5%) was present along with ^{99m}TcO$_4^-$. Purification of the wash with Sep-Pak light alumina N cartridge conditioned by acidified Millipore water (pH 2) resulted in only the TcO$_4^-$ species. Activity yields for ^{99m}Tc averaged 84% of the calculated theoretical yields. Additionally, the percent recovery of MoO$_3$, the precursor for both Mo metal and Mo$_2$C, was consistently high at 85% ensuring a good life cycle for this target material. While outside the scope of this CRP, similar processes were also developed for the production of ^{186}Re from enriched ^{186}W targets using these techniques.

REPORTS BY THE PARTICIPANTS OF THE COORDINATED RESEARCH PROJECT

TECHNOLOGY DEVELOPMENT FOR ^{99m}Tc DIRECT PRODUCTION UNDER PROTON BEAM FROM C18 CYCLOTRON AT NATIONAL SCIENCE LABORATORY

A. AVETISYAN, R. DALLAKYAN, R. SARKISYAN, A. MELKONYAN, M. MKRTCHYAN, G. HARUTYUNYAN, N. DOBROVOLSKY, S. SERGEEVA

A. I. Alikhanyan National Science Laboratory (Yerevan Physics Institute)
Foundation, Yerevan, Armenia

Abstract

An alternative way of accelerator production of ^{99m}Tc on cyclotrons for medical purposes is under active consideration in recent years in the world. The technique of direct production (bypassing the intermediate phase of the parent ^{99}Mo isotope) of ^{99m}Tc on cyclotron proton beams is actively developed in many scientific centers in recent years [1-9].

This method promised to be successful especially taking into account a huge number of medical cyclotrons around the world. The serious technology problems for powdered molybdenum use as target material, expensive enriched ^{100}Mo recovery for multiple times irradiation, high power target module extensive cooling requirement should be resolved. Technologies of above mentioned procedures have been developed to provide higher efficiency of ^{99m}Tc direct production.

1. INTRODUCTION

The C18 cyclotron (produced by IBA, Belgium, Fig. 1) is in the stage of installing in the Isotope Production Center in Armenia. An appropriate technology of ^{99m}Tc production on its proton beam has been developed at the National Science Laboratory after. A. Alikhanyan (Yerevan Physics Institute). There is an opportunity to develop the technology of ^{99m}Tc direct production using parallel beam from that cyclotron. Three tasks of that activity namely Mo target preparation technology development, target cryogenic cooling and Molybdenum recovery for multiple uses were investigated in the present work.

2. MOLYBDENUM TARGET PREPARATION TECHNOLOGY DEVELOPMENT

2.1. Target module description

For irradiation of solid targets in the standard specification of the C18 cyclotron a targets module is used (Fig. 2), in which the target itself is fixed by pneumatic clamps. During the irradiation, the target is cooled by a helium flow on the front side and by a water stream under a pressure of about 8 bars on the rear side.

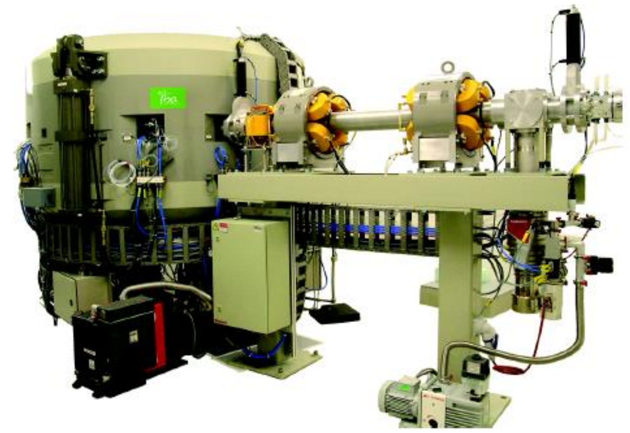

FIG. 1. General view of the C18 cyclotron with extracted beam pipe.

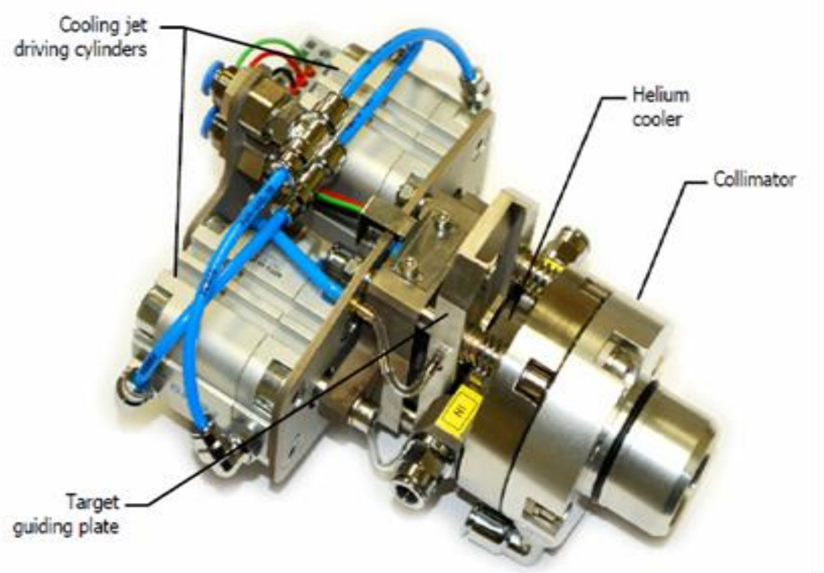

FIG. 2. The general view of the Nitra Solid Compact TS06 target module.

The target itself is a metallic disk with a central deepening in which the material for irradiation is located. In Fig. 3, that area is marked as “target area”.

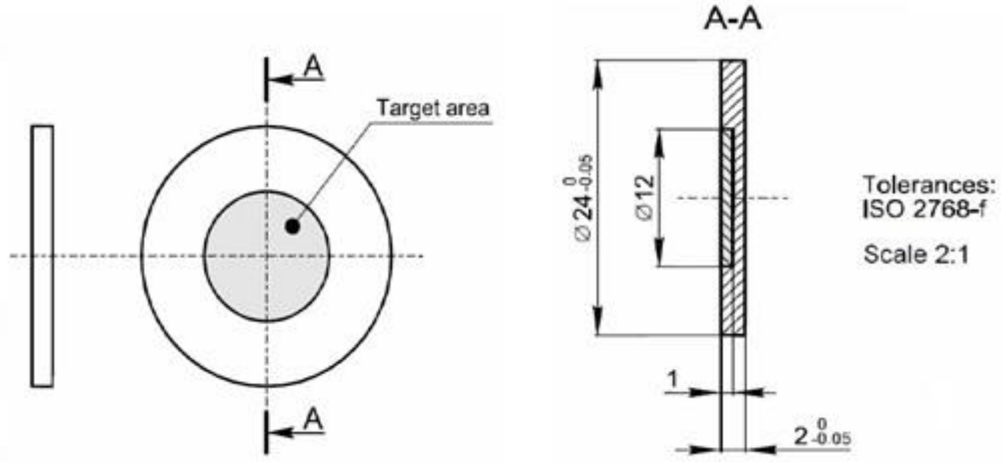

FIG. 3. Solid state target disk.

2.2. Regular targets preparation method

The target consists of a metallic disk (see Fig. 3) [10] and the material for irradiation placed in the target area.

The requirements to the target disk are as follows: high mechanical strength and high thermal conductivity for effective evacuation of the heat produced during irradiation and chemical inactivity.

In terms of durability and chemical inactivity, niobium and titanium are a good fit. The thermal conductivity of niobium is twice as better as that of titanium.
^{100}Mo or natural molybdenum ^{nat}Mo fine powder is used as material for irradiation in order to produce ^{99m}Tc. It is required to make a solid disk from the powder to place it in the target area. There has been usually used the method of powder metallurgy, where the fine powder is first compressed then roasted at high temperatures. The edges of powder grains melt and join each other, creating a quasi-solid structure.
The different-scale images of the compressed powder taken by an electron microscope are shown in Fig. 4 ([1] (page 140).

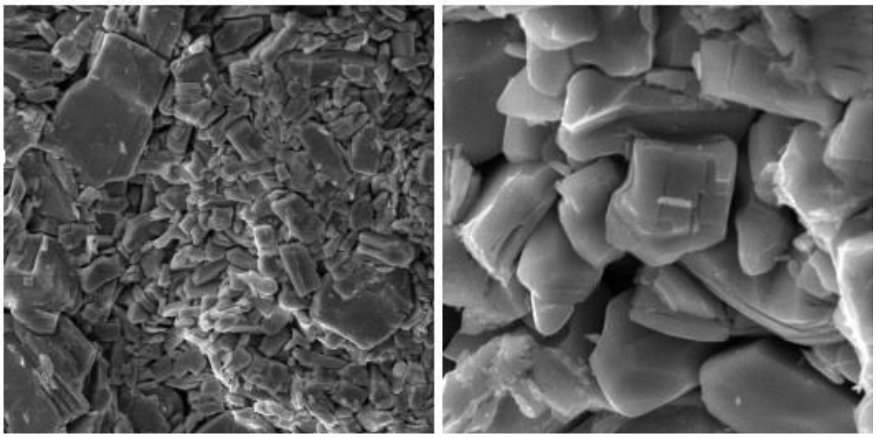

FIG. 4. Molybdenum powder grains images of different scale after thermal processing taken by an electron microscope.

We have developed a natural molybdenum powder compression method using a press (Fig. 5) that can exert a force of ~40000 N.

FIG. 5. A press with a matrix and a punch for pressing of molybdenum into a disk.

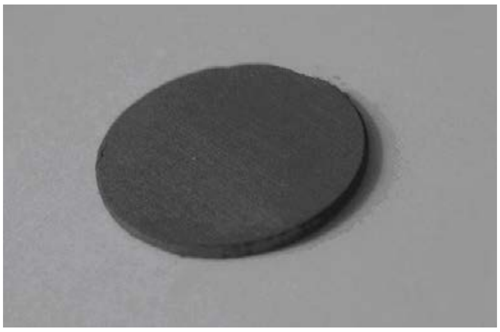

FIG. 6. A tablet of natural molybdenum obtained by the compression method.

However, without additional processing the tablet does not have enough durability and can crash while set up in the target area or its evacuation after the irradiation.

The increase the mechanical durability, we have developed a tablet surface burning method using a focused laser beam. A solid-state laser with the following specifications has been used:

Wave length	1.6 µm
Impulse energy	250 MJ
Impulse repetition frequency	40 Hz
Impulse duration	200 µsec

A special device for burning has been developed. The laser beam was held through a beam expander and then was focused by a lens having a focal distance of F=150 mm. The light spot’s diameter in the focus varied within the range of 150-300 µm.

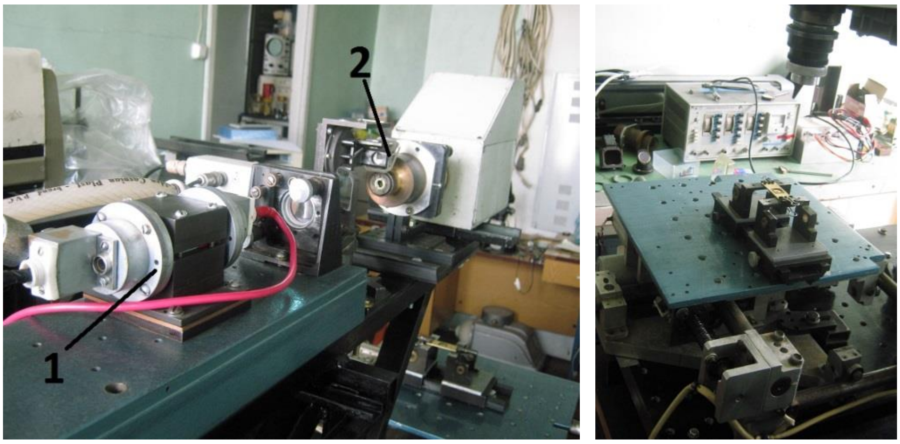

FIG. 7. The automatic tablet processing device for molybdenum target laser processing: the solid-state laser (left) and the 2-dimensional coordinate table with remote computer control (right). 1- solid state laser, 2- beam expander.

The molybdenum powder is melted in trace of laser, creating a solid strip of molybdenum with a width of a few hundred micrometers. The images of a tablet after orthogonal processing with a laser beam are shown in Fig. 8.

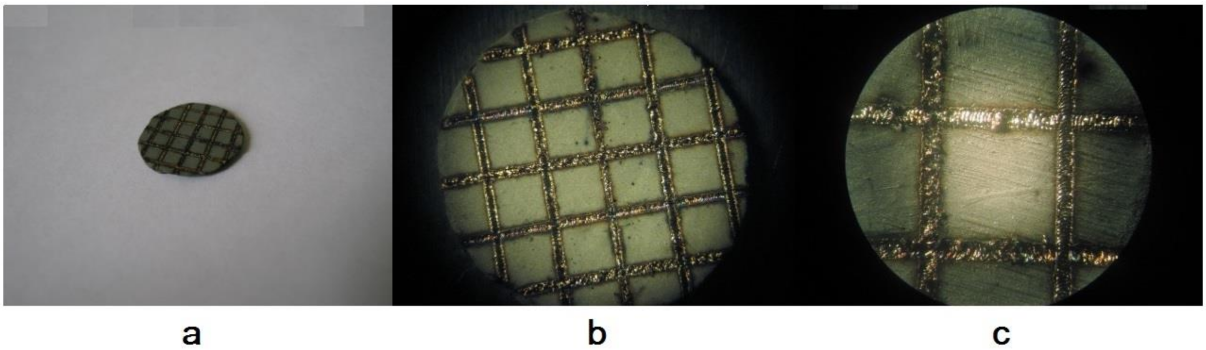

FIG. 8. Molybdenum tablet processed by a laser beam at different magnifications: a) general view, b) x20 times zoomed under optical microscope c) x42 times zoomed.

It is well known that Mo oxidizes in the air at T>600°C. During laser processing the temperature of molybdenum tablet surface is more than 2700°C for a very short time. That creates an anxiety that a part of metallic Mo could be transformed to MoO_3. To check the possibility, the laser processing was performed in a special airtight box filled with inert gas neon. Three identical tablets were prepared to check the possibility of oxidizing. One was simply pressed without any laser processing. The second tablet was processed by a laser in air atmosphere, and the third one underwent the same laser processing in a neon atmosphere. As a calibration point, the pure MoO_3 powder has been tested. All four samples were investigated under X-ray phase analysis. The results are presented in Fig. 9.

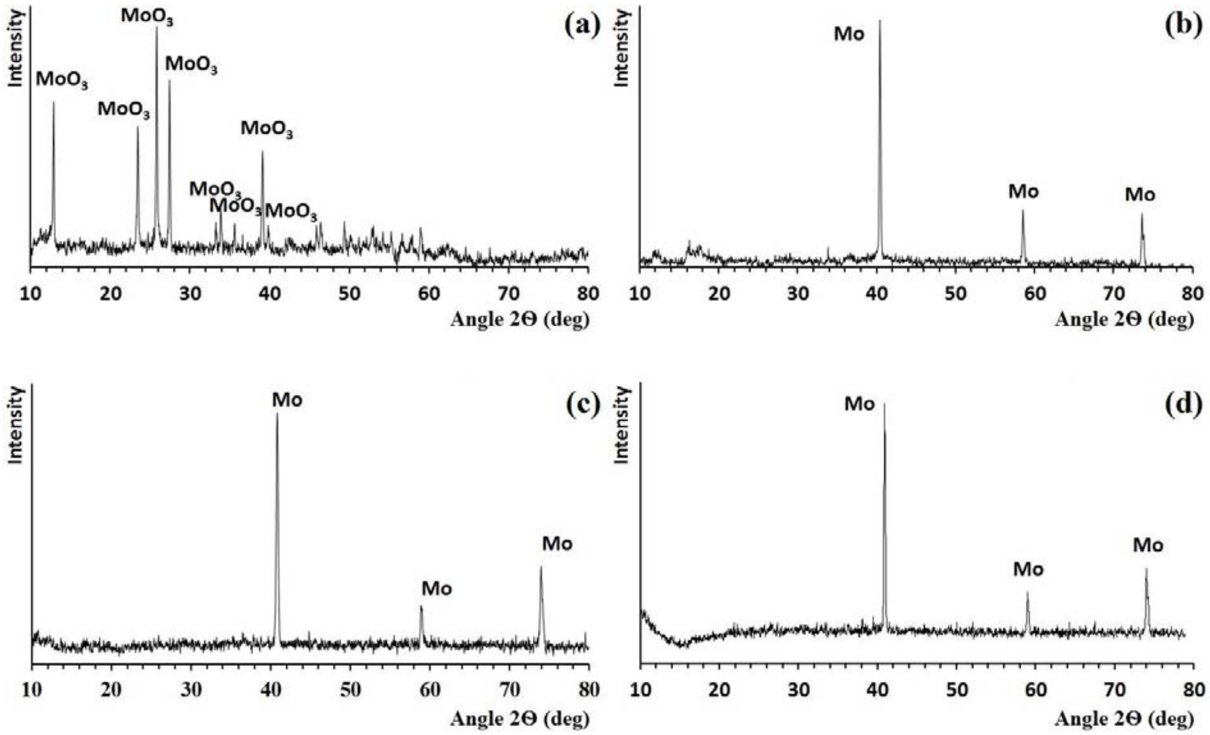

FIG. 9. X-ray phase analysis spectra a) for MoO_3 powder, b) metallic Mo pressed to tablet without any additional processing, c) metallic Mo pressed to tablet and processed under laser beam in air atmosphere, d) metallic Mo pressed to tablet and processed under laser beam in neon atmosphere.

These results show that during laser processing Mo did not transform to MoO_3 neither in the air nor in the neon atmosphere. That could be due to very short time of high temperature presence, which is not enough for the slow chemical process of oxidizing.

After such processing, the mechanical strength of tablets should increase. The reason for such an increase is that the melted stripes of metallic molybdenum on the surface of the tablet play the role of steel fittings. For objective estimation of such assumption, a device for the measurement of the relative strength of tables is made. The strength of tablets was measured with and without processing.

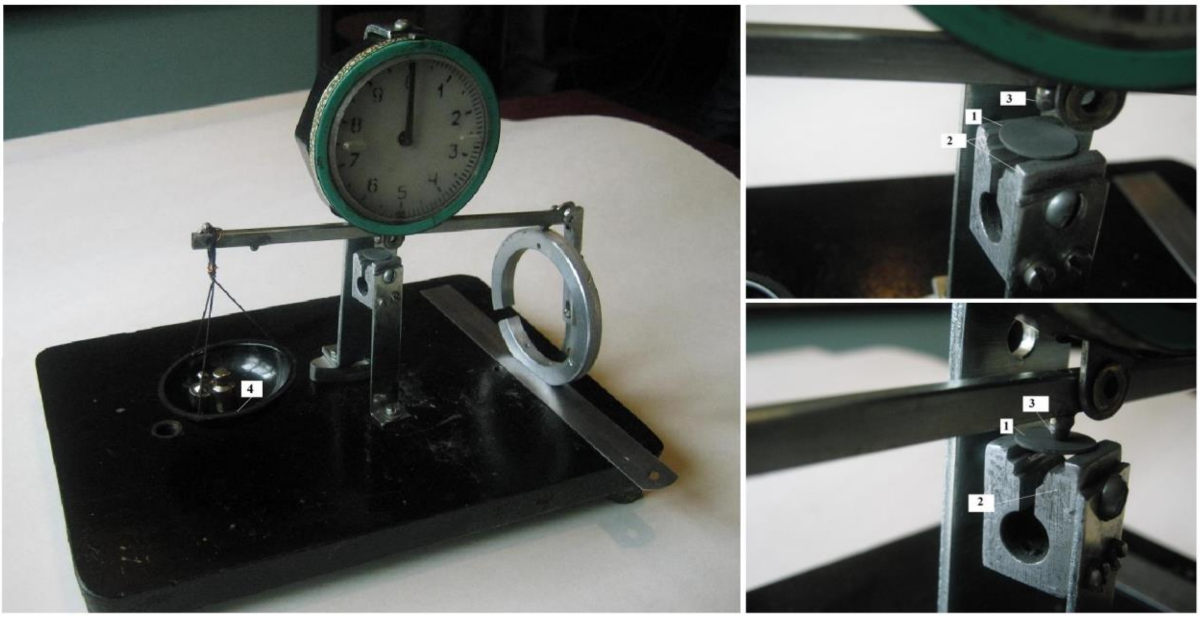

FIG. 10. Tablet top mechanical strength measurement device. The molybdenum tablet (1) is set on support (2), the steel ball (3) presses against the tablet with a force determined by the mass of the weights in the scale dish (4). Upper right picture - before strength measurement, bottom right picture - the ball presses against the tablet surface.

The tablets relative strength measuring device is shown in Fig. 10. The pressure of steel ball (3) on the tablet (1) is determined by the mass of weights in the scale dish (4). At a certain point, the tablet breaks under the pressure.

Ten tablets with approximately the same characteristics were made. The durability of five tablets having not undergone and five tablets having undergone laser processing has been measured. The results of measurements are shown in Table 1 and Table 2.

TABLE 1. RELATIVE STRENGTH OF TABLETS WITHOUT LASER PROCESSING

№	**Diameter (mm)**	**Thickness (mm)**	**Weight (mg)**	**Mechanical strength (a.u.)**
1	9	0.8	580	445
2	9	0.76	560	476
3	9	0.7	570	560
4	9	0.72	540	426
5	9	0.74	535	436

TABLE 2. RELATIVE MECHANICAL STRENGTH OF TABLETS AFTER LASER PROCESSING

№	Diameter (mm)	Thickness (mm)	Weight (mg)	Mechanical strength (a.u.)
1	9	0.75	560	884
2	9	0.78	570	844
3	9	0.79	570	724
4	9	0.80	580	604
5	9	0.76	535	644

The mechanical strength increased more than 1.5 times after laser treatment as is seen from the tables above. The developed technique of laser treatment of the surface of compressed molybdenum powder tablets can be used to make real solid targets for irradiation by proton beam of the cyclotron.

2.3. Tablet (disc) target preparation technique by laser treatment

Using the above-mentioned technique the disk targets were made in accordance with the drawings in Fig. 3. The fine powder of natural molybdenum was compressed in the central part of the disc (Fig. 11).

FIG. 11. Disc type target with compressed natural molybdenum powder (the central circle).

Further, to increase the surface strength of the molybdenum pressed in the center of the target disk, its surface was treated similarly as in case of individual tablets. The processing parameters remained the same. The result is shown in Fig. 12.

FIG. 12. Target disk with pressed molybdenum therein after the laser treatment (left), with x40 magnification (right).

However, the molybdenum powder pressed into the center of the target disk has insufficient adhesion to the disk and may fall out during transportation after irradiation. Therefore, additional treatment with a laser beam was performed at four diametrically opposite points, providing sufficient adhesion, as is shown in Fig. 13.

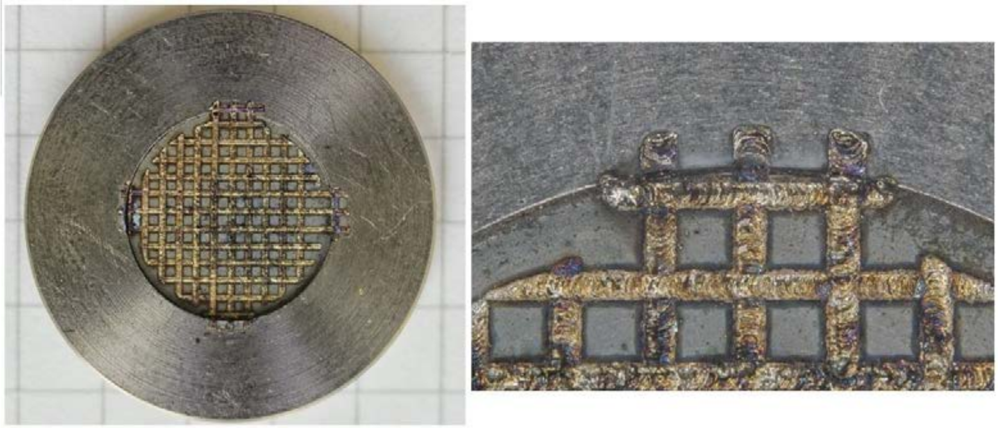

FIG. 13. Target disc with molybdenum after the additional strengthened adhesion at four points (left side), at x30 magnification (right).

3. ^{99m}Tc SEPARATION

The direct extraction of ^{99m}Tc from the irradiated material is chosen. For that, a centrifuge extractor with Methyl Ethyl Ketone (MEK) solvent technology was chosen. This technology has been successfully used for many years in Russia [11]. The irradiated Mo oxidized in H_2O_2 peroxide, then dissolved in KOH alkali and then MEK liquid is added to that solution. The Mo dissolves in KOH while ^{99m}Tc dissolves in MEK so that we have mixture of two solutions with very different densities. The centrifuge extractor was designed at the A.N. Frumkin Institute of Physical Chemistry and Electrochemistry in Moscow [12] and allows the separation of the two elements with high purity, followed by the separation of the ^{99m}Tc from MEK by evaporation. The complete automated system commissioned from the Moscow “Federal center of nuclear medicine projects design and development” and developed by FMBA (Russia company) was installed in a “hot” cell shown in Fig. 14, tested by MoO_3 irradiated under electron beam from LUE20 showing good results [13]. It will be used also for extraction of ^{99m}Tc from Mo irradiated under proton beam from C18 is under commissioning and suggested first beam on September 2015.

FIG. 14. Main part of the centrifuge extractor complex.

4. CRYOGENIC COOLING

As it was mentioned above the NIRTA solid target technology provides the target cooling by a helium flow on the front side and by a water stream under a pressure of about 8 bars on the rear side during the irradiation. That provides around 500 W thermal power utilization which means for beam energy Ep=18 MeV the maximum intensity Ip~30 μA while the C18 cyclotron could provide up to 100 μA. One of the ways to increase the cooling efficiency is to decrease the temperature of cooling element dramatically – e.g. up to liquid nitrogen temperature.

The ideology of that is the following. The thermal stream is an equivalent of electric current in Ohm’s low. While our task is increasing the thermal stream for better cooling there are only 2 ways namely to increase the thermal conductivity or to increase the potential is equivalent of difference between warm and cold parts. Because development of thermal conductivity is limited due to powder consistence the only way is increasing of difference between heated target and cooler. The liquid nitrogen could be a good alternative to simple water cooling.

For that a test layout has been mounted using solid state CW laser with wave length 1.06 μm. The laser beam with a maximum power 50 W was directed to the front face of target prepared from Mo pressed powder (see Fig. 15 and 16). The temperature of face was measuring by infrared thermometer - pyrometer which was preliminary calibrated for correct measurement in the green area of light.

Test shows the following results.

- Without cooling the face temperature of target under laser heating is rising up in the time and achieves the plateau with value of 500 degree centigrade.
- While liquid nitrogen cooling has been on the face temperature of target under laser heating is rising up in the time and achieves the plateau with value of 320 degree centigrade.
- No cooling has been applied directly to the front of target.

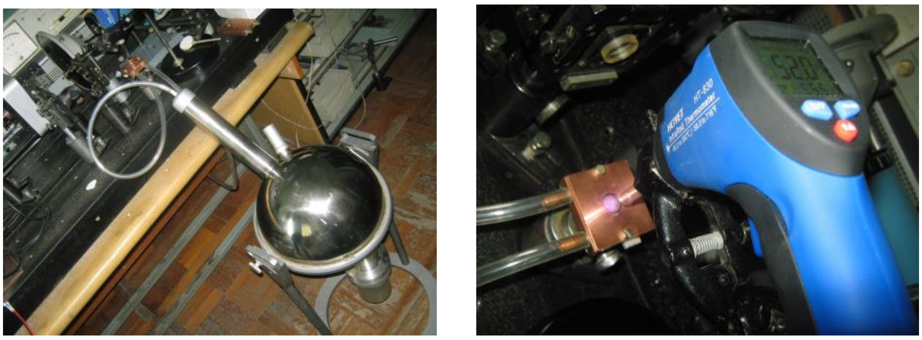

FIG. 15. Laser system for heating simulation and cryogenic cooling system. On the right picture the red spot on the center of target is an infrared radiation of heated target.

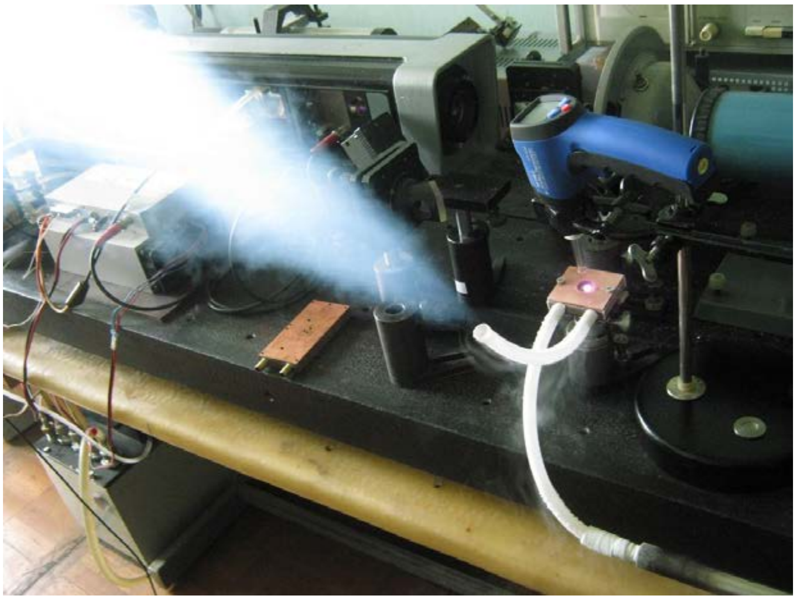

FIG. 16. Laser beam heating and liquid nitrogen cooling test.

Results of this test are following:

- This was simply qualitative test to show that cryogenic cooling could work in general.
- The effective cooling decreases the temperature of target front for 180 degrees centigrade (from 500 to 320 degrees centigrade – for about 1.5 times).
- The simulation of heating by means of laser beam is not absolutely correct because during irradiation under proton beam the evolution of heat takes place along the beam direction on whole length while under irradiation under laser beam it happens only on the very thick slice of target. So the way of thermal stream in the second case is much longer and total thermal resistance is higher. It can suggest that under proton beam the efficiency of cryogenic cooling would be higher.

Preliminary estimation shows that for such a cooling will spent 5-7 liter of liquid nitrogen per hour which is a good price for more effective cooling and therefore much more output of final product.

These investigations should be continued under CO_2 laser beam with a maximum beam power up to 500 W.

5. MOLYBDENUM RECOVERY FOR MULTIPLE USES

Due to very high cost of enriched ^{100}Mo it should be recovered after irradiation and ^{99m}Tc extraction. The recycling strategy is shown on Fig. 17.

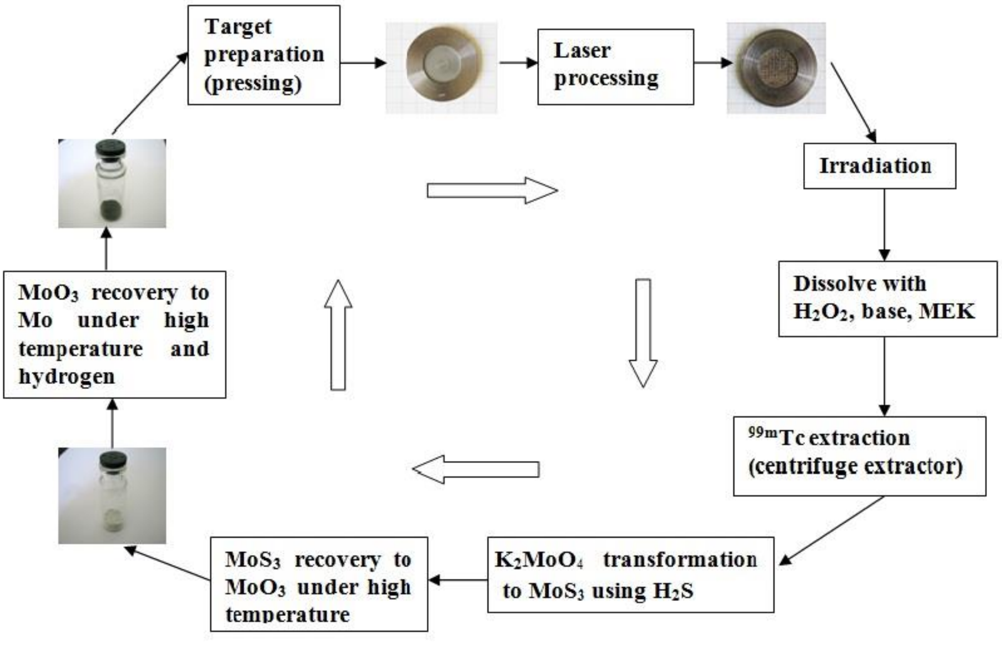

FIG. 17. The recycling strategy of ^{99m}Tc production.

We decided to use a combination of processes for Mo recovery after extraction of ^{99m}Tc from irradiated Mo.

The chemistry processing has been designed as follows.

First step – recovery of MoS_3 from K_2MoO_4 solution, **second step** – transformation of MoS_3 to MoO_3, and on **third step** – recovery of metallic Mo from MoO_3.

On the first step the following reaction is carried out. The hydrogen sulfide put in alkaline solution. Hydrogen sulfide 3-5 fold excess of an alkaline solution fed. The process proceeds according to the following reactions

$$K_2MoO_4 + 4H_2S = MoS_3 + K_2S + 4H_2O$$

To produce hydrogen sulfide a laboratory method based on the action of 20-30% hydrochloric acid for the iron sulfide was used. That work should be carried out under the hood.

$$FeS + 2HCl = FeCl_2 + H2S\uparrow$$

In alkaline environment molybdenum sulfide precipitate does not fall because formed soluble potassium thiomolybdate formed

$$MoS_3 + K_2S = K_2MoS_4$$

Then a neutralization of the alkaline solution of hydrochloric acid should be done by following reactions:

$$K_2MoS_4 + 2HCl = MoS_3\downarrow + HCl + H_2S$$

Molybdenum sulfide precipitates as an amorphous black-brown flock.

The precipitate was washed with distilled water from the chlorine ions

The washed precipitate was annealed in a muffle furnace feeding for two modes of air

$$MoS_3 = MoS_2 + S \qquad \text{by } T = 250\text{-}300°C$$

$$2MoS_2 + 7O_2 = 2MoO_3 + 4SO_2 \qquad \text{by } T = 500\text{-}600°C$$

Parallel reactions can take place:

$$MoS_2 + 6MoO_3 = 7MoO_2 + 2SO_2$$

$$2MoO_2 + O_2 = 2MoO_3$$

The resulting pitch, white-gray crushed to a powder.To provide all above mentioned action a laboratory layout has been ordered, purchased and mounted with intensive exhaust hood (see Fig.18).

FIG.18. Exhaust hood with Mo recycling trial layout.

On the final state recovery of metallic Mo from MoO_3 is carried out via hydrogen reduction by following reaction

$MoO_3 + 3H_2 \rightarrow Mo + 3H_2O\uparrow$ (under 700°C temperature in a special furnace).

6. CONCLUSION

A new technology of molybdenum target preparation using laser beam processing to the front of tablet has been created and tested. The laser beam applying to press-fitted Mo tablet increased the mechanical strength and its thermal conductivity.

The centrifuge extractor with **M**ethyl **E**thyl **K**etone (**MEK**) solvent technology was chosen for ^{99m}Tc extraction from the irradiated Mo. The complete semi-automated system was installed in a "hot" cell, tested by MoO_3 irradiated under electron beam from LUE20 showing good results. It will be used also for extraction of ^{99m}Tc from Mo irradiated under proton beam from C18 is under commissioning and suggested first beam on September 2015

The option of target cryogenic cooling has been preliminary tested using liquid nitrogen. Test shows good result and should be continue under higher laser beam intensity and under real proton beam.

The system of Mo recycling has been designed, mounted and tested. Final test is in progress.

So that all components of system for testing a ^{99m}Tc direct production technology are ready for waiting a proton beam from C18 suggested on September 2015.

The article - A.Avetisyan, R.Dallakyan, R.Sargsyan, A.Melkonyan, M.Mkrtchyan, G.Harutyunyan, N.Dobrovolsky “The powdered molybdenum target preparation technology for ^{99m}Tc production on C18 cyclotron” has been submitted to the International Journal of Engineering Science and Innovative Technology.

Acknowledgment

This work was performed under the financial support of Armenian State scientific budget and IAEA CRP Contract 18029. The authors gratefully thank Dr. Thomas Ruth (TRIUMF, Canada) for his great support of this activity.

References

[1] INTERNATIONAL ATOMIC ENERGY AGENCY, 2nd RCM on "Accelerator-based Alternatives to Non-HEU Production of Mo-99 / Tc-99m", October 7-11, 2013, Legnaro, Italy, http://www-naweb.iaea.org/napc/iachem/working_materials/TR-RCM2-Final-Report-Draft-oct-22nd.pdf.

[2] INTERNATIONAL ATOMIC ENERGY AGENCY, 1st Research Coordination Meeting on “Accelerator-based Alternatives to Non-HEU Production of ^{99}Mo/^{99m}Tc”, 16 - 20 April 2012, Vancouver, Canada, http://www-naweb.iaea.org/napc/iachem/working_materials/RC-1212-1-report.pdf.

[3] RUTH, T., Accelerating production of medical isotopes, NATURE,|Vol **457(29)** January (2009).

[4] GAGNON, K., et al., Cyclotron Production of ^{99m}Tc: Experimental measurement of the ^{100}Mo(p,x)^{99}Mo, ^{99m}Tc and ^{99g}Tc excitation functions from 8 to 18 MeV, Nucl. Med. and Biology **38** (2011) 907-916.

[5] CERVERA, M., ^{99m}Tc Production processes: an examination of proposals to ensure stable north american medical supplies, http://www.cvmbs.colostate.edu/erhs/Health%20Physics/99mTc_Production_in_North_America.pdf.

[6] NAGAI, Y., HATSUKAWA, Y., Production of ^{99}Mo for nuclear medicine by ^{100}Mo(n; 2n)^{99}Mo, Journal of the Physical Society of Japan Vol. **78**, No. 3, March, (2009) 033201.

[7] MOORE, R. S., Production of ^{99m}Tc and ^{99}Mo,PXIE_PX-DOC-1102-V2 **31**, Oct(2012).

[8] INTERNATIONAL ATOMIC ENERGY AGENCY, Production and Supply of Molybdenum-99, IAEAGC (**54**)/INF/3 Suppl., Vienna (2010).

[9] BERTSCHE, K., Accelerator production options for ^{99}Mo, International Particle Accelerator Conference (IPAC), Kyoto, Japan, May (2010), http://accelconf.web.cern.ch/AccelConf/IPAC10/papers/mopea025.pdf.

[10] Nirta Solid Compact Model TS06 Operation manual.

[11] M. P. Zykov, V. N. Romanovskii, D. W. Wester et al., Use of extraction generator for preparing a ^{99m}Tc radiopharmaceutical, Radiochemistry, Vol. **43**, No. 3, (2001) 297-300.

[12] EGOROV, A.V., ZIKOV, M.P., KORPUSOV, G.V., ROMANOVSKY, V.N., FILYANIN, A.J., Production of ^{99m}Tc on the centralized generator in St. Petersburg, The Journal of Nucl. Med. and Biology Vol. **38**, No. 3, (1994) 399-402.

[13] AVAGYAN, R., AVETISYAN, A., KEROBYAN, I., DALLAKYAN, R., Photo-production of ^{99}Mo/^{99m}Tc with electron linear accelerator beam, Nucl. Med. and Biology **41** (2014) 705–709.

ACCELERATOR-BASED ALTERNATIVES TO NON-HEU PRODUCTION OF ^{99}Mo/^{99m}Tc

S.A. MCQUARRIE[a], K. GAGNON[a], J. ANDERSSON, J. WILSON[a], E. SCHIRRMACHER[a], B. THOMAS[a], R. LECOMTE[b], S. SELIVANOVA[b], H. SENTA[b], B. GUÉRIN[b], E. TURCOTTE[b], A. ZYUZIN[c] and A.J.B. MCEWAN[a]

[a] University of Alberta, Faculty of Medicine and Dentistry
Edmonton, Alberta
Canada

[b] Centre Hospitalier Universitaire de Sherbrooke
Sherbrooke, Quebec
Canada

[c] Advanced Cyclotron Systems
Richmond, British Columbia
Canada

Abstract

The consortium led by University of Alberta has completed two new cyclotron facilities, the Medical Isotope and Cyclotron Facility (MICF, Edmonton, AB) and the Centre d'imagerie moléculaire de Sherbrooke (CIMS, Centre Hospitalier Universitaire de Sherbrooke, QC), to help address the expected problems in the supply of ^{99}Mo/^{99m}Tc generators from aging nuclear reactors. We have developed a unique approach to demonstrate that cyclotron-produced ^{99m}Tc is feasible. Information presented in this report will summarize the creation and implementation of a cyclotron laboratory and associated GMP facility for the production of cyclotron-based ^{99m}Tc. The processes leading to the final production scheme, as well as ^{99m}Tc/^{100}Mo separation and subsequent QA/QC trials are reviewed, including summary of the regulatory processes that are hoped will lead to approval for the use of [^{99m}Tc]TcO_4^- in the health care system.

1. INTRODUCTION

The information reported in this document represent the collaborative effort of our consortium, the University of Alberta (U of A), Advanced Cyclotron Systems Inc. (ACSI) and the Centre Hospitalier Universitaire de Sherbrooke (CHUS). In order to best evaluate the potential of cyclotron-produced ^{99m}Tc, our consortium set a series of objectives; the successful completion of each was necessary to prove that a safe product, [^{99m}Tc]TcO_4^- could be economically produced in sufficient quantities to meet the needs of a local/regional nuclear medicine community. A brief review highlighting these necessary steps are presented with sufficient generality so that they could be adapted for other cyclotron-produced radiopharmaceuticals.

These objectives can be broadly classified into cyclotron targetry, target processing, and the development of GMP facilities and procedures required to ensure patient safety when using cyclotron-produced [^{99m}Tc]TcO_4^- instead of reactor-derived [^{99m}Tc]TcO_4^- [1-3]. During the optimization stage, we took into account the economic impact for all steps leading to the final product. The resulting financial model is still under development but indicates that a cyclotron can be used to produce clinically useful quantities of [^{99m}Tc]TcO_4^- at a price similar to that available for reactor-produced [^{99m}Tc]TcO_4^-.

2. CYCLOTRON-PRODUCED ^{99m}Tc

Building on the early work of Beaver and Hupf [4], we sought to test whether significant quantities of [^{99m}Tc]TcO$_4^-$ could be made to meet the needs of the nuclear medicine community in times of shortage or the unavailability of reactor-based [^{99m}Tc]TcO$_4^-$. Initial experiments at the University of Alberta commenced in 2009 using a TR19/9 cyclotron and our promising results were first reported internationally at the Workshop on Cyclotron Targetry and Target Chemistry in Denmark [5]. Our next goals were to 1) verify ^{99m}Tc production cross-sections and assess the production of ^{99g}Tc in order to measure the ^{99m}Tc/^{99g}Tc ratio and thereby predict its potential impact on specific activity when compared reactor-derived [^{99m}Tc]TcO$_4^-$, 2) using thermal modeling techniques, design a cyclotron target that could withstand the elevated thermal loads expected during high-current irradiations, and 3) design, build and evaluate different cyclotron targets taking into account the results predicted by the thermal model. Particular emphasis was paid to the interface between the ^{100}Mo and the target body (substrate) to ensure maximum heat transfer and physical stability of the interface during subsequent handling.

2.1. ^{99m}Tc and ^{99g}Tc Cross-Section Measurements

When this project began in 2009 there were large cross-section discrepancies in the then current literature; our goal was to re-evaluate the cross sections for the ^{100}Mo(p,2n)^{99m}Tc and ^{100}Mo(p,pn)^{99}Mo reactions. The methods are described in Refs [6,7]; only the results are summarized here.

Thick target yields were calculated from the measured ^{99m}Tc cross-sections assuming 100 percent ^{100}Mo and fitting the cross-section data with a 2nd order polynomial. Values were reported for proton energy loss with the ^{100}Mo of 18→10 MeV, and 22→10 MeV (cross-sections extrapolated to 22 MeV from a polynomial curve fit). Thick target yields for ^{99m}Tc were determined to be 14.2 mCi (526 MBq)/μAh for 18-10 MeV, and 18.2 mCi (674 MBq)/μAh for 22→10 MeV. FIG 1 compares the evaluated cross-sections for the direct production of ^{99m}Tc to previously published cross section data.

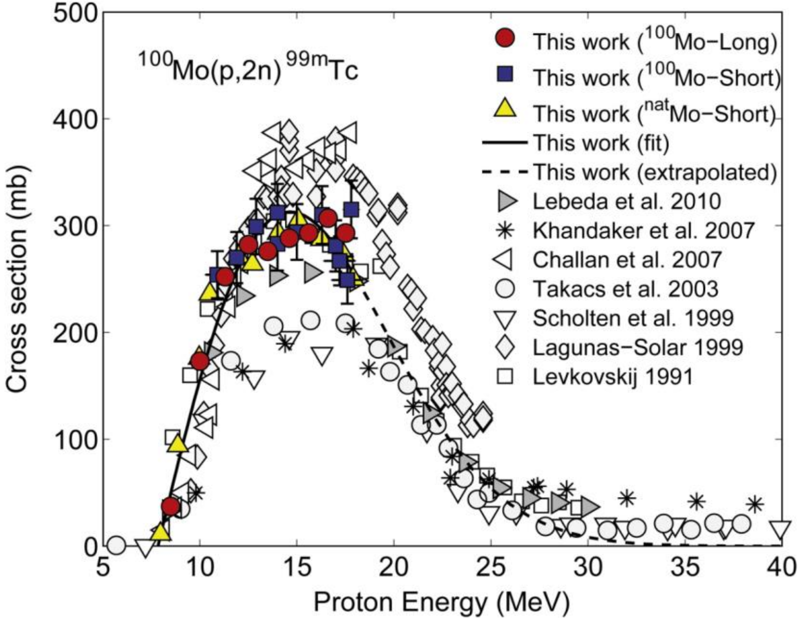

FIG. 1. Experimental excitation function for the ^{100}Mo(p,2n)^{99m}Tc reaction. Error bars for the short ^{100}Mo irradiations are included.

As we are not only interested in optimizing the yield of ^{99m}Tc, but also in determining its specific activity, we measured the experimental ^{100}Mo(p,2n)^{99g}Tc cross-section in the energy range of 8 – 18 MeV, using ICP-MS to evaluate ^{99g}Tc. These results are presented in FIG 2 with the observation that the ratio of ^{99m}Tc to $^{99m+99g}$Tc nuclei is similar to the ^{99}Mo/^{99m}Tc generator standard eluted at a 24 hr frequency.

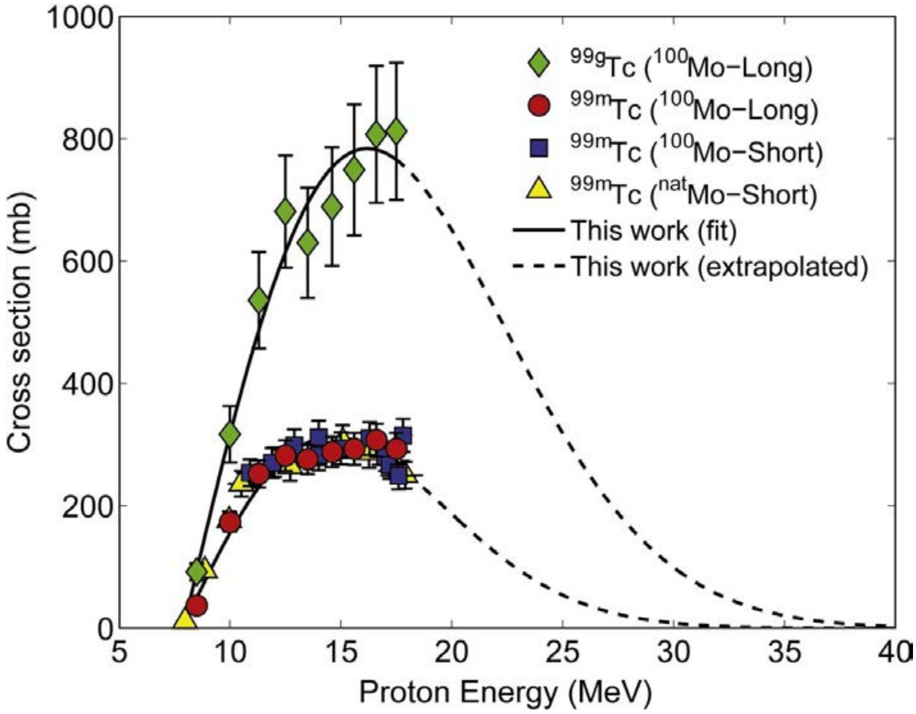

FIG. 2. Experimental excitation function for the ^{100}Mo(p,2n)^{99g}Tc and ^{100}Mo(p,2n)^{99m}Tc reactions.

2.2. Thermal Modelling

Although radionuclide production yields may be improved by increasing the beam current, the maximum beam current is often dictated by the thermal performance of a target. This limitation is commonly observed for solid targets as these materials often demonstrate poor thermal conductivities and low melting points. In this case we are interested in improving the power handling capability of our ^{100}Mo solid targets through choice of the target substrate and optimization of the water flow-rate and of the shape and location of the cooling channels on the back of the substrate. We have investigated the use of finite element analysis to model both heat transfer and turbulent flow, followed by experimental validation [8,9].

For the purpose of validating the model a target plate with simplistic geometry was used that was equipped with a thermocouple to perform real-time measurements during irradiation as shown in FIG 3. Target plates of both copper and zirconium were tested because of their markedly different thermal properties: copper is an excellent thermal conductor with a thermal conductivity, *k*, of 401 $Wm^{-1}K^{-1}$ (@ 300 K), while zirconium is a relatively poor thermal conductor with *k* equal to 22.6 $Wm^{-1}K^{-1}$ (@ 300 K). Irradiations were performed with proton currents up to 80 μA (17.5 MeV) for the copper plate and 50 μA (15.5 MeV) for zirconium.

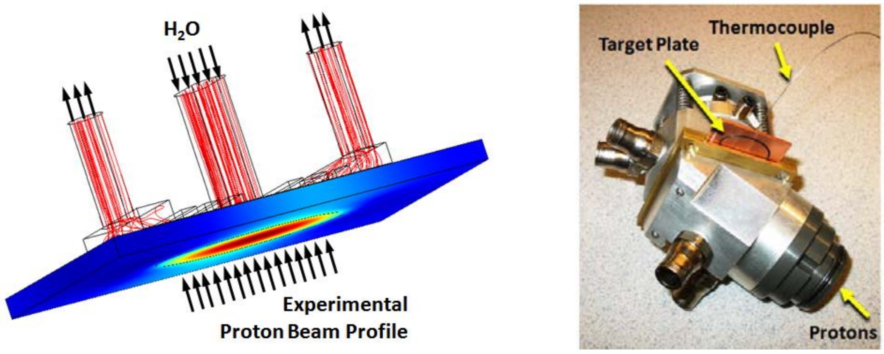

FIG. 3. Schematic diagram of the thermal model (right) and the experimental validation apparatus used to measure thermal characteristics of a cyclotron sold-target (left).

The 3D heat transfer and turbulent flow of the cooling water were modelled using the COMSOL Multiphysics® v. 3.5a. steady-state general heat transfer and k-ε turbulence models, respectively. Experimental input parameters to the model include the cooling water temperature, cooling water flow rate, target plate/cooling water channel geometry; a sample proton beam profile was obtained experimentally using radiochromic film [10]. The temperature dependent material properties (i.e. thermal conductivity, density, heat capacity, etc.) were defined using COMSOL's built-in material library.

The results of this work suggest that our geometric configuration is best described by the convective heat transfer coefficient proposed by Chang et al [11]. The experimental measurements performed in this study have allowed us to select a convective heat transfer model, which is capable of accurately predicting the target plate temperature for materials with widely varying thermal properties.

2.3. Cyclotron Targets

The University of Alberta successfully completed the design and testing of a ^{100}Mo target using sintering technology for the TR19 cyclotron [1,12,13]. Critical parameters were optimized during the sintering process, including the type of atmosphere used and the temperature of the oven, the substrate on which the molybdenum was sintered, and the pressure at which the molybdenum is pressed. The best results were obtained when the molybdenum was sintered at 1600°C under a reducing atmosphere (5% H_2 in Ar) for 4 hours, with the resulting molybdenum achieving a density of ca. 8.2 gcm^{-3}. Aluminum oxide was the substrate of choice due to its low activation and acceptable thermal properties.

Although this target was used to successfully demonstrate the ability of a cyclotron to produce adequate quantities of ^{99m}Tc targets, the beam current (~100 μA) was sub-optimal to meet the needs of a regional radiopharmaceutical distribution network.

In order to meet the anticipated needs for regional supply, new high-current (500 μA) TR24 cyclotrons (24 MeV) were selected. These were installed in the newly-constructed purpose-built MICF and CIMS. This necessitated a complete overhaul and re-design of the ^{100}Mo target based on adapting the solid-target irradiation-station supplied by ACSI. The main focus of our next phase of target research was to 1) select a target substrate to hold the ^{100}Mo in place during irradiation and transfer to a recovery hot-cell, and 2) discover a process to bond the ^{100}Mo to the target substrate while optimizing thermal heat transfer and physical stability.

Based on our studies on the TR19 and its activation properties, aluminum was our substrate of choice. Irradiations were performed step-wise on aluminum “blank” targets up to a maximum of 6 hours at 500 µA (Ep = 22 MeV). Note that all irradiations were performed with no entrance window (under cyclotron vacuum) so that only the rear of the target was cooled.

Bonding ^{100}Mo to the substrate was a challenging process, and one that we are still optimizing [14]. Starting with natural abundance molybdenum, we first developed a method for preparing foil-like pieces of rigid molybdenum from powder of the desired dimensions (i.e. ~20 mm × 80 mm × 100 µm). Molybdenum densities in excess of 10 g/cm^3 were obtained. We have also optimized the bonding of this molybdenum to the target support to ensure adequate heat-exchange. Our current efforts are now focused on scale-up of target fabrication and minimizing losses of molybdenum during the fabrication process. Losses are currently on the order of ~20%, with increased efficiency expected as the process is further optimized.

As of late 2013, we have started to use our process for fabricating targets using enriched ^{100}Mo. This is in contrast to natural abundance molybdenum (which is made of 7 stable molybdenum isotopes – ^{100}Mo only comprising ~10%). Use of the expensive enriched ^{100}Mo is critical for achieving a product of high yield and high quality. The enriched ^{100}Mo targets showed similar characteristics compared with natural isotopic abundance molybdenum. A series of photos noting the transition from the low current TR19 targets to the high current TR24 targets is given in FIG 4.

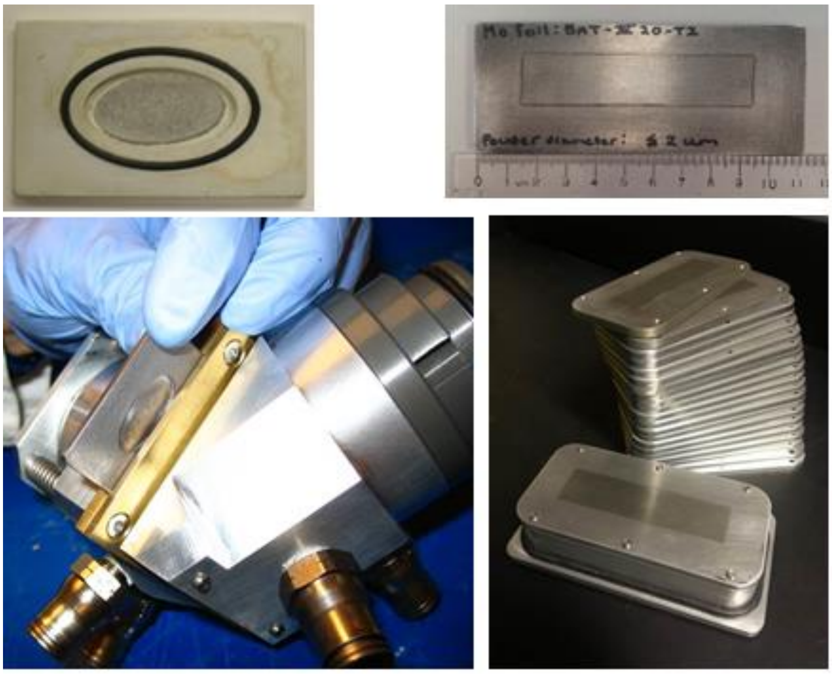

FIG. 4. Photos of target transition from the small low-current TR19 targets (left –top and bottom), to initial/preliminary foil studies (right - top), to our present (as of January 2014) high-current TR24 targets (right - bottom).

The first ^{100}Mo target irradiations on our TR24 were performed in January 2014, with targets irradiated with beam currents of ~250 µA. These preliminary tests made 10x more ^{99m}Tc than we had made previously on the TR19 cyclotron. A provisional patent application was filed on our “high current” target technology on March 27, 2014.

Before irradiating further ^{100}Mo targets, a number of irradiations were performed step-wise on aluminum “blank” targets up to a maximum of 6 hours at 500 µA. Given the success of the “blanks”, we followed up with further target irradiations on ^{100}Mo targets. All irradiations were performed at 22 MeV. In August 2014, eight aluminum target plates with Mo-100 were irradiated in 50 µA steps (i.e. from 150 µA to 500 µA) for 15 minutes each. The yields were consistent and independent of irradiation current, with the average and standard deviation of the experimentally measured saturated yield being 6.1 ± 0.2 GBq/µA. This was approximately 90% of the expected/extrapolated theoretical yield. With the experimentally determined saturated yields, we therefore expect to make 1.5 TBq (41 Ci) after 6 hrs of irradiation. Six of the eight target plates looked virtually identical before and after irradiation, while two of the plates had points where the Mo-100 had small burn spots (FIG 5, left). This was not clearly correlated to current or to significant drops in yield (FIG 5, right). Further scale-up is currently underway.

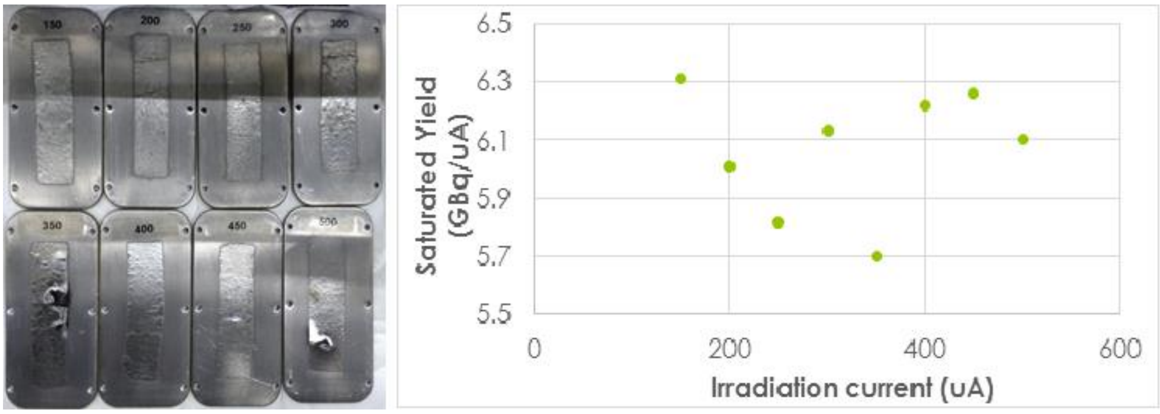

FIG. 5. Photo of irradiated targets. Beam current (µA) is shown at the top of each target (left). Saturated yield vs Current for the eight irradiated Mo-100 targets (right).

2.4. Separation of ^{99m}Tc/^{100}Mo and Production of $^{99m}TcO_4^-$

After the production of ^{99m}Tc via the ^{100}Mo(p,2n)^{99m}Tc reaction, there is a requirement for separating ^{99m}Tc from bulk ^{100}Mo [15]. Efficient and timely dissolution of the ^{99m}Tc/^{100}Mo is the first of the two critical chemistry steps; the second is the isolation/purification of the ^{99m}Tc product. Although a number of separation methods have been demonstrated, the potential of using an automated system for both steps is particularly attractive for the routine use in a good manufacturing practice (GMP) regulatory environment.

2.5. Dissolution Technology

Due to the significant amount of radioactivity present following irradiation, this dissolution must be performed within a hot cell (i.e. it cannot be performed bench-top). Furthermore, although we have remote manipulators for handling of radioactive objects within the hot cells, automation of the dissolution process is essential for minimizing radiation exposure to personnel, and for the purpose of ensuring process reliability and reproducibility. To this end, we have leveraged and adapted a cassette-based automated chemistry system to introduce chemicals to the ^{100}Mo dissolution chamber.

Dissolution testing using a statistical screening design was performed to determine the critical factors in the dissolution process. Some of the variables tested included annealed and un-annealed targets, dissolution temperatures and varying concentrations of the solvent, hydrogen peroxide. The time for complete dissolution of the target and the amount of leftover hydrogen peroxide were measured. The H_2O_2 concentration and volume of H_2O_2 was found to be a major factor in the quest to reduce the dissolution time. At present, dissolution of annealed, bonded and irradiated molybdenum targets can be achieved in approximately 40 minutes.

2.6. Separation Technology

Separations were performed on an automated chemistry unit. Resins were evaluated with regard to [^{99m}Tc]pertechnetate and [^{99}Mo]molybdate adsorption and desorption. [^{99m}Tc]pertechnetate and [^{99}Mo]molybdate was obtained from generators (Edmonton Radiopharmaceutical Centre), eluted using NaCl and $(NH_4)_2CO_3$ (1.5M) respectively. All commercial resins were activated according to the manufacturer's specification, and $(NH_4)_2CO_3$ (3M, 20 mL) was used to condition all resins before loading of pertechnetate and molybdate. Loading solutions consisted of $(NH_4)_2CO_3$ (1.5M) [^{99m}Tc]pertechnetate or [^{99}Mo]molybdate in NaCl. After loading, the resins were washed with Na_2CO_3 (1M, 3 mL), and then eluted with deionized water (D.I. H_2O) (10 mL) unless otherwise stated. Separations were performed using a loading solution containing 300 mg Mo powder dissolved in 10 mL H_2O_2 and 10 mL $(NH_4)_2CO_3$ (3 M). After loading, the column was washed with 5 mL $(NH_4)_2CO_3$ (1 M) followed by 1.5 mL D.I. H_2O. The [^{99m}Tc]TcO_4^- was eluted using 10 mL D.I. H_2O and passed through a strong cation exchange column and an alumina column. The [^{99m}Tc]TcO_4^- was eluted from the alumina column using 10 mL of isotonic saline.

2.7. Commercial SPE cartridges

We evaluated commercial reversed phase resins for their potential of separating pertechnetate from molybdate [16,17]. Pertechnetate adsorbed strongly on the RP-SPE cartridge Chromabond® HR-P (Macherey-Nagel GmbH & Co.) however none of the solvents used (H_2O, MeCN, DCM and DMSO) were successful in desorbing the pertechnetate. In addition 0.4% of the ^{99}Mo was adsorbed on the HR-P cartridge. Oasis® HLB (Waters Inc.) was successful in retaining pertechnetate but acetonitrile was needed for desorption. It was however encouraging that no [^{99}Mo]molybdate breakthrough to the Tc fraction was observed. Waters tC18 plus and Phenomenex Strata® C18-U did not successfully retain pertechnetate.

2.8. Synthesis of PS-DVB-PEG resin

PS-DVB-PEG resin synthesis consisted of grafting polyethylene glycol (PEG) to polystyrene beads according to previously published methods. In short, a 500 mL, three necked round bottom flask with magnetic stirrer and condenser was capped with a drying tube. It was put in an oil bath on a heat/stir plate and was equipped with thermometer. Chloromethylated polystyrene: 1% divinylbenzene copolymer beads (3.0 – 3.5 g) were pre-swelled in diethylene glycol dimethyl ether (anhydrous, 99.5%, 40 mL) or THF (anhydrous, with inhibitor, ≥99.9%, 60 mL) by stirring for 15 min at room temperature. Polyethyleneglycol methyl ether (average MW 2,000 or 5,000, 20-25 g) was added to the system, and NaH (600 mg) was slowly added over 30 min. The oil bath was then heated to 70°C (gentle reflux for THF) for 17 hours. The NaH was quenched with isopropanol (IPA,

≥99.5%) until no reaction could be noticed. The resin was then washed with IPA and twice with deionized water and filtered using a Buchner funnel.

Total synthesis time was 20 hours, and the yield of the synthesis was over 2.5 g PS-DVB-PEG resin per g polystyrene starting material. Elemental analysis indicated a carbon content of 69-76%. Recovery of ^{99m}Tc was 82 ± 9 % (n=5, all different batches). The “in-house” produced PEG resins showed similar adsorption characteristics as ABEC™ resin obtained from Eichrom Technologies LLC, however elution profiles of the pertechnetate were more variable between batches of the in-house synthesized resin. These interesting differences could not be attributed to synthesis or resin analysis (elemental analysis). To determine the adsorption due to PEG grafted on the beads, PS-DVB-Cl and PS-DVB-OH were included in the study. As expected, pertechnetate did not adsorb on the resins. The PEG resins all exhibited very low ^{99}Mo retention and thus low breakthrough to the Tc fraction. The highest breakthrough observed was 0.08% for the PS-DVB-PEG resin.

2.9. PEG coated C18 cartridges

C-18 cartridges containing 3 g of resin were coated by pouring PEG3000 solution through the cartridge and then washing with deionized water (D.I. H_2O). PEG concentration in the final product was evaluated by iodine visualization TLC. Recovery of ^{99m}Tc was 92 ± 4 % (n=4). Greater than 99.5 % of the ^{99}Mo was present in the load/wash fractions (n=2) thus allowing for minimal losses in terms of recycling enriched ^{100}Mo. The PEG3000 concentration in the final product was lower than the limit of detection for our TLC spot test (0.1 mg/mL), pH was 6 and the product was clear and colorless.

2.10. Tentagel N-OH

Tentagel N-OH (Rapp Polymere), was identified, tested, and found to give high yields (i.e. >98%). As with the other resins we tested, Tentagel N-OH was not originally designed for separation of ^{99m}Tc (rather it is used for peptide synthesis), but its properties were such that we observed superior results using this resin than we had observed with ABEC. As product quality is imperative, and in accordance with guidelines from Health Canada, the International Conference on Harmonization, the European Medicines Agency, and the Food and Drug Administration, the U of A has implemented a quality by design approach to our process development. To date, using the Tentagel N-OH resin, we have implemented an 8-factor, 16-run D-optimal design to assess critical process parameters in the production of ^{99m}Tc. Factors assessed include load molarity, load temperature, load time, resin mass, SPE column diameter, wash molarity, elution temperature, and elution speed. Further optimization studies are underway. We are focused on moving forward with the Tentagel N-OH resin for commercial-scale production of cyclotron-based ^{99m}Tc.

2.11. Automation

Process automation is imperative for minimizing radiation exposure to personnel, and for the purpose of ensuring process reliability and reproducibility. Furthermore, automation also allows for digital process trending of system parameters (e.g. pressure, flow rates, etc.), thus facilitating optimization and troubleshooting. With regards to automation of the chemistry for extracting ^{99m}Tc from the irradiated and dissolved ^{100}Mo target material, numerous separation units have been evaluated at the U of A. As none of the commercial units are traditionally used for ^{99m}Tc extraction, there was a need for reprogramming and reconfiguring the chemistry unit to suit our processing scheme. It should also be noted that the U of A always had a strong focus on commercial level production and has therefore employed cassette based automated systems since "day 1" for ease of scale-up and regulatory approval. An initial cyclotron test using the optimized dissolution and separation conditions together with complete automation yielded 106 GBq (decay corrected to EOB) of [^{99m}Tc]TcO_4^-.

3. ^{100}Mo RECYCLING

The high costs associated with the isotopic separation of ^{100}Mo from natural molybdenum makes target recycling very attractive. While recycling of enriched molybdenum has been reported for oxide-based targets (e.g. in the context of ^{94}Mo), the main challenge in recycling metallic targets arises from the conversion of the metallic molybdenum to molybdate that is required for ^{99m}Tc extraction. Metallic recycling strategies therefore require isolation and purification of the molybdate, followed by subsequent conversion back to molybdenum metal.

In developing a process for recycling enriched metallic ^{100}Mo, all chemicals which are used in either of the dissolution and ^{99m}Tc extraction processes were carefully considered as their efficient removal is critical prior to radiopharmaceutical formulation. We have successfully optimized a ^{99m}Tc extraction strategy that is compatible with the proposed target recycling methodology [11,12]. To allow for evaporative isolation and purification of the molybdate, this procedure used hydrogen peroxide to dissolve the target, and ammonium carbonate to basify the dissolved target solution prior to extraction of pertechnetate. Following isolation, purification, and hydrogen reduction to convert the molybdate to the metal, an overall enriched ^{100}Mo metal-to-metal recovery of 87% was obtained (ongoing optimization is expected to further improve recovery).

This "recycled" ^{100}Mo was used to produce three more targets. These targets were once again irradiated and the recovered quality of the ^{99m}Tc from the "new" and "recycled" targets was compared. No differences in the ^{94g}Tc, ^{95g}Tc, or ^{96g}Tc radionuclidic impurities were noted between these two sets, and all batches of [^{99m}Tc]-pertechnetate had a pH, radiochemical purity, and Al^{3+} concentration that were within USP limits. Isotopic composition of the recycled ^{100}Mo was not found to change post-irradiation as determined via inductively coupled plasma mass spectrometry (ICP-MS). As a further test, [^{99m}Tc]-MDP was prepared following irradiation of "recycled" ^{100}Mo, and its biodistribution was evaluated by imaging the uptake in a rabbit. The results were compared with biodistribution of reactor-based [^{99m}Tc]-MDP, and qualitatively, no significant differences in uptake were noted. A schematic of the overall separation scheme is given in FIG 6.

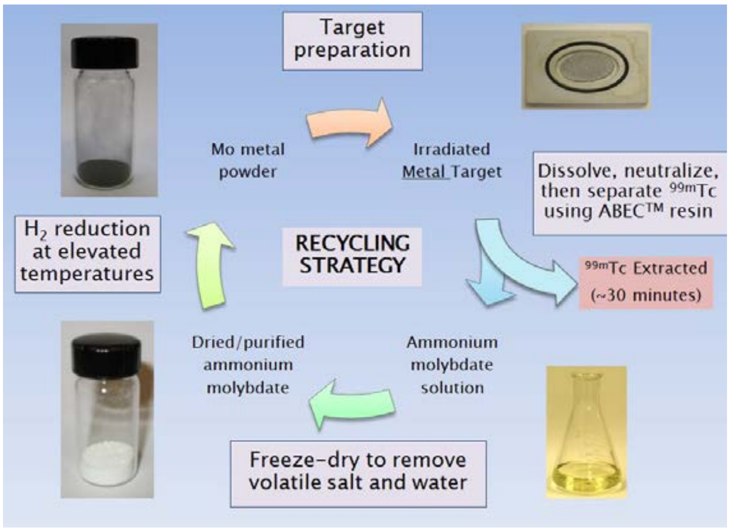

FIG. 6. Summary of the Process Implemented for the Production of ^{99m}*Tc and Recycling of the Enriched* ^{100}*Mo.*

These recycling studies were recently published in Ref [17]; and with further considerations with regards to co-production of radionuclide contaminants ^{96}Nb and ^{97}Nb addressed in [6]. It is expected that the technology developed for this project will provide a platform for reliable large-scale ^{100}Mo recycling. Further assessment of the build-up of chemical, radionuclidic, and isotopic impurities as a function of ^{100}Mo recycling strategy and an assessment of number of times a target can be recycled is ongoing. A dedicated ICP-MS system (allowing for radioactive samples) was purchased to aid in the assessment of these impurities.

4. QUALITY ASSURANCE PROGRAM AND GMP

We will soon seek regulatory approval from Health Canada for cyclotron produced sodium pertechnetate. In this section we will summarize the necessary steps leading to regulatory approval (in Canada) with the goal of providing a template that might be useful in other jurisdictions.

4.1. Engagement of a National Health Regulatory Agency

In order to define the necessary regulations that need to be satisfied we participated in two Health Canada sponsored radiopharmaceutical workshops. One in December 2013 which was general to radiopharmaceuticals (i.e. not just ^{99m}Tc), and one in June 2014 that was specific to alternative production strategies for ^{99m}Tc. During the December workshop, in the session on cyclotron-based ^{99m}Tc, questions regarding radionuclidic purity, validation of radiolabelling, and GMP compliance were brought forward by Health Canada. The June 2014 workshop was a platform whereby the non-reactor-based ^{99m}Tc/^{99}Mo projects from across Canada provided a status update.

Our regulatory initiatives are based in part on the information exchanged in these workshops. On the radionuclidic purity front, we believe the new batches of ^{100}Mo are of adequate purity to minimize the radiation dose to patients from any co-produced byproducts. In accordance with guidelines from Health Canada, the International Conference on Harmonization, the European Medicines Agency, and the Food and Drug Administration, the U of A has implemented a quality by design (QbD) approach to our process validation [20]. The QbD approach is being used for the dissolution, separation chemistry, and ultimately the downstream radiolabelling. We are also developing a quality assurance program which includes a master validation plan addressing not only the ^{99m}Tc production process, but also quality control processes, equipment qualification, environmental monitoring procedures, raw material handling, etc.

4.2. Proposed Release Specifications

The planned release specifications for cyclotron-produced ^{99m}Tc (produced via the ^{100}Mo(p,2n) reaction) in the chemical form of sodium pertechnetate are based on the current sodium pertechnetate for injection chapters in the USP and the Eu Pharm. (USP 38 and Eu Pharm 8.5).

While the USP does not have separate chapters for fission and non-fission derived pertechnetate like the Eu Pharm does, the paragraph about radionuclidic purity specifies two different sets of acceptance criteria based on the production method.

Both compendial sources specify that the sodium pertechnetate injection has to be sterile, and the USP chapter also specifies the bacterial endotoxin limit as 175/V, with V being the maximum recommended dose in mL. The USP stipulates that the sterility test be started on the day of manufacture, which is not possible in Canada due to the unavailability of approved testing labs holding radioactive licenses. The U of A therefore proposes to initiate the sterility test as soon as the sample is decayed. As the maximum recommended dose of sodium pertechnetate is dependent on multiple, difficult-to-control factors such as transportation times and the use of sodium pertechnetate per se or its use in the reformulation of diverse kits, we propose to define the maximum recommended dose as the entire batch volume. The bacterial endotoxin acceptance criterion is < 8.75 EU/mL.

The pH specification in the USP chapter is 4.5-7.5 whereas both Eu Pharm chapters state 4.0-8.0. Both values are in keeping with the traditional pH acceptance ranges for radiopharmaceuticals in the respective jurisdictions. The U of A proposes to use the tighter range of 4.5-7.5 to facilitate product approval in North America as well as Europe.

The aluminum specification in the USP is 10 ppm, while the EuPharm limits it to 5 ppm, and the compendial test methods differ as well. The U of A will again use the tighter acceptance criterion of ≤ 5 ppm, and proposes to use a simplified test method that will have to undergo full method validation to replace the compendial methods.

The radiochemical purity is specified as ≥ 95% in both compendial sources with different test methods. The EuPharm uses a 2 h descending paper chromatography, which seems to be less practical than the USP method, which is based on ascending paper chromatography. The U of A proposes to use an ascending chromatography, which can clearly differentiate between colloids and pertechnetate, and which will be validated with generator-derived pertechnetate as reference material.

Radionuclidic identity is demonstrated through the photopeak of Tc-99m at 140 keV (USP) or 141 keV (Eu Pharm), as the half-life is too long to be used for identification in a pre-release test.

The main deviation from current compendial texts has to be the specification for radionuclidic purity. Most of the potential impurities listed in the USP and the EuPharm are specific to the ^{99}Mo/^{99m}Tc generator production route (such as iodine-131, strontium-98, strontium-90, and ruthenium-103). However, the limit for molybdenum-99 can be used regardless of the production method for pertechnetate. The USP limit is 0.015% of Mo-99, whereas the EuPharm limit is 0.1% Mo-99. As for previous tests, the U of A proposes to adopt the tighter specification of 0.015% Mo-99. Other known impurities for the ^{100}Mo(p,2n) derived pertechnetate are ^{94}Tc (g and m), ^{95}Tc, ^{96}Tc, ^{93m}Tc, ^{93g}Tc, ^{95m}Tc, ^{97m}Tc, ^{96}Nb, and ^{97}Nb. These radioisotopic impurities are most easily controlled through judicious selection of the isotopic impurities in the enriched ^{100}Mo used for the target [1,22]. We have worked with our supplier (Isoflex USA, San Francisco, CA) to achieve an appropriate ^{100}Mo enrichment profile (typical: ^{92}Mo<0.003%, ^{94}Mo<0.003%, ^{95}Mo<0.003%, ^{96}Mo<0.003%, ^{97}Mo<0.003%, ^{98}Mo<0.17%, ^{100}Mo<99.8%). The low amount of the problematic isotopes ^{97}Mo and ^{98}Mo will result in a significant lowering of patient radiation dose [23].

The U of A has proposed individual limits for all those known, identified impurities, with the exception of ^{94m}Tc and ^{94g}Tc, which cannot readily be quantified individually. With the exception of ^{95m}Tc and ^{97m}Tc, all those impurities can be detected and quantified in a pre-release test with a suitable set-up (high-purity Ge detector or equivalent) on a lead-shielded sample. For the two impurities that can only be detected post-release, the usual process validation applies. The individual impurity levels as proposed by U of A (see Table 1) were chosen based on lower detection and quantification limits, and on radiation dosimetry calculations. For all impurities that have a shorter half-life than ^{99m}Tc, the stated specifications have to be met 120 min after the end of bombardment (which is the earliest estimated release time for the lot). For all impurities with a half-life longer than ^{99m}Tc, the stated specifications have to be met at the expiry time of the lot. Validated spreadsheets are used for decay calculations of all identified impurities to either 120 min post EOB, or the expiry time to minimize the time necessary for the test. Both pre-release and post-release radionuclidic purity tests are easy to perform and do not require much time. For the pre-release test, a QC sample of defined ^{99m}Tc content is placed inside a lead shield designed to fully absorb the 140 keV emission of ^{99m}Tc. Once this sample is placed onto the HPGe detector in a defined geometry, acquisition is started. The HPGe detector software then prints an automatic quantitative report, which is used in conjunction with an Excel spreadsheet to automatically calculate and display the radionuclidic impurities. The sample is then stored, and used again for the post-release test, which is identical to the prerelease test, but performed without the lead-shield in place.

The radiation exposure of the patient due to the presence of radionuclidic impurities is dependent not only on the individual impurity and its specific emission, but also on its residence time and biodistribution, which in turn depends on its chemical form [22,24]. For all technetium impurities, it is an acceptable assumption that they are present in the same chemical form as ^{99m}Tc, but for other nuclides such as ^{99}Mo, ^{96}Nb, and ^{97}Nb this assumption is likely untrue. Nevertheless, as there is insufficient information about those biodistribution data, it was assumed that each individual identified impurity shows the same in vivo behaviour as ^{99m}Tc. Another factor to consider is the time-point of injection, since the impurity profile of the same lot of pertechnetate will change over time with the decay of short-lived impurities. Final release specifications will be based on patient dosimetry. Note that radionuclidic impurity specifications listed in Table 1 are useful during the development stage, but that other, simpler tests are likely to be used once we are in routine clinical production.

TABLE 1. DRAFT RADIONUCLIDIC IMPURITY SPECIFICATIONS FOR CYCLOTRON-PRODUCED [^{99m}Tc]TCO$_4$ USED DURING THE DEVELOPMENT STAGE

Specification	Radionuclide
≤ 0.015%	^{99}Mo
≤ 0.02%	^{94}Tc (m+g)
≤ 0.05%	^{95g}Tc
≤ 0.05%	^{96g}Tc
≤ 0.003%	^{93m}Tc
≤ 0.02%	^{93g}Tc
≤ 0.005%	^{96}Nb
≤ 0.001%	^{97}Nb
≤ 0.001%	^{95m}Tc
≤ 0.02%	^{97m}Tc

An additional release specification at U of A is the test for residual ethanol. Due to a multi-use transfer line that is rinsed with ethanol, the ethanol content has to be measured pre-release. U of A proposes to use the standard ≤ 5,000 ppm specification from the USP residual solvent chapter.

5. CLINICAL TRIALS

As of June 2015, the U of A is still the only group globally to have completed a Clinical Trial with cyclotron produced ^{99m}Tc – a critical step towards ensuring market adoption across Canada and the world [18]. This study was performed using [^{99m}Tc]TcO$_4^-$ from the TR19 cyclotron, and included case-matched patients imaged with reactor-based [^{99m}Tc]TcO$_4^-$ (FIG 7). A blinded case-control comparison showed that uptake, clearance, and biodistribution patterns were identical for the two sources of ^{99m}Tc. No hematological or biochemical toxicity was associated with the cyclotron-based injections.

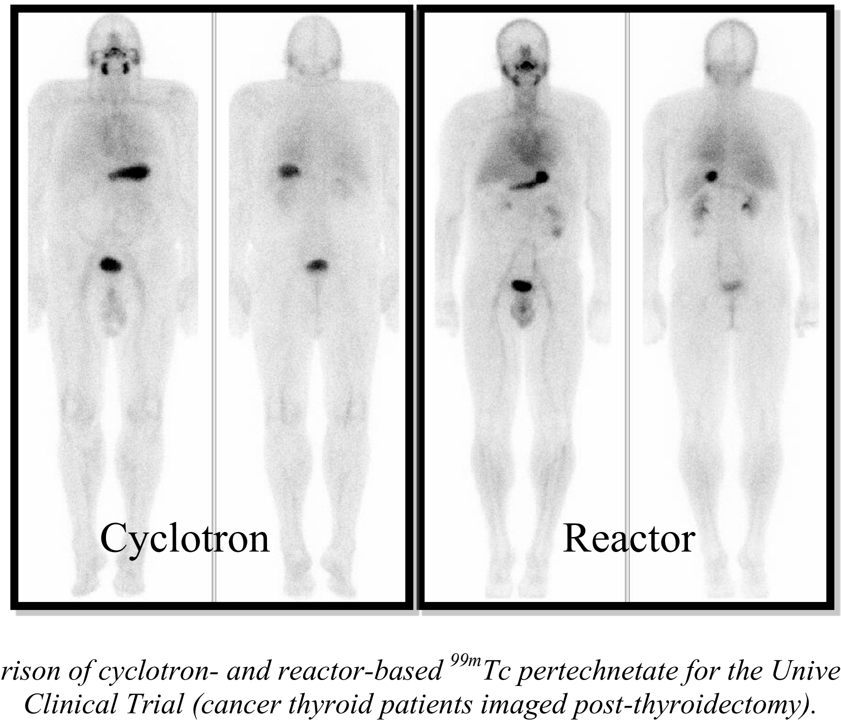

FIG. 7. Comparison of cyclotron- and reactor-based ^{99m}Tc pertechnetate for the University of Alberta Clinical Trial (cancer thyroid patients imaged post-thyroidectomy).

A second trial with ^{99m}Tc produced using a TR24 cyclotron at 24 MeV is currently underway at CHUS [23]. The recruitment of patients receiving cyclotron-produced [^{99m}Tc]TcO_4^- was completed in April 2015, while the recruitment of the case-matched patients in the conventional [^{99m}Tc]TcO_4^- arm of the trial is ongoing (recruited 5 out of 20). Preliminary results showed that the 5 case-matched patients had identical biodistribution patterns for the cyclotron and generator produced radiotracers (FIG 8). Image definition and contrast were equivalent and without particular features allowing discrimination between Tc production methods. No adverse effects were observed.

FIG. 8. Whole-body scans with cyclotron-produced (left) and generator-eluted (right) ^{99m}Tc-pertechnetate for the Centre Hospitalier Universitaire de Sherbrooke clinical trial (suspected Graves' disease for both patients).

5.1. Infrastructure at the University of Alberta for the Production of Clinical Grade $^{99m}TcO_4^-$

A new facility has been recently built at the University of Alberta to house state-of-art GMP radiopharmacy manufacturing rooms, radiopharmaceutical chemistry research labs, cyclotron targetry and engineering labs and a 500 µA 24 MeV cyclotron (TR24 from ACSI) with 4 external beam lines and 2 automated solid-target loading stations.

As part of this facility (Medical Isotope and Cyclotron Facility or MICF, Figure 11), a laboratory was completed and dedicated to target research and development with a focus on solid targets. To facilitate access and integration with cyclotron operations, this laboratory is ideally situated adjacent to the cyclotron operator room, the cyclotron engineering room, and the solid target hotcell room for automated download of irradiated solid targets. General comments on the building layout and major equipment requirements are summarized below to illustrate some of the necessary components for this specialized facility. Where appropriate, construction timelines and equipment commissioning times are shown to provide the reader with some insight into the time necessary to complete a similar project, with the recognition that there will be country to country variations in both building construction and equipment installation and validation.

6. CONSTRUCTION

Construction of the Medical Isotope and Cyclotron Facility (MICF) on the South Campus of the U of A commenced October 2011. Substantial completion of the building (Phase I) was achieved in December of 2012 – i.e. a short 14 months. Although substantial completion of the building was achieved December 2012, several University research labs, as well as additional office and teaching space were not completed until early 2014. These labs offer space for 3 PIs to leverage the unique research and infrastructure opportunities at MICF.

6.1. Key Infrastructure Related to ^{99m}Tc Production

6.1.1. The TR24 Cyclotron

The TR24 variable energy, high-current cyclotron (FIG 9) is located within a concrete bunker on the west side of the building (accessible via a ~2.5 m thick concrete door – FIG 10). This cyclotron has two sets of double "Y" beamlines, thus offering the capability for dual target irradiation using a combination of four target stations. This offers redundancy, as well as the opportunity for simultaneous production of more than one isotope. The cyclotron is equipped with two high-current target stations (FIG 11), each which allows for remote and fully automated mechanical docking/undocking and pneumatic recovery into one of the two shielded cyclotron laboratory hot cells (FIG 12).

FIG. 9. The TR24 cyclotron at MICF (high voltage pit below in open in photo, and one set of "Y" beamlines readily visible on the right).

Approval from Canada's nuclear regulatory agency, the Canadian Nuclear Safety Commission (CNSC) to commission the cyclotron was obtained January 7, 2013. The first extracted beam was achieved March 29, 2013 with scale-up to 500 µA taking place during April and May. Extraction has proven to be limited to ~500 µA, which (after collimator "spill") has led to maximum extended "on-target" irradiation currents of ~420 µA. All radiation field measurements performed around the vault shielding during cyclotron operation were acceptable and within design specifications. Technical challenges associated with this newly designed cyclotron have been largely resolved in the latter months of 2013.

Additional licences that are required for the cyclotron as we move forward include both servicing and operating licences. Our service licence was granted January 2014, and our operating licence was issued June 2014.

FIG. 10. Entrance to concrete bunker is achieved via motorized ~2.5 m thick concrete door.

FIG. 11. One of the two high current target stations at MICF. Having two target stations provides redundancy and reliability for ^{99m}Tc production.

FIG. 12. Solid-target receiving hot cells at MICF for safe handling of high levels of radioactivity. The left hot cell is for automated pneumatic transfer of the irradiated ^{100}Mo target from the cyclotron. The right hot cell is used for dissolving the irradiated ^{99m}Tc/^{100}Mo target.

6.1.2. Target Research and Development Laboratory

In support of the ^{99m}Tc efforts, MICF houses a laboratory dedicated to solid target research and development (FIG 13). This lab is equipped with a 1600˚C tube furnace for target annealing and a 25 ton heated (to ~600˚C) press for bonding of the annealed molybdenum onto a target support plate. The lab is also equipped to reclaim the ^{100}Mo raw material (following chemical separation performed within the building's GMP radiopharmacy). Facilitating access and integration with cyclotron operations, this laboratory is ideally situated adjacent to the cyclotron operator room, the cyclotron engineering room, and the solid target cyclotron hot cell room.

As our approach opts to use molybdenum metal as a target material, molybdate isolation will be performed by lyophilization with subsequent reduction to be performed using our 1100˚C rotary furnace. For characterization purposes, the lab facility is also equipped with a high purity germanium detector that will be used to evaluate the radionuclidic purity of both the ^{99m}Tc product and the recycled ^{100}Mo. This lab will also house an ICP-MS unit that can be used for assessing the ^{99m}Tc specific activity, as well as the isotopic composition of the enriched ^{100}Mo target material.

FIG. 13. MICF target development lab showing heated press (left), rotary furnace (far counter straight ahead), sintering furnace (free standing under large ventilation system), and two fume hoods.

6.1.3. GMP Radiopharmacy

The GMP radiopharmacy contains a series of rooms and areas designed with different air classifications (from unclassified through to Class B). Each room is dedicated for preparation of radiopharmaceuticals using different types or classes of isotopes (e.g. ^{99m}Tc, ^{18}F, radioiodine, therapeutic isotopes, etc.). One of the rooms is dedicated to the isolation of ^{99m}Tc from the irradiated ^{100}Mo target material (FIG 14). The goal of the activities in this room is to isolate a ^{99m}Tc product that is equivalent to that which is obtained using the conventional reactor-based ^{99}Mo/^{99m}Tc generator. The hot cells in this room are currently equipped with four automated chemistry units (Neptis, ORA, Rue de la Gendarmerie 50/B – 5600 Philippeville – Belgium).

Selection of Neptis was based on a comparison of multiple units (described in further detail below in the R&D section). The infrastructure at U of A now consists of four identical Neptis units which will be used to demonstrate reliable daily production over a four month period as well as for validation studies in preparation of our Health Canada New Drug Submission.

FIG. 14. The GMP laboratory dedicated to separation of the ^{99m}Tc from the irradiated and dissolved ^{100}Mo target material. A Neptis automated chemistry unit can be seen in the upper-right hot cell.

6.1.4. Quality Control (QC) Instrumentation

For characterization purposes, we have acquired significant analytical testing equipment for assessing and optimizing the quality of the cyclotron-based ^{99m}Tc product. Several of these pieces of equipment would not normally be required for a standard radiopharmacy, but are critical for process development and optimization purposes. Instrumentation available at MICF for characterizing the ^{99m}Tc quality includes, but is not limited to, a high purity germanium detector (to assess radionuclidic purity), a TOC analyzer (to assess leachable organic carbon from the solid phase extraction resin), an ICP-MS (to assess isotopic composition of the molybdenum target material), an ICP-OES (to assess chemical composition of the ^{99m}Tc product), a TLC reader (to assess radiochemical purity of the ^{99m}Tc product and/or ^{99m}Tc labelled radiopharmaceutical), an endotoxin tester (to ensure endotoxin levels in the ^{99m}Tc product are within safe limits for injection), and so on. For regulatory purposes, we are in the process of implementing a strict quality assurance program to ensure this critical instrumentation undergoes rigorous and continued qualification testing.

6.1.5. Unique Access and Purpose-Built Design

There are several unique design features of MICF that greatly enhance the accessibility and facilitate future flexibility of infrastructure modification at this facility. These include, but are not limited to, an access corridor (behind the 8 existing hot cells that line the cyclotron corridor), a trap-door above the single standalone hot cell (for which rear access is not possible), and access to all labs and GMP/radiopharmacy space from above via the 2nd floor interstitial space. Expansion opportunity was also planned in this facility in the context of hot cells, with mechanical and electrical services in place for an additional nine hot cells within the building.

6.1.6. Research and Teaching Space

In addition to the target development laboratory for cyclotron target research, and the GMP radiopharmacy space, which provides a platform for translation of new radiopharmaceuticals from the bench into clinic, MICF also includes organic chemistry facilities for precursor synthesis and development, as well as three radiochemistry labs for research and teaching. Administrative space requirements at MICF are modest and additional teaching/training areas (e.g. classrooms, workstations, etc.) exist to augment the capabilities of the facility for the U of A in building training capacity for highly qualified personnel.

7. STATUS OF THE ^{99M}TC PROGRAM AT THE UNIVERSITY OF ALBERTA

The U of A and its partners have completed the optimization process for Tc production, Tc/Mo separation and, under GMP conditions, are finalizing the pertechnetate manufacturing processes. To aid on our application to Health Canada, we have completed one clinical trial (2012) and are about halfway through a second trial (CHUS). Our application will be augmented with the submission of all applicable SOPs, process specification for the manufacturing of $^{99m}TcO_4$ in a Neptis automated synthesizer and all QA/QC pre- and post-release specifications.

We are currently exploring the commercial scale-up of target manufacturing under appropriate ISO standards to produce reliable and cost-effective solution for the cyclotron production of ^{99m}Tc.

Acknowledgements

The work presented in this document was made possible through the collaborative efforts of our partners at CHUS and ACSI and through financial support from the Government of Canada: the Non-reactor-based Isotope Supply Contribution Program, Isotope Technology Acceleration Program, Western Economic Diversification, and the Western Economic Partnership Agreement; from the Government of Alberta: Alberta Innovates; and from the University of Alberta.

References

(manuscripts, abstracts and conference presentations)

[1] GAGNON, K., Cyclotron Production of Technetium-99m, University of Alberta PhD Thesis, (2012).

[2] GUÉRIN, B., et al., Cyclotron production of ^{99m}Tc: An approach to the medical isotope crisis, J. Nucl. Med. **51** (2010) 13N–16N.

[3] BEAVER, J., HUPF, H., Production of ^{99m}Tc on a medical cyclotron: a feasibility study, J. Nucl. Med. **12** (1971) 739–741.

[4] GAGNON, K., et al., Cyclotron production of ^{99m}Tc via the ^{100}Mo(p,2n)^{99m}Tc reaction, 13th International Workshop on Targetry and Target Chemistry, Roskilde, Denmark, July (2010).

[5] GAGNON, K., et al., Cyclotron production of ^{99m}Tc: experimental measurement of the ^{100}Mo(p,x)^{99}Mo, ^{99m}Tc, and ^{99g}Tc excitation functions from 8 to 18 MeV, Nucl. Med. Biol. **38** (2011) 907–916.

[6] GAGNON K., et al., Letter to the Editor: Experimental cross section measurements for the ^{100}Mo(p,x)^{101}Tc, ^{96}Nb, and ^{97}Nb reactions in the energy range of 10 to 18 MeV, *Nucl. Med. Biol.* (2012), 39:923–925.

[7] AVILA-RODRIGUEZ, M.A., et al., Proceedings of the COMSOL Conference, (2007) 359.

[8] GAGNON, K., et al., Thermal modelling of a solid cyclotron target using finite element analysis: An experimental validation. Presented at the 13th International Workshop on Targetry and Target Chemistry, Roskilde, Denmark, July 2010.

[9] AVILA-RODRIGUEZ, M.A., et al., The use of radiochromic films to measure and analyze the beam profile of charged particle accelerators, Appl Radiat Isot. **67** (2009) 2025-2028.

[10] CHANG, C.T., et al., Confined single- and multiple-jet impingement heat transfer—I. Turbulent submerged liquid jets, Int. J. Heat Mass Transfer **38** (1995) 833.

[11] GAGNON, K., et al., Target preparation and recycling of molybdenum for the cyclotron production of ^{99m}Tc, Oral presentation at the 19th International Symposium on Radiopharmaceutical Sciences, Amsterdam, Aug 28-Sept 2, 2011.

[12] WILSON, J., et al., Target preparation and recycling molybdenum for the cyclotron production of ^{99m}Tc (US Patent filed April 2012).

[13] THOMAS, B.A., et al., Solid ^{100}Mo target preparation using cold rolling and diffusion bonding, Presented at the 15th International Workshop on Targetry and Target Chemistry, Prague, August 2014.

[14] ANDERSSON, J.D., et al., Separation of molybdenum and technetium. Presented at the 14th International Workshop on Targetry and Target Chemistry, Mexico, August 2012.

[15] ANDERSSON, J.D., et al., Tentagel® as chromatography media for processing cyclotron produced ^{99m}Tc. Poster presentation at the Annual Meeting of the Society of Nuclear Medicine and Molecular Imaging, Vancouver, BC, June 2013.

[16] ANDERSSON, J.D., et al., Separation of TcO_4^- and MoO_4^{2-} using a PEG coated C18 SPE cartridge. Poster presentation at the Annual Meeting of the Society of Nuclear Medicine and Molecular Imaging, Vancouver, BC, June 2013.

[17] GAGNON K., et al., Cyclotron production of ^{99m}Tc: Recycling of enriched ^{100}Mo metal targets, Applied Radiation and Isotopes, 70 (2012) 1685–1690.

[18] A.J.B. McEwan, S. McQuarrie, D. Abrams, K. Gagnon, J. Wilson, E. Turcotte, B. Guerin, R. Lecomte, Technetium-99m (Tc-99m) pertechnetate (TcO_4^-) imaging with cyclotron produced Tc-99m compared with generator Tc-99m. Society of Nuclear Medicine Meeting, June, (2012) Miami, Florida

[19] SELIVANOVA S.V., et al., Clinical quality sodium pertechnetate Tc-99m is reached with cyclotron at 24 MeV, 27th Annual Congress of the European Association of Nuclear Medicine, October 18-22, 2014, Gothenburg, Sweden

[20] ANDERSSON, J.D., et al., An initial quality by design (QbD) case study: Critical process parameter screening experiments for processing of cyclotron produced ^{99m}Tc. Submitted to the Annual Congress of the European Association of Nuclear Medicine, October 2014, Gothenburg, Sweden.

[21] SELIVANOVA S.V., et al., Isotopic purity of ^{100}Mo target is paramount for cyclotron production of clinical quality ^{99m}Tc, American Chemical Society 248th National Meeting, August 2014, San Francisco, CA, USA.

[22] SELIVANOVA S.V., et al., Radiation dose from cyclotron-produced ^{99m}Tc-radiopharmaceuticals based on their experimentally determined isotopic composition, Symposium on Technetium and Other Radiometals in Chemistry and Medicine (TERACHEM 2014), September 10-13, Bressanone, Italy. Nuclear Medicine and Biology **41 (7)** (2014) 649.

[23] SELIVANOVA S.V., et al., Phase I clinical trial using sodium pertechnetate ^{99m}Tc produced by medium-energy cyclotron. Society of Nuclear Medicine Meeting, June 6-10, 2015, Baltimore, MD, USA, Journal of Nuclear Medicine **56** (supplement 3) (2015) 475.

[24] SELIVANOVA S.V., et al., Radioisotopic purity of sodium pertechnetate ^{99m}Tc produced with a medium-energy cyclotron: implications for internal radiation dose, image quality, and release specifications, Journal of Nuclear Medicine 56 (10) 2015 1600-1608.

A COMPLETE SOLUTION TO PRODUCING ^{99M}Tc VIA PROTON BOMBARDMENT OF ^{100}Mo

THOMAS J. RUTH

TRIUMF and the British Columbia Cancer Agency
Vancouver, Canada

Abstract

The production of ^{99m}Tc via the ^{100}Mo(p,2n) reaction has been developed to the point of going into Clinical Trials with the ultimate goal of using the cyclotron produced ^{99m}Tc (CPTc) in clinical practice as an adjunct to generator ^{99m}Tc. The entire cycle of target production, irradiation, chemical separation, recovery of target material and preparation of targets using the recycled ^{100}Mo have been performed. In addition theoretical calculations for the excitation functions for (p,n), (p,2n) and (p,3n) reactions were performed covering the energy range from 6 MeV up to 24 MeV. Based on these results the production of the various Tc-isotopes was performed using standard commercially available ^{100}Mo enrichments including the distributions of accompanying Mo-isotopes. These results were used to estimate the radiation dosimetry for several radiopharmaceuticals using commercial kits in comparison to generator produced ^{99m}Tc.These results have been published in peer reviewed papers.

This process approach was established for two types of cyclotrons, the 16.5 MeV PETtrace from GE Healthcare and an ACSI 19 MeV TR19 cyclotron. A TR30 cyclotron operating at 24 MeV has been used to measure yields of ^{99m}Tc at this higher energy as well as co-produced Tc-isotopes that may contribute to increased radiation dosimetry to the patient depending upon the Mo target composition and irradiation conditions.

To date we have produced greater than 9 Ci of ^{99m}Tc on the TR19 cyclotron multiple times as well as 4.7 Ci at 16.5 MeV and >32 Ci at 24 MeV.

We have developed a simple ion-chamber based quality control protocol that will provide a *go/no-go* decision that will enable the producer/end user to decide on the use of the ^{99m}Tc radiopharmaceutical based on potential increases in radiation dose due to contributing Tc-isotopes.

Thus we have developed a production process following GMP procedures and have published multiple papers documenting and validating our approach.

1. INTRODUCTION

Feasibility of cyclotron production of ^{99m}Tc via the ^{100}Mo(p,2n)^{99m}Tc reaction was demonstrated in the early seventies [1]. Subsequently, a number of theoretical and experimental studies investigated cross sections, yields, as well as other aspects of accelerator-based isotope production [2-5](see for example: Sholten et al. 1999, Takacs et al. 2003, Gagnon et al 2011, Qaim, et al.).

The Government of Canada funded three projects based on accelerators to investigate the commercial production of ^{99}Mo and/or ^{99m}Tc. One was based on the photo transmutation of ^{100}Mo into ^{99}Mo (^{100}Mo(γ,n)^{99}Mo) and two based on proton irradiation of ^{100}Mo to produce ^{99m}Tc directly (via ^{100}Mo(p,2n)^{99m}Tc). One of the cyclotron teams involved collaborations between the University of Alberta, the University of Sherbrooke and Advanced Cyclotron Systems, Incorporated (ACSI, Richmond, BC, Canada). The other team is a collaboration amongst TRIUMF, British Columbia Cancer Agency, the University of British Columbia, all in Vancouver; the Lawson Health Research Institute in London, Ontario and the Centre for Probe Development and Commercialization (CPDC) in Hamilton, Ontario. The TRIUMF consortium aimed to investigate the feasibility of using existing PET cyclotrons as the platform.

Overall Technical Goals for Cyclotron-based Production included:

- Establish optimal irradiation conditions to maximize yield and purity which involves defining the beam energy range (effecting yield and purity), current (which effects yield)
- Target characteristics (the enrichment of ^{100}Mo, the isotopic composition of other Mo isotopes which will impact purity, establish the target plate capable of being irradiated at high power (beam current and energy), the encapsulation of the target to enable target transfer, and establish the ability to recycle the enriched ^{100}Mo)
- The optimal time of irradiation will impact the production
- Establish a reliable, high yielding chemical separation system that could operate under Good Manufacturing Processes (GMP)
- Define the operating parameters for a complete production system including Quality Control procedures

2. SPECIFIC GOALS

In addition to performing theoretical calculations and determining excitation functions for the possible radionuclides from the irradiation of Mo isotopes the actual production quantities of ^{99m}Tc needed to be established under production conditions. The production rates for ^{99m}Tc, the mix of impurities that are coproduced need to be identified and quantified. These results will impact the shelf-life and ultimately radiation dosimetry associated with this approach.

The ability to label certain radiopharmaceutical kits is highly dependent upon the specific activity of the ^{99m}Tc (the ratio of ^{99m}Tc to all Tc –isotopes including ^{99g}Tc).

The radionuclide mix in the production of ^{99m}Tc has implications in production and disposal of waste, in recycling the enriched ^{100}Mo target material and patient radiation dose that could be associated with any radionuclidic impurities in the final radiopharmaceutical product.

The US Pharmacopeia defines ^{99m}Tc as being derived from fission produced ^{99}Mo while the European Pharmacopeia includes the production of ^{99}Mo by other routes such as the ^{98}Mo(n,γ)^{99}Mo reaction. Thus to allow acceptance of the cyclotron produced ^{99m}Tc, the regulatory authorities have to understand the implications of the quality of cyclotron produced material on the safety and diagnostic efficacy for the patient.

With all of these parameters in mind the production specifications need to be established which define the energy range, length of irradiation, establishing transport criteria, the shelf-life, and the protocol for recycling of target materials.

Ultimately whether this approach will be adopted into widespread use will depend upon the economic factors associated with providing healthcare.

For these studies the aim was to demonstrate that existing medical cyclotrons could be used to produce sufficient quantities of ^{99m}Tc to be commercially viable. We chose two platforms, the 16.5 MeV for the GE PETtrace and 18 MeV for the ACSI TR-19 cyclotrons, both of which are widely available throughout the world. See Figure 1. Although IBA 18 MeV cyclotrons were not involved in the program, they could be configured to produce ^{99m}Tc in a similar manner as were the TR cyclotrons.

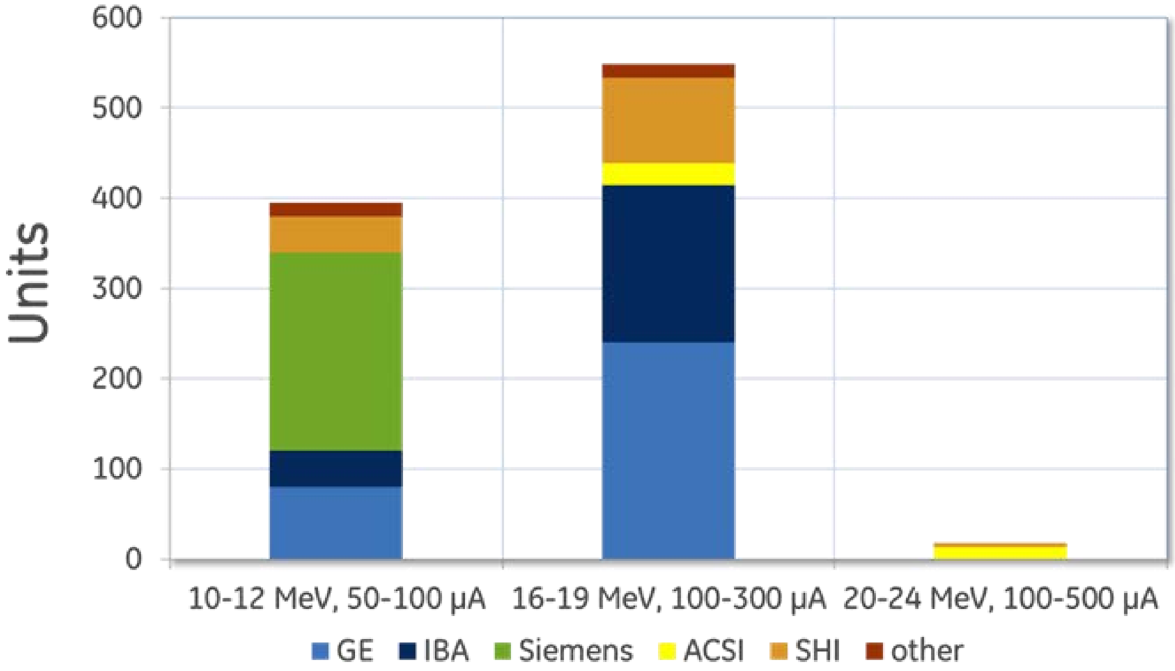

FIG. 1. This graph illustrates the number of cyclotrons of various extracted beam energies attributed to the respective manufacturer; Data from cyclotron survey conducted by D. Schlyer 2013.

Only cyclotrons with proton beam energies greater than 16 MeV are considered since the yield below 15 MeV [4] does not allow for widespread distribution. That said such low energy machines. That said, such machines may have potential for local production.

3. FINAL REPORT, JUNE 2015

Over the period of the program we have finalized target production process for the TR19 [6] and PETtrace cyclotrons [7] as well as completing the target transfer capsules for these systems [8]. The TR19 target is based on a slanted target while the PETtrace uses an orthogonal target due to space constraints.

The target preparation for the TR19 makes use of electrophoretic [6] approach to deposit the molybdenum metal on a tantalum metal surface followed by sintering at 1700 C. The process involves using fine grain molybdenum powder suspended in a polar organic solvent, stirring vigorously while applying the voltage with the target plate serving as the cathode. After coating the Ta foil, it is allowed to air dry and then sintered. This approach produces a robust target that has been tested to 450 µA (theoretical thermal calculations indicate that he target should be capable of withstanding greater than 500 µA). The porous nature of the target allows for it to easily dissolve in peroxide as described below.

FIG. 2. The top photo shows the aluminum target capsule for holding the ^{100}M plate on a tantalum backing. The capsule serves as the transfer module as well as the dissolution chamber for dissolving the Mo plate from its backing. This target system was used with the TR19 cyclotron where 240 μA average proton beam current (peak value of 260 μA) of 18 MeV protons yielded 9.4 Ci (348 Gbq) following an irradiation for 6 hours. The theoretical yield at 300 μA is 15.4 Ci (570 Gbq).

FIG. 3. The target plate shown in this photograph shows a ^{100}Mo plate irradiated with 450 μA beam of 24 MeV protons for 6 hours. The yield was greater than 32 Ci (1.2 TBq). A TR30 cyclotron was used since the TRIUMF team does not have a 24 MeV cyclotron.

The PETtrace target is manufactured by pressing and sintering a Mo metal disc followed by brazing on to a copper backing. This target has been tested to 130 μA.

FIG. 4. The top picture shows the transfer capsule for the ^{100}Mo target shown in the lower photo. This type target has been irradiated at 130 µA for 6 h on the PETtrace cyclotron which delivers 16.5 MeV protons. The recovered yield was 4.7 Ci (174 GBq) compared to the theoretical yield of 4.9 Ci (181 GBq) [7].

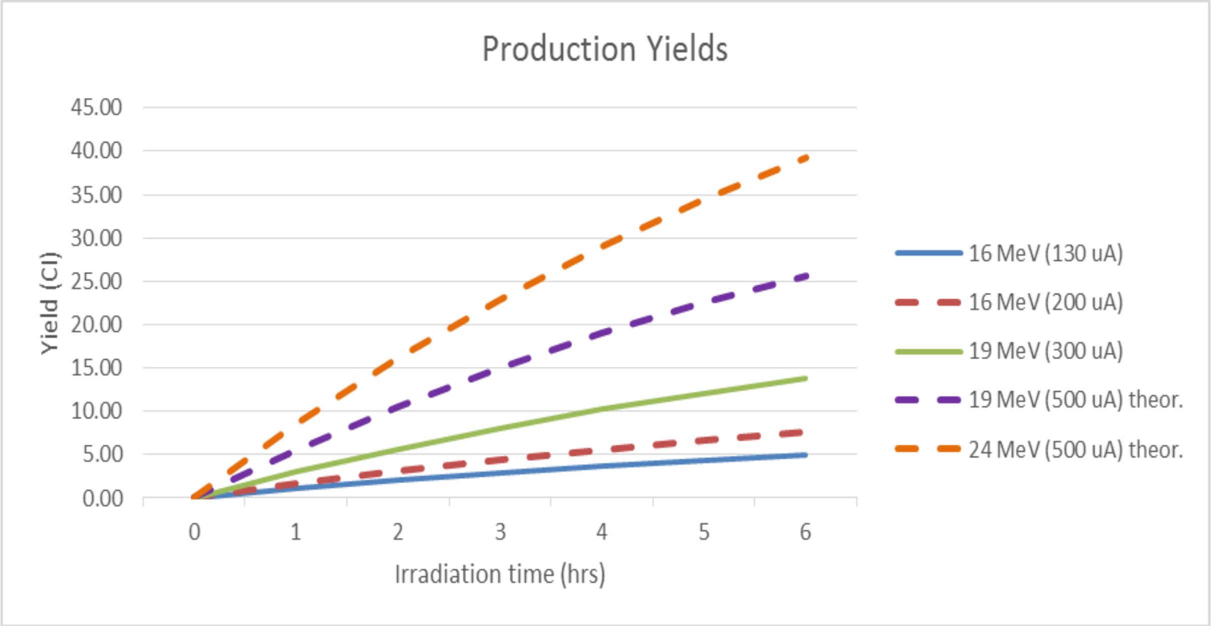

FIG. 5. This illustrates the yield of ^{99m}Tc as a function of energy and beam current. Clearly for a particular cyclotron (energy) the beam current is the crucial parameter.

Using these targets we have produced multicurie quantities of ^{99m}Tc multiple times and have followed the decay over several days to ascertain the composition of the Tc-isotopic mix. The actual mix of Tc-isotopes is highly dependent upon the isotopic composition of the Mo target material. In Table I below is a list of Tc-isotopes that can be produced during irradiation of ^{100}Mo targets which contain varying amounts of other Mo-isotopes depending upon the enrichment of ^{100}Mo. As discussed later the impact on radiation dosimetry and image quality was assessed.

TABLE 1. Tc-ISOTOPES PRODUCED IN THE PROTON BOMBARDMENT OF Mo TARGET MATERIAL. ALSO LISTED IS THE RADIATION DOSIMETRY ASSOCIATED WITH EACH OF THESE ISOTOPES.

Tc isotope	**Half-life**	**Emission energies (intensity) (keV (%))**	**Patient Dose Sv/MBq)**	**Remarks**
^{93m}Tc	43.5min	511 (4.5); 2644.58 (14.3)	8.73	Not considered in imaging study because of short half-life.
^{93g}Tc	2.75h	1362.9(66.2); 1520.3 (24.4)	7.82	Considered in imaging study
^{94m}Tc	52min	511(140); 871(94.2)	51	Not considered in imaging study because of short half-life.
^{94g}Tc	4.88h	702.7 (99.6); 849.7 (95.7); 871.1 (99.9)	96.6	Considered in imaging study
^{95m}Tc	61d	204.1(63.2); 582.1(30); 835.2 (26.6)	187	Considered in imaging study
^{95g}Tc	20d	765.8 (93.8)	77.7	Considered in imaging study
^{96m}Tc	51.5min	1200.2 (1.1)	1.79	Not considered in imaging study because of short half-life and weak gamma emission.
^{96g}Tc	4.28d	778.1 (99.8); 812.5 (82); 849.9 (98); 1126.9 (15.2)	446.0	Considered in imaging study; The worst impurity which highly increases patient dose.
^{97m}Tc	91d	96.5 (3)	145	Not considered in imaging study Gamma has low energy cannot be detected in 140 keV window.

As part of our efforts to understand production parameters we have operated the TR19 at >200 μA on target for more than 6 hours with a peak beam current of 260 μA. During this 6 hour run we have lowered the beam current to 200 μA on the Mo target while running 60 μA on a standard water target for ^{18}F production demonstrating that those facilities with dual beam capability can produce ^{99m}Tc without interfering with their PET radionuclide production program. It should be noted that the beam currents indicated here are not limitations. The TR19 has been modified to be capable of extracting 300 μA. Once this level has been established routinely we will move to this higher level.

4. CHEMISTRY

The target transfer capsule has been designed to not only hold the target plate during transfer between hot cell and cyclotron but to also serve as the dissolution vessel. The electrophoretic plated targets are porous in nature and can be dissolved from the tantalum backing with the addition H_2O_2 [8]. The solution is transferred from the target vessel and further prepared by drying and dissolving in 4N NaOH base before adding to a pegylated ion column [9] where the pertechnetate is trapped allowing molybdate and other ions to pass through to the waste. The pertechnetate is eluted with water.

The eluted pertechnetate is trapped on an alumina column which will trap any molybdate. Following elution with saline we have found a chemically pure Tc product [8, 10]. Colorimetric assays determined the levels of alumina and molybdenum. Depending upon the isotopic composition of the Mo target material will dictate the Tc-isotopic impurities as indicated above.

The molybdate in the waste solution can be purified via ion exchange and reduced to metal powder suitable for introduction into the electrophoretic plating system by temperature stepped hydrogen reduction. To date we have demonstrated a recovery efficiency of 93% with a range of 91-95%. This was for a small number of relatively small samples and expect the efficiency will be higher for bulk solutions. While the recovered molybdenum was chemically pure we have not determined the isotopic composition of the Mo. However expectations are that this will not be different from the starting material at the level of production we anticipate.

The initial automated chemistry was designed and built in-house [10]. However recognising the need to have a system that will meet GMP specifications we have engaged a commercial partner to prepare a chemistry system that will use disposable units as illustrated in the figure below.

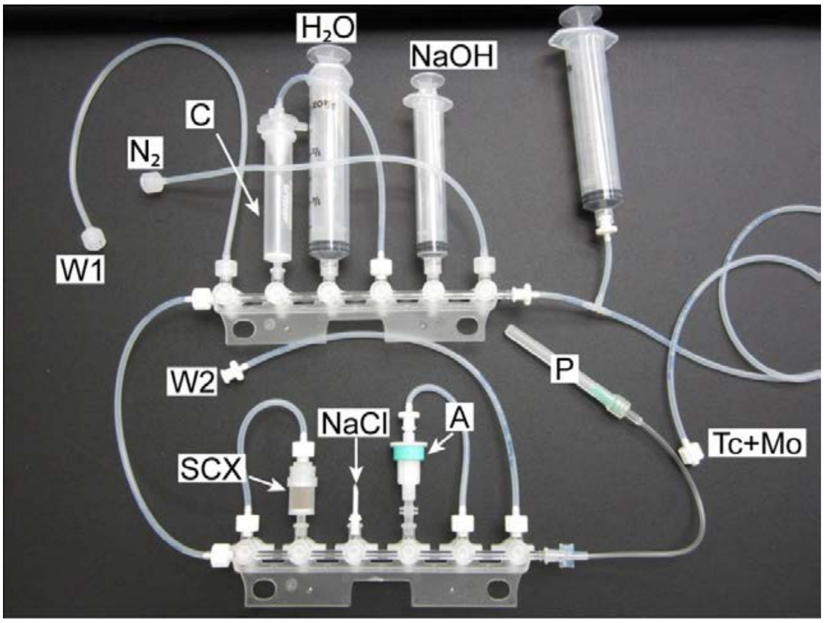

FIG. 6. An example of a disposable reagent kit for the separation and isolation of ^{99m}*Tc [8].*

Shown in Figure 6 are the components used for the automated purification system. The two syringes at the top are initially filled with water (H_2O) and sodium hydroxide 4N NaOH. The raw target dissolution is loaded via the *luer* connector labeled 'Tc+Mo'. The ChemMatrix resin (C) is in a standard solid phase separation reservoir. Nitrogen is connected to one end of the kit (N_2). The two waste vessels are indicated as W1 (molybdate recovery) and W2. The strong cation exchange resin (SCX), the sodium chloride vial (NaCl), the alumina column (A) completes the kit. The product is eluted at location 'P', normally through a 0.22 µm filter.

The processing time is less than 90 minutes with an efficiency of 92.7 ± 1.1%. The resulting radiochemical purity is >99.99% as TcO_4^-. Analysis for trace impurities indicate that there is <10 Bq ^{99}Mo and < 5 ppm of Al^{3+}. There is no evidence of non-Tc impurities. The fluid path is disposable consistent with GMP.

We have labeled cold radiopharmaceutial kits (acidic, basic and neutral) with cyclotron produced ^{99m}Tc and found that they labeled well and the labeled radiopharmaceutcals met the quality criteria.

5. CLINICAL TRIALS

In preparation for an application for a Clinical Trial in human subjects we have completed a Good Laboratory Practice preclinical study in rodents, finalized the GMP production process and are in the process of defining the acceptance criteria for molybdenum enrichment including all Mo isotopes as well as defining the irradiation parameters.

The enrichment and irradiation parameters are interconnected and should not be considered separately. Also the conditions will impact the shelf-life and the patient radiation dose. Our goal is keep the radiation dose increase to ≤ 10% when compared to ^{99m}Tc eluted from a generator.

6. RADIATION DOSIMETRY

In order to have the cyclotron approached adopted for routine use several aspects had to be addressed which included the impact on radiation dosimetry to patients, the impact on image analysis and interpretation as well as the QC protocols that addresses the overall safety of the produced ^{99m}Tc including indirectly the above concerns.

7. ASSESSMENT OF RADIATION DOSE

Using ^{100}Mo targets with the following compositions (Table II) the quantity of Tc-isotopes produced was determined in relationship to that of ^{99m}Tc [11].

TABLE 2. ^{100}Mo TARGETS ALONG WITH THE OTHER Mo-ISOTOPES.

Target	Mo92	Mo94	Mo95	Mo96	Mo97	Mo98	Mo100
Batch A	0.08	0.07	0.09	0.11	0.08	0.51	99.03
Batch B	0.003	0.003	0.003	0.003	0.003	0.17	99.815

Figure 7 illustrates the ratio of Tc-impurities relative to ^{99m}Tc.

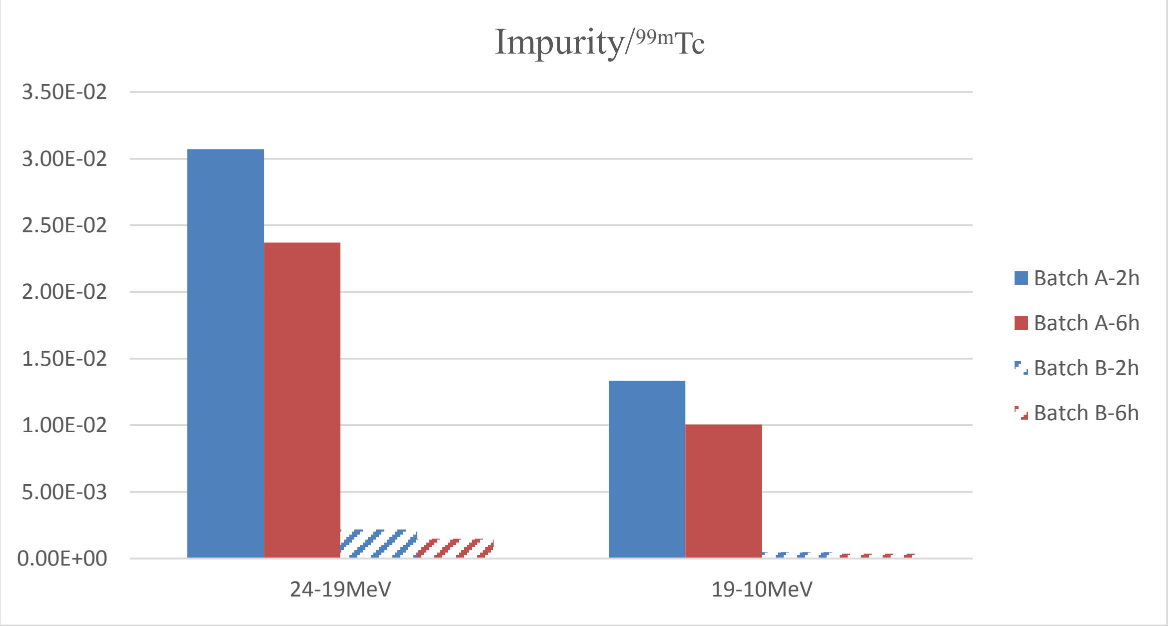

FIG. 7. Relative increase in patient dosimetry based on the Tc-isotopic impurities produced using Mo targets with the Mo-isotopic distribution as presented in Table II. The effect of the length of bombardment is also illustrated.

It is significant to note that both targets contain over 99% ^{100}Mo. However Batch A has an isotopic distribution for $^{92-98}$Mo that results in unacceptable increases in radiation dose over all energy ranges but particularly above 20 MeV, while Batch B yields very low dose increases. These results were used to guide us in proposing the specifications for ^{100}Mo targets shown in Table IV.

8. IMPACT ON IMAGE DATA

In order to determine the impact of higher energy photons associated with the Tc-isotope impurities phantom studies were perform. Point spread function were determine from line sources imaged with a standard clinical SPECT camera. The line source were filled with equivalent quantities of ^{99m}Tc as produced form a clinical ^{99}Mo/^{99m}Tc generator and from cyclotron production using a target composed of high purity ^{100}Mo.

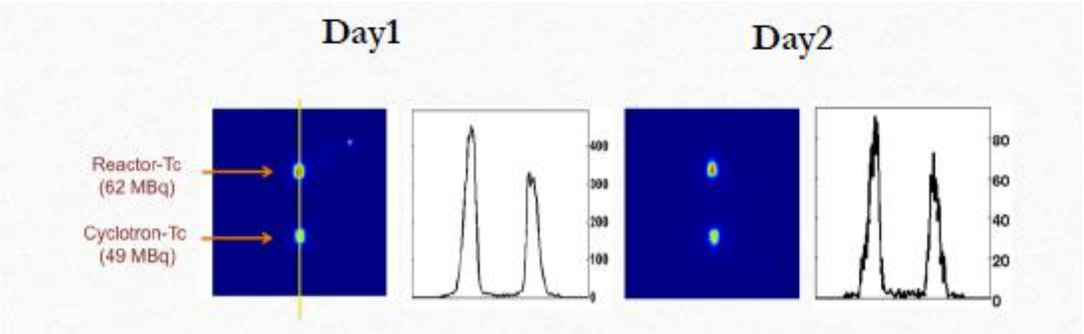

FIG. 8. Line spread functions for ^{99m}Tc produced form generators in comparison to cyclotron produced ^{99m}Tc. See text.

The profiles were measured on two separate days to emphasize the possible influence of longer lived Tc-isotopes which emit higher (>500 keV) energy photons. It is clear that there is no measurable difference between generator ^{99m}Tc and cyclotron ^{99m}Tc, even after 24 hour decay.

9. QUICK RELEASE BASED ON DOSE CALIBRATOR ASSESSMENT

9.1. Overview

We have developed a simple and fast dose-calibrator-based method for measuring γ emission rates from Tc impurities per MBq of ^{99m}Tc. While our approach does not enable direct estimation of the activity of *each* Tc impurity, it does provide a direct measurement of γ emission rates from impurities, which can be used to estimate radiation dose increases (relative to pure ^{99m}Tc) to patients injected with cyclotron produced ^{99m}Tc (CPTc)-based radiopharmaceuticals, and could be used in place of routine γ spectroscopy to rapidly estimate the levels of radionuclidic impurities present in CPTc samples.

9.2. Challenges for quick-release testing of the RNP of cyclotron-produced ^{99m}Tc

It is important to develop simple product release tests to ensure that, for every cyclotron-produced ^{99m}Tc (CPTc) batch, patient radiation dose remains below acceptable levels. This is a challenging task because it requires detection of minute quantities of radioactive Tc impurities in the presence of much higher ^{99m}Tc activities. Since radioactive Tc isotopes can be identified by their gamma (γ) emissions, γ spectroscopy has been used to determine RNP in proof-of-principle studies [4, 8, 12, 13]. However, the overwhelming presence of ^{99m}Tc and the count-rate limitations of γ spectroscopy systems preclude fast, accurate, and precise measurement of small amounts of Tc impurities; in practice, determining RNP by γ spectroscopy requires analyzing multiple spectra acquired over many days [8]. An alternative approach would be to acquire emission spectra of CPTc samples encapsulated by a lead shield. This would reduce count rates by attenuating 140-keV photons emitted from ^{99m}Tc while at the same time transmitting high-energy (>500 keV) photons emitted from impurities. However, spectrum analysis would remain non-trivial because in some cases two different Tc isotopes emit photons with the same energy (e.g. ^{94g}Tc and ^{96g}Tc both emit 850-keV photons) and most isotopes emit multiple photons. Due to the complexity of the resulting γ emission spectra and analysis thereof, we opted for a simpler solution.

9.3. Solution: A dose-calibrator-based quick-release test

We have developed a method that only requires two dose calibrator readings: one DC reading of a CPTc source placed in a lead shield is compared to a second reading of the same source in air. Since DCs are sensitive to a large range of activities, the in-air and in-lead readings are sensitive and insensitive to ^{99m}Tc, respectively, while both measurements are sensitive to impurities. A similar methodology is used to identify ^{99}Mo contamination in generator-produced ^{99m}Tc [14, 15], and ^{124}I and ^{64}Cu contamination in cyclotron-produced ^{123}I and ^{67}Cu, respectively [16, 17].

A challenge with this approach is that DCs are not energy-discriminators. Therefore, the activity a particular Tc impurity cannot be estimated from knowledge of its γ emission energies. At best, the total activity of all Tc impurities may be estimated. However, even this is challenging because it would require knowledge of the DC dial setting for Tc impurities. Choosing the appropriate dial setting would require a-priori knowledge of the relative abundance of each Tc impurity, which is highly sensitive to changes in production conditions. This presents a situation where one needs to know what she or he is measuring prior to measuring it.

However, while the relative abundance of each Tc impurity may change from one production to the next, the γ emission energies will not. Furthermore, the average emission energies for most of the Tc impurities that are expected to be present in QC samples are tightly grouped in the 700 keV to 830 keV range. We have demonstrated both experimentally and theoretically that the ratio of in-lead to in-air readings is linearly related to γ emission rates from Tc impurities per MBq of ^{99m}Tc over a large range of clinically-relevant production conditions. Importantly, the constant of proportionality relating the ratio of in-lead to in-air readings to the γ emission rates from Tc impurities per MBq of ^{99m}Tc is relatively insensitive to changes in production conditions, and therefore does not require a-priori knowledge of the Tc impurity profile. In practice, this constant of proportionality needs to be determined by acquiring in-lead and in-air DC readings of CPTc sample(s) with known γ emission rate(s). In addition to the DC readings, this would require estimating the γ emission rates by (for example) γ spectroscopy for one (or a few) calibration batches. The resulting calibration curve could then be used for all subsequent DC readings.

We have demonstrated DC-based estimates of the γ emission rates from Tc impurities per MBq of ^{99m}Tc are highly sensitive to the presence of ^{93g}Tc, ^{93m}Tc, ^{94g}Tc, ^{94m}Tc, ^{95m}Tc, ^{95g}Tc, and ^{96g}Tc, which are the primary contributors to increases in radiation dose (relative to pure ^{99m}Tc) to patients injected with CPTc-based radiopharmaceuticals.

9.4. Dosimetry-based release criteria

Patient radiation dose from ^{99m}Tc impurities relative to that from ^{99m}Tc can be estimated directly from the γ emission rates from Tc impurities per MBq of ^{99m}Tc. *This enables establishing dosimetry-based clinical-release criteria that can be tested using commercially-available dose calibrators.* While estimating patient radiation dose requires knowledge of the Tc impurity profile, we have shown the patient radiation dose per γ emission rate varies little with production conditions. Therefore, a single threshold on the γ emission rate from Tc impurities per MBq of ^{99m}Tc can be derived using an average of the Tc impurity profiles that are expected to be produced. In practice, this average could be determined experimentally from calibration run(s) or could be determined theoretically based on the expected production conditions. This results in a pass/fail test that is highly sensitive to CPTc batches that would exceed predefined limits for the increase in patient radiation dose due to Tc impurities.

Simulated measurements were performed to estimate the ratio of dose calibrator (DC) readings with and without a lead shield to attenuate the effect of ^{99m}Tc in relationship to ratio of the emission rate from Tc-impurities to the activity of ^{99m}Tc.

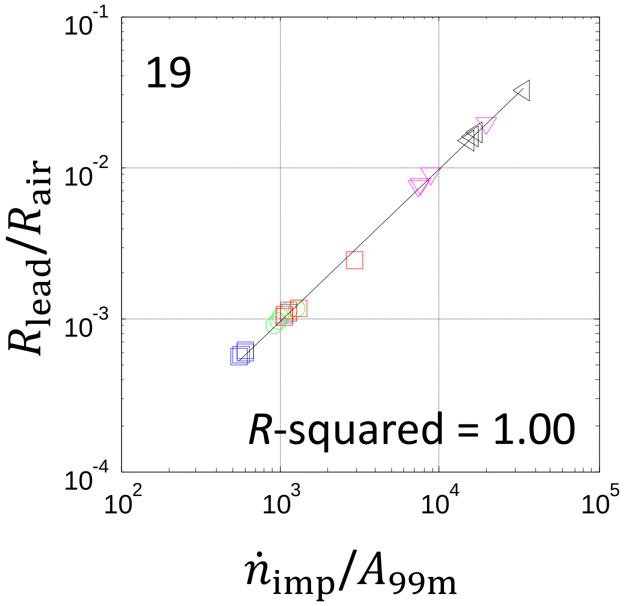

FIG. 9. Plot of the ratio of DC readings with and without lead to the emission rate for Tc-impurities to the activity of ^{99m}Tc.

TABLE 3. TARGET COMPOSITION USED IN THE SIMULATION STUDY DESCRIBED IN FIGURE 9

	Target				
Isotope					
^{92}Mo	0.003	0.006	0.06	0.09	0.005
^{94}Mo	0.003	0.0051	0.03	0.06	0.005
^{95}Mo	0.003	0.0076	0.04	0.10	0.005
^{96}Mo	0.003	0.0012	0.05	0.11	0.005
^{97}Mo	0.003	0.0016	0.08	0.08	0.01
^{98}Mo	0.17	0.41	0.47	0.55	2.58
^{100}Mo	**99.82**	**99.54**	**99.27**	**99.01**	**97.39**

Irradiation conditions:

- 6 hour irradiation
- 10-MeV exiting proton energy

Measurement conditions:

- Veenstra Dose Calibrator
- Biodex Moly-assay shield
- Measurements performed at 2, 4, 6, 12, and 24 hours after EOB

- Performed an experimental validation of this approach using a 19-MeV cyclotron at the British Columbia Cancer Agency

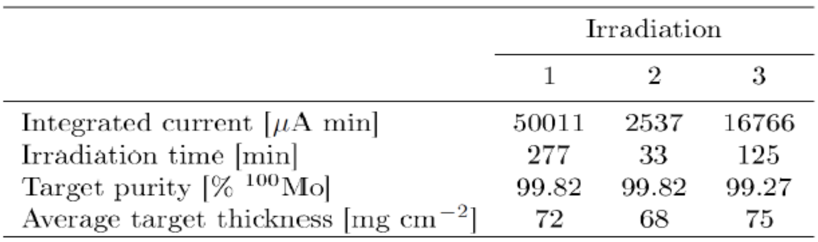

	Irradiation		
	1	2	3
Integrated current [μA min]	50011	2537	16766
Irradiation time [min]	277	33	125
Target purity [% ^{100}Mo]	99.82	99.82	99.27
Average target thickness [mg cm^{-2}]	72	68	75

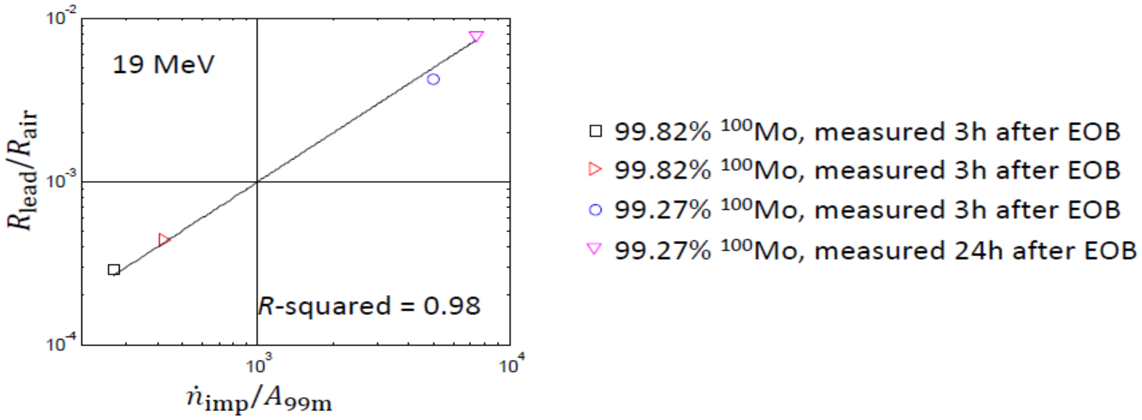

FIG. 10. The experimental results showing the plot of the ratio of DC readings with and without lead to the emission rate for Tc-impurities to the activity of ^{99m}Tc for the conditions shown in the figure.

Both theoretical calculations and experiments show that many other stable and radioactive isotopes can be produced spontaneously [13, 18]. Optimizing reaction conditions to maximize ^{99m}Tc production yield and minimize contributions from other nuclides becomes crucial. In particular, target composition and thickness, energy and intensity of the proton beam, irradiation time and radiation dose estimates for different injection times must be determined.

Manual calculations of all the production yields and doses are very time consuming. Therefore, we have created a graphical user interface [19] that would automate these calculations. This GUI not only helps us to calculate the activity of each potential product, but it can also be used to predict its gamma emissions to assist in the analysis of the observed gamma spectra. Moreover, the impact of different technetium (Tc) impurities on patient dosimetry can be evaluated [11]. In this study, experimental data for ^{99m}Tc productions is compared with the theoretical estimations obtained from the GUI.

Clearly the output from the GUI is highly dependent upon the accuracy of the reference data used for the calculations. Where possible, we have used experimental data instead of the theoretical inputs.We have used the GUI to determine the Tc-isotope yields based on a series reaction conditions to understand how target materials impact the dosimetry. Using these results we have developed what consider simple and conservative set of criteria for acceptance of the enriched Molybdenum target material. (see Table III). In addition, the ^{98}Mo values mitigate the impact of higher energy due to the ^{98}Mo(p,3n)^{96}Tc reaction.

TABLE 4. RECOMMENDED SPECIFICATIONS FOR ^{100}MO TARGET

Isotope	**Proposed % isotopic Purity to Maintain Patient Dose Increase of ~10% compared to pure $^{99m}TcO_4$**		
	$\leq$ 20 MeV[1]	20 – $\leq$22 MeV[2]	22 - $\leq$24 MeV[3]
^{92}Mo	0.03	0.03	0.03
^{94}Mo	0.03	0.03	0.03
^{95}Mo	0.03	0.03	0.03
^{96}Mo	0.03	0.03	0.03
^{97}Mo	0.03	0.03	0.03
^{98}Mo	6	0.8	0.25

(The columns represent the Mo-isotope recommended maximal Mo-isotopic composition for the typical energy ranges that would be used in direct production of ^{99m}Tc).

[1] Maximum increase in patient dose of 10.1% at 20 MeV, 18 hours after EOB.
[2] Maximum increase in patient dose of 10.1% at 22 MeV, 18 hours after EOB.
[3] Maximum increase in patient dose of 11.0% at 24 MeV, 18 hours after EOB

These specifications are aimed at keeping the increase in patient radiation dose to approximately 10% above that from generator produced ^{99m}Tc radiopharmaceuticals due to possible contamination from Tc-isotopic impurities. Using these limits will hopefully make it easier to document ^{100}Mo target material from the certificate of analysis form the supplier.

9.5. Clinical Use of Cyclotron Produced ^{99m}Tc

In establishing an approach to using CPTc in the clinical setting we performed a preclinical trial in order to establish and validate the protocols for a full clinical trial in human subjects. As part of that effort we proposed the specifications for use in humans. A Clinical Trial Application (CTA) has been submitted to Health Canada in June 2015 based o a 60 patient study using pertechnetate in thyroid studies.

10. CONCLUSION

TABLE 5. PROPOSED SPECIFICATIONS FOR CYCLOTRON PRODUCED PERTECHNETATE

Parameter	Acceptance Criteria	Test Method
Visual Appearance	Clear, colourless, no particles	Visual Inspection
Radionuclidic purity	Isotopes other than ^{99m}Tc contribute an emission rate of less than 6,000 emissions per second per MBq of ^{99m}Tc	Modified Molybdenum shield assay
Radionuclidic identity	Half-life between 5.72 and 6.32 hours or main gamma photopeak at 140 keV	USP <821> Half-life determination or gamma spectroscopy
Radiochemical purity	≥ 95%	TLC-Radiometric
Radiochemical identity	Rf = 0.8 - 1.0	TLC-Radiometric
pH	4.5 to 7.5	USP <791> (pH paper)
Aluminum content	< 10 µg/mL of solution (10 ppm)	Colorimetric assay
Molybdenum content	< 30 µg/mL of solution (30 ppm)*	Photometric assay
Hydrogen peroxide content	< 50 µL/mL of solution (50 ppm)	Colorimetric assay

Bacterial endotoxins	No more than 175/V USP endotoxin units per mL (V = final vial volume in mL)	USP <85> (Gel-clot or kinetic-chromogenic)
Sterility (retrospective)	No growth	USP <71> (Direct inoculation)

References

[1] BEAVER J.E., HUPF, H.B., Production of ^{99m}Tc on a medical cyclotron: a feasibility study. J. Nucl Med. **12** (1971) 739–741.

[2] SCHOLTEN, B., LAMBRECHT, R.M., COGNEAU, M., VERARUIZ, H., QAIM, S.M., Excitation functions for the cyclotron production of ^{99m}Tc and ^{99}Mo, Appl. Radiat. Isot. **51** (1999) 69–80.

[3] TAKÁCS, S., SZÜCS, Z., TÁRKÁNYI, F., HERMANNE, A., SONCK, M., Evaluation of proton induced reactions on ^{100}Mo: new cross sections for production of ^{99m}Tc and ^{99}Mo, J. Radioanal. Nucl. Chem. **257** (2003) 195–201.

[4] GAGNON, K., BÉNARD, F., KOVACS, M., RUTH, T.J., SCHAFFER, P., WILSON, J.S., MCQUARRIE, S.A., Cyclotron production of ^{99m}Tc: experimental measurement of the ^{100}Mo(p,x)^{99}Mo, ^{99m}Tc, and ^{99g}Tc excitation functions from 8 to 18 MeV, Nucl. Med. Biol. **38** (2011) 907-916.

[5] QAIM, S.M., Sudár, S., Scholten, B., Koning, A.J., Coenen, H.H., Evaluation of excitation functions of ^{100}Mo(p,pn)^{99}Mo and ^{100}Mo (p,2n)^{99m}Tc reactions: estimation of long-lived Tc-impurity and its implication on the specific activity of cyclotron-produced ^{99m}Tc, Appl. Radiat. Isot. **85** (2014) 101–113.

[6] HANEMAAYER, V., BENARD, F., BUCKLEY, K.R., KLUG, J., KOVACS, M., LEON, C., RUTH, T.J., SCHAFFER, P., ZEISLER, S.K., Solid targets for ^{99m}Tc production on medical cyclotrons, J. Radioanal. Nuc. Chem. **299** (2014) 1007-1011.

[7] SCHAFFER, P., BÉNARD, F., BERNSTEIN, A., BUCKLEY, K., CELLER, A., COCKBURN, N., CORSAUT, J., DODD, M., ECONOMOU, C., ERIKSSON, T., FRONTERA, M., HANEMAAYER, V., HOOK, B., KLUG, J., KOVACS, M., PRATO, F.S., MCDIARMID, S., RUTH, T.J., SHANKS, C., VALLIANT, J.F., ZEISLER, S., ZETTERBERG, U., ZAVODSZKY, P.A., Direct production of ^{99m}Tc via ^{100}Mo(p,2n) on small medical cyclotrons, Physics Procedia **66** (2015) 383-395.

[8] BÉNARD, F., BUCKLEY, K.R., RUTH, T.J., ZEISLER, S.K. KLUG, J., HANEMAAYER, V., VUCKOVIC, M., HOU, X., CELLER, A., APPIAH, J-P., VALLIANT, J., KOVACS, M.S., SCHAFFER. P., Implementation of multi-curie production of ^{99m}Tc by conventional medical cyclotrons. J. Nuc. Med. **55** (2014) 1017-1022.

[9] BENARD, F., ZEISLER, S.K., VUCKOVIC, M., LIN, K-SYAN, ZHANG, Z., COLPO, N., RUTH, T.J., SCHAFFER, P., Cross-linked polyethylene glycol beads to separate ^{99m}Tc-pertechnetate from low specific activity molybdenum. J Nuc Med. **55** (2014) 1910-1914.

[10] MORLEY, T.J., DODD, M., GAGNON, K., HANEMAAYER, V., WILSON, J., MCQUARRIE, S.A., ENGLISH, W., RUTH, T.J., BENARD, F., SCHAFFER, P. An automated module for the separation and purification of cyclotron-produced ^{99m}TcO$_4^-$, Nucl. Med. Biol. **39** (2012) 551-559.

[11] HOU, X., A CELLER, A., GRIMES, J., BÉNARD, F., RUTH, T., Theoretical dosimetry estimations for radioisotopes produced by proton induced reactions on natural and enriched molybdenum targets, Phys. Med. Biol. **57** (2012) 1499-1515.

[12] LAGUNAS-SOLAR, M.C., KIEFER, P.M., CARVACHO, O.F., LAGUNAS, C.A., YAPO, C., Cyclotron production of NCA ^{99m}Tc and ^{99}Mo, An alternative non-reactor supply source of instant ^{99m}Tc and ^{99}Mo/99mTc generators, Int. J. Rad. App. Inst. A **42 (7)** (1991)) 643-657.

[13] LEBEDA, O., VAN LIER, E.J., ŠTURSA, J., RÁLIŠ, J., ZYUZIN, A., Assessment of radionuclidic impurities in cyclotron produced ^{99m}Tc, Nucl. Med. Biol. **39** (2012) 1286-1291.

[14] LO, H.H., BERKE, R.A., POTSAID, M.S., A simple method of correcting ^{99}Mo breakthrough from a ^{99m}Tc -^{99}Mo generator, Radiology **93 (5)** (1969) 1198-1199.

[15] RICHARDS, P., O'BRIEN, M., Rapid determination of ^{99}Mo in separated ^{99m}Tc, J. Nucl. Med. **10 (7)** (1969) 517-517.

[16] DENARDO, G.L., KUKIS, D.L., SHEN, S., DENARDO, S.J., Accurate measurement of copper-67 in the presence of copper-64 contaminant using a dose calibrator, J. Nucl. Med. **37 (2)** (1996) 302-306.

[17] PALMER, D.W., RAO, S.A., A simple method to quantitate iodine-124 contamination in iodine-123 radiopharmaceuticals, J. Nucl. Med. **26 (8)** (1985) 936-940.

[18] CELLER, A., HOU, X., BÉNARD, F., RUTH T., Theoretical modelling of yields for proton induced reactions on natural and enriched molybdenum targets, Phys. Med. Biol. **56** (2011) 5469-5484.

[19] HOU, X., CELLER, A., VUCKOVIC, M., BUCKLEY, K., BÉNARD, F., SCHAFFER, P., RUTH. T., Graphical user interface for yield and dose estimations for cyclotron-produced technetium, Phys. Med. Biol. **59** (2014) 3337-3352.

NUCLEAR DATA FOR ACCELERATOR PRODUCTION OF ^{99m}Tc

S. TAKACS

Institute for Nuclear Research, Hungarian Academy of Sciences
Debrecen, Hungary

Abstract

As an alternative to reactor produced ^{99}Mo/^{99m}Tc generator technology, direct production of ^{99m}Tc on accelerators is considered. There are a number of methods of using accelerators to produce ^{99m}Tc and/or ^{99}Mo. Direct production of ^{99m}Tc on highly enriched ^{100}Mo target using cyclotrons can be interesting for energies up to 25 MeV, so as to minimize the impurities from additional open reaction channels. To estimate the quality of the accelerator produced ^{99m}Tc all the possible reaction routes should be mapped which could be potentially involved in this technology. However, a well-defined excitation function for the ^{100}Mo(p,2n)^{99m}Tc primary reaction is needed, in order to achieve acceptable good results in assessing the quality of the accelerator-produced ^{99m}Tc by model calculations. Most of the available experimental cross section data sets for the ^{100}Mo(p,2n)^{99m}Tc reaction have the same general shape while their amplitudes are different. A large difference, more than a factor of two may, indeed, be observed between the lowest and the highest datasets values.

Based on experimental and theoretical cross section data thick target yields for production of ^{99m}Tc, ^{99}Mo and other radionuclides may involve in the real production of ^{99m}Tc were calculated and the results were evaluated. Considering actual irradiation circumstances, proton energy, beam intensity, irradiation time, target composition, irradiation geometry activity and target construction the resulting activity of the main radionuclides ^{99m}Tc and ^{99}Mo can be different. Using a newly developed calculation tool the production of ^{99m}Tc can be modeled, together with the possible co-produced other Tc, Ru, Mo, Nb and Zr stable and radioisotopes.

1. INTRODUCTION

Efforts and studies are going on for studying alternative production routes of ^{99}Mo and ^{99m}Tc all over the world [1-4]. Direct production of ^{99m}Tc with accelerators is one of the proposed alternative utilizing the ^{100}Mo(p,2n)^{99m}Tc reaction on highly ^{100}Mo-enriched target material [5]. This Coordinated Research Project (CRP) is aiming to develop an alternative direct production of ^{99m}Tc using dedicated high current cyclotrons.

As an alternative to reactor produced ^{99}Mo/^{99m}Tc generator technology, the direct production of ^{99m}Tc on cyclotrons is considered. ^{99m}Tc can be produced in several reaction but only the ^{100}Mo(p,2n)^{99m}Tc and ^{100}Mo(p,x)^{99}Mo reactions are investigated in the frame of this CRP. Other possible accelerator based reactions on molybdenum target are listed here:

^{100}Mo(p,2n)^{99m}Tc	**^{100}Mo(p,x)^{99}Mo**
^{100}Mo(d,3n)^{99m}Tc	^{100}Mo(d,x)^{99}Mo
^{98}Mo(d,n)^{99m}Tc	^{98}Mo(d,p)^{99}Mo
^{98}Mo(p,γ)^{99m}Tc	^{100}Mo(p,2p)^{99}Nb → 99Mo
^{97}Mo(d,γ)^{99m}Tc	^{100}Mo(γ,n)^{99}Mo
^{96}Mo(α,p)^{99m}Tc	^{97}Mo(α,2p)^{99}Mo

These reactions have different importance regarding the required technical and technological developments of large scale production of ^{99m}Tc.

Proton induced reactions have the highest cross sections when comparing to other bombarding particles (deuteron, alpha) for producing ^{99m}Tc and ^{99}Mo, consequently they have the highest yields too. It requires use of highly enriched ^{100}Mo target in order to be able to produce large amount of activity with minimal radio and chemical contaminations. Although the ^{100}Mo(p,2n)^{99m}Tc and ^{100}Mo(p,x)^{99}Mo reactions have obvious importance in accelerator produced ^{99m}Tc and the cross sections and yields of these reactions were studied extensively by several groups, no full agreement can be found among the published data.

2. ACCEPTED WORK PLAN FOR ATOMKI

- Collection and selection of the experimental cross section data for the reactions involved in the production process (depending on the bombarding energy the number of important reactions can be between 50 and 200)
- Selection of the possible best cross section data predicted by different theoretical models for those reactions for which no experimental data are available.
- To build up a dedicated database containing cross section data (from threshold up to 30 MeV) for the reactions can be important regarding the ^{99m}Tc production
- Determine the amount of different radionuclide produced during irradiation as function of bombarding energy, irradiation time and cooling time for the different available target enrichments.
- Analysis of the calculated radionuclide profiles in order to determine optimal production parameters.
- Determination of the maximal (theoretical) specific activity for various irradiation parameters and target compositions.
- Determine the time dependence of the specific activity of the ^{99m}Tc product

3. DESCRIPTION OF RESEARCH CARRIED OUT

Direct accelerator production of ^{99m}Tc is possible on enriched ^{100}Mo target with yield high enough to provide suitable amount of activity to cover the local and regional needs. Predicted quality of accelerator produced ^{99m}Tc, based on the ^{100}Mo(p,2n)^{99m}Tc reaction, was studied by calculating and comparing the yields of the main and the side reactions. After collecting the available experimental cross section data of the ^{100}Mo(p,2n)^{99m}Tc reaction it was found that data sets showed large differences. A large disagreement more than a factor of two may, indeed, be observed between the lowest and the highest datasets values. We aimed to clear that situation by performing new experiments in which the excitation functions and thick target yields were measured for the two main the ^{100}Mo(p,2n)^{99m}Tc and ^{100}Mo(p,x)^{99}Mo reactions.

3.1. Measurements of the cross section of 100Mo(p,2n)99mTc and 100Mo(p,x)99Mo reactions

New experiment was performed at Atomki to determine the excitation function of the two main reactions, ^{100}Mo(p,2n)^{99m}Tc and ^{100}Mo(p,x)^{99}Mo, up to E_p=18MeV using the standard stacked target technique and activation method on Mo target with natural isotopic composition. Another experiment at higher upper energy, E_p=36.4MeV, was performed at the VUB cyclotron laboratory. Additionally, results from one of our earlier experiments, reported in 2003 [6], were re-evaluated by using up to date nuclear decay data with the aim to improve the quality of experimental data sets. Experiments were made relative to the ^{nat}Ti(p,x)^{48}V monitor reaction.

Cross section values deduced in those three independent experiments, using the latest evaluated nuclear decay data for the radionuclides involved, provided data sets in very a good agreement with each other indicating sound results of the cross section of ^{100}Mo(p,2n)^{99m}Tc and ^{100}Mo(p,x)^{99}Mo reactions.

3.2. Benchmark experiment

A benchmark experiment was carried out at Atomki to check and to validate the deduced cross section data. In this experiment we have measured the thick target yield of the ^{100}Mo(p,2n)^{99m}Tc and ^{100}Mo(p,pn)^{99}Mo reactions by irradiating a thick Mo target with natural isotopic composition and measuring the produced activity. The decay of the irradiated Mo target was followed for several days and about 100 measured activity points were compared with the values deduced by calculation based on our latest experimental cross section data measured for both ^{100}Mo(p,2n)^{99m}Tc and ^{100}Mo(p,pn)^{99}Mo reactions. We found excellent agreement among the experimental and calculated values confirming the validity of the measured cross section data of the ^{100}Mo(p,2n)^{99m}Tc and ^{100}Mo(p,pn)^{99}Mo reactions.

3.3. Development of a Reaction Network Calculation Tool

A Reaction Network Calculation Tool (RNCT) was developed with calculating capabilities to estimate the yields of different Ru, Tc, Mo, Nb and Zr isotopes may be formed in a series of direct and indirect reactions during the production process. Experimental cross section data are not available for all the reactions involved in accelerator production of ^{99m}Tc. The available experimental excitation functions were collected and completed with data from the TENDL library for those reactions for which no proper experimental data were available.

Technetium isotopes have primary importance regarding the specific activity of the final ^{99m}Tc product. They are produced in (p,xn) reactions on Mo target. In general the (p,xn) reactions are well represented in the TENDL library. Data for Mo target isotopes in the TENDL library generally agree with the experimental data of (p,xn) and (p,pn) reactions well, but reactions with gamma or complex particles in the exit channel, like (p,γ), (p,αn), etc., are not described so well.

On the experience gathered and the new requirements arisen during the period of CRP we worked on the development and improvement of the Reaction Network Calculation Tool. It is now capable to predict by calculation the amount of ^{99m}Tc and the amount of co-produced unwanted Tc isotopes as well as the amount of other stable and radioactive isotopes of Ru, Mo, Nb and Zr. The calculation can be done as function of target composition, bombarding energy and irradiation time. Decay production of the investigated radioisotopes is also included in the latest version.

The RNCT applies numerical integration of the cross sections weighted by the stopping power to estimate the thick target yield. The reactions cross sections are taken from experimental works and from the TENDL-2013 data library based on TALYS code version 1.6 calculations.

In the latest version of the RNCT the upper bombarding energy was set to 30 MeV in order to limit the number of reactions contribute to the unwanted activity. The number of reactions having reaction threshold energy less than E_p=30MeV is around 200.

The Reaction Network Calculation Tool can be used to model most of the aspects of the accelerator production of ^{99m}Tc for variety of possible cyclotron infrastructure.

4. RESULTS OBTAINED

4.1. Experimental results

Cross sections were determined in three independent experiments for the ^{100}Mo(p,2n)^{99m}Tc and ^{100}Mo(p,x)^{99}Mo reactions, using stacked target technique, activation method and the latest evaluated nuclear decay data of ^{99}Mo and ^{99m}Tc. The measurements were done relative to the ^{nat}Ti(p,x)^{48}V monitor reaction. The three data sets are in good agreement with each other and are confirmed in another independent benchmark experiment.

4.1.1. Cross section of the ^{100}Mo(p,2n)^{99m}Tc reaction

Analyzing the available experimental cross section data sets of the ^{nat}Mo(p,x)^{99m}Tc and ^{100}Mo(p,2n)^{99m}Tc reactions one can find large differences in the amplitudes among different data sets. In figure 1 experimental cross section data for the ^{100}Mo(p,2n)^{99m}Tc reaction are collected including our latest results published in [7].

The available cross section database of the ^{100}Mo(p,2n)^{99m}Tc reaction contains several datasets now, but a critical evaluation of the experimental data is urgently needed. Qaim et al. gave a comprehensive analysis of the available data in 2014 [8] introducing an effective cross section and using a theoretical approach. However, when datasets are different from each other in such an extent, there should be some among them that are basically not correct, therefore could not be involved in the evaluation and should be rejected. As a first step of the data analyses, these erroneous datasets should be identified and corrected whenever possible otherwise they should be discarded. The reduced database thus obtained is more suitable for preparing recommended values for the reaction. To overcome this problem, we performed new experiments using the stacked target foil technique, activation method and high resolution gamma-spectrometry for determining cross sections of the ^{100}Mo(p,2n)^{99m}Tc reaction in well controlled conditions, in order to be able to provide a limit for the amplitude of the excitation function. The experiments were made in reference to the ^{nat}Ti(p,x)^{48}V monitor reaction. In each experiment the complete excitation function of the ^{nat}Ti(p,x)^{48}V reaction was re-measured in full agreement with the recommended values. The results of the new measurements performed at Atomki and at VUB to determine the excitation function of the ^{100}Mo(p,2n)^{99m}Tc reaction, and re-evaluation of one of our earlier experiments using up to date nuclear decay data provided very good agreement among each other.

The production yield and the specific activity of ^{99m}Tc estimated theoretically basically depend on the cross sections used in the calculation. Therefore it is very important to determine the cross sections of the ^{100}Mo(p,2n)^{99m}Tc reaction with high confidence level. In our three independent experiments we got almost the same result for the maximal cross section value. These three experiments yielded a σ_{max}=237±16mb maximum cross section at E_p=15.7 MeV proton energy with a relatively wide plateau of the excitation function for the ^{100}Mo(p,2n)^{99m}Tc reaction using the latest evaluated nuclear decay data. The coinciding results of the three independent experiments can provide a strong base for selecting and deselecting the available experimental data sets and narrow the list of experimental works with accepted results. However, in the reaction network calculation the weighted average of these three experimental results was used.

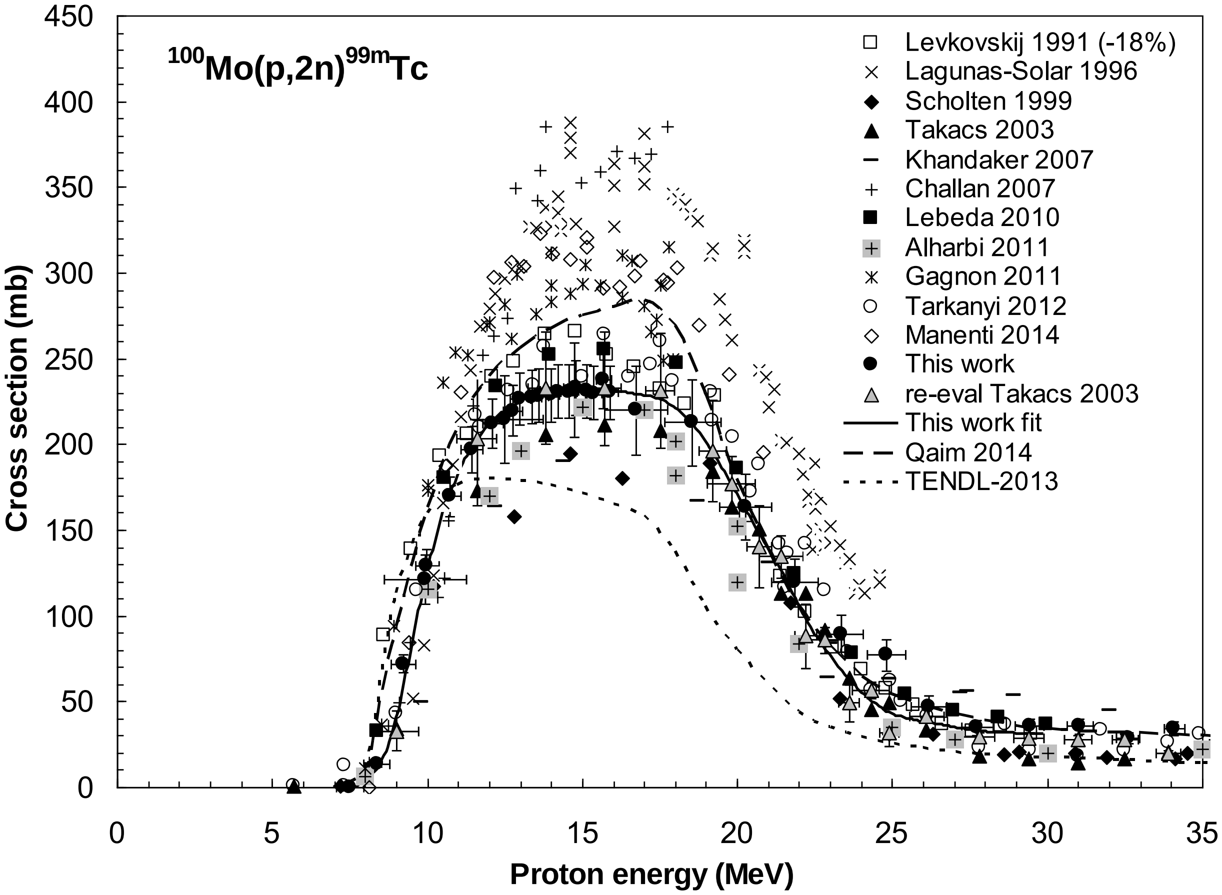

FIG. 1. Cross section data published for the $^{100}Mo(p,2n)^{99m}Tc$ reaction.

4.1.2. Cross section of the $^{100}Mo(p,x)^{99}Mo$ reaction

In figure 2 selected experimental cross sections of the $^{100}Mo(p,x)^{99}Mo$ reaction are collected together with the results of our two new experiments and results of the re-evaluated measurements published in 2003 [6]. Our new results are not different very much from the earlier one consequently the calculated yield is also quite similar.

The re-evaluation of the 2003 experiment, using the latest nuclear decay data of the radionuclides involved, resulted in practically the same values for the $^{100}Mo(p,x)^{99}Mo$ process as were published before, except the small hump in the E_p=20MeV and E_p=25MeV region which is not present there anymore. In the E_p=25-38MeV energy region the original and the re-evaluated as well as the new experimental data are in good agreement. These datasets are among the highest ones when comparing to other available datasets above E_p=25MeV. On the contrary below E_p=15MeV our new cross section data are among the lowest ones. This behaviour is confirmed by the benchmark experiment.

In Table1 and Table2 the numerical values of the newly measured cross sections and the re-evaluated ones for the $^{nat}Mo(p,x)^{99m}Tc$ and $^{100}Mo(p,2n)^{99m}Tc$ reactions are presented respectively.

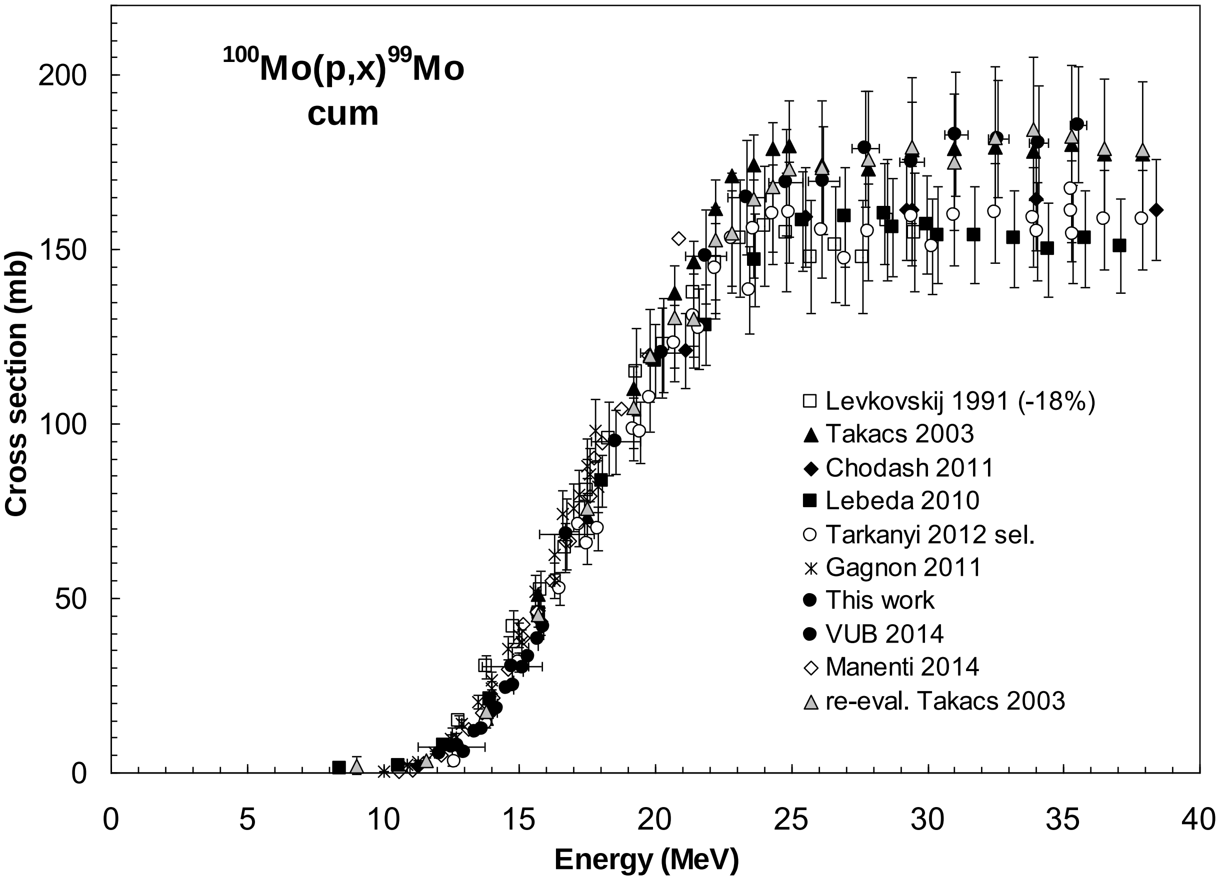

FIG. 2. Selected experimental cross section data sets of the ^{100}Mo(p,x)^{99}Mo reaction.

TABLE 1. NUMERICAL VALUES OF THE CROSS SECTIONS MEASURED IN THIS WORK NORMALIZED TO 100% ENRICHED ^{100}Mo TARGET FOR THE ^{100}Mo(p,2n)^{99M}TC AND FOR THE CUMULATIVE CROSS SECTIONS FOR THE ^{100}Mo(p,x)^{99}MO REACTIONS. DATA FROM THE E_P=16 MeV AND E_P=36.4 MeV IRRADIATIONS ARE COMBINED AND PRESENTED AS ONE EXPERIMENT

	^{100}Mo(p,2n)^{99m}Tc	^{100}Mo(p,x)^{99}Mo
Energy MeV	Sigma mb	Sigma mb
35.54 ± 0.32	25.4 ± 3.0	185.8 ± 16.5
34.09 ± 0.35	34.2 ± 4.0	180.6 ± 16.3
32.60 ± 0.39	28.8 ± 3.4	181.6 ± 16.8
31.04 ± 0.43	35.7 ± 4.2	183.0 ± 17.8
29.42 ± 0.47	36.0 ± 4.3	174.9 ± 17.4
27.73 ± 0.51	34.8 ± 4.1	178.8 ± 16.6
26.18 ± 0.57	47.5 ± 5.6	169.8 ± 15.5
24.80 ± 0.62	77.1 ± 9.1	169.1 ± 15.3
23.37 ± 0.68	89.7 ± 10.6	165.0 ± 16.5
21.85 ± 0.75	119.4 ± 14.1	148.0 ± 13.6
20.26 ± 0.83	163.6 ± 19.4	120.3 ± 13.0
18.56 ± 0.91	212.6 ± 25.2	94.8 ± 9.2
16.73 ± 1.00	220.1 ± 26.0	68.4 ± 10.2
15.89 ± 0.25	230.2 ± 15.6	41.9 ± 3.88
15.68 ± 0.25	237.5 ± 16.2	38.4 ± 3.44
15.35 ± 0.26	230.0 ± 15.7	33.2 ± 4.34
15.13 ± 0.27	231.2 ± 15.7	30.3 ± 2.78
14.78 ± 0.27	232.8 ± 15.9	25.2 ± 2.79
14.74 ± 1.10	231.6 ± 27.4	30.6 ± 5.4
14.56 ± 0.28	230.8 ± 15.7	24.1 ± 1.34
14.21 ± 0.29	230.7 ± 15.7	18.4 ± 2.99
13.97 ± 0.29	228.8 ± 15.6	17.3 ± 3.11
13.61 ± 0.30	228.4 ± 15.5	12.6 ± 1.17
13.37 ± 0.30	227.7 ± 15.5	11.6 ± 1.29
13.00 ± 0.31	226.6 ± 15.2	5.8 ± 0.69
12.75 ± 0.32	219.7 ± 14.9	7.9 ± 2.69
12.51 ± 1.21	214.7 ± 25.4	7.4 ± 5.6
12.10 ± 0.33	212.2 ± 14.4	
11.43 ± 0.35	197.2 ± 13.4	5.4 ± 0.73
10.72 ± 0.36	169.9 ± 11.5	
9.99 ± 0.38	129.6 ± 8.9	
9.93 ± 1.33	121.6 ± 14.4	
9.21 ± 0.40	72.2 ± 5.1	
8.38 ± 0.41	13.3 ± 1.3	

TABLE 2. THE ORIGINAL AND THE RECALCULATED CROSS SECTION DATA OF THE ^{100}Mo(p,x)^{99}Mo AND ^{100}Mo(p,2n)^{99m}Tc REACTIONS IN THE TAKACS 2003 EXPERIMENT [6]

	^{100}Mo(p,x)^{99}Mo	^{100}Mo(p,2n)^{99m}Tc	^{100}Mo(p,x)^{99}Mo	^{100}Mo(p,2n)^{99m}Tc
Energy MeV	Sigma mb	Sigma mb	Sigma re-eval mb	Sigma re-eval mb
5.7 ± 0.78		0.7 ± 0.7		
9.0 ± 0.71		34.7 ± 11.5	2.0 ± 2.6	33.0 ± 11.5
11.6 ± 0.64		173.5 ± 39.2	3.6 ± 0.6	203.2 ± 39.2
13.8 ± 0.58	15.7 ± 1.5	205.8 ± 32.5	17.7 ± 2.0	233.1 ± 32.5
15.7 ± 0.53	51.2 ± 6.3	211.2 ± 33.4	45.4 ± 5.1	232.6 ± 33.4
17.5 ± 0.48	73.6 ± 7.9	208.3 ± 33.4	75.8 ± 8.5	231.2 ± 33.4
19.2 ± 0.44	110.2 ± 12.9	184.6 ± 29.4	104.7 ± 11.8	196.0 ± 29.4
19.8 ± 0.76	120.1 ± 15.3	163.2 ± 18.3	119.6 ± 13.2	176.9 ± 15.9
20.7 ± 0.40	137.6 ± 16.0	150.9 ± 24.1	130.6 ± 14.7	140.5 ± 24.1
21.4 ± 0.70	146.6 ± 20.5	113.4 ± 12.7	130.3 ± 14.4	134.5 ± 12.1
22.2 ± 0.36	161.7 ± 19.2	113.5 ± 18.7	152.9 ± 17.2	88.3 ± 18.7
22.8 ± 0.65	171.3 ± 22.5	91.7 ± 10.3	154.8 ± 17.2	85.9 ± 7.7
23.6 ± 0.33	174.4 ± 20.2	63.5 ± 10.8	164.5 ± 18.5	49.2 ± 10.8
24.3 ± 0.60	179.0 ± 29.1	45.5 ± 5.1	167.9 ± 18.6	56.6 ± 5.1
24.9 ± 0.30	179.8 ± 20.3	49.7 ± 8.1	173.0 ± 19.4	31.8 ± 8.1
26.1 ± 0.56	174.1 ± 26.0	33.4 ± 3.7	173.4 ± 19.2	41.8 ± 3.8
27.8 ± 0.51	173.3 ± 20.9	18.3 ± 2.1	175.9 ± 19.5	29.2 ± 2.6
29.4 ± 0.48	178.5 ± 24.0	17.1 ± 1.9	179.4 ± 19.9	29.0 ± 2.6
31.0 ± 0.44	178.8 ± 20.5	14.5 ± 1.6	175.1 ± 19.4	27.7 ± 2.5
32.5 ± 0.41	179.4 ± 26.8	17.1 ± 1.9	182.1 ± 20.2	28.2 ± 2.5
33.9 ± 0.38	178.0 ± 23.4	21.0 ± 2.4	184.6 ± 20.5	20.1 ± 1.8
35.3 ± 0.35	180.0 ± 23.2	15.4 ± 1.7	182.5 ± 20.2	22.6 ± 2.0
36.5 ± 0.32	177.4 ± 24.0	21.5 ± 2.4	179.1 ± 19.8	9.0 ± 0.8
37.9 ± 0.30	177.4 ± 21.9	20.9 ± 2.3	178.5 ± 19.8	6.8 ± 0.6

4.1.3. Results of Benchmark experiment

A benchmark experiment was performed to check the excitation functions of the ^{100}Mo(p,2n)^{99m}Tc and ^{100}Mo(p,x)^{99}Mo reactions by irradiating a thick Mo target with natural isotopic composition with a proton beam at E_p=18MeV, I_p=50nA at Atomki. The irradiation lasted for 5 minutes only. The decay of the generated activity in the target was followed for several days with a high resolution HpGe gamma-spectrometer by acquiring about 100 complete spectra of the activated target. The count rate for the photo-peak of the E_γ=140.5keV gamma-line was determined for each spectra and was compared with the values deduced from analytical formulas representing the production and decay of ^{99m}Tc and ^{99}Mo in this actual experiment using the cross section data determined earlier in three independent experiments and the latest approved decay parameters. Correction for absorption of the E_γ=140.5keV gamma photon in the thick Mo target also was introduced. We found very good agreement between the calculated count rate curve and the one measured directly in the benchmark experiment for the ^{100}Mo(p,2n)^{99m}Tc reaction. In case of the ^{100}Mo(p,2n)^{99}Mo reaction to reach the best agreement between the experimental values and the theoretically calculated curve the experimental cross section values used in the calculation had to be decreased by 4%. This correction factor is far within the experimental uncertainties of the measured data points, which in any case are higher than 8%.

In this benchmark experiment both reactions, the ^{100}Mo(p,2n)^{99m}Tc and ^{100}Mo(p,x)^{99}Mo, were cross checked. The spectra measured close to the EOB can be used to

confirm the ^{99m}Tc production while spectra measured four days or later after EOB can be used to check the production of ^{99}Mo. Figure 3 shows the experimental count rate measured for the E_γ=140.5keV gamma-line and calculated from analytical equations describing the activation and decay processes using basic considerations.
Considering the maximum of the different datasets reported earlier for the cross sections of the ^{100}Mo(p,2n)^{99m}Tc reaction they were between σ_{max}=195mb and σ_{max}=388mb, while our newly determined and confirmed value is σ_{max}=(237±16)mb.

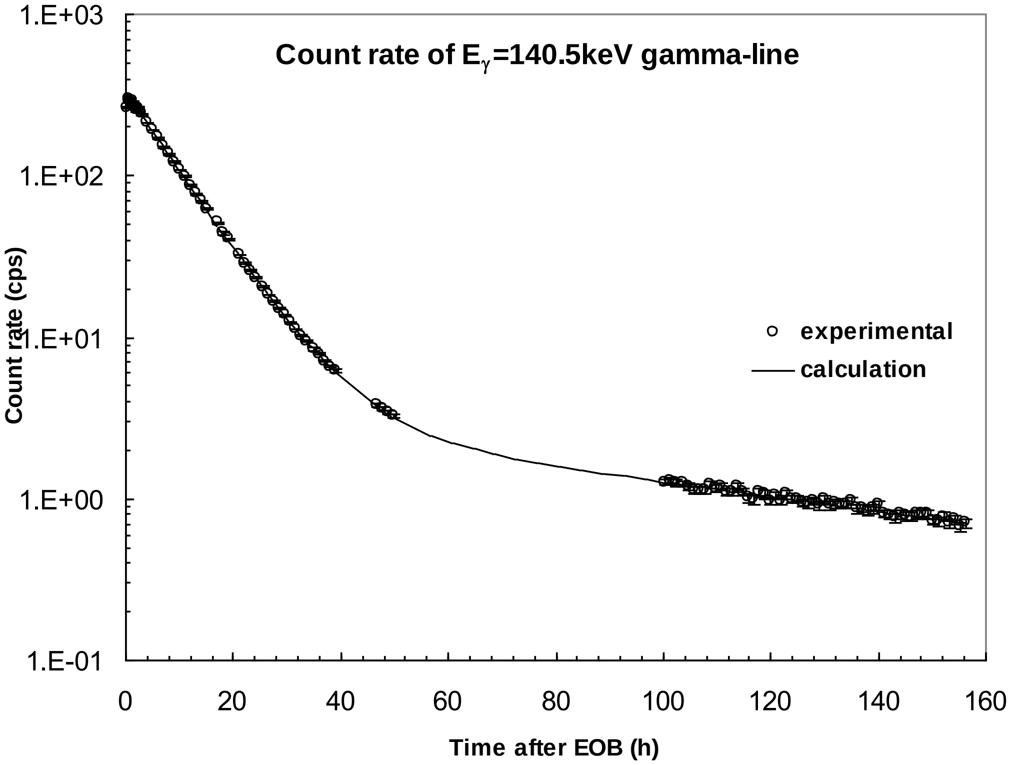

FIG. 3. Calculated and measured count rate of the E□=140.5keV gamma line for a thick Mo target irradiated with E_p*=17.9MeV protons.*

4.2. Development of a Reaction Network Calculation Tool

It is well known that activation and decay rate of any radionuclides can be calculated by using the reaction cross section and the decay parameters of the radionuclide in question. To estimate the amount of ^{99m}Tc and the amount of the co-produced unwanted radionuclides present in the target at any time (during irradiation and after the end of bombardment), when irradiating a ^{100}Mo enriched target material, both direct and indirect processes were considered in the development of the calculation tool. The RNCT was developed by using the following assumptions and constrains.

- The list of the possible isotopes produced during irradiation was mapped and beside the production of different Tc isotopes production of Ru, Mo, Nb and Zr isotopes were also considered in the calculation.
- For limiting the number of reactions included in the calculation an upper limit, $E_{threshold}$=30 MeV, was set for the reaction threshold energies.
- All possible production routes were considered in the calculation.
- Secondary reactions were not included in the calculation.

- Contribution of different production routes leading to the formation of the same reaction product is summed up when estimating the final number of reaction products present in the target.
- Experimental cross section values are used for the two main reactions ^{100}Mo(p,2n)^{99m}Tc and ^{100}Mo(p,x)^{99}Mo
- Cross section data were taken from the TENDL data library for the other reactions.
- For indirect or decay production routes decay chains up to 5 levels are considered.
- The actual differential equations were solved analytically by direct integration.
- No approximations were used and no processes were neglected, instead the well known exact mathematical formulae describing the formation and decay of stable and radioactive reaction products during irradiation and cooling periods were applied in the calculation.
- A target thickness which corresponds to the proton range from bombarding energy down to E_p=7.8MeV, to the threshold energy of the ^{100}Mo(p,2n)^{99}Tc reaction is considered to minimize the amount of unwanted activity and minimize the amount of necessary target material.

The calculation tool was developed in MS Excel format. It provides the number of the different Tc atoms present in the target (following production and decay of technetium nuclides in time) for mass numbers from 90 to 101 as function of bombarding energy, target composition, irradiation and cooling time. In the extended version of the calculation tool estimating the production and decay of the amount of Ru, Nb and Zr radionuclides can also follow the chemical impurities of the target. Change of the original isotopic composition of the reused enriched molybdenum-100 target material is also possible by calculation.

4.2.1. Collection of reaction cross sections

Experimental cross section data of proton induced reactions on stable isotopes of Mo are not available for each reaction considered in the production of ^{99m}Tc. For the two main reactions, ^{100}Mo(p,2n)^{99m}Tc and ^{100}Mo(p,x)^{99}Mo, several experimental data sets exist with relatively large differences. For rest of the reactions only limited number of experimental data sets is available. The available experimental data were compared with the corresponding data taken from the TENDL on-line data library [9]. The experimental cross section data measured on Mo target with natural isotopic composition were compared with the linear combination of the data from TENDL database. The comparison showed that the theory generally can predict on an acceptable level the cross section of the (p,xn) reactions, but underestimates the cross section of meta-stable states with some exemption. Regarding the theoretical excitation functions that can be used in the calculation they have deviation from the experimental cross section values an average of 20% in both direction. Although in a few cases even higher deviations exist, the received calculation result still can be considered as "good approximation" regarding the deduced trends and relative values as function of bombarding energy and/or irradiation time.

In the actual calculations the latest experimental cross section values are used for the two main reactions ^{100}Mo(p,2n)^{99m}Tc and ^{100}Mo(p,x)^{99}Mo and the excitation functions provided by the TENDL on-line data library are used for the rest of the reactions.

4.2.2. Reactions involved in ^{99m}Tc production

Figure 4 summarizes the possible direct and indirect reactions involved in proton bombardment of ^{100}Mo target for production of ^{99m}Tc and ^{99}Mo radionuclides. The production and decay scheme of ^{99m}Tc is relatively complex. Bombarding ^{100}Mo target with proton several direct reactions can take place. Direct production of ^{99m}Tc and ^{99g}Tc in the ^{100}Mo(p,2n) reaction, direct production of ^{99}Mo in the ^{100}Mo(p,pn) reaction and direct production of ^{99m}Nb and ^{99g}Nb in the ^{100}Mo(p,2p) reaction are possible. The relatively low amount of short lived ^{99m,g}Nb quickly decay to ^{99}Mo, while ^{99}Mo decays to ^{99m}Tc and ^{99g}Tc. Almost 100% of ^{99m}Tc decays to ^{99g}Tc and just minor amount of ^{99m}Tc decays to ^{99}Ru. The corresponding decay data are collected in table 3. The complexity of the production and decay scheme of the ^{99m}Tc and ^{99}Mo radionuclide pair is increased by the common E_{γ}=140.5keV gamma line emitted during disintegration of the radionuclides. This complexity and possible experimental difficulties may explain the large deviations among the different data series reported from different laboratories.

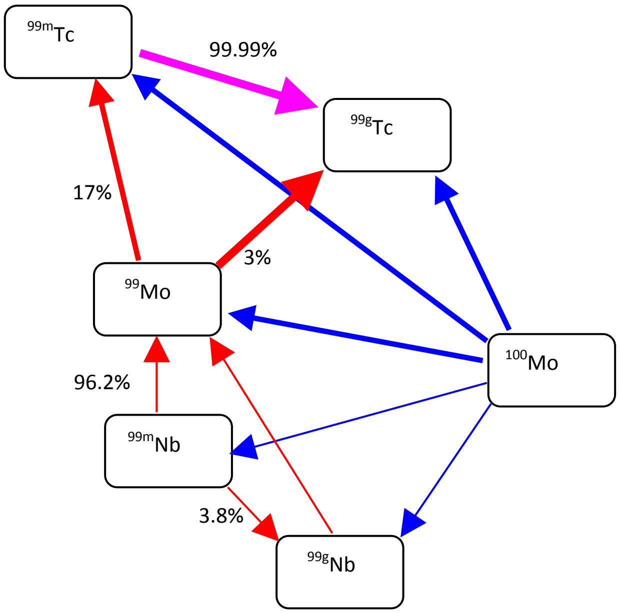

FIG. 4. Possible direct and indirect reactions involved in proton bombardment of ^{100}Mo target for production of ^{99m}Tc and ^{99}Mo radionuclides.

Regarding a single peak in a gamma-spectrum, the peak area (i.e. the total number of counts in the peak) once removed the background, is generally proportional with the number of decays occurring in the sample during the applied acquisition time. However, in the gamma-spectrum of an activated Mo foil the E_{γ}=140.5keV gamma peak is more complex the counts can have four different origins:

- Decay of direct produced ^{99m}Tc, (Eq.1)
- Decay of ^{99m}Tc produced during irradiation exclusively by decay of ^{99}Mo, (Eq.2)
- Decay of ^{99m}Tc produced after EOB by decay of ^{99}Mo, (Eq.3)
- Prompt gamma radiation that follows the decay of ^{99}Mo, (Eq.4)

The corresponding contributions to the total peak area T_{γ} acquired during a t_m measuring time after a t_b irradiation and t_c cooling time for a given Mo target foil can be described by the following four equations for the above four components, respectively.

$$T_{\gamma}\left(direct\right)_{D} = \varepsilon_{d}\varepsilon_{\gamma_{2}}\varepsilon_{t}N_{t}N_{b}\sigma_{2}\left(1-e^{-\lambda_{2}t_{b}}\right)\frac{1}{\lambda_{2}}e^{-\lambda_{2}t_{c}}\left(1-e^{-\lambda_{2}t_{m}}\right) \tag{1}$$

$$T_{\gamma}\left(decay\right)_{x} = \varepsilon_{d}\varepsilon_{\gamma_{2}}\varepsilon_{t}\frac{fN_{t}N_{b}\sigma_{1}}{\left(\lambda_{1}-\lambda_{2}\right)}\left[\lambda_{1}\left(1-e^{-\lambda_{2}t_{b}}\right)-\lambda_{2}\left(1-e^{-\lambda_{1}t_{b}}\right)\right]\frac{1}{\lambda_{2}}e^{-\lambda_{2}t_{c}}\left(1-e^{-\lambda_{2}t_{m}}\right) \tag{2}$$

$$T_{\gamma}\left(decay\right)_{y} = \varepsilon_{d}\varepsilon_{\gamma_{2}}\varepsilon_{t}\frac{fN_{t}N_{b}\sigma_{1}}{\left(\lambda_{1}-\lambda_{2}\right)}\left(1-e^{-\lambda_{1}t_{b}}\right)\left[e^{-\lambda_{2}t_{c}}\left(1-e^{-\lambda_{2}t_{m}}\right)-\frac{\lambda_{2}}{\lambda_{1}}e^{-\lambda_{1}t_{c}}\left(1-e^{-\lambda_{1}t_{m}}\right)\right] \tag{3}$$

$$T_{\gamma}\left(direct\right)_{M} = \varepsilon_{d}\varepsilon_{\gamma_{1}}\varepsilon_{t}N_{t}N_{b}\sigma_{1}\left(1-e^{-\lambda_{1}t_{b}}\right)\frac{1}{\lambda_{1}}e^{-\lambda_{1}t_{c}}\left(1-e^{-\lambda_{1}t_{m}}\right) \tag{4}$$

Where

N_t	surface density of target atoms, [atom/cm^2]
N_b	number of bombarding particles per unit time, [proton/sec]
σ_i	activation cross sections, [cm^2]
f	decay branching ratio of ^{99}Mo to ^{99m}Tc
ε_d	detector efficiency
ε_γ	corresponding gamma intensity
ε_t	dead time correction
λ_i	decay constant, [1/sec]
t_b	bombarding time, [sec]
t_c	cooling time, [sec]
t_m	acquisition time, [sec]
i	the *i=1* index refers to the ^{99}Mo parent radionuclide, *i=2* is referred to the ^{99m}Tc daughter radionuclide instead.

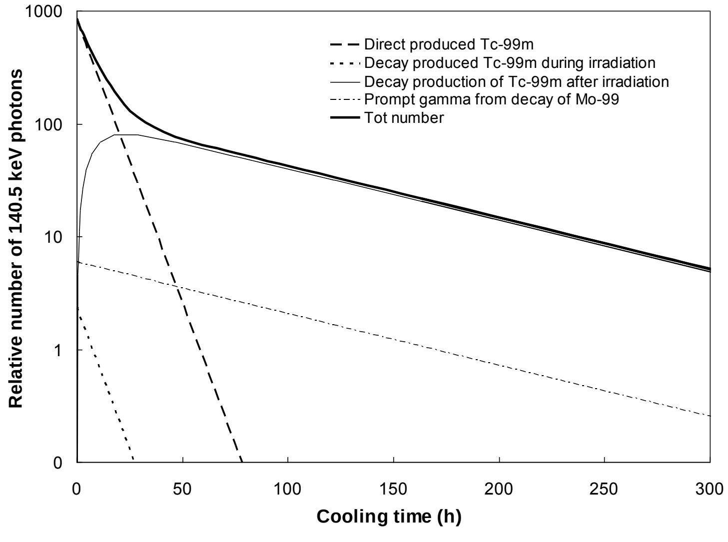

Fig. 5. Relative contributions to the total peak area of the E_{γ}=140.5keV gamma line of the four components as function of the cooling time. (EOB=0).

Beside the main reactions, in which ^{99m}Tc and ^{99}Mo are produced, several other reactions take place on the lower mass stable Mo isotopes present in the ^{100}Mo-enriched target material in minor amount and additional Tc, Ru, Mo, Nb and Zr stable and radionuclides are produced. The amounts of activation products depend on many parameters, such as reaction cross section, bombarding energy, beam intensity, irradiation time, target composition, post irradiation processing time etc. Production of ^{99m}Tc in the irradiated Mo target is continued after the stop of irradiation by decay of the co-produced ^{99}Mo present in the target. This post irradiation production is only stopped by the chemical separation of technetium from the target. With the help of the developed calculation tool most of these processes can be modeled.

TABLE 3. NUCLEAR DECAY DATA OF ^{99m}Tc AND ^{99}Mo USED IN THE EXPERIMENTAL WORKS AND IN THE CALCULATION TOOL, TAKEN FROM [10], AND [11]. DATA WITH * ARE FROM [12]

	Half life	Decay mode	E_γ keV	I_γ %	Contributing reactions	Q-value MeV	Threshold MeV
^{99}Mo	65.9496* h	β^-, 100%	140.5	4.72*	^{100}Mo(p,pn)	-8.29	8.38
			181.1	6.01*	^{100}Mo(p,d)	-6.07	6.13
		^{99}Mo→^{99m}Tc	739.5	12.12*	^{99}Nb decay		
		87.6%*	140.5 (equilibrium)	89.6*			
^{99g}Nb	15 sec	β^-, 100%	137.7	81.0	^{100}Mo(p,2p)	-11.15	11.26
^{99m}Nb	2.6 min	β^-, 96.2% IT, 3.8%	97.8	6.7			
^{99g}Tc	2.14x10^{3*} year	β^-, 100%	89.5	6.5x10^{-4}	^{100}Mo(p,2n)	-7.72	7.79
^{99m}Tc	6.0082* h	IT, 99.9963% β^-, 0.0037%	140.5	88.5*			
^{90g}Nb	14.6 h	EC, 48.8%	141.18	66.8	^{94}Mo(p,αn)	-8.96	9.05
		β^+, 51.2%	1129.22	92.7	^{92}Mo(p,^{3}He)	-11.79	11.92
^{90m}Nb	18.8 sec	IT, 100%	122 (?)	(?)			
^{90}Mo	5.67 h	EC, 100%	122.37	64	^{92}Mo(p,t)	-14.30	14.45
			257.34	78			

* Data are taken from [13].

The standard atomic weight (A_{Mo}=95.96(2)g) and the isotopic composition of molybdenum (^{92}Mo:14.525(15)%, ^{94}Mo:9.1514(74)%, ^{95}Mo:15.8375(98)%, ^{96}Mo:16.672(19)%, ^{97}Mo:9.5991(73)%, ^{98}Mo:24.391(18)% and ^{100}Mo:9.824(50)%) were taken from a IUPAC Technical Report 2009 [13] and were used in the calculations.

In table 4 nuclear data are collected for the possible side reactions of Tc radionuclides other than ^{99}Tc.

TABLE 4. NUCLEAR DATA OF THE REACTIONS IN WHICH CONTAMINATING TC RADIONUCLIDES (OTHER THAN ^{99}TC) ARE PRODUCED USING HIGHLY ENRICHED ^{100}Mo TARGET. DECAY DATA WERE TAKEN FROM NuDAT2.6 DATABASE [14]

Nuclide	Half-life	Decay mode (%)	Eγ (keV)	Iγ (%)	Contributing reactions	Q-value (MeV)
^{101}Tc	14.2 min	β^-(100)	306.83	89	^{100}Mo(p,γ)	+7.44
^{100}Tc	15.46 s	β^-(99.9982) EC(0.0018)	539.52	6.60	^{100}Mo(p,n)	-0.95
^{98}Tc	4.2 10^6 y	β^-(100)	652.4	100	^{100}Mo(p,3n)	-16.68
					^{98}Mo(p,n)	-2.47
					^{97}Mo(p,γ)	+6.17

^{97g}Tc	4.21 10^{6} y	EC(100)	No		^{100}Mo(p,4n)	-23.96
			gamma		^{98}Mo(p,2n)	-9.74
					^{97}Mo(p,n)	-1.1
					^{96}Mo(p,γ)	+5.7
					^{97m}Tc decay	
^{97m}Tc	91. d	IT(96.06)	96.5	0.32	^{100}Mo(p,4n)	-24.06
		EC(3.94)			^{98}Mo(p,2n)	-9.84
					^{97}Mo(p,n)	-1.2
					^{96}Mo(p,γ)	+5.6
^{96g}Tc	4.28 d	EC(100)	778.2	99.76	^{100}Mo(p,5n)	-33.43
			812.5	82	^{98}Mo(p,3n)	-19.22
			849.9	98	^{97}Mo(p,2n)	-10.58
			1126.85	15.2	^{96}Mo(p,n)	-3.75
					^{95}Mo(p,γ)	+5.39
					^{96m}Tc decay	
^{96m}Tc	51.5 min	IT(98.0)	778.2	1.9	^{100}Mo(p,5n)	-33.47
		EC(2.0)	1200.15	1.1	^{98}Mo(p,3n)	-19.25
					^{97}Mo(p,2n)	-10.61
					^{96}Mo(p,n)	-3.79
					^{95}Mo(p,γ)	+5.36
^{95g}Tc	20 h	EC(100)	765.79	93.8	^{98}Mo(p,4n)	-27.09
					^{97}Mo(p,3n)	-18.45
					^{96}Mo(p,2n)	-11.63
					^{95}Mo(p,n)	-2.47
					^{94}Mo(p,γ)	+4.89
^{95m}Tc	61 d	EC(96.12)	582.1	30.0	^{98}Mo(p,4n)	-27.13
					^{97}Mo(p,3n)	-18.49
					^{96}Mo(p,2n)	-11.67
					^{95}Mo(p,n)	-2.51
					^{94}Mo(p,γ)	+4.85
^{94g}Tc	293 min	EC(100)	702.67	99.6	^{98}Mo(p,5n)	-37.02
			849.74	95.7	^{97}Mo(p,4n)	-28.38
			871.05	99.9	^{96}Mo(p,3n)	-21.56
					^{95}Mo(p,2n)	-12.41
					^{94}Mo(p,n)	-5.04
^{94m}Tc	52 min	EC(100)	871.05	94.2	^{98}Mo(p,5n)	-37.1
					^{97}Mo(p,4n)	-28.46
					^{96}Mo(p,3n)	-21.64
					^{95}Mo(p,2n)	-12.48
					^{94}Mo(p,n)	-5.11
^{93g}Tc	2.75 h	EC(100)	1362.94	66.2	^{97}Mo(p,5n)	-37.00
			1520.28	24.4	^{96}Mo(p,4n)	-30.18
					^{95}Mo(p,3n)	-21.03
					^{94}Mo(p,2n)	-13.66
					^{92}Mo(p,γ)	+4.08
^{93m}Tc	43.5 min	IT(77.4)	943.7	2.92	^{97}Mo(p,5n)	-37.4
		EC(22.6)	391.83	58.3	^{96}Mo(p,4n)	-30.58
					^{95}Mo(p,3n)	-21.42
					^{94}Mo(p,2n)	-14.05
					^{92}Mo(p,γ)	+3.69

4.2.3. *Specific activity of ^{99m}Tc and radio contaminants*

The specific activity and the amount of contaminating radionuclides depend on the bombarding energy. Generally using higher bombarding proton energy the production yield is also higher. However, in practice the beam energy should be limited since at higher energies more contaminating Tc radioisotopes are co-produced. The enrichment level of ^{100}Mo in the target never can reach 100%, therefore other stable Mo isotopes in minor amount are always present in the target material. Bombarding Mo target with proton beam ^{99m}Tc can be produced directly in the (p,2n) reaction and also in the decay of parallel produced ^{99}Mo. Production can be made by low and medium energy, high intensity commercial cyclotrons on an appropriate design of enriched ^{100}Mo target. Depending on the bombarding energy, the target thickness and the applied irradiation parameters such as beam current, irradiation time and cooling time different amounts of ^{99m}Tc and other co-produced Tc radionuclides are produced and present in the target at EOB. These processes are modelled by using the calculation tool and the results and conclusions are presented below.

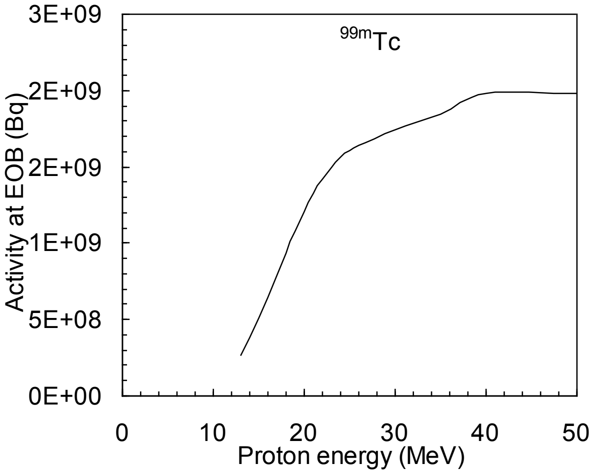

FIG. 6. Activity of ^{99m}Tc at EOB after a 3h and 1μA irradiation as function of bombarding energy

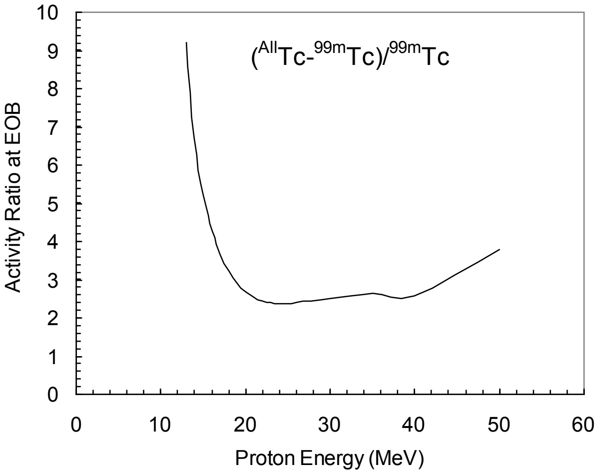

FIG. 7. Relative activity of all contaminating Tc radionuclides compared to ^{99m}Tc at EOB after a 3h and *1μA* irradiation as function of bombarding energy.

Figure 6 shows the production yield of ^{99m}Tc as the function of bombarding energy for fixed 3 hour irradiation time and 1 μA bombarding proton beam at EOB. As it is expected the production yield is increasing with increasing bombarding energy. In Figure 7 the relative activity of all contaminating Tc radionuclides is presented. The total activity is compared to the activity of ^{99m}Tc at EOB after a 3h and 1 μA irradiation as function of bombarding energy. At low energies, where the cross section of the ^{100}Mo(p,2n) reaction is low, the total activity of the contaminating other Tc radionuclides is quite high. Mainly due to presence of the short-lived ($T_{1/2}$=15.8s) ^{100}Tc formed in the ^{100}Mo(p,n) reaction. Fortunately this reaction product is decaying quickly and in practice does not really influences the specific activity of ^{99m}Tc. Other reactions on lighter mass Mo isotopes also result in production of Tc radioisotopes other than ^{99m}Tc. The lower the enrichment level of the ^{100}Mo target material the higher of the ratio of the contaminating radioisotopes produced. To avoid unwanted radio-contaminants the enrichment level of the ^{100}Mo target material should be as high as possible and the bombarding proton energy should be kept below the threshold of the reactions in which the unwanted radioisotopes are produced.

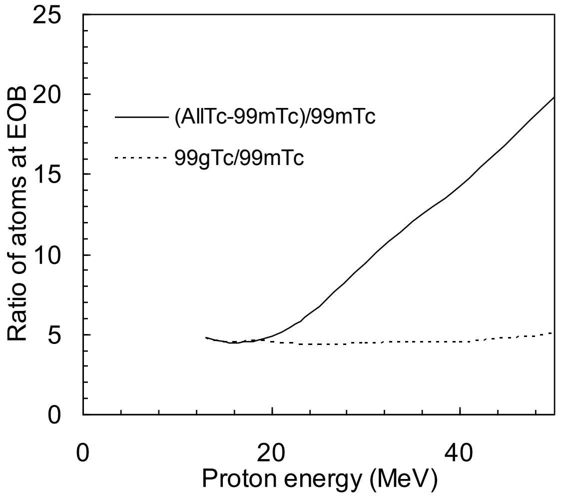

FIG. 8. Relative amount of the contaminating Tc radionuclides in the target at EOB after a 3h and 1 μA bombardment.

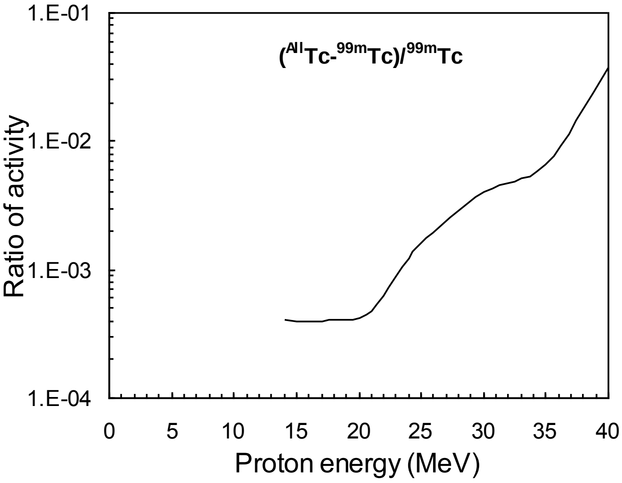

FIG. 9. Relative activity of co-produced Tc radionuclides after a 3h and 1 μA irradiation and 1h cooling time as function of bombarding energy.

Figure 8 illustrates the relative amount (number of atoms) of all contaminating technetium isotopes compared to the number of ^{99m}Tc present in the target at EOB as function of bombarding proton energy. Also the relative number of ^{99g}Tc/^{99m}Tc is represented. While the total number of other co-produced Tc radionuclides is increasing rapidly with increasing bombarding energy above 20 MeV, the relative number of ^{99g}Tc remains almost constant at around five. In figure 9 the relative activity of the co-produced Tc atoms is presented as function of bombarding proton energy applying a 1h cooling time after EOB. Comparing Fig 7 and Fig 9 the significant effect of a 1 hour of cooling time on the relative activity can be noted. This difference is explained by the decay of the short lived ^{100}Tc.

Investigating the effect of the irradiation time it was found that due to the several longer lived Tc reaction products a longer irradiation results in a higher Tc contamination level. Therefore the irradiation time always should be kept as short as possible by maximizing the beam intensity.

Regarding the quality of the enriched target material and the acceptable level of different unwanted radionuclides the initial bombarding energy should be limited at different values. Depending on the bombarding proton energy not only the ^{99m}Tc radionuclide is produced but a series of other Tc isotopes too. Since the half-life of ^{99m}Tc ($T_{1/2}$=6.01h) is much shorter than the half-life of its mother ^{99}Mo ($T_{1/2}$ =65.95h) the post irradiation processes should be started as soon as possible in order not to lose activity of ^{99m}Tc since the decay of ^{99}Mo can compensate only fraction of the activity loss of ^{99m}Tc by applying long cooling time. Beside ^{99m}Tc ($T_{1/2}$=6.01h) the long lived ^{99g}Tc ($T_{1/2}$=2.1 10^5year) radioisotope is always co-produced. However, due to the very long half-life its activity is very low but considering that the cross section for producing ^{99g}Tc [15] is much higher than the cross section to produce ^{99m}Tc considerable amount of ^{99g}Tc is produced during irradiation. Above E_p=17MeV bombarding proton energies the amount of the long lived ^{98}Tc ($T_{1/2}$=4.2 10^6year) radioisotope produced in the ^{100}Mo(p,3n) reaction is increasing considerable. Above 24 MeV proton energy another long lived Tc radioisotope is produced, ^{97g}Tc ($T_{1/2}$=4.0 10^6year). Depending on the enrichment level of the target material other reactions also can take place producing unwanted radio contaminants. Presence of the very long lived technetium radionuclides may not influence critically the quality of the SPECT images but can lower considerably the specific activity of the ^{99m}Tc product.

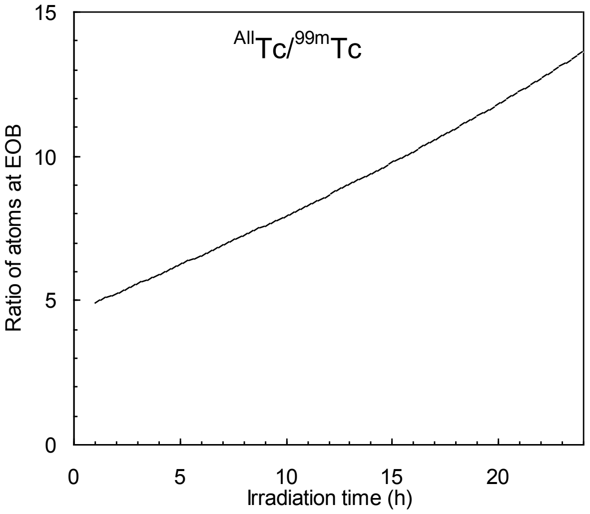

FIG. 10. The relative number of other co-produced Tc radionuclides is increasing with longer irradiation time calculated for E_p=17MeV bombardment.

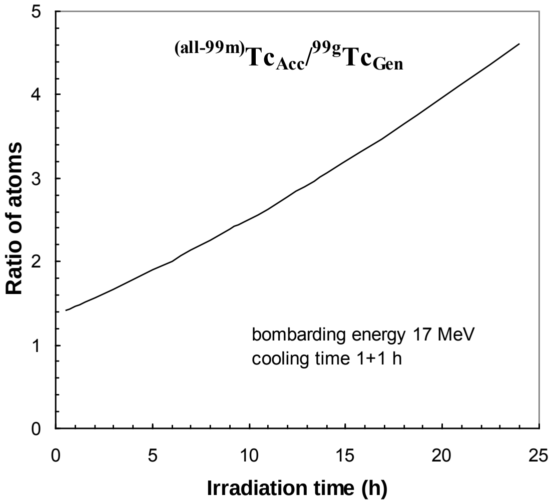

FIG. 11. Relative number of contaminating Tc atom for same amount of accelerator and generator produced ^{99m}Tc. (Ep=17MeV, 2h of cooling time after EOB).

In Table 5 the relative amount of co-produced Tc radionuclides are collected for different irradiation conditions.

TABLE 5. RELATIVE AMOUNT OF TC RADIONUCLIDES IN THE TARGET AT EOB AFTER 6 H IRRADIATION FOR DIFFERENT ENRICHMENT LEVELS OF THE TARGET

Energy MeV	^{99m}Tc	^{99g}Tc	^{98}Tc	^{97m}Tc	^{97g}Tc	^{96m}Tc	^{96g}Tc	^{95m}Tc	^{95g}Tc	^{94m}Tc	^{94g}Tc	^{93m}Tc	^{93g}Tc	total
	enriched 1													
17	1	5.14	0.06	2E-02	8E-02	4E-05	5E-04	7E-05	2E-04	2E-05	2E-04	1E-06	3E-05	5.3
24	1	4.92	1.90	2E-02	1E-01	1E-03	2E-02	9E-05	3E-04	1E-05	2E-04	4E-06	8E-05	7.0
26	1	4.91	2.82	2E-02	1E-01	2E-03	4E-02	1E-04	4E-04	1E-05	2E-04	4E-06	1E-04	7.9
32	1	4.96	4.73	1E-01	9E-01	6E-03	1E-01	6E-04	4E-03	2E-05	3E-04	6E-06	1E-04	10.9
	enriched 2													
17	1	5.14	0.01	4E-03	1E-02	7E-06	9E-05	6E-05	2E-04	2E-05	2E-04	1E-06	3E-05	5.2
24	1	4.92	1.87	4E-03	2E-02	2E-04	3E-03	4E-05	2E-04	2E-05	3E-04	4E-06	8E-05	6.8
26	1	4.91	2.79	4E-03	2E-02	4E-04	6E-03	5E-05	2E-04	2E-05	3E-04	4E-06	1E-04	7.7
32	1	4.96	4.70	1E-01	8E-01	1E-03	1E-02	1E-04	7E-04	2E-05	3E-04	6E-06	2E-04	10.6

Enriched 1: ^{100}Mo 97.39%, ^{98}Mo 2.58%, ^{97}Mo 0.01%, ^{96}Mo 0.005%, ^{95}Mo 0.005%, ^{94}Mo 0.005%, ^{92}Mo 0.005%
Enriched 2: ^{100}Mo 99.54%, ^{98}Mo 0.41%, ^{97}Mo 0.0016%, ^{96}Mo 0.0012%, ^{95}Mo 0.0076%, ^{94}Mo 0.0051%, ^{92}Mo 0.006%.

5. TARGET CONSIDERATIONS

It is a technical and technological challenge to design and build a target of enriched ^{100}Mo that can withstand and dissipate the large power transferred by the high intensity proton beam. As basic requirements the target should have large surface, an optimized thickness, good cooling and glancing irradiation geometry.

The highly enriched, expensive ^{100}Mo target material should be recovered and use again after suitable cooling time and proper target preparation. For any very strict target technology the change of the isotopic composition of the enriched material is unavoidable. For E_p=17 MeV bombarding proton energy the required amount of target material is about 2.8 10^{21} atoms/cm2 (for a target thickness correspond to energy loss of the proton beam of E_p=(17 – 7.8)MeV, dx=430 μm). In an E_p=17MeV and 3h irradiation cycle the number of reactions occurs on the ^{100}Mo content of the target is estimated to be 1.5 10^{14} 1/μA.
Supposing a beam intensity of I_p=100μA the number of reactions that takes place on the ^{100}Mo target isotopes is in the order of 10^{16} during each 3h irradiation. That is 5 orders of magnitude less than the number of ^{100}Mo atoms in the target. However, during successive reuse and irradiation of the same target material under the same irradiation conditions the small changes are accumulating and the isotopic composition of the target gradually changes. In figures 12a and 12b the estimated small relative changes of the target composition is shown.

TABLE 6. ESTIMATED METALLIC ^{100}MO TARGET THICKNESS AT DIFFERENT BOMBARDING PROTON ENERGIES OPTIMIZED FOR ^{99m}Tc PRODUCTION THRESHOLD ENERGY 7.8MeV

Beam energy	Range of particles	Projected range	Optimized target thickness
		at 10 degree	at 10 degree
(MeV)	(µm)	(µm)	(µm)
17	594	103	74
24	1069	186	157
26	1226	213	184

Reactions can take place on all of the stable Mo isotopes in the target. The amount of the different Mo target isotopes is decreasing mainly by the production rate of the (p,xn) reaction and increasing by the production rate of the (p,pxn) reactions and by the decaying rate of the corresponding mother radionuclides. Since the cross section of the (p,xn) reactions is generally higher than the cross section of the (p,pxn) reactions an overall decrease can be expected in the amount of the different Mo target isotopes. Considering that the amplitudes of the (p,xn) reactions on the neighboring mass Mo isotopes are quite similar the amount of each minor Mo target isotope have about the same negative changing rate except for the ^{97}Mo and ^{96}Mo which are fed by the (p,α) and (p,αn) reactions on ^{100}Mo respectively through the decay of the corresponding Nb radionuclides and therefore have positive changing rate. The large positive "gain" of the ^{97}Mo target isotope can be explain by the ^{100}Mo(p,α)^{97}Nb reaction, which occurs on the most abundant stable ^{100}Mo isotope in the target.

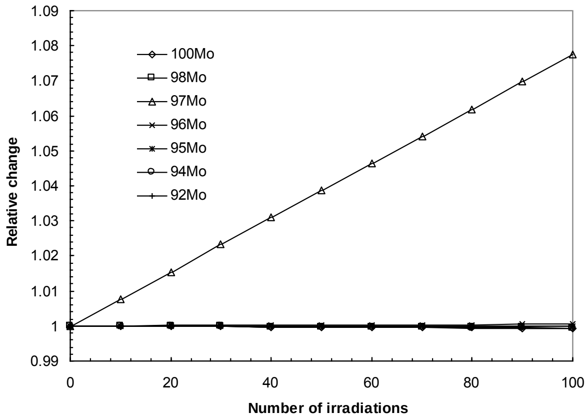

FIG. 12a. The relative change of the amount of different Mo target isotope as function of number of irradiations. Large positive change can be expected for ^{97}Mo.

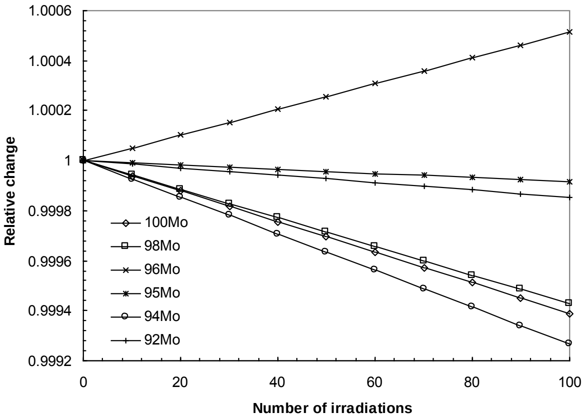

FIG. 12b. The relative change of the amount of different Mo target isotope as function of number of irradiations. ^{96}Mo has a positive change while ^{92,94,95,98,100}Mo are decreasing.

The change in the target composition would slightly affect the isotopic composition, specific activity and relative dose of the final ^{99m}Tc product. However, compensating the mass loss, which occurs during reprocessing, by adding fresh enriched target material the overall change will be even less significant. Beside the slow change in the isotopic composition of the enriched target material a gradual increase of the amount of Ru, Nb and Zr as chemical contaminations is also expected as function of successive irradiations.

6. SUMMARY AND CONCLUSIONS

- The available experimental data sets for the ^{100}Mo(p,2n)^{99m}Tc and ^{100}Mo(p,x)^{99}Mo reactions are not in good agreement and may contain systematic errors.
- New experimental cross section data with higher confidence level were established.
- Two experiments were performed and one re-evaluated in well controlled circumstances and the shape and amplitude of the ^{100}Mo(p,2n)^{99m}Tc reaction was confirmed relative to the ^{nat}Ti(p,x)^{48}V monitor reaction.
- The new proposed cross section data were crosschecked in a thick target yield benchmark experiment and very good agreement was found.
- A Reaction Network Calculation Tool (RNCT) was developed in MS Excel format to model and study the accelerator production of ^{99m}Tc.
- All possible production routes were considered in the calculation.
- Contribution of different production routes leading to the formation of the same reaction product is summed up when estimating the final number of reaction products present in the target.
- For indirect or decay production routes decay chains up to 5 levels are considered.
- No approximations were used and no processes were neglected, instead the well known exact mathematical formulae describing the formation and decay of stable and radioactive reaction products during irradiation and cooling periods were applied in the calculation.
- The actual differential equations were solved analytically by direct integration.
- The list of the possible isotopes produced during irradiation was mapped and beside the production of different Tc isotopes production of Ru, Mo, Nb and Zr isotopes were also considered in the calculation.
- For limiting the number of reactions included in the calculation an upper limit, $E_{threshold}$=30MeV, was set for the reaction threshold energies.
- Updated nuclear decay data of the ^{99}Tc-^{99}Mo pair were included in the calculation tool.
- Experimental cross section data are not available for all the reactions involved in accelerator production of ^{99m}Tc.
- Excitation functions provided by nuclear model calculations based on the TALYS code and appropriate input parameters agree with the experimental data of (p,xn) reactions quite well, but reactions with gamma or complex particles in the exit channel, like (p,γ), (p,αn), etc., are not described so well.
- Highly enriched ^{100}Mo as target material is needed for accelerator production of ^{99m}Tc to reduce the amount of contaminating technetium in the product.
- A target thickness which corresponds to the proton range from bombarding energy down to E_p=7.8MeV, to the threshold energy of the ^{100}Mo(p,2n)^{99}Tc reaction is considered to minimize the amount of unwanted activity and minimize the amount of necessary target material.

- Contribution by indirect production of ^{99m}Tc by decay of ^{99}Mo is low.
- The bombarding proton energy for production of ^{99m}Tc can be set to around 17 MeV below the threshold energy of the ^{100}Mo(p,3n)^{98}Tc reaction.
- About 5 times more ^{99g}Tc than ^{99m}Tc radionuclides are present in the target at EOB
- The ^{99g}Tc / ^{99m}Tc atom ratio is almost independent of the bombarding energy
- The numbers of contaminating Tc atoms, other than ^{99g}Tc, are increasing rapidly with bombarding energy above 25 MeV.
- The ^{99g}Tc / ^{99m}T atom ratio is higher for accelerator produced ^{99m}Tc than for the standard ^{99}Mo/^{99m}Tc generator eluted every 24-h
- Calculations show that in any circumstances the total amount of contaminating Tc radionuclides in accelerator produced ^{99m}Tc is higher than in the same amount of generator produced ^{99m}Tc based on 24 h elution intervals.
- The higher contamination level may affect the preparation of ^{99m}Tc-chelates.
- Activity of the contaminating Tc impurities in accelerator produced ^{99m}Tc can be several orders of magnitude higher than the activity of Tc impurity in the generator produced case. It very much depends on the composition of the target material, beam energy, irradiation and cooling times.
- Lower bombarding energy reduces the level of radio contaminating isotopes.
- Short irradiation with maximal beam intensity result in less radio contamination of the ^{99m}Tc product.
- The expensive ^{100}Mo target material should be handled centralized.
- Considering that the ^{99m}Tc has $T_{1/2=}$6.01h half-life the fraction of ^{99m}Tc in the target is decreasing after EOB therefore relatively quick post irradiation processing is required.
- Production should be made on daily basis and transport of the ^{99m}Tc product should be organized properly which would require good logistic.
- Proper recovery method should be developed for reuse of the expensive ^{100}Mo enriched material.
- Successive irradiations slowly change the composition of the original target material by changing the amount of initial Mo isotopes and reducing the amount of ^{100}Mo.
- The largest relative change can be expected in the amount of ^{97}Mo isotope.
- The change in target composition slowly would affect the isotopic composition, relative activity and relative dose of the final product.
- Successive irradiations gradually build up the amount of Ru, Nb and Zr elements in the target up to 100 ppm levels which may invoke additional chemical treatments to purify the recycled target material.

As a general conclusion regarding accelerator production of ^{99m}Tc: To provide the required amount of ^{99m}Tc activity in a possible best quality the shortest irradiation time with minimized beam energy and maximized beam intensity with short post irradiation processing time should be applied.

References

[1] INTERNATIONAL ATOMIC ENERGY AGENCY, Non-HEU Production Technologies for Molybdenum-99 and Technetium-99m, Nuclear Energy Series: No. NF-T-5.4, IAEA, Vienna (2013).

[2] INTERNATIONAL ATOMIC ENERGY AGENCY, Technetium-99 Radiopharmaceuticals: Status and Trends, IAEA Radioisotope and Radiopharmaceuticals Series, No. 1, IAEA, Vienna, 2009.

[3] OECD, The supply of Medical Radioisotopes: Review of Potential Molybdenum 99/Technetium-99m Production Technologies, NEA, Nuclear development, November 2010, Paris.

[4] NATIONAL RESEARCH COUNCIL, Medical Isotope Production Without Highly Enriched Uranium, Washington, DC: National Academies Press (2009) 69.

[5] BÉNARD, F., BUCKLEY, K.R., RUTH, T.J., ZEISLER, S.K., KLUG, J., HANEMAAYER, V., VUCKOVIC, M., XINCHI HOU, CELLER, A., APPIAH, J-P., VALLIANT, J., KOVACS, M.S., SCHAFFER, P., Implementation of Multi-Curie Production of ^{99m}Tc by Conventional Medical Cyclotrons. Journal of Nuclear Medicine, **55** (2014) 1017-1022.

[6] TAKÁCS, S., SZŰCS, Z., TÁRKÁNYI, F., HERMANNE, A., SONCK M., Evaluation of proton induced reactions on ^{100}Mo: new cros ssections for production of ^{99m}Tc and ^{99}Mo, J.Radioanal.Nucl.Chem. **257** (2003) 195–201.

[7] TAKÁCS, S., HERMANNE, A., DITRÓI, F., TÁRKÁNYI, F., AIKAWA, M., Reexamination of cross sections of the ^{100}Mo(p,2n)^{99m}Tc reaction, Nucl. Instr. Meth. B **347** (2015) 26-38.

[8] QAIM, S.M., SUDÁR, S., SCHOLTEN, B., KONING, A.J., COENEN, H.H., Evaluation of excitation functions of ^{100}Mo(p,d+pn)^{99}Mo and ^{100}Mo(p,2n)^{99m}Tc reactions: Estimation of long-lived Tc-impurity and its implication on the specific activity of cyclotron-produced ^{99m}Tc, Applied Radiation and Isotopes **85** (2014) 101–113.

[9] KONING, A.J., ROCHMAN, D.**,** TENDL-2013: TALYS-based Evaluated Nuclear Data Library. Nuclear Research and Consultancy Group (NRG) Petten, The Netherlands, Release date: December 23, 2013, URL: http://www.talys.eu/tendl-2013/.

[10] NUCLEAR STRUCTURE AND DECAY DATA ON-LINE LIBRARY, Nudat 2.6, National Nuclear Data Center, Brookhaven National Laboratory, USA, URL: http://www.nndc.bnl.gov/nudat2/.

[11] Q-value Calculator (QCalc), http://www.nndc.bnl.gov/qcalc/.

[12] BÉ, M.M., CHISTÉ, V., DULIEU, C., CHECHEV, V., KUZMENKO, N., HELMER, R., NICHOLS, A., SCHÖNFELD, E., DERSCH, R., Monographie BIPM-5, Table of Radionuclides, Vol. **1**, A=1 to 150, 2004, Ed. BIPM, France.

[13] WIESER, M.E., BERGLUND, M., Atomic weights of the elements 2007, Pure Appl. Chem., Vol. **81**, No. 11, (2009) 2131–2156, doi:10.1351/PAC-REP-09-08-03 (IUPAC Technical Report).

[14] NATIONAL NUCLEAR DATA CENTER, Brookhaven National Laboratory, based on ENSDF http://www.nndc.bnl.gov/nudat2/reCenter.jsp?z=42&n=57.

[15] GAGNON, K., BÉNARD, F., KOVACS, M., RUTH, T.J., SCHAFFER, P., WILSON, J.S., MCQUARRIE, S.A., Cyclotron production of ^{99m}Tc: Experimental measurement of the ^{100}Mo(p,x)^{99}Mo, ^{99m}Tc and ^{99g}Tc excitation functions from 8 to 18 MeV, Nucl Med Biol. **38** (2011) 907-916.

CYCLOTRON PRODUCTION OF ^{99m}Tc AND DEVELOPMENT OF A NEW METHOD OF SEPARATION OF $^{99m}TcO_4^-$ FROM THE IRRADIATED MOLYBDENUM TARGET

MALAY KANTI DAS[a], MADHUSMITA[a], SANKHA CHATTOPADHYAY[a], SUJATA SAHA DAS[a], MD. NAYER ALAM[a], LUNA BARUA[a], ANIRBAN DE[b], UMESH KUMAR[a], SIDDHARTHA DATTA[c]

[a]Radiopharmaceuticals Laboratory, Regional Centre, Board of Radiation and Isotope Technology (BRIT), Variable Energy Cyclotron Centre (VECC), Kolkata – 700 064, India

[b]Accelerator Technology Group, Variable Energy Cyclotron Centre, Kolkata – 700 064, India

[c]Chemical Engineering Department, Jadavpur University, Kolkata-700 032, India

Abstract

The direct production of ^{99m}Tc through (p, 2n) reaction on a natural molybdenum target was investigated. Extrapolated thick target yield for 1h, 3h and 6h irradiation as a function of incident proton energy (upto 20MeV) was calculated from the irradiated natural molybdenum targets. Separation of technetium radionuclide from the irradiated ^{100}Mo target by a new method using Dowex-1 ion exchange resin as well as well as by the standard solvent extraction (with methyl ethyl ketone) method was studied. The quality of the final pertechnetate solution was assessed. Recovery of target material as molybdenum trioxide has been achieved and preliminary experiment on reduction of ammonium molybdate to metallic Mo with hydrogen at high temperature was carried out.

1. INTRODUCTION

It is known that ^{99m}Tc is the most important radioisotope used in the preparation of radiopharmaceuticals for diagnostic nuclear medicine. More than 80% of the administered radiopharmaceuticals are prepared from this radioisotope. Traditionally, ^{99m}Tc is being obtained indirectly from a radioisotope generator, ^{99}Mo/^{99m}Tc, by the decay of its parent radioisotope, ^{99}Mo. The major amount of ^{99}Mo used to make the generators is produced by fission of ^{235}U in a nuclear reactor. Five old reactors (NRU of Canada, HFR of Netherlands, BR2 of Belgium, Safari-1 of South Africa and Osiris of France) meet almost entire global demand of ^{99}Mo. Because of the steady supply of ^{99}Mo (and hence ^{99m}Tc) over the years from these reactors, production of ^{99m}Tc by the direct route via the ^{99}Mo(p, 2n)^{99m}Tc reaction in a cyclotron did not gain sufficient importance, though the production of large amount of ^{99m}Tc by this route was demonstrated long back [1]. The renewed interest to study this production route as an alternate source of ^{99m}Tc started only a few years back when the nuclear medicine community faced the scarcity of ^{99m}Tc due to planned and unplanned shutdown of a couple of reactors (NRU, Canada; HFR-Patten, Netherlands) which were used to meet the major share of global demand of ^{99}Mo. So, the researchers started to study thoroughly the various aspects of ^{99m}Tc production in a cyclotron. Research activities in this direction include the study of the excitation function of ^{99m}Tc and other isotopic and nonisotopic active/stable isotopes produced concurrently by proton induced reactions on Mo target [2, 3, 4, 5 , 6 , 7 , 8 , 9 , 10], development of a target irradiation system which can utilize high beam current [11], development of a fast chemical separation method [12, 13 , 14], recovery of ^{100}Mo from the irradiated target [15] and assessment of the directly produced ^{99m}Tc for the preparation of radiopharmaceuticals [9,12]. It may be noted that various isotopes of Nb, Zr and Y could be produced at trace level (3, 8, 10, 15) when enriched ^{100}Mo is irradiated with proton beam. The amount of these impurity isotopes produced depends on the enrichment level of ^{100}Mo used for irradiation as well as beam energy. Radioisotopes of Nb and Zr further decays and ultimately produce stable isotope of Mo, Zr and Y. While Zr, Nb and Y can be separated from the irradiated ^{100}Mo target, it is not possible to separate the Mo isotopic impurities by chemical means due to the obvious reason. Since these Mo isotopic impurities are the decay products of some of the directly or indirectly produced Nb radioisotopes (e.g.^{100}Mo (p, α)^{97}Nb→^{97}Mo) , it is possible to control their level, to some extent, if irradiation of shorter duration at high current is used for ^{99m}Tc production and a fast chemical separation of Nb, Zr and Y radioisotopes from the recovered ^{100}Mo solution (obtained after the chemical separation of ^{99m}Tc from the irradiated target) are practised. It may be noted that even the use of purest ^{100}Mo will induce ^{97}Mo impurity in the recovered ^{100}Mo through the concomitant nuclear reaction, ^{100}Mo(p, α)^{97}Nb→^{97}Mo (Half life of ^{97}Nb is 72.1 min) In the present work the authors have studied the yield of ^{99m}Tc produced from the proton irradiation of a natural molybdenum metal target as a function of incident proton energy, developed a new method of separation of the Tc radioisotopes from the irradiated natural molybdenum target, assessed the quality of the TcO_4^- in general and its radionuclidic purity (RNP) in particular as a function of time after the chemical separation of ^{99m}Tc from proton irradiated ^{100}Mo target, recovered molybdenum from the irradiated target and purified it from nonisotopic contaminants and reduced ammonium molybdate to metallic molybdenum with hydrogen at high temperature.

2. EXPERIMENTAL

2.1. Materials

Reagents such as hydrochloric acid, nitric acid, ammonium carbonate, sodium hydroxide pellets, hydrogen peroxide etc., were of analytical grade and were procured from E. Merck, India. Mo foils and Cu monitor foils were purchased from H. Cross Co. NJ 07074, USA, and Material Research Corporation, New York, USA, respectively. Anion exchanger: Dowex-1x8 (Cl^- form, 200–400 mesh), capacity 3–5 meq/g of dry the resin and natural Mo metal powder (<150 μm, 99.99%) were purchased from Sigma Chemical Co. St. Louis, MO. 63174, USA. Aluminium oxide, active basic and acidic (100–200 mesh), Brockman grade-1 (Prabhat Chemicals, Mumbai, India) were used in preparing the purification columns. [^{99}Mo]Na_2MoO_4 in 5N NaOH (150mg Mo/ml: 1.11–2.22 GBq/ml) used in optimizing the separation of ^{99m}Tc from ^{99}Mo and the cold kits (MDP and MIBI) were obtained from the Radiopharmaceutical Division, BARC and BRIT, Mumbai, India. Enriched ^{100}Mo (99.805%) was obtained from Isoflex, USA, San Francisco, CA 94129, USA and its isotopic composition is shown in Table-1.

TABLE 1. ISOTOPIC COMPOSITION OF ENRICHED Mo

Isotope	Abundance, %
^{100}Mo	99.805
^{98}Mo	0.170
^{97}Mo	0.005
^{96}Mo	0.005
^{95}Mo	0.005
^{94}Mo	0.005
^{92}Mo	0.005

Zr metal was purchased from H. Cross Co. NJ 07074, USA. Paper chromatography (PC) strips (3 MM Chr, 20 mm width) were purchased from Whatman International Limited, England.

2.2. Target preparation

Two types of targets were irradiated. For irradiation at low beam intensity and for short duration, natural Mo foils (25micron) in a stack (containing 4-7 foils, 10mm x 10mm, with an 8-10 micron thick natural Cu monitor foil placed just before the first Mo foil) were used. Circular (10 mm diameter) ^{nat}Mo & ^{100}Mo metal pellet targets were used in the irradiations of longer duration and at higher beam intensities (upto 3µA). These Mo pellets were prepared by pressing about 400-500mg natural or enriched Mo metal powder in a dice plunger at 980MPa pressure. Zr-metal pallet was prepared by pressing about 350mg natural Zr metal powder in a dice plunger at 980MPa pressure.

2.3. Target irradiation

All the irradiation experiments were carried out with 16/18/20 MeV protons using the cyclotron of Variable Energy Cyclotron Centre (VECC), Kolkata. The beam current was measured by placing a natural copper monitor foil (8-10 mg/cm^2 thick) in front of the target. For beam current measurement the ^{nat}Cu(p, x)^{62,63,65}Zn cross-section data recommended by International Atomic Energy Agency [16] were used. In case of Mo-foil stack irradiation, stacks containing 4-7 ^{nat}Mo foils (each 25 micron thick) were irradiated with a proton beam (energy window: 8-20 MeV, current: 10-250nA) for 1-5 minutes. In order to irradiate the stacked foil targets at lower incident beam energy, 100µm, 200 µm, 300 µm, 400 µm, thick Mo foils were used in between the Cu monitor foil and the Mo stack, to degrade the proton energy from 20/18/16 MeV to a lower value. The actual "on target" beam energy falling on the individual foil in a stack was determined using the energy-range formula and tables [17].The radioactivity in each Mo foil in the stack was assessed 1.5h after the end of irradiation (EOI). ^{nat}Mo pellet (about 400mg) targets irradiated at 1-3 µA, 16/18MeV beam intensity for 1- 6 hour were used to standardize the chemical separation of Tc-radionuclides from Mo and other co-produced non-isotopic impurities (e.g. radioisotopes of Nb , Zr or Y)) and to study the recovery of Mo from the irradiated target. ^{100}Mo metal pellets were irradiated at 18MeV. RNP of the ^{99m}Tc obtained from the enriched Mo target was studied as a function of time.

For the preparation of Nb, Zr and Y radiotracers, Zr-metal pallet (1mm thick, w=0.301gm) was irradiated in the in-house cyclotron of the Variable Energy Cyclotron Centre (VECC) with 18MeV, 1µA proton beam for 22hrs.

2.4. Gamma ray spectrometry

The radioactivity of samples was measured on a 30cc HPGe detector coupled to an ORTEC 92X Spectrum master and a personal computer loaded with ORTEC Maestro II software. The detector used had 10% efficiency relative to a 3″ × 3″ NaI(Tl) detector and an energy resolution (FWHM) of 1.74 keV at the 1332 keV γ-peak of ^{60}Co. A standard ^{152}Eu source was used for the energy as well as for the efficiency calibration. The radionuclides were identified by their characteristic photo peaks and half-lives. In order to avoid any interference of counts from the same gamma energy of another radioisotope, carefully selected characteristic gamma energies of the respective radioisotopes were used for the activity measurement. The gamma energies used for the radioactivity measurement of different radioisotopes are listed in Table 2. All the nuclear data of these radioisotopes used for calculation were taken from the available reference [18]. The radioactivity measurement of all the radioactive samples was carried out at a suitable distance (0.5-25cm) from the detector so that the dead time is below 10%. Total error in the yield was estimated in the standard way: the independent errors of the linearly contributing processes (beam current measurement-8%, statistical error in the counting-4% and uncertainty in the sample geometry-5%) were summed quadratically and the square root of the sum was taken. Thus, the total error estimated in the yield was about 10.2%.

TABLE 2. NUCLEAR DATA USED IN ESTIMATION OF VARIOUS RADIOISOTOPES

Radionuclide	$t_{½}$	E_γ(keV)	I_γ(%)
^{62}Zn	9.193 h	596.56	26.
^{63}Zn	38.47 min	669.62	8.2
^{65}Zn	243.93 d	1115.539	50.04
^{99m}Tc	6.0067 h	140.511	89.022
^{99}Mo	65.976 h	181.068	6.14
		739.500	12.26
^{96}Tc	4.28 d	812.54	82
^{95}Tc	20.0 h	765.789	93.8
^{95m}Tc	61 d	204.117	63.2
^{94}Tc	4.883 h	702.7	99.6
^{94m}Tc	52 min	1868.68	5.7
		1522.1	4.5
^{93}Tc	2.75 h	1362.94	66.2
^{92m}Nb	10.15 d	934.44	99.15
^{95m}Nb	3.61 d	235.69	24.8
^{95g}Nb	34.99 d	765.80	99.8
^{95}Zr	64.03 d	756.72	54.38
^{88}Y	106.626 d	898.0	93.7

Direct counting of foils irradiated for short duration:

Radioactivity in the irradiated foils were measured about 1.5h after the EOI in order to estimate the activity of the radioisotopes having shorter half-life (e.g. ^{94m}Tc having $t_{½}$ 52 min). Typical assay live times were 300 sec for these samples. The radioactivity in the same irradiated foils were also measured for a longer duration and at a closer distance from the detector at different time points post irradiation in order to obtain a better counting statistics of those radioisotopes having longer half-lives. It is known that if the decay of the radioisotope during the measurement time is ignored, it will result in inaccuracy in radioactivity measurement. It has been calculated that when the measurement time duration is significantly longer compared to the half-life of the radioisotope (i. e. when duration of assay live time is larger than about 3/100th of the half-life of the radioisotope being assayed) the error in the activity estimation is increased beyond 1%. In such situation the actual activity at the start of measurement was calculated using the following formula:

$$A_{SOC} = \frac{c\,\lambda\,t_R}{(1-e^{-\lambda t_R})\varepsilon_\gamma I_\gamma t_L}$$

where, A_{SOC} = activity of the sample counted at the start of counting, c = total count of the sample for time t_L, λ = decay constant of the radioisotope counted, ε_γ = detector efficiency for the particular gamma energy counted, I_γ = gamma ray intensity of the characteristic gamma peak of the radioisotope counted t_R = real time of counting, t_L = live time of counting.

From the radioassay data of each foil that was irradiated for 5 min, yields of various radioisotopes were calculated. Then by adding the yield of a particular radioisotope in successive foils, the cumulative yield (in 5 min irradiation) of that radioisotope in the thick target was calculated as a function of incident proton energy. From these data thick target yield for 1h, 3h or 6h irradiation was calculated using the following formula:

$$A_t = A_{t'} \frac{\phi\ (1-e^{-\lambda t})}{\phi'(1-e^{-\lambda t'})}$$

where A_t= activity at the end of 1h, 3h or 6h irradiation, $A_{t'}$ = activity at the end of 5min irradiation, λ=decay constant of the isotope under consideration, $\emptyset'$= proton flux during the 1h, 3h or 6h irradiation, $\emptyset$= proton flux during the 5min irradiation.

2.5. Target dissolution

Irradiated target was dissolved following a reported method [15]. The irradiated target was taken in a conical flask and 3ml H_2O_2 (30% w/w, E. Merck, India, Purified) was added to it and the flask was heated (50-60 ^oC) in a water bath. When the target reacted completely with H_2O_2, the flask was brought to room temperature and 1ml of 3M ammonium carbonate was added drop wise to yield a clear solution.

2.6. Preparation of the basic alumina column (required in MEK separation)

5g of dry basic alumina obtained commercially was used directly for making this column, 80mm (H) x 14mm (dia.).

2.7. Anion exchange resin column (7mm×1mm) preparation

A slurry of 15 mg Dowex-1 x 8, Cl^- resin in 2ml water was taken in a syringe and pushed into a polypropylene tube (internal diameter 1 mm, the other end of the tube was packed with some glass wool) to make the resin column. Both the ends of the tube were fitted with miniature barbed polypropylene fittings. The column was preconditioned by passing 10 ml of normal saline solution followed by washing with 5ml water.

2.8. Preparation of the acidic alumina column (required in Dowex-1-HNO_3 acid separation)

A slurry of 1.5g acidic alumina in 5ml water was poured into a glass column, 12mm (H) x 8mm (dia.), containing a sintered disc at the bottom. Excess liquid was drained off with the help of a vacuum pump and the column was washed thoroughly with 10ml saline. Both the ends of the column were closed with silicon rubber septa having a small hole at the centre for insertion of a needle. Care was taken to avoid entrapment of any air bubbles in the column bed. A liquid trap was connected in-line with the vacuum pump (purchased from Waters, Milford, USA) to prevent any accidental contamination of the pump.

2.9. Chemical separation of the Tc-radionuclides from the irradiated thick ^{nat}Mo target

2.9.1. Separation by MEK solvent extraction method

The solution obtained after the dissolution of the irradiated target was thoroughly agitated with 5ml MEK in a vortex mixer. After standing for few minutes, the two layers got separated. The upper organic layer containing the Tc radionuclides was collected with a pipette and passed through a basic alumina column to trap any Mo impurity present in the extracted organic layer. The aqueous layer containing the molybdenum target material was preserved for the recovery of molybdenum. Aliquots of the radioactive solution were taken from all the radioactive solutions handled before and after the separation for the estimation of separation efficiency using γ-ray spectrometry in an HPGe detector.

The chemistry of separation and recovery of ^{99m}Tc from Mo using methyl ethyl ketone (MEK) solvent extraction technique has been automated, named TCM-AUTOSOLEX (Technetium automated solvent extraction) generator and tested widely for the separation of ^{99m}Tc from (n,γ) ^{99}Mo [19]. Precise separation of aqueous phase from the organic phase was achieved by controlling with an indigenously developed conductivity detector. The evaporation of the organic phase was done in a temperature controlled water bath to prevent charring. The entire system has been automated and controlled by a user friendly PC based graphical user interface that actually supervises process via an embedded system based electronic controller (Fig.1 & Fig.2).

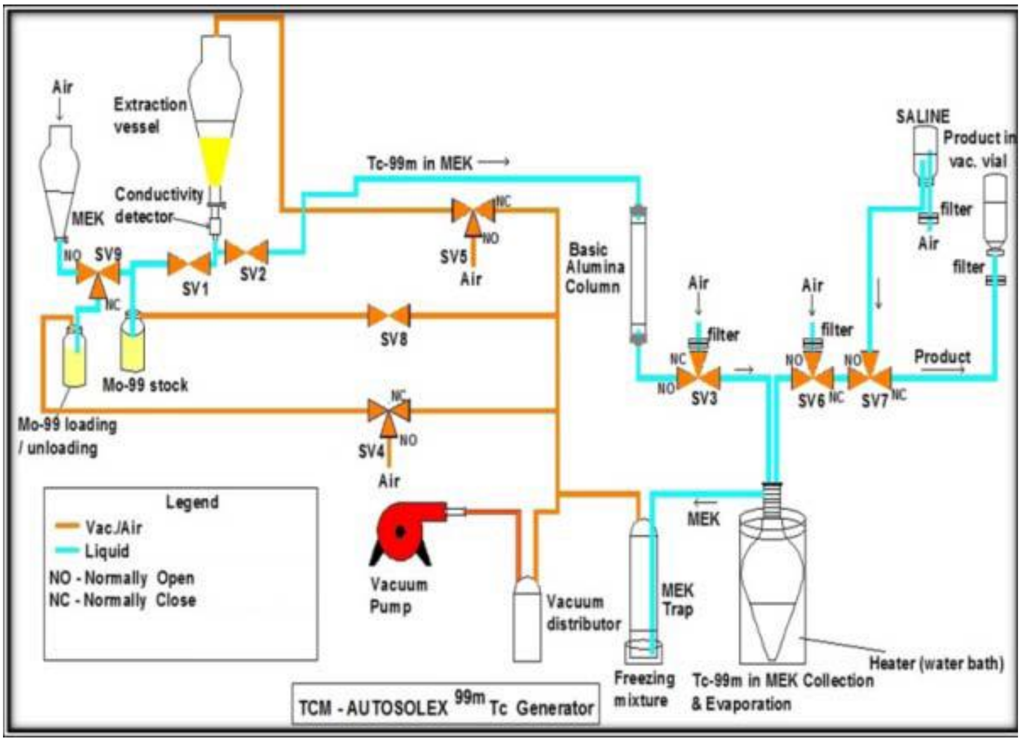

FIG. 1. Process diagram of TCM-Autosolex generator.

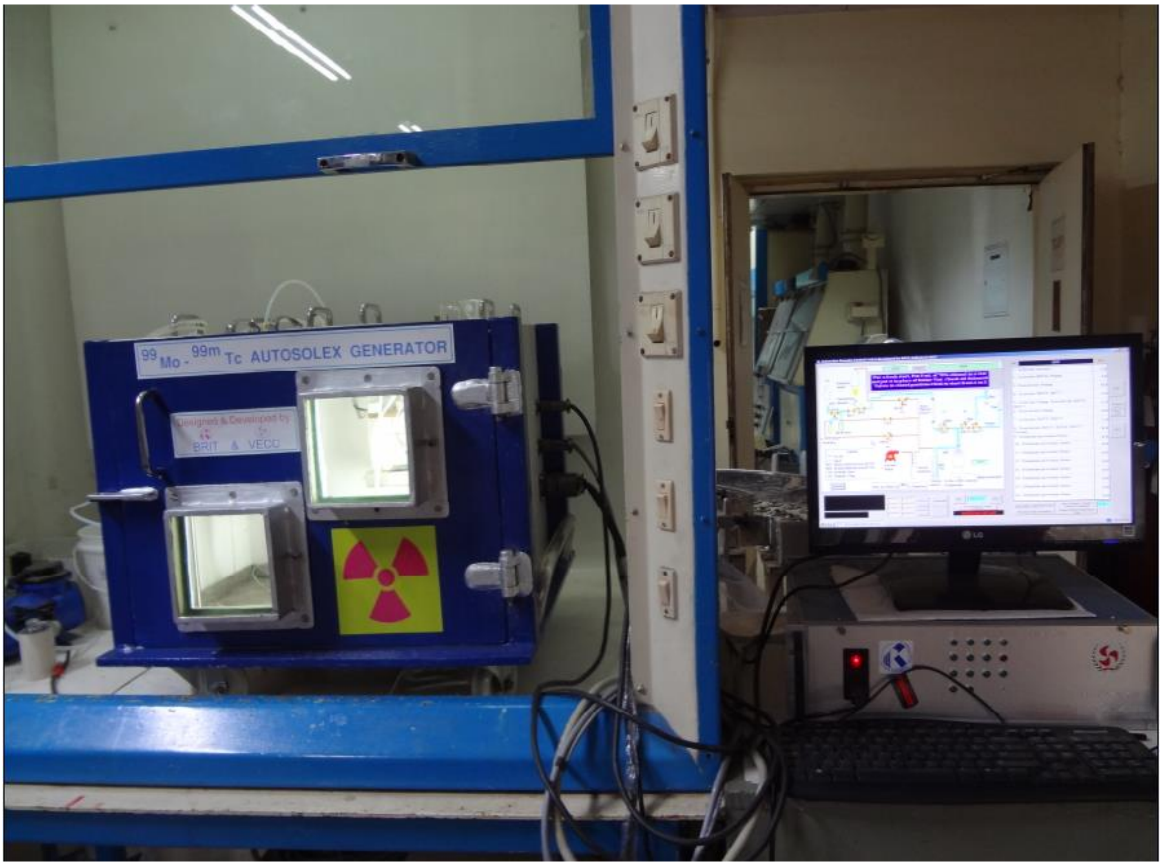

FIG. 2. TCM-AUTOSOLEX Separation Module.

2.9.2. Separation by Dowex-1 resin and HNO_3 method

The flowchart of this separation procedure is shown in Fig.3. In this method, at first with the help of a vacuum pump the molybdate/pertechnetate solution was allowed to pass through the resin column, which immobilized the pertechnetate and allowed the molybdate to flow. The molybdate solution was collected in the molybdenum collection vial.

The Mo line and the resin column were washed with 1ml of water and the washing was also collected in the molybdenum collection vial. The resin column was then washed with 5ml of water and the washing was collected in the waste collection vial. 4ml of 4M HNO_3 was passed through the resin column to elute ^{99m}Tc into the evaporation vial. The HNO_3 line & the resin column were washed with 1ml water and the washings were collected in the evaporation vial. The evaporation vial was then heated while a flow of air was passed through the HNO_3 acid line. HNO_3 was thus evaporated out completely and the evaporated HNO_3 was trapped in a NaOH bath. The evaporation vial was then cooled and the requisite volume (10ml) of saline was added. Sodium pertechnetate in saline thus obtained was passed through a small acidic alumina column (1.5g), a millipore filter (0.22μm) and then collected in a vacuum vial. This method was tried using both molybdate/pertechnetate radioactivity obtained from cyclotron target and reactor production of ^{99}Mo.

The chemistry of separation and purification of ^{99m}Tc based on Dowex-HNO_3 technique has been automated, named as TCM-AUTODOWNA (Fig. 4, & Fig, 5), which utilizes abundantly available ^{99}Mo(n,γ) produced by (n,γ) reaction in BARC reactors and also compatible for cyclotron produced ^{99m}Tc using enriched ^{100}Mo. The evaporation of nitric acid was done in a temperature controlled water bath under vacuum and collected in ice cooled sodium hydroxide trap. The entire system has been automated and controlled by a user friendly PC based graphical user interface that actually supervises process via an embedded system based electronic controller [20].

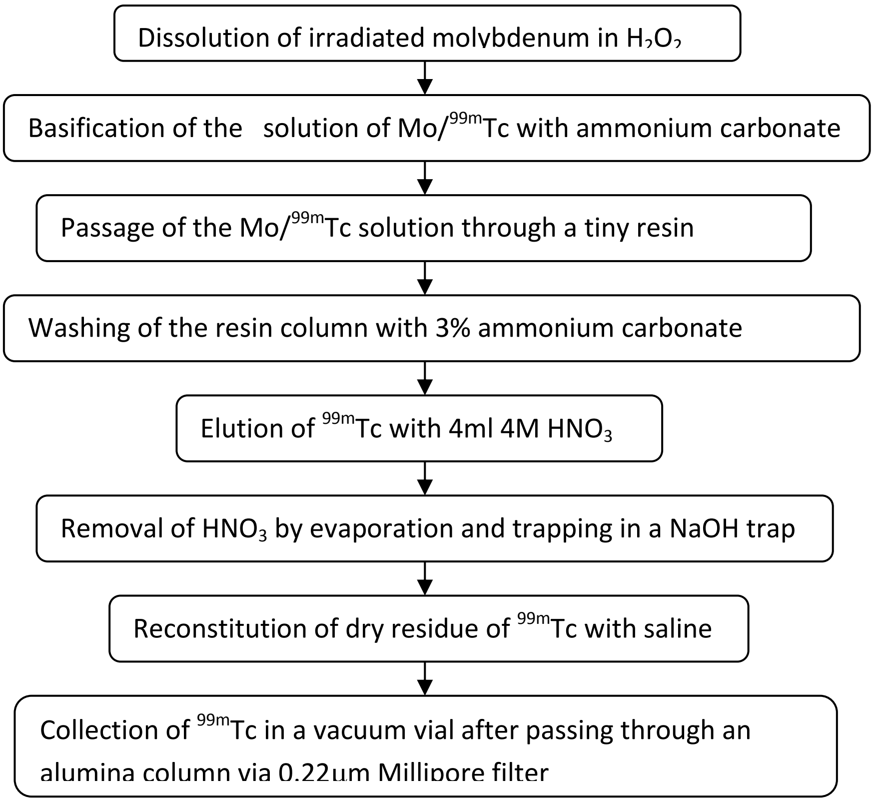

FIG. 3. Separation and purification of ^{99m}Tc from the irradiated molybdenum target using Dowex 1 column.

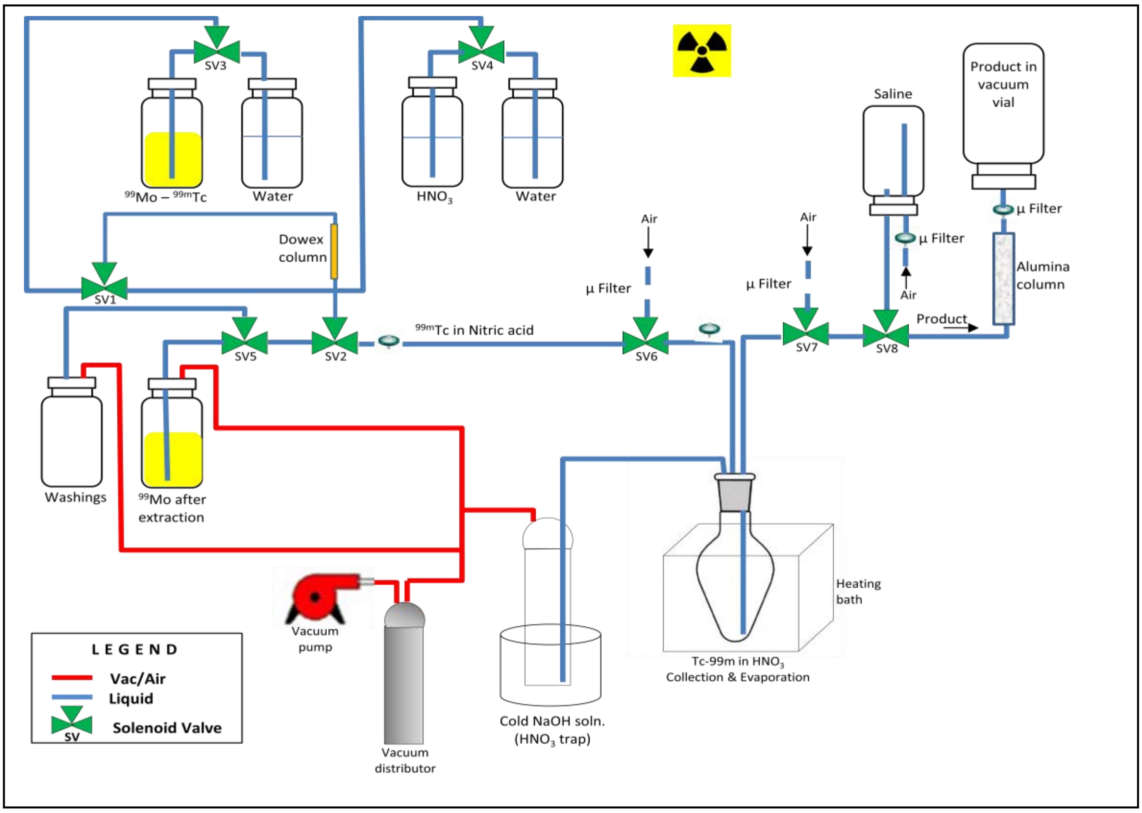

FIG. 4. Process diagram of TCM-AUTODOWNA

FIG. 5. ^{99m}*Tc-TCM-AUTODOWNA Module.*

2.9.3. Studies on Nb, Zr and Y contamination in the final ^{99m}*Tc preparation*

This particular experiment was carried out to study the path of Nb, Zr or Y isotopes in the two separation methods used. Nb, Zr or Y isotopes could be produced directly through various nuclear reactions on Mo isotope or indirectly through the decay of a particular radioisotope produced through a primary reaction; the amount of which depends on the energy of proton as well as the enrichment level of ^{100}Mo used. Moreover, the purest ^{100}Mo will produce ^{97}Nb ($t_{1/2}$= 74min) through ^{100}Mo (p, α) reaction.
For the present study, the ^{92m}Nb ($t_{1/2}$= 10.2d), ^{95}Nb ($t_{½}$= 3.61 d), ^{95}Zr ($t_{½}$=64d) and ^{88}Y($t_{½}$=106.6d) tracers required were produced in the cyclotron through the irradiation of a natural Zr metal pellet. One day after the end of the irradiation the target was dissolved in 10ml conc. HCl and 2ml HF. Diluted sample was prepared taking 0.1ml out of 12ml in 5ml 6M HCl. An aliquot from this stock solution was used mixes in the solution containing Mo (both natural Mo and ^{99}Mo) and ^{99m}Tc. The resultant solution was used to separate Mo and Tc. Both the Mo and Tc fractions were checked for the presence of Nb, Zr and Y radioisotopes.

2.10. MDP and MIBI Labelling

2ml of the radioactive Tc-pertechnetate solutions obtained from the two separation methods were added separately to the freeze-dried kit vials of MDP and MIBI. The ^{99m}Tc-MDP preparation vials were kept at room temperature for 10min while the ^{99m}Tc-MIBI preparation vials were kept in a boiling water bath for 10min for the completion of the labelling reactions.

2.11. Quality assessment tests

The radioactive pertechnetate solutions obtained from the two separation methods were checked for the clarity, pH, radionuclidic purity (RNP) and radiochemical purity (RCP).

The clarity of the solution was checked by visual inspection and pH was evaluated using a suitable pH indicating paper.

2.11.1. Radionuclidic purity (RNP) and radiochemical purity (RCP)

The RNP of the final product was estimated using a calibrated HPGe detector. The RCP of radioactive TcO_4^- solution was evaluated by paper chromatography using Whatman paper strip (10cm x 1cm) and MEK as mobile phase. Radionuclidic purity due to the presence of other Tc radioisotopes in the final ^{99m}Tc preparation was checked in an HPGe detector as a function of time by counting an aliquot of decayed ^{99m}Tc sample. The RCP of ^{99m}Tc-MDP was evaluated by developing the Whatman paper strip (10cm x 1cm), spotted with the sample, in MEK solvent and saline. The radiochemical purity of ^{99m}Tc-MIBI was evaluated by developing the Whatman paper strip (10cm x 1cm), spotted with the sample, in MEK solvent and ethanol.

2.11.2. Chemical purity

MEK, molybdenum and aluminium contents in the final radioactive TcO_4^- solution were determined by turbidity/color tests using iodoform, potassium thiocyanate and chromazural-S tests, respectively, as per BRIT, Mumbai, India monograph.

MEK content test: 200µl of 1N NaOH, 200µl of 0.1N I_2, 50 µl of the test solution and 150µl distilled water were taken in a test tube. The turbidity produced in the sample was compared with that of the standard (0.1% v/v).
Molybdenum content test: 50µl of the test sample, 50µl of 10% KCNS and 10% $SnCl_2$ were taken in a test tube. The orange-red colour produced in the sample was compared with that of the standard (10ppm).

Aluminium content test: 10µl of the test sample, 30µl of acetate buffer (0.1 M sodium acetate & 0.1 M acetic acid, pH = 4.6) and 10µl of chromazural-S (2.7 mM) were taken in a test tube. The reddish pink colour produced in the sample was compared with that of the standard(10ppm).

Nitrate (NO_3^-) content test: The level of nitrate ion in the final radioactive TcO_4^- solutionswas measured using colorimetric test strips (Merck, Germany,Cat. No. 1.10020.0001). This test strips measure the nitrate ion concentration semi-quantitatively by visual comparison of the reaction zone of the test strip with the fields of a colour scale which can measure 10-500 mg/l of NO_3^-.

Hydrogen Peroxide (H_2O_2) content test: Similarly, the presence of hydrogen peroxide in the final radioactive TcO_4^- solutionswas measured using colorimetric test strips (Merck, Germany, Cat. No. 1.10011.0001). This test strips measure the peroxide concentration semi-quantitatively by visual comparison of the reaction zone of the test strip with the fields of a colour scale, which can measure 0.5-25 mg/l of peroxide.

2.12. Recovery of Mo from the irradiated target

The aqueous fraction containing ammonium molybdate obtained after solvent extraction with MEK or the eluate obtained after passing the load solution through the resin column in the Dowex-1 resin and HNO_3 method can be used to recover the enriched target material. In order to standardize the Mo recovery, 500mg of Mo metal was dissolved as per the method described in section 2.5. To this solution 200µCi of ^{99}Mo was added. Then from this solution the ^{99m}Tc and ^{99}Mo fractions were separated by the two separation methods described above. Total ^{99}Mo activities in the solution before separation and in the Mo fraction obtained after separation were estimated. In the Mo fraction, molybdenum was present as ammonium molybdate. This fraction also contained some ammonium carbonate which was used during Mo metal dissolution step.

2.12.1. Conversion of molybdate to MoO_3

The Mo fraction obtained in each separation process was separately heated in a small vial. Care was taken to avoid any loss of this solution during heating. When all the solvent evaporated out, the dry residue obtained was heated for one hour at about 700 °C. The residue turned light yellow in colour after this heating step. On cooling, the colour of the residue turned gray. The weight of the dry powder obtained was recorded. It was also noted that, commercial MoO_3 also turned yellow on heating.

2.12.2. Characterization of recovered molybdenum compound by X-ray diffraction

Recovered MoO_3 was characterized by X-ray powder diffraction method. For the purpose of comparison, XRD was also performed on commercially available (Loba Chemie, Mumbai, India, GR grade) sample of MoO_3 (unheated and heated at 700°C). The crystalline phases of the powder were identified in the D8 Advance (Bruker, Germany) X-ray diffractometer using monochromatized Cu K_α source (1.5418 angstrom radiation).

2.12.3. Purification of recovered ^{100}Mo from possible non-isotopic contaminants

It has been noticed that in both the ^{99m}Tc and Mo separation methods employed in this study, traces of Nb, Zr or Y isotopes if present in the solution used before separation are collected in the Mo fraction. It is therefore advised to purify the recovered ^{100}Mo before recycling. Solvent extraction of Mo has been reviewed in literature [21]. It has been reported [22] that Mo can be extracted in diethyl ether with 80-90% yield from an acidic solution. We have developed a fast method of separation of Nb, Zr and Y isotopes from the ^{100}Mo solution (obtained after the separation of ^{99m}Tc directly produced) using the solvent extraction with ether in order to improve the purity of the recycled ^{100}Mo. The method is briefly described in the following paragraph.

The aqueous solution containing known amount of Mo that was preserved after ^{99m}Tc separation (as described above) was doped with ^{99}Mo, ^{95}Nb, ^{95}Zr and ^{88}Y and taken in a conical flask and evaporated to dryness (avoid overheating that may convert the molybdate to MoO_3). Then the residue was taken up in 9ml 10M HCl containing 6ml 30% H_2O_2 so that the resultant solution becomes 6M with respect to HCl. Mo was extracted from this solution with 15ml ether. The extraction step was repeated 5-6 times. All the ether fractions were pooled together in a conical flask. Aliquots of the radioactive solution handled before and after the separation were collected for the estimation of separation efficiency Mo from ^{95}Nb, ^{95}Zr and ^{88}Y tracer using γ-ray spectrometry in an HPGe detector. The ether phase was first evaporated to dryness and then heated strongly at about 700 °C for an hour to get MoO_3. Weight of the recovered MoO_3 was noted.

2.12.4. Preliminary studies on reduction of natural ammonium molybdate to Mo metal with hydrogen at high temperature

The reduction method of ammonium molybdate to molybdenum metal consists of three step process. In the first step, ammonium molybdate is converted into molybdenum oxide at 600°C for about 4hrs under atmospheric condition. In the second step, molybdenum oxide produced in the first step is reduced with 100% hydrogen atmosphere with a continuous flow rate of 0.5 litre per min at 1050°C for 6 hrs. Flushing of the furnace with nitrogen gas is essential before introduction of hydrogen to remove all air from the furnace. Finally, in the third step, the reduced metal produced in the second step is heated at 200°C in a vacuum furnace for about 2 hrs to remove traces of adsorbed moisture.

2.12.5. SEM and EDS analysis of the Mo sample obtained by the reduction of natural ammonium molybdate with hydrogen

SEM analysis of the reduced Mo powder has been carried out in Zeiss (model no. EVO50) Scanning electron microscope (made in Germany) to determine the particle size of the reduced Mo powder. Simultaneously, EDS analysis of the reduced Mo sample to check the purity of the conversion was performed in the said instrument supported by INCA EDS analysis software.

3. RESULTS AND DISCUSSION

3.1. Stacked foil irradiation: Thick target yield of ^{99m}Tc

Radioactivity of various Tc radioisotopes produced in each foils in the stacks, irradiated for 5min, was determined from the gamma spectrometry data. Then the yield of Tc radioisotopes in each foil for 5min irradiation with 1μA proton beam was calculated as a function of the incident proton energy (Fig. 6). From these data by adding up the radioactivity of the respective radioisotope in successive foils, the thick target yield (TTY) for 5 min irradiation with 1μA proton beam was calculated and plotted as a function of the incident proton energy (Fig.7).

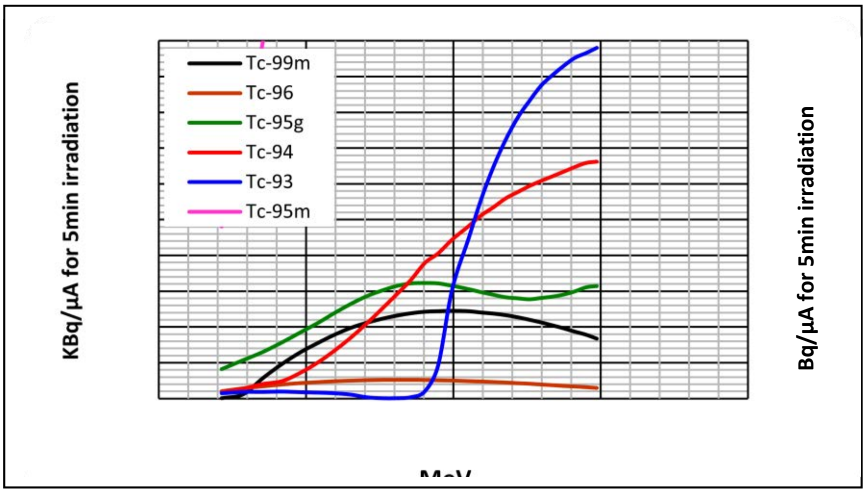

FIG.6. Yield of Tc radionuclides formed in individual 25 micron natural Mo foil in 5min irradiation with 1μA proton beam ^{95m}Tc activities are expressed in Bq/μA and follows the secondary axis.

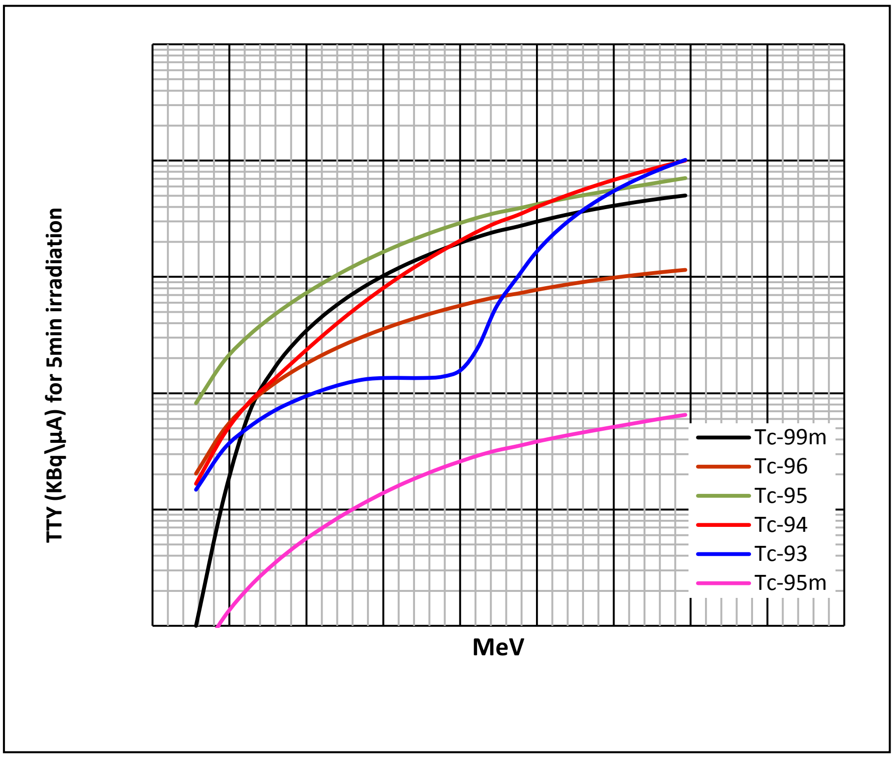

FIG.7. Thick target yield of Tc radionuclides formed in 5min irradiation of a natural Mo target with 1µA proton beam.

It may be noted that the direct production of all these Tc radioisotopes (except ^{99m}Tc) can take place through more than one channel. However, ^{99m}Tc can only be produced directly through ^{100}Mo(p, 2n) reaction. For this reason the experimental TTY data obtained from this study can be directly extrapolated for enriched ^{100}Mo target. The TTY of ^{99m}Tc thus calculated at the end of irradiation (EOI) for 100% enriched ^{100}Mo target for 1h, 3h, and 6h irradiations is represented in Fig.8 It is evident from this figure that if an 100% enriched ^{100}Mo target is irradiated at 20→8MeV, 100µA proton beam for 1h, 3h, and 6h, it will produce about 60, 160, 272 GBq of ^{99m}Tc at EOI, respectively.

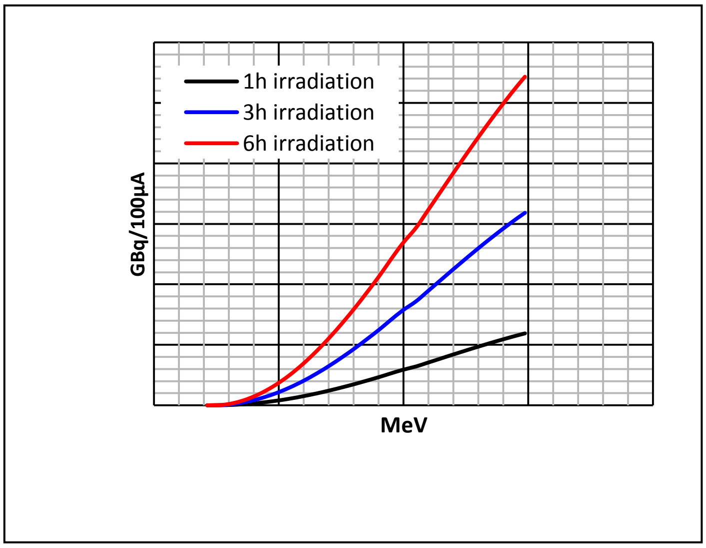

FIG.8.Thick target yield of ^{99m}Tc obtained (present work) from 1h, 3h & 6h irradiation of an enriched ^{100}Mo target with 100µA proton beam.

3.2. Chemical separation

3.2.1. Dowex-1 resin and HNO_3 method

In the new Dowex-1 resin and HNO_3 method, pertechnetate was bound efficiently (95%) and eluted from the resin with very high yield (90%). ^{99}Mo along with the non-radioactive molybdenum target material ended up in the waste stream. The overall yield of ^{99m}Tc in both the separation methods was about 80%.

3.3. Quality assessment of purified 99mTc

A challenge in the development of cyclotron produced ^{99m}Tc is to ensure that the quality of the final pertechnetate preparation to be equivalent to that obtained from a ^{99}Mo/^{99m}Tc generator.

At the end of the chemical separation, the product was evaluated for radionuclidic, radiochemical and chemical purity using the standard quality assessment protocols. The quality assessment results are summarized in Table 3. The radiochemical purity of the pertechnetate preparation was found to be 99%. The efficacy in labelling of MDP and MIBI with the pertechnetate solution obtained from either of the separation method was typically more than 95%.

In both the separation processes no ^{99}Mo was detected in the product vial containing radioactive TcO_4^-. It was found from the simulation studies that 99.8% Nb was removed in the washing process and 0.07% of initial amount of Nb was present in the eluted ^{99m}Tc obtained in the Dowex method. Nb peak was absent in the organic fraction obtained in the MEK solvent extraction process. Level of Zr and Y present in the final radioactive $^{99m}TcO_4^-$ obtained by the solvent extraction method was below the detection level. In the Dowex separation method Zr level in the eluted ^{99m}Tc was 2.5% of initial amount of Zr in the load solution. Level of Y in the eluted ^{99m}Tc obtained in the Dowex method was not estimated conclusively. Since traces of Nb, Zr and Y radioisotopes are produces in irradiation of enriched ^{100}Mo target, they will not contaminate the product beyond acceptable level in either of the separation process.

MEK content in the final product was found to be less than 0.1% (v/v). In both the methods of separation, nonradioactive molybdate content in the final pertechnetate solution was within the acceptable limit (less than 10 ppm). Al^{3+} levels were below the limits (less than 10 ppm) set for generator-produced pertechnetate. For both the processes, the pH of the final product solution was between 6 and 7. Paper chromatography showed that the pertechnetate obtained by processing of the targets irradiated in cyclotron was identical in radiochemical purity with the generator produced pertechnetate and no colloid was formed. The concentration of nitrate ions in the final pertecnetate solution was matching with 10 mg/l NO_3^- colour zone in the test strip, which is much less than the LD_{50} value of nitrate (1267 mg/kg, oral-rat). The concentration of H_2O_2 in the final radioactive TcO_4^- solutions was matching with 2-5 mg/l H_2O_2 colour zone, which is much less than the LD_{50} value of peroxide (1232 mg/kg, oral-rat).

TABLE 3. TYPICAL DATA FOR THE QUALITY CONTROL TESTS OF NA^{99M}TCO$_4$ PREPARED IN CYCLOTRON AND FROM ALUMINA COLUMN GENERATOR

Q. C. Parameter	TcO_4^- obtained from cyclotron by Dowex-1	MEK method	TcO_4^- obtained from Generator
Clarity	Clear	Clear	Clear
pH	6-7	6-7	6-7
^{99}Mo breakthrough	$<10^{-4}$ %	$<10^{-4}$ %	$<10^{-4}$ %
RC Purity	>99 %	>99 %	99%
<u>Chemical Purity</u>			
Al and Mo	< 10 ppm	< 10 ppm	< 10 ppm
Nitrate	< 10ppm	--	
Peroxide level	< 5ppm	< 5 ppm	-
MEK content	-	<0.1% (v/v)	-

Radionuclidic purity (RNP) of final pertechnatate solution was evaluated from the decayed pertechnetate samples and it was found that RNP was greater than 99.9% even at 24h after the separation. The detailed analysis of level of different Tc radionulides are listed in Table-4.

TABLE 4. OTHER RADIOTECHNETIUM IMPURITIES IN THE FINAL ^{99m}Tc PREPARATION AT DIFFERENT TIME POINTS AFTER THE END OF SEPARATION (AS % OF ^{99m}TC ACTIVITY)

Impurity	EOB	After 6h	After 12h	After 24h
^{95g} Tc	1.46E-04	2.09E-04	3.86E-04	1.02E-03
^{95m} Tc	5.30E-06	9.29E-06	2.11E-05	8.39E-05
^{96}Tc	3.97E-05	6.70E-05	1.46E-04	5.40E-04

3.4. Recovery of Mo from the irradiated target

Recovery of molybdate (ammonium molybdate) obtained in the two separation methods was estimated from the counting data and the recovery yield was found to be about 100% in both the methods. Ammonium molybdate when heated seems to break down into MoO_3 and ammonia. Conversion yield of molybdate was estimated by gravimetric method. From the weight of MoO_3 recovered, the recovery yield of Mo was estimated to be more than 94.5% (n=3).

3.4.1. Characterization of recovered molybdenum compound by X-ray diffraction

The spectral pattern of the synthesized powder matches with the commercial MoO_3 (unheated and heated at 700°C), but the intensity of the peaks is more close to the commercial heated MoO_3 powder (Fig. 9). The 2θ values for the major peaks at 12.8, 23.6, 25.8, 27.5, 33.6 and 39.2 resemble the JCPDS 85-2405 file, having monoclinic structure (space group P21/m, a: 3.954, b: 3.687, c: 7.095). This result confirms that our recovered Mo is chemically in the form of MoO_3.

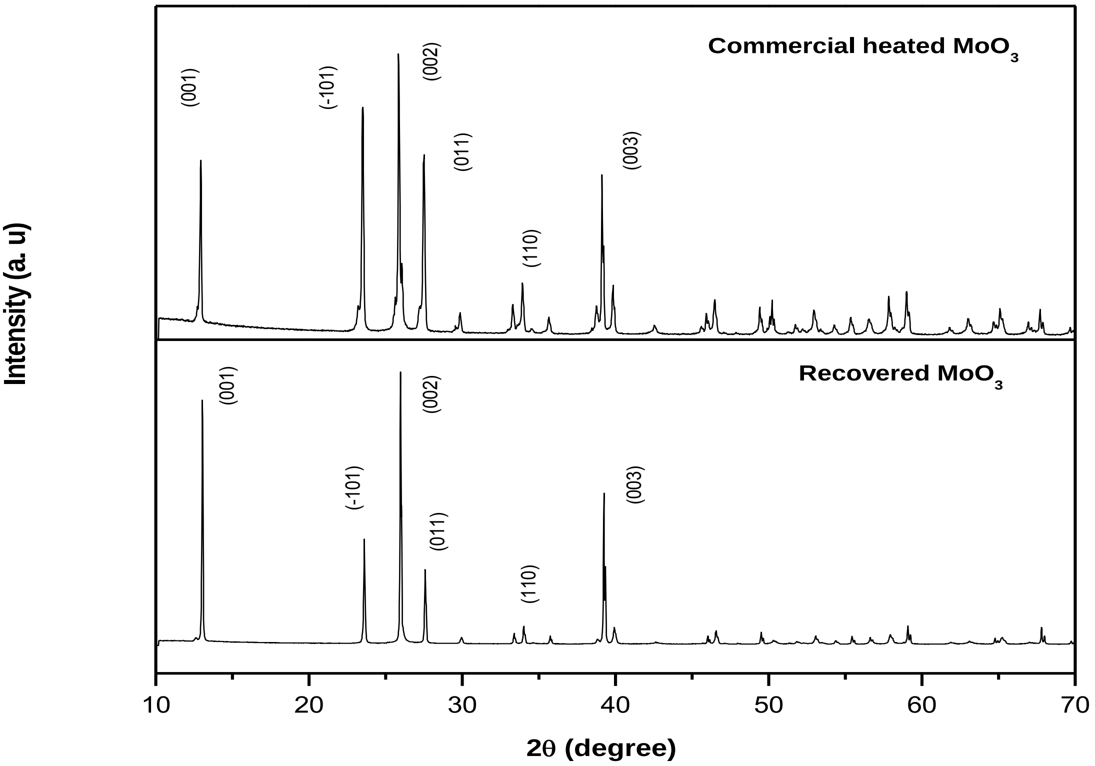

FIG.9. XRD of the recovered $^{nat}MoO_3$ and commercial $^{nat}MoO_3$.

3.4.2. Purification of recovered 100Mo from possible non-isotopic contaminants

Radiometric estimation showed that about 84% Mo is recovered after purification with 2.1%, 0.9% and 0.3% of the initial amount of Nb, Zr and Y isotopes in it, respectively. Gravimatric estimation of the purified Mo as MoO_3 indicated 94% recovery of Mo.

Various radioioisotopes of Nb , Zr and Y may be produced at trace level. Radioisotopes of Nb and Zr further decays and ultimately produce stable isotope of Mo, Zr and Y. While Zr, Nb and Y can be separated from the irradiated ^{100}Mo target, it is not possible to separate the Mo isotopic impurities by chemical means due to the obvious reason. Since these Mo isotopic impurities are the decay products of some of the directly or indirectly produced Nb radioisotopes, it is possible to control their level to some extent if irradiation of shorter duration at high current is used for ^{99m}Tc production and a fast chemical separation of Nb, Zr and Y radioisotopes from the recovered ^{100}Mo solution (obtained after the chemical separation of ^{99m}Tc from the irradiated target) are practised. It may be noted that even the use of purest ^{100}Mo will induce ^{97}Mo impurity in the recovered ^{100}Mo through the concomitant nuclear reaction, ^{100}Mo(p, α)^{97}Nb→^{97}Mo (Half life of ^{97}Nb is 72.1 min). The level of induced ^{97}Mo impurity in the recycled ^{100}Mo can be reduced by 56% if the separation of ^{97}Nb from the ^{100}Mo solution recovered after isolation of ^{99m}Tc is completed within 1 h after the end of irradiation. For other Nb radioisotopes which have longer half life and decay to a stable Mo isotope, the level of induced Mo isotopic impurity level after the chemical separation will be lesser if identical irradiation and separation time schedule is followed. Thus practice of purification of recovered ^{99}Mo by solvent extraction will result a better quality ^{99}Mo for the purpose of reusing it for the ^{99m}Tc production.

3.4.3. Preliminary studies on reduction of natural ammonium molybdate to Mo metal with hydrogen at high temperature

The ammonium molybdate was successfully reduced to Mo metal which was confirmed from the EDS spectrum. Fig. 10 shows the EDS spectrum and this analysis primarily detects the presence of a single molybdenum phase. The particle size of the reduced Mo metal powder was in the range of 0.45 µm to 1 µm which was confirmed from the SEM analysis and shown in Fig. 11.

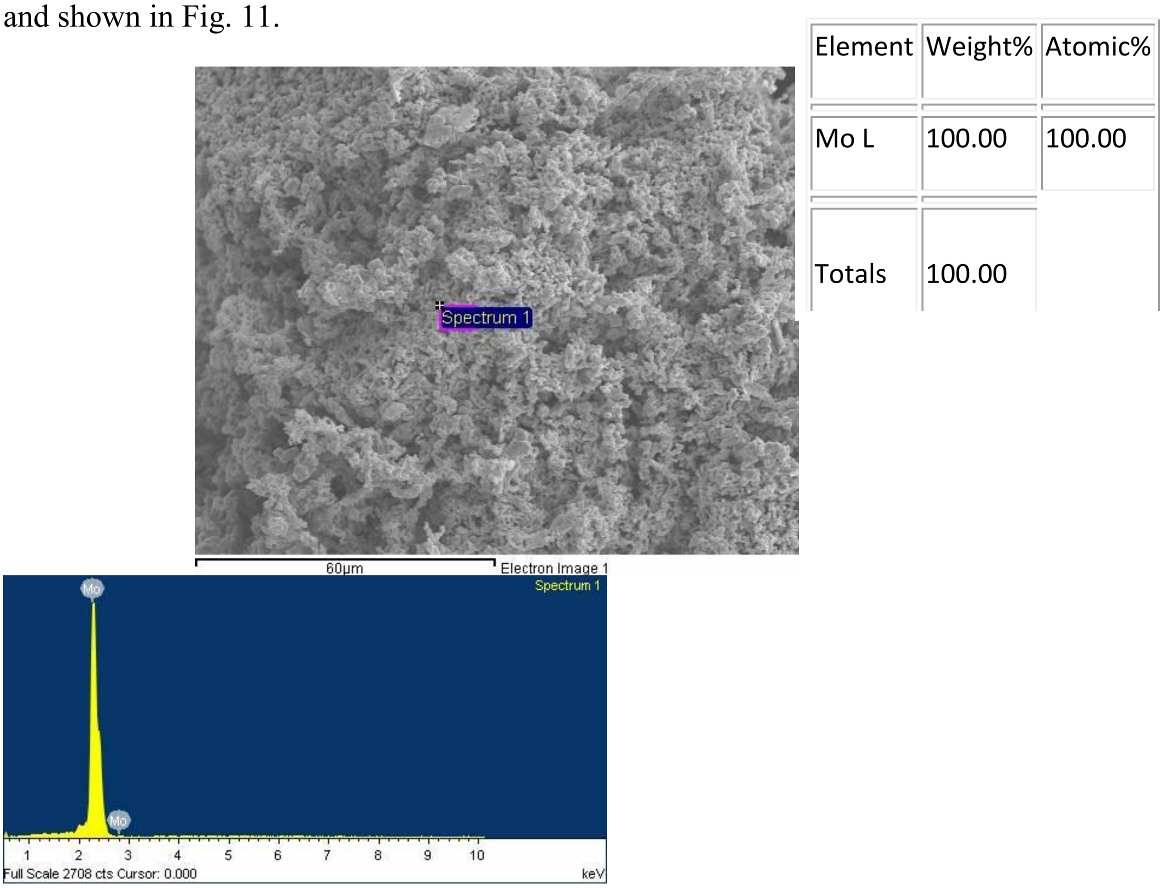

Element	Weight%	Atomic%
Mo L	100.00	100.00
Totals	100.00	

FIG. 10. EDS analysis showing only molybdenum phase.

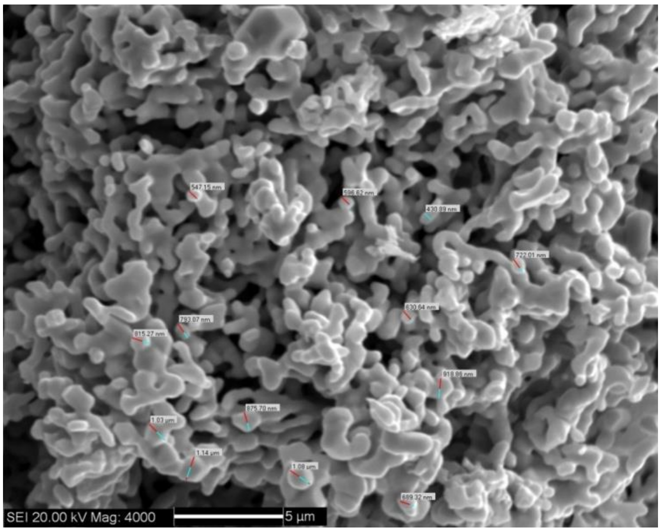

FIG. 11. Individual powder size range is from 0.45 µm to 1 µm.

4. CONCLUSION

Present study of ^{99m}Tc yield in stacked foil irradiation shows that proton irradiation of enriched ^{100}Mo target at 20→8MeV, 100μA proton beam for 1h, 3h, and 6h, will produce about 60, 160 and 272 GBq of ^{99m}Tc at EOI, respectively. The new chemical separation method developed recovers more than 80% of ^{99m}Tc from the irradiated target. The recovered pertechnetate has acceptable radionuclidic, radiochemical and chemical purity for labelling of biomolecules for clinical applications. Purification of the recovered ^{99}Mo by the newly developed solvent extraction method will reduce the level of nonisotopic contaminants like Nb, Zr and Y making it more suitable for repeated use as target material for ^{99m}Tc production. Recovered Mo-100 (after separation of ^{99m}Tc) as molybdate was successfully converted to Mo metal by reduction with hydrogen at high temperature.

Acknowledgment

The work was performed in part under a research contract between the International Atomic Energy Agency (IAEA) and the Board of Radiation and Isotope Technology (BRIT), India (Research Contract no. 17159). The authors thank Dr. A.K. Kohli, Chief Executive, BRIT for encouragement. The authors are grateful to Dr. D.K. Srivastava, Director, VECC and cyclotron operators for target irradiations. Thanks are due to Target Laboratory of VECC for extending help in preparing thick Mo pellets from Mo powder. The authors thank the Material Science Section of VECC for extending help in XRD experiments. The authors also thank Shri A.C. Dey and Shri Prabhakar Naskar, BRIT, Mumbai for extending their help in making AUTOSOLEX module. We sincerely acknowledge the generous help provided by Mr. S, Sarkar, Associate Group Director, Chemical Technology Group, BARC and his group in carrying out the reduction of ammonium molybdate to metallic molybdenum.

References

[1] BEAVER, J., HUPF, H., Production of ^{99m}Tc on a medical cyclotron: A feasibility study, J. Nucl. Med. **12** (1971) 739.

[2] LEVKOVSKIJ, V., Activation cross section nuclides of average masses (A=40-100) by protons and alpha-particles with average energies (E=10-50 MeV), Data accessed from the NNDC EXFORdatabase (2010), <http://www.nndc.bnl.gov/exfor/>.

[3] LAGUNAS-SOLAR, M.C., KIEFER, P.M., CARVACHO, O.F., et al., Cyclotron production of nca ^{99m}Tc and ^{99}Mo -an alternative non-reactor supply of instant ^{99m}Tc and ^{99}Mo/^{99m}Tc generator, Appl. Radiat. Isot. **42** (1991) 643.

[4] SCHOLTEN, B., LAMBRECHT, R., COGNEAU, et al., Excitation functions for the cyclotron production of ^{99m}Tc and ^{99}Mo, Appl. Radiat. Isot. **51** (1999) 69.

[5] TAKÁCS, S., SZUCS, Z., TÁRKÁNYI, F., et al., Evaluation of proton induced reactions on Mo-100: new cross sections for production of Tc-99m and Mo-99, J. Radioanal. Nucl. Ch. **257** (2003) 195.

[6] Challan M., Comsan M., Abou-Zeid M., Thin target yields and EMPIRE-II predictions on the accelerator production of technetium-99m, Nucl. Rad. Phys. **2** (2007) 1.

[7] KHANDAKER, M., UDDIN M., KIM K., et al., Measurement of cross-sections for the (p,xn) reactions in natural molybdenum. Nucl. Instr. Meth. Phys. Res. **B 262** (2007) 171.

[8] LEBEDA, O., PRUSZYŃSKI, M., New measurement of excitation functions for (p,x) reactions on ^{nat}Mo with special regard to the formation of ^{95m}Tc, $^{96m+g}$Tc, ^{99m}Tc and ^{99}Mo, Appl. Radiat. Isot. **68** (2010) 2355.

[9] GAGNON, K., BÉNARD, F., KOVACS, M., et al., Cyclotron production of ^{99m}Tc: Experimental measurement of the ^{100}Mo(p,x)^{99}Mo, ^{99m}Tc and ^{99g}Tc excitation functions from 8 to18 MeV, Nucl. Med. Biol. **38** (2011) 907.

[10] TÁRKÁNYI, F., DITRÓI, F., HERMANNE, A., et al., Investigation of activation cross-sections of proton induced nuclear reactions on ^{nat}Mo up to 40 MeV: New data and evaluation, Nucl. Instr. Meth. Phys. Res. **B 280** (2012) 45-73.

[11] TARGHOLIZADEH, H., RAISALI, G., JALILIAN, A.R., et al., Cyclotron production of technetium radionuclides using a natural metallic molybdenum thick target and consequent preparation of [Tc]-BRIDA as a radio-labelled kit sample, Nukleonika **55** (2010) 113.

[12] MORLEY, T.J., DODD, M., GAGNON, K., et al., An automated module for the separation and purification of cyclotron-produced $^{99m}TcO_4^-$, Nucl. Med. Biol. **39** (2012) 551.

[13] CHATTOPADHYAY, S., DAS, S.S., DAS, M.K., GOOMER, N.C., Recovery of ^{99m}Tc from $Na_2[^{99}Mo]MoO_4$ solution obtained from reactor-produced (n,γ)^{99}Mo using a tiny Dowex-1 column in tandem with a small alumina column, Appl. Radiat. Isot. **66** (2008)1814.

[14] MCALISTER, D.R., HORWITZ, E.P., Automated two column generator systems for medical radionuclides. Appl. Radiat. Isot. **67** (2009) 1985.

[15] GAGNON, K., WILSON, J.S., HOLT, C.M.B., ABRAMS, D.N., MCEWAN, A.J.B., MITLIN, D., MCQUARRIE, S.A., Cyclotron production of ^{99m}Tc: Recycling of enriched ^{100}Mo metal targets, Appl. Radiat. Isot. **70** (2012) 1685.

[16] INTERNATIONAL ATOMIC ENERGY AGENCY (2009), http://www-nds.iaea.org/medical/ monitor_reactions.html.

[17] ANDERSEN, H.H., ZIEGLER, J.F., Hydrogen Stopping Powers and Ranges in All Elements, Pergamon Press, New York (1977).

[18] NuDat 2.6 (2013), http://www.nndc.bnl.gov/nudat2.

[19] CHATTOPADHYAY S., BARUA L., SAHA DAS S., et al., Pharmaceutical grade sodium [^{99m}Tc] pertechnetate from low specific activity ^{99}Mo using an automated ^{99}Mo/^{99m}Tc-TCM-autosolex generator, J. Radioanal. Nucl. Chem. **302** (2014) 781.

[20] CHATTOPADHYAY S., DAS, S.S., BARUA L., et al., An automated computer controlled module for preparation of sodium [^{99m}Tc] pertechnetate using (n,γ) ^{99}Mo-molybdate solution: TCM-AUTODOWNA generator, Proceedings in 46th Annual Conference of Indian Soc. of Nuclear Medicine (SNMICON-2014) during 11th Dec-14th Dec. 201, SINP, Kolkata, Page No. 26-27.

[21] SCADDEN, E. M., BALLOU, N. E., The Radiochernistry of Molybdenum, National Academy of Sciences, National Research council, Nuclear Science Series. US Atomic Energy Commission (1960).

[22] SWIFT, E., A new method for the separation of gallium from other element, J. Am. Chem. Soc. **46** (1924) 2378.

ACCELERATOR-BASED ALTERNATIVES TO NON-HEU PRODUCTION OF Tc-99m

J. ESPOSITO[a], M. BELLO[B], A. BOSCHI[C,d], G. CICORIA[e] ,L. De NARDO[b] G. Di DOMENICO[d], A. DUATTI[f], M. GAMBACCINI[b], M. GIGANTI[c], L. GINI[g], F. GROPPI[g], U. HOLZWARTH[h], M. LORIGGIOLA[a] G. LUCCONI[e,] S. MANENTI[g], M. MARENGO[e], P. MARTINI[a,b,], L. MELENDEZ-ALAFORT[i], A. NEGRI[j], V. PALMIERI[a], M. PASQUALI[c,d], G. PUPILLO[a,d] A. ROSTATO[i,] A. ROSSI[a] H. SKLIAROVA[a], A. TAIBI[d], L. UCCELLI[c,k], N. UZUNOV[l]

[a] INFN, Legnaro National Laboratories, Legnaro (Padua), Italy.
[b] Physics Department, Padua University and INFN Padua branch, Italy.
[c] Morphology, Surgery and Experimental Medicine Department, Diagnostic Imaging Section, Ferrara University, Italy .
[d] Physics and Earth Sciences Department., Ferrara University, and INFN Ferrara branch, Italy.
[e] Nuclear Medicine Department, St. Orsola Malpighi Hospital, Bologna, Italy
[f] Department of Chemical and Pharmaceutical Sciences, Ferrara University, Italy.
[g] Accelerator and Applied Superconductivity Lab., Physics Department, Milan University and INFN Milan branch Italy.
[h] Institute for Health and Consumer Protection, Joint Research Centre, European Commission, Ispra,VA, Italy.
[i] Department of Oncology Surgery, Padua University, Italy.
[j] Oncology Research Centre of Veneto Region (IOV), Padua, Italy.
[k] Nuclear Medicine Department. St. Anna Hospital, Ferrara, Italy
[l] Faculty of Natural Sciences, Shumen University, Shumen, Bulgaria.

Abstract

The current, nuclear-reactor-based ^{99}Mo/^{99m}Tc productions experienced some shortage in recent years, thus forcing the scientific community to find out alternative solutions. Among them, the use of particle accelerators to produce either ^{99}Mo or ^{99m}Tc is one of the most interesting and promising approach. For this reason, in the framework of LARAMED (Laboratory of Radionuclides for Medicine) project at Legnaro National Laboratories of the Istituto Nazionale di Fisica Nucleare (LNL-INFN), research activities are underway since the kick-off of the IAEA CRP. The final goal is to establish feasible technical solutions to get alternative, accelerator-driven, ^{99m}Tc production routes on a routine basis, which might possibly be implemented by cyclotron-based Nuclear Medicine Depts. in hospitals, in order to meet new future radionuclide shortage. A summary of activities performed in the last CRP period (2014-2015), and a recall of items already reported in previous report are here outlined.

1. THEORETICAL STUDIES AIMED AT ^{99m}Tc DIRECT PRODUCTION BY PROTON ACCELERATORS

The theoretical studies aimed at the assessment of the optimal proton irradiation condition (i.e. beam energy, irradiation time) and evolution analyses post EOB of the most important parameters, taking into account the ^{100}Mo-enriched (>99 %) molybdenum metal target configuration, have already been performed and results already published. More detailed information may be found in the paper by Esposito et al. [1] and partly in the in the former RCM report [2].

2. ^{99m}Tc PRODUCTION WITH CYCLOTRON ACCELERATED PROTONS: EXPERIMENTAL EXCITATION FUNCTION AND THICK TARGET YIELDS OF ^{100}Mo(p,2n)^{99m}Tc, ^{100}Mo(p,2n)^{99g}Tc AND ^{100}Mo(p,x)^{99}Mo

The excitation functions were measured using the stacked-foil technique and covering the proton energy range from 8 MeV to 21 MeV. The stack of thin foils consists of alternating high purity aluminium, highly ^{100}Mo-enriched molybdenum foils and one titanium beam monitor foil. We used ^{100}Mo-enriched (99.05% level) molybdenum, in metallic form, as target material, from ISOFLEX Isotopes [3]. ^{100}Mo-enriched metal foils having 20-25µm ±2% nominal thickness and the following isotopic composition (0.08% ^{92}Mo, 0.05% ^{94}Mo, 0.1% ^{95}Mo, 0.11% ^{96}Mo, 0.07% ^{97}Mo, 0.54% ^{98}Mo, 99.05% ^{100}Mo) were prepared following a melting-laminating process, at the LNL nuclear target laboratory. The experimental value of target thickness was accurately measured by weighting technique, followed by additional measurements using a high-precision thickness meter instrument, in order to assess foils thickness homogeneity.

Stacks foils were irradiated in different irradiation experiments at the JRC-Ispra (VA) laboratory using the Scanditronix MC40 cyclotron. All irradiations were carried out at different incident energies in the range from 8 MeV to 21 MeV, 100 nA typical beam current and 1-hour beam time. After irradiations, targets were soon transported to INFN LASA lab in Segrate (Milan), to get gamma spectrometry measurements. Activities were measured without any chemical processing, by using a calibrated high-purity germanium (HPGe) detector (EG&G Ortec, 15% relative efficiency, FWHM = 2.2 keV at 1.33 MeV). All foils were measured in the same geometrical position as that used for the detectors calibration sources, in order to avoid corrections for different geometries. The distance from the detector cap was chosen in order to reduce dead time and pile up errors to negligible values (< 0.1%). The first measurements of the samples generally started within a few hours after end of bombardment (EOB) and measurements continued periodically for about one month, in order to follow the ^{99}Mo decay: counts in the peak in the region of interest exceed 10,000. The experimental excitation function for each target were calculated from the thin-target yield, taking into account also the decay factor to correct for the decay during the counting time and the growing factor to correct the decay during the irradiation time. Details on the procedure followed may be found in the paper by Manenti et. al. [4]

In Figs 1 and 2 are reported the experimentally measured excitation functions for ^{100}Mo(p,2n)^{99m}Tc and ^{100}Mo(p,x)^{99}Mo, compared with the data present in literature. The great difficulty in the determination of the ^{100}Mo(p,2n)^{99m}Tc cross-section, is related to the fact that ^{99m}Tc emits only 140.511 keV and 142.63 keV photons and at these energies there is the contribution of the same gamma emission due to the decay of ^{99}Mo. Furthermore, the contribution for the indirect production of ^{99m}Tc must be taken into account. This indirect production results from ^{99}Mo decay, both during and post irradiation. There is also a possible contribution related to the production of ^{90}Nb (γ-emissions at 141.2 keV (69.0%) and 1129.1 keV (92.0%)), that can be produced by nuclear reactions induced by protons on ^{92,94,95}Mo. In our experiments, there was no evidence of the presence of ^{90}Nb, so in the determination of ^{99m}Tc cross sections, all the different contributions related to ^{99}Mo and the decay of ^{99m}Tc were taken into consideration, as reported in deeply detail in [4]. From a critical analysis of the completely experimental procedure [4], we pointed out some of the reasons that could justify the large disagreement among literature data, about the ^{100}Mo(p,2n)^{99m}Tc cross section determination. That has been checked be due to: (i) an inaccurate determination of the calibration curve, (ii) the use of different nuclear data or (iii) not applying the corrections for the determination of the direct ^{99m}Tc production.

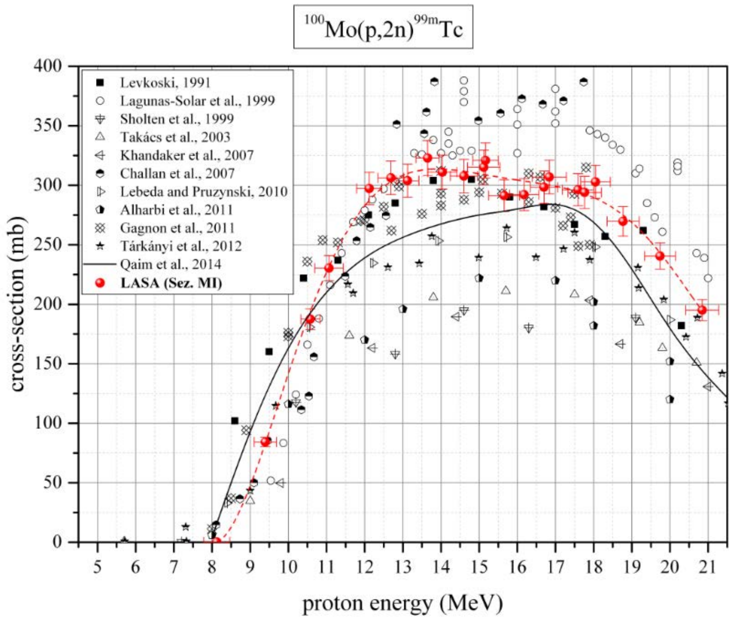

FIG. 1. Excitation functions for $^{100}Mo(p,2n)^{99m}Tc$ nuclear reaction. For sake of clarity, literature data are plotted without error bars. Only our data have been fitted with a polynomial curve [4].

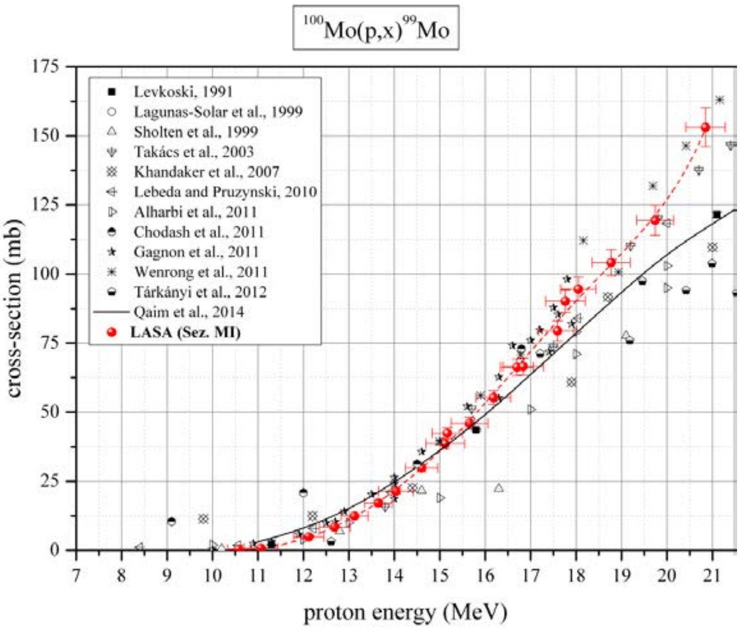

FIG. 2. Excitation functions for $^{100}Mo(p,x)^{99}Mo$ nuclear reactions. For sake clarity, literature data are plotted without error bars. Only our data have been fitted with a polynomial curve [4].

Moreover, in our case, the solution of the exact differential equation for the decay curve, starting from the End Of an Instantaneous Bombardment (EOIB) was derived.

On the other hand, the other important isomer state, ^{99g}Tc, is much more difficult to be determined; indeed being an almost pure beta emitter γ-ray spectrometry may not be used. The ICP-MS technique was therefore used for evaluating the ^{99g}Tc content and, ultimately, the excitation function. The direct ^{99g}Tc excitation function was determined using ICP-MS in combination with γ-ray spectrometry, in order to correct for the indirect ^{99g}Tc contributions produced by the complete decay of ^{99m}Tc and ^{99}Mo. Just some of the experimentally measured excitation function points for ^{100}Mo(p,2n)^{99g,dir}Tc reaction is plotted in Fig 3, compared with the data present in literature. Full data will be available in the near future in a dedicated paper in peer-reviewed journal. It is anyway clear how the unique former e.f. fitted curve proposed some years ago seems to underestimate the ^{99g}Tc production basically in the 16-25 MeV region. The net production appears to be larger than expected.

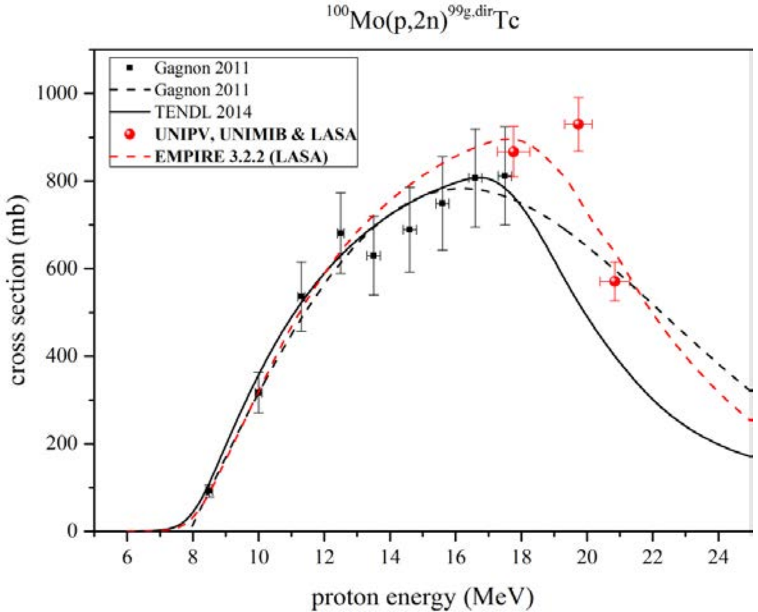

Fig. 3. The excitation functions for ^{100}Mo(p,x)^{99g,dir}Tc nuclear reaction.

At last, the experimental thin-target yields were fitted and these mathematical functions were integrated to bear the thick-target yields (Figure 4).

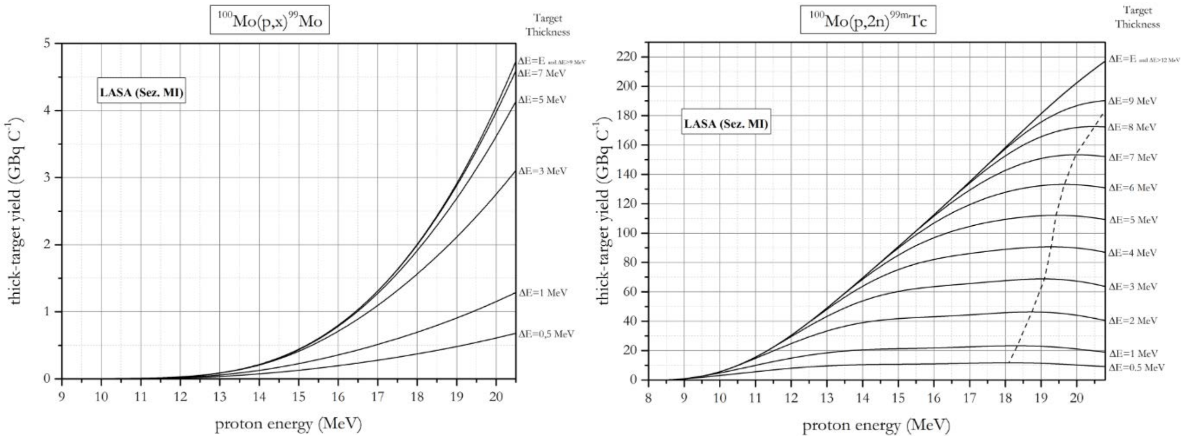

FIG. 4. (left) Calculated ^{99}Mo thick-target yields versus proton beam energy and different energy loss in the target (corresponding to different target thickness);(right) Some data relying the production of ^{99m}Tc. The couples of (E, ΔE) values on the calculated locus of maxima (---) corresponding to optimized thick-target yield are also plotted.

As obtained from the experimental results presented in [4] and reported here, it is our opinion that the optimal energy range for the production of ^{99m}Tc (with no ^{9x}Tc contaminants other than the ^{99g}Tc isomeric state from ^{100}Mo) via cyclotron route is 12–17 MeV. The cross section indeed achieves its maximum value in this energy range. Furthermore, for energies larger than about 17 MeV there is a sharp increase of the side production of the very long-lived radioisotopic impurities, basically due to the production of ^{98}Tc ($t_{1/2}$= 4.2E+6 y) (^{100}Mo(p,3n)^{98}Tc, E_{th} = 16.85 MeV). This energy interval is a theme of debate in between the different research centres, especially being no any current Pharmacopoeia monograph establishing values for the Radionuclidic Purity (RNP) and Isotopic Purity (IP) for the cyclotron production Tc. On the other hand, it must be pointed out that the specific activity – the most important parameter in this kind of applications - must be experimentally determinated, in order to consider a larger (or different) energy range, for improving the accelerator-^{99m}Tc activity production.

3. DEVELOPMENT OF AN AUTOMATIC SEPARATION/EXTRACTION MODULE FOR THE CYCLOTRON ^{99m}Tc PRODUCTION VIA ^{100}Mo-ENRICHED MOLYBDENUM METAL TARGETS

The purpose of this work was to develop a completely automatic extraction module for the ^{99m}Tc separation and purification process from enriched ^{100}Mo metal targets. Several techniques, (based upon both chemical and physics processes) are known to obtain separation of technetium from molybdenum; among them, the most used ones are the ABEC technique (Aqueous Biphasic Extraction Chromatography), the so-called Chattopadhyay's method with ion exchanger cartridges (Dowex-1 x 8) and the solvent extraction method with MEK (Methyl Ethyl Ketone) [5]. Preliminary experimental studies pointed out that the solvent extraction technique is one of the most efficient methods, thanks to the selective affinity of the pertechnetate ($^{9x}TcO_4^-$) for MEK and the affinity of the binegative molybdate (MoO_4^{2-}) for the aqueous phase, providing high extraction yield of high quality ^{9x}Tc from molybdenum metal targets. The solvent extraction technique in general involves the following steps:

(1)dissolution of the irradiated target of molybdenum (VI) oxide (MoO_3) in NaOH 5N (aqueous phase);

(2)extraction of ^{99m}Tc from the aqueous alkaline solution of molybdate into the organic phase (MEK).

Starting from this method, and applying some improvements and corrections to the original procedure aimed at the optimization of operator's radioprotection, a preliminary semi-automated extraction module was developed [6]. In particular, a revised and optimized procedure started with the dissolution of the metal target in H_2O_2 and NaOH; addition of MEK and vortex mixing with the alkaline solution, that contained molybdate and other by-products, caused the selective extraction of $[^{99m}TcO_4]^-$ into the organic phase. The final product has been easily purified from organic solvents and molybdate residuals by the passage through silica and alumina columns. Finally, $[^{99m}TcO_4]^-$ was collected from the alumina column with saline. In 35 minutes, the semi-automatic module allowed to recover about 80% of the initial activity. Purity values of final pertechnetate saline solution were in agreement with values imposed by Pharmacopoeia for the generator-obtained product. The extraction was then completely automated and controlled, in order to ensure an optimal operator radioprotection and faithful reproducibility of the process.

As a next step, an automatic and remote controlled prototype was assembled by using proper modular units shown in Figure 5. In order to test the efficiency of the module six ^{100}Mo (99.05%) enriched molybdenum metal foils (∅=0.9cm, total thickness=143μm, total mass=124.5mg) were irradiated in stacked foils configuration for 70 min at 25 μA with a proton beam with energy 19.2-17 MeV at JRC Ispra cyclotron and then treated with the automatic procedure.

A detailed quality control (QC) analysis of the final pertechnetate solution was performed, in order to determine isotopes and impurity amounts, Mo breakthrough, percentage of organic solution etc. results are enlisted in Table 1. The module allows for the recovery of more than

90% of the ^{99m}Tc initial activity within 70 minutes [7]. Details on the optimized process set up will be available in a dedicated paper next to be submitted to a peer-reviewed journal.

FIG. 5. The automatic and remote controlled/operated Tc-99m Solvent Extraction Module.

TABLE 1. RADIONUCLIDIC (RNP), CHEMICAL (CP) AND RADIOCHEMICAL (RCP) PURITY VALUES; MDA: INDICATES THE MINIMUM DETECTABLE ACTIVITY

RNP	^{xx}Nb in final eluate	<MDA
	^{xx}Mo in final eluate	<MDA
	^{99m}Tc	>99%
CP	pH	4,5-5
	Mo	<5ppm
	Al	<5ppm
	MEK	<0.0004% (v/v)
RCP	$^{99m}TcO_4^-$	100%

4. PRECLINICAL SPECT-CT IMAGING STUDIES WITH CYCLOTRON PRODUCED ^{99m}Tc

In vivo multimodality imaging studies (SPECT-CT) were performed by using both the generator- and accelerator-produced ^{99m}Tc pertechnetate and the labeled radiopharmaceuticals (RF): HMPAO (CERETC™) and tetrofosmine (MYOVIEW™). Molybdenum ^{100}Mo (99.05%) metal targets, were irradiated at JRC-ISPRA (VA, Italy). The energy was chosen in order to test the effectiveness of the chemical separation procedure having a mixture of different Tc-radionuclides yielded. Targets were then treated with the automatic, MEK-based solvent extraction (SE) method, module system. An aliquot of the final elute was finally added to RF kit, following the standard preparation procedure. The determination of radionuclidic purity of the ^{99m}Tc-eluate was performed by standard γ-spectrometry and the determination of radiochemical purity (RCP) of ^{99m}Tc-pertechnetate, ^{99m}Tc-HMPAO and ^{99m}Tc-tetrofosmine was checked by radio-TLC. WIST rats, previously anesthetized, were injected into the jugular vein using generator- and cyclotron-^{99m}Tc pertechnetate, HMPAO and tetrofosmine . All the experimental procedure was carried out strictly following the current regulation. Whole-body SPECT-CT biodistribution studies were carried out with the hybrid YAP(S)PET-CT small-animal scanner [8,9] shown in Figure 6.

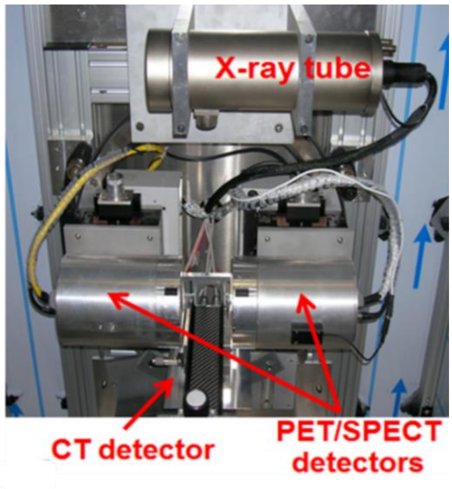

FIG. 6. The YAP-(S)PET-CT scanner for small animals.

CT images have been acquired, by using optimized parameters, and corrected for non-uniformity of the beam and detector response (*flat image*), dark current and readout noise (*dark image*). SPECT-images were corrected for injection time, injected activity and reconstructed by using the iterative Expected Maximization-Maximum Likelihood (EM-ML) technique, with the possibility to include scatter correction. In case of accelerator-produced Tc, the scatter contribution due to higher-energy γ-rays emitted in the decay of some Tc-isotopes (shown in Table 2), has been corrected by selecting appropriate energy windows. On the other hand, the standard spectral energy range [140-250] keV has been selected to get the imaging reconstruction of the generator ^{99m}Tc-labelled pharmaceutical.

TABLE 2. TECHNETIUM ISOTOPES DETECTED IN THE CYCLOTRON PRODUCED TC-ELUATE AND DECAY PROPERTIES FROM NUDAT 2.6 DATABASE [10].

Isotope (half-life)	γ-ray energy [keV] (Int.%)
Tc-99m (6.01 h)	140.511 (89)
Tc-93 (2.75h)	1362.9 (66.2)
Tc-94g (4.88 h)	702.7 (99.6)
	849.7 (95.7)
	871.1 (99.9)
Tc-95g (20.0 h)	765.8 (93.8)
	1073.7 (3.74)
Tc-96g (4.28 d)	778.2 (99.8)
	812.5 (82)
	849.9 (98)
	1126.9 (15.2)

In vivo SPECT-CT preclinical imaging studies in a rat animal model, by using a high-resolution small-animal scanner, confirmed a superimposable biodistribution behavior of heart and brain perfusion of ^{99m}Tc-radiopharmaceuticals labeled with both cyclotron- and generator-produced Tc. As an example, one of the preliminary imaging test showing the biodistribution comparison, using the ^{99m}Tc-labelled MYOVIEW pharmaceutical is shown in Figure 7.

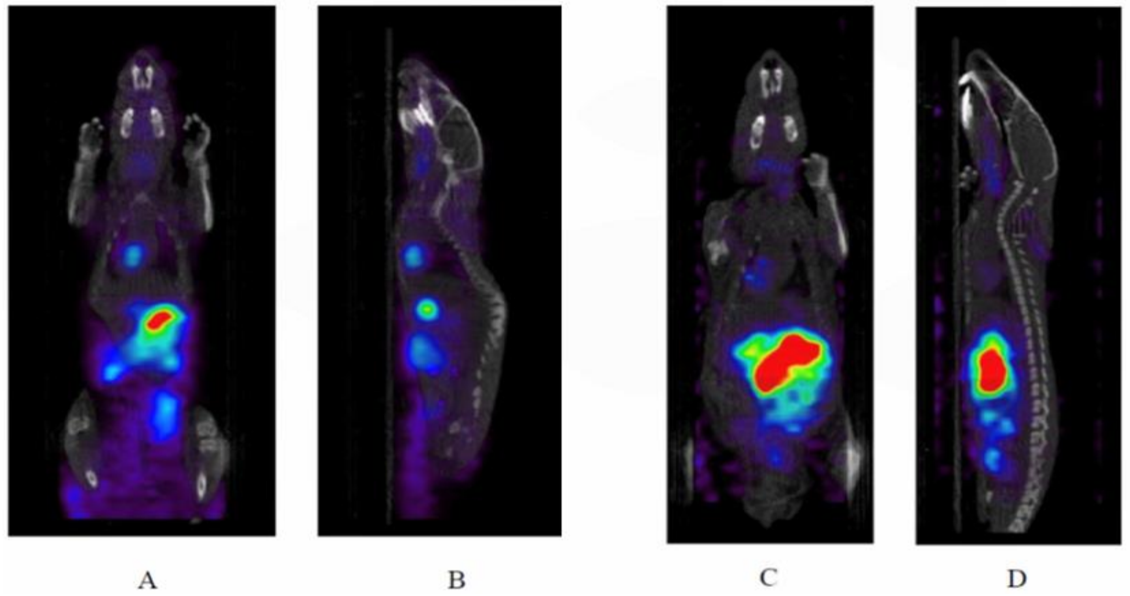

FIG.7. One of the preliminary in-vivo comparison of experimental imaging result studies about the ^{99m}Tc-labelled MYOVIEW radiopharmaceutical. Images marked A and B show the coronal and sagittal sections of SPECT-CT scans of a rat using generator labeled compound. Images C and D show the same scans but using the accelerator-^{9x}Tc instead.

5. DEVELOPMENT OF LOW-BACKGROUND, HIGH-SENSITIVITY B-SPECTROMETER BASED ON TDCR METHOD FOR ^{99g}Tc ACTIVITY/E.F. ALTERNATIVE ESTIMATION

Although the production of accelerator-Tc impurities can be limited as much as possible by using highly enriched ^{100}Mo targets and an appropriate energy window for the incoming proton-beam, the co-production of the ^{99g}Tc isomer cannot be prevented. The e.f. peak for the ^{100}Mo(p,2n)^{99g}Tc,^{99m}Tc reaction routes are indeed in the same energy range. The ^{99g}Tc, a long half-life ($2.111 \cdot 10^5$ y), almost pure β-emitter (End-point energy E=293.5 keV, I=99.9984%), is produced by decay of ^{99m}Tc and ^{99}Mo as well.

In order to have a precise evaluation of ^{99g}Tc content in the final product, therefore estimating in the proper way the ^{99g}Tc/^{99m}Tc isomer ratio, which has also an impact on the Isotopic Purity (IP) estimation, a digital β-spectrometer based on the Triple to Dual Coincidence Ratio (TDCR) method was developed [11, 12]. The detection system is based upon three R329-02 Hamamatsu photomultiplier tubes (PMTs) arranged symmetrically at an angle of 120° each other (see Figure 8). The sample is vertically inserted in the optical chamber, by using a piston and an optical shutter, to avoid light infiltration. The chamber and the piston have been designed and built at the INFN Ferrara branch. Signals from PMTs are individually processed by the stand-alone CAEN DT5720B desktop module, a 4-channel fast digitizer characterized by a 250 MS/s, 12-bit ADC, 125 MHz bandwidth and 4 ns Trigger Time Tag resolution. The number of dual and triple coincidence events is obtained by analyzing off-line the output files of the digitizer with a homemade software, allowing the setting up of the appropriated parameters, such as coincidence time interval. In order to test the effectiveness of the TDCR-spectrometer, ^{99g}Tc calibrated sources have been used. For each measurement, both the TDCR system and with a commercial β-counter TriCarb 2810TR (Perkin Elmer), equipped with two PMTs have been performed.

Activities were calculated by using the TDCR-07c software developed at Laboratoire National Henri Becquerel [13]. The background contribution (dark signal) was estimated by measuring a blank sample (containing only the SC). A simplified estimation of the activity has been also performed, by calculating the ratio $A = (N_D)^2/N_T$; the expected discrepancy with the activity estimated by using the TDCR method is less than 1%, being $K > 0.9$. Table 3 reports the activities obtained by using the TDCR β-spectrometer, the expected values of ^{99g}Tc standard solution (calculated by weight), as well as activities measured with the commercial β-counter.

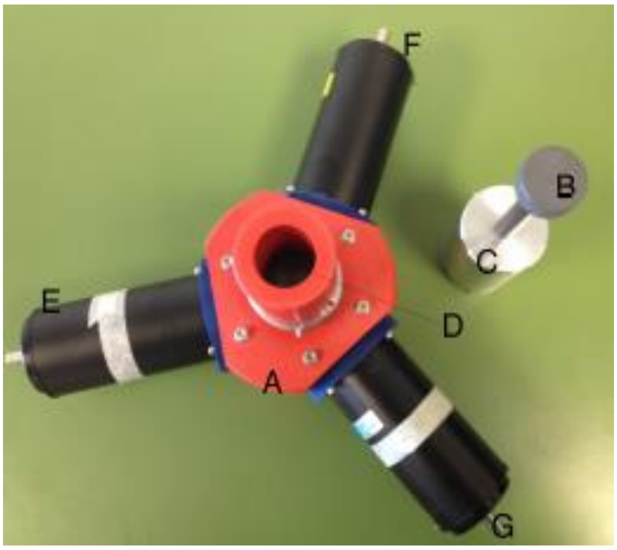

FIG. 8. The β-spectrometer: A. Optical Chamber; B. Piston; C. Cylinder for vial insertion; D. Shutter; E,F,G. Photomultiplier Tubes.

TABLE 3. RESULTS OF MEASUREMENTS ON THE REFERENCE ^{99g}Tc SAMPLES

	K	Activity (Bq)			
	N_T/N_D	Simplified TDCR	TDCR	β-counter	Expected
0.1 ml	0.927	3850 ± 20	3880 ± 40	3840 ± 80	3700 ± 185
0.4 ml	0.927	14870 ± 60	14910 ± 150	14870 ± 290	14800 ± 740

Results show that the activities obtained by using the TDCR β-spectrometer are in excellent agreement with the ones measured by the commercial β-counter. In comparison with the expected ^{99g}Tc activities, both measurements seem to slightly overestimate the reference values; this can be explained by considering the uncertainty associated to the volume taken from the standard solution. The development of the TDCR spectrometer is going on, in order to be optimized for the measurement of low-level ^{99g}Tc activity, by developing a dedicated shielding and optimizing the acquisition and data analysis software.

6. IMAGING QUALITY STUDIES OF ACCELERATOR-^{9x}**Tc**

Two ~4 GBq each ^{99m}Tc activity experimental yield tests, have been performed, in order to assess the whole Cyclotron-Produced-Tc (CPTc) chain up to the CPTc-labelled pharmaceutical. Both ^{99m}Tc samples produced by proton bombardment (1hr time, 19 MeV, 25µA) on ^{100}Mo-enriched (99.05%) molybdenum metal target with the related ^{99m}Tc extraction and purification procedure (referred to as "accelerator-produced ^{99m}Tc" or "AP ^{99m}Tc") have been analysed in the Laboratory for Radiopharmaceuticals and Molecular Imaging (LARIM) at the INFN Legnaro Labs. Several types of experiments/theoretical estimations have been performed, to estimate the imaging quality, i.e. (1) gamma spectrometry analyses of the gamma emitters in the solution, (2) studies on the image gamma-ray background with respect to the relative activities of other technetium isotopes in the solution and (3) computational dosimetry studies about the impact on the absorbed dose in organs but using the real spectrometry data.

6.1. Assessment of CPTc Impurities

Small fraction of the AP ^{99m}Tc solutions with activities of the order of tens kBq have been used for gamma-spectrometry analysis. The gamma-ray spectrometry measurements were carried out using a low-background setup of the Geophysics Laboratory of the LNL, INFN and the University of Ferrara. High-volume germanium detectors with 80% relative efficiency and energy resolution of 2.1 keV were used for the spectra acquisition. The detectors output was connected to 7611 Silena spectroscopy amplifier and an EtherNIM 919E Ametek ADC converter controlled by the Maestro 32 program. Several technetium isotopes, such as shorter-half-time ^{93}Tc ($T_{1/2}$ = 2.75h) and ^{94g}Tc ($T_{1/2}$ = 4.88h) as well as relatively longer decaying technetium ones ^{95g}Tc ($T_{1/2}$ = 20h) ^{95m}Tc ($T_{1/2}$ = 102.72h) and ^{96}Tc ($T_{1/2}$ = 1464h), have been determined in the samples from the two irradiation experiments. The measured isotope activities of both samples, recalculated for EOB+ 9 hrs after the target irradiation, are shown in Table 4 and are related to the minimum ^{9x}Tc impurities' activity relative to ^{99m}Tc one.

Comparison between values from both irradiations tests clearly point out that relative contribution from Tc impurities is unchanged. Moreover, the relative activities of ^{96}Tc, ^{95}Tc and ^{95m}Tc measured in the two experiments do not differ within experimental uncertainties. Some difference is seen for the shorter-half-life isotopes of ^{93}Tc and ^{94}Tc, which is likely due to the efficiency recalibration procedure used for the delayed gamma-ray spectra, collected during the second measurement test.

TABLE 4. ^{9x}Tc RELATIVE ACTIVITIES RECORDED IN BOTH IRRADIATION EXPERIMENTS (EOB+9HRS)

Nuclide	*Experiment I (June.2014)* A_{Tc9x} / A_{Tc99m} (%)	*Experiment II (Nov. 2014)* A_{Tc9x} / A_{Tc99m} (%)
^{96g}Tc	0.03 ± 0.01	0.029 ± 0.0045
^{95m}Tc	0.0013 ± 0.0003	0.0014 ± 0.0002
^{95g}Tc	0.20 ± 0.04	0.22 ± 0.03
^{94g}Tc	0.08 ± 0.02	0.12 ± 0.03
^{93g}Tc	0.07 ± 0.02	0.14 ± 0.04
Total	0.38% ± 0.09%	0.50% ± 0.11%

6.2. Influence of the higher-energy gamma-ray emitters on images' background

Technetium isotopes other than ^{99m}Tc emit gamma rays in the energy range of 200 keV – 1350 keV. The energy window of diagnostic tools for standard ^{99m}Tc imaging procedure is usually set in a narrow interval around 140 keV, so that gamma rays from technetium impurities that directly reach the scintillator do not affect the image quality. However, this energy window could be achieved by the gamma rays that have undergone large-angle Compton scattering with (eventually) consequent multiple forward Compton scattering in the matter (tissues). Such an effect increase the background signal thus compromising the images quality during diagnostic procedures using CPTc. A simple experimental setup, based on the use of a system of capillary tubes as shown in Figure 9 (left), was used to test the influence of such an effect. The system was immersed in water to simulate the effect of tissue Compton scattering and the container was placed above the collimator of a gamma-ray camera with an opening upward. The quantity of water was chosen to cover slightly the highest of the capillary tubes. Thus the amount of Compton backscattered gamma rays in the water was higher around the lowest capillary tube.

Solutions with activity of 1 mCi were circulating in the system containing the three-capillary-tubes and the dedicated feeding circuit. Images of the system in air and immersed in water were collected for AP ^{99m}Tc 20 hours after the target irradiation. For comparison, similar measurements were conducted in air and in water using 1.24 mCi ^{99m}Tc eluate from a generator (GP ^{99m}Tc) (Mallinckrodt pharmaceuticals). All the obtained images were corrected for the uniformity (details can be found in [14]) and photo-peak position (details may be found in the paper by Uzunov et al. [15]). The corrected image data were reconstructed into an image of 512 × 512 pixels, using an energy window of ±10% at the peak of 140 keV. The resulting background fits are shown in Figure 9 (right).

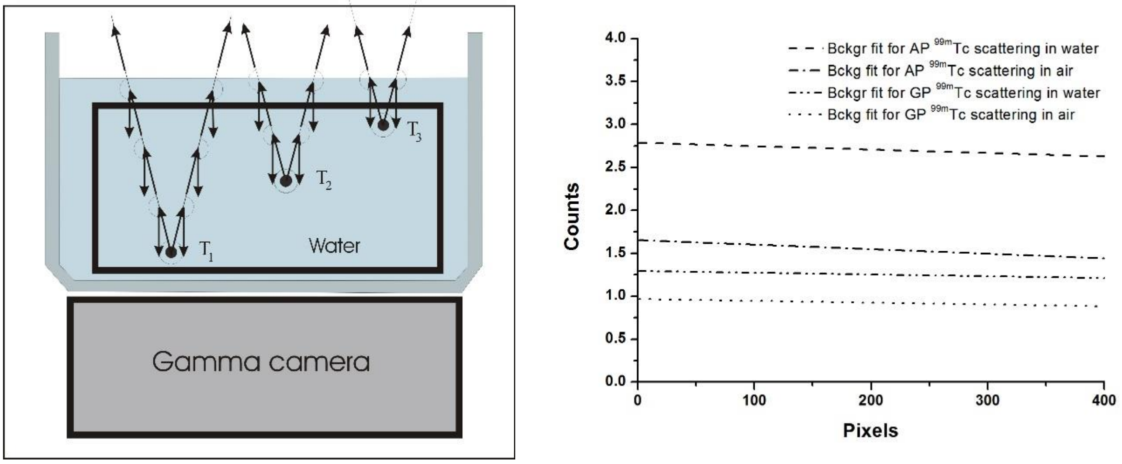

FIG. 9. (left) Sketch of the three capillary tubes, indicated as T1, T2, and T3, and the gamma camera. The larger the water layer above the capillary tube, the bigger the number of Compton backscattered gamma rays beneath; (right) Average background fits derived from the profiles of the system of capillary tubes with circulating AP ^{99m}T and the GP ^{99m}Tc, obtained in air and immersed in water.

The comparison reveals slightly higher background rate of the AP ^{99m}Tc images (a factor of 1.5 – 2) and, as shown in Figure 9, a slightly higher slope of the images' background obtained with AP ^{99m}Tc. The later indicates on higher-energies Compton backscattering of the gamma rays emitted by the other technetium isotopes. However, it is worth noting that the background measurements were carried out long after the end of the chemical extraction of the AP ^{99m}Tc and the relative activity of the other isotopes versus the ^{99m}Tc one had higher values, thus admitting relatively large error in the background evaluation. More details will be provided soon in a submitted paper to peer-reviewed journal.

7. ABSORBED DOSE COMPUTATIONAL STUDIES

As it can be seen from Table 4 the AP ^{99m}Tc contains some amounts technetium impurities. It is therefore important to calculate their impact on the patient radiation dose with respect to the GP ^{99m}Tc. Just a few considerations of a dedicated study and some of the results obtained are here reported. A comprehensive study is underway and aimed at being submitted to peer-reviewed journal.

Four radiopharmaceuticals, commonly used in the nuclear medicine clinic have been studied: Pertechnetate (used in clinical diagnostic of thyroid function and morphology) [16]; SESTAMIBI (widely used on cardiac scans for diagnosis of heart disease) [17]; Hexamethylpropyleneamine Oxime (i.e. HMPAO), used as tracers of brain function [18]; and Disodium Etidronate (i.e. HEDP) (a phosphonate commonly used for defining bone metastasis in cancer patients) [19]. According to the Medical Internal Radiation Dose (MIRD) method, the time integral of the activity of the isotope distributed inside the organ A_h gives the total number of decays or cumulated activity in the source organ ($\tilde{A}_h$) expressed per unit of initial activity (MBq h/MBq):

$$\tilde{A}_h = \int_{t=0}^{t=\infty} A_h \, dt.$$

The cumulated activity for each radionuclide in the main source organs was calculated for all the radiopharmaceuticals studied using the biokinetics models published by the International Commission on Radiological Protection (ICRP). Pertechnetate and Phosphonate biokinetic models were obtained from publication 53 (ICRP, 1988) [20] and SESTAMIBI and HMPAO models from the publication 80 (ICRP, 1998) [21]. The cumulated activity in bladder ($\tilde{A}_b$) for all 4 radiopharmaceuticals was calculated using the kidney-bladder model presented in ICRP publication 106 [22], which considers that the effect of kidney residence time can be neglected. For phosphonates, which are eliminated mainly by the kidney, the number of decays, that occurred in this organ, was calculated by using the kidney-bladder model from ICRP 53. For the other 3 radiopharmaceuticals eliminate predominantly by Gastro-Intestinal (GI) system, the number of decays that occurred in this tract were calculated using the GI model report on ICRP publication 30. The cumulated activity in the source organs, after the administration of the radiopharmaceutical mentioned before was calculated for the cyclotron produced Tc isotopes found in our experiments (see Table 4).
The absorbed dose in the target organs (r_k) was calculated using the following equation:

$$\tilde{D}(\mathrm{r_k} \leftarrow \mathrm{r_h}) = \boldsymbol{\tilde{A}_h}\, \boldsymbol{S}(\mathrm{r_k} \leftarrow \mathrm{r_h}),$$

where $\tilde{D}(r_k \leftarrow r_h)$ is the mean absorbed dose to a target organ from a source organ, $\tilde{A}_h$ is the cumulated activity in the source organ and $\boldsymbol{S}$ is a dose factor that can be calculated from the following equation:

$$\boldsymbol{S}(\mathrm{r_k} \leftarrow \mathrm{r_h}) = \frac{\mathrm{K}\sum_{\mathrm{i}} \Delta_i\, \phi_i\, (\mathrm{r_k} \leftarrow \mathrm{r_h})}{\mathrm{m_k}},$$

where $\boldsymbol{K}$ is a unit conversion constant, $\boldsymbol{\Delta_i}$ is the equilibrium dose constant for radiation $\boldsymbol{i}$ (in g.rad/µCi.h unit), $\boldsymbol{m_k}$ is the mass of the target organ and $\phi_{\mathrm{i}}(\mathbf{r_k} \leftarrow \mathbf{r_h})$ is the absorbed fraction in the target organ $\mathbf{r_k}$ for radiation $\boldsymbol{i}$ emitted in the source organ $\mathbf{r_h}$. The mean total absorbed dose $\tilde{D}(\mathrm{r_k})$ to a target organ $\mathrm{r_k}$ is then the sum of the absorbed dose contributions from all the source organs $\mathrm{r_h}$:

$$\tilde{D}(\mathrm{r_k}) = \sum_h [\boldsymbol{\tilde{A}_h}\, \boldsymbol{S}(\mathrm{r_k} \leftarrow \mathrm{r_h})]$$

OLINDA/EXM 1.1 software [23] was applied for radiation dosimetry calculations using an adult male phantom by adding the cumulated activity in the source organs for each real technetium impurities experimentally measured and radiopharmaceutical, calculated previously. Then, the total absorbed dose in the target organs, produced by the mixture of technetium radioisotopes at 3 different times after irradiation (9, 14, and 19hrs post EOB), was calculated using the next equation:

$$\tilde{D}\ \mathrm{r_k} \leftarrow \mathrm{r_h} = \sum_j \boldsymbol{f_j}\, \tilde{D}(\mathrm{r_k} \leftarrow \mathrm{r_h})j\,,$$

where $\boldsymbol{f_j}$ is the fraction of the total activity corresponding to each radioisotope $\boldsymbol{j}$ and $\tilde{D}(\mathbf{r_k} \leftarrow \mathbf{r_h})\,\boldsymbol{j}$ is the dose contribution from the source organ to the target organ per unit of activity from each technetium isotope.

From the analyses of data in Table 5 and taking into account the constraints, it may be concluded that the small activities of other technetium isotopes contribute to a slight increase of the absorbed dose. Bone marrow is the organ that exhibits higher difference between the absorbed dose obtained with a GP ^{99m}Tc and an AP ^{99m}Tc. Phosphonate showed the highest bone marrow dose difference to be about 8.5% 11.8% and 17.7% for 9, 14, and 19 h irradiations respectively. However, for Sestamibi, Pertecnetate and HMPAO the difference is lower than 8%, 10% and 14% after 9, 14, and 19 h irradiations respectively.

TABLE 5. CALCULATED ABSORBED DOSE IN THE MAIN ORGANS AFTER ADMINISTRATION OF 4 RADIOPHARMACEUTICALS PREPARED WITH AP ^{99m}Tc.

	9h	14h	19h	Tc-99m
Tc Sestamibi (h) (Rest study)				
Brain	2.23E-03	2.28E-03	2.36E-03	2.12E-03
Heart wall	5.78E-03	5.85E-03	5.98E-03	5.54E-03
Kidney	3.53E-02	3.55E-02	3.59E-02	3.43E-02
Liver	8.48E-03	8.57E-03	8.74E-03	8.12E-03
Lung	3.04E-03	3.09E-03	3.19E-03	2.88E-03
Red marrow	3.91E-03	3.99E-03	4.13E-03	3.68E-03
Tc Pertechnetate				
Small intestine	1.66E-02	1.68E-02	1.71E-02	1.60E-02
Stomach wall	9.84E-03	9.92E-03	1.01E-02	9.47E-03
Kidney	4.88E-03	4.95E-03	5.07E-03	4.64E-03
Red marrow	3.80E-03	3.87E-03	4.02E-03	3.56E-03
Thyroid	2.25E-02	2.25E-02	2.27E-02	2.20E-02
Urinary bladder	1.85E-02	1.86E-02	1.90E-02	1.78E-02
Tc Phosphonate				
Kidney	8.60E-03	8.73E-03	8.98E-03	8.20E-03
Red marrow	4.79E-03	4.93E-03	5.19E-03	4.41E-03
Osteogenic cells	3.56E-02	3.60E-02	3.65E-02	3.49E-02
Urinary bladder	4.96E-02	4.98E-02	5.03E-02	4.82E-02
Tc HMPAO				
Brain	7.23E-03	7.42E-03	7.77E-03	6.77E-03
Small intestine	9.24E-03	9.37E-03	9.61E-03	8.83E-03
Stomach wall	4.03E-03	4.11E-03	4.26E-03	3.78E-03
Kidney	3.33E-02	3.37E-02	3.43E-02	3.22E-02
Liver	8.80E-03	8.91E-03	9.12E-03	8.40E-03
Red marrow	3.47E-03	3.56E-03	3.71E-03	3.23E-03

8. TECHNOLOGICAL DEVELOPMENTS TO DESIGN AND TEST A HIGH SPECIFIC POWER HEAT REMOVAL (e.g. >10 kW) TARGET SYSTEM. ASSESSMENT OF VIABLE PROCESSES IN ORDER TO FIND OUT THE OPTIMAL WAY TO MOLYBDENUM DEPOSITION TECHNIQUE

The problem of heat removal from narrow irradiation area is crucial for the effectiveness of the nuclear reaction for radioisotope having medical interest. Sometimes high power targets require extremely high efficiency of heat dissipation, which can be provided only by liquid metal cooling. Difficulty lays in the fact that the liquid metal alloys are normally chemically aggressive, and all the metals that are good heat conductors suffer from the liquid metal embrittlement. Therefore, use of specific protective coatings is mandatory.

Refractory metals such as niobium (Nb), zirconium (Zr) and tantalum (Ta), as their alloys or oxides, have high melting point and excellent chemical resistance. Chemical stability of material is necessary for high corrosion resistance, but not enough. The microstructure of material is also of primary importance. In a case of thin films, atomic diffusion is no longer determined by regular bulk processes but is controlled by grain boundaries and other defects in the material. Grain boundaries and extended defects offer paths, which can carry atoms rapidly across the films thereby dominating the atomic traffic. Therefore, avoidance of prolonged through the film voids and grain boundaries is a first necessary requirement for the barrier. Diffusion through the amorphous layers is very difficult due to the irregularity of the atomic structure.

Sputtering is a standard method for deposition of thin film of both conductive and non-conductive materials as well as materials with high melting point as refractory metals. We proposed to use sputtering technique as deposition method because it provides also a possibility of microstructure control. In order to find out the most effective protective coatings, the coatings content, microstructure and barrier properties have been correlated with deposition parameters such as substrate temperature, applied bias, deposition rate, sputtering gas pressure, multilayer periodicity and multilayer deposition method, etc. Aluminated quartz used as a substrate allowed us to verify the protection efficiency of the desirable coatings as diffusion barriers. The modelling corrosion test was based on the extreme susceptibility of aluminum to liquid gallium corrosion.

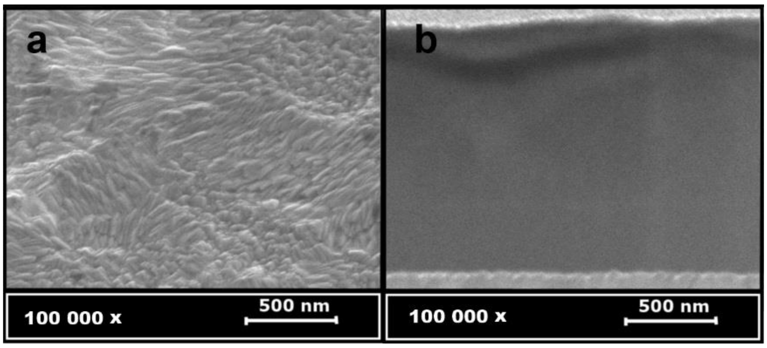

FIG. 10. SEM of the surface (a) and cross-section (b) of amorphous niobium oxide protective coating.

The main coating systems studied include:

- Pure Nb coatings obtained at different conditions
- Niobium oxide coatings
- Niobium-niobium oxide multilayer system
- Nb-Ta, Nb-Zr, Ta-Zr alloy systems of different composition

As far as all niobium coatings obtained by magnetron sputtering are columnar, the grain boundaries provide a fast diffusion path for active species of corrosive media to penetrate and to corrode the substrate. Amorphous niobium oxide films obtained by reactive magnetron sputtering (Figure 10) showed superior barrier properties according to the corrosion tests performed [24]. In order to prevent degrading of brittle niobium oxide at high pressures, multilayers combining high ductility of niobium with superior diffusion barrier efficiency of niobium oxide were proposed. The intercalation of niobium oxide interlayers was proved to interrupt the columnar grain growth of niobium during sputtering, resulting in improved diffusion barrier efficiency of obtained multilayers. The thin layer multilayer coating architecture with 70 nm bi-layer thickness was found preferential because of higher thermal stability [25].

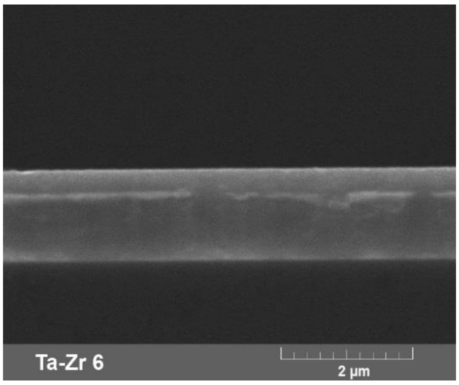

FIG. 11. SEM of the cross section of amorphous Ta47Zr53 alloy protective coating.

Since amorphous metal alloys (metallic glasses) are well-known to perform a high corrosion resistance, the glass forming ability, microstructure and diffusion barrier efficiency of binary alloys containing chemically inert Nb, Ta, Zr were investigated [26]. Nb–Ta, Nb–Zr and Ta–Zr 1.5 µm thick films of different alloy composition were co-deposited by magnetron sputtering. Though co-sputtered Nb–Ta and Nb–Zr alloy films of different contents were crystalline, Ta–Zr alloy was found to form dense amorphous microstructures in a range of composition with 30–73% atomic Ta. The diffusion barrier efficiency of Nb–Zr and Nb–Ta alloy coatings decreased with increase of Nb content. The diffusion barrier efficiency of sputtered Ta–Zr alloy coatings increased with the transition from nanocrystalline columnar microstructure to amorphous for coatings with 30–73 at.% Ta (Figure 11). Further details may be found in the papers by H. Skliarova et al. [24, 25, 26]

9. ACCELERATOR-BASED PRODUCTION OF ^{99}Mo: A COMPARISON BETWEEN THE ^{100}Mo(p,x) AND ^{96}Zr(α,n) REACTIONS

The production of high Specific Activity (SA) ^{99}Mo has also been investigated as parallel INFN dedicated research activity, by performing a new measurement of the ^{96}Zr(α,n)^{99}Mo reaction route [27]. This work has been carried out in collaboration with ARRONAX facility (Accelerator for Research in Radiochemistry and Oncology at Nantes Atlantique) [28]. The charge particle-induced reactions for the production of ^{99}Mo, i.e. the ^{100}Mo(p,x)^{99}Mo and ^{96}Zr(α,n)^{99}Mo routes, were compared with SA values generally demanded worldwide for standard ^{99}Mo/^{99m}Tc generator systems [29], i.e. up to SA = 370 TBq/g for large-sized generators (^{99}Mo activity of 7.4 TBq), up to SA = 37 TBq/g for medium-sized generators (^{99}Mo activity of 740 GBq) and SA = 0.37 TBq/g for small-sized generators (^{99}Mo activity of 7.4 GBq) [30].

Estimations of ^{99}Mo activity and SA at the End Of Bombardment (EOB) were performed for these p- and α-induced reactions, taking into account ideal target (100% enriched) and commercially available enriched materials. In particular, the isotopic composition of the 99.05% enriched Mo-100, supplied by ISOFLEX company [3] (^{92}Mo 0.08%, ^{94}Mo 0.05%, ^{95}Mo 0.10%, ^{96}Mo 0.11%, ^{97}Mo 0.07%, ^{98}Mo 0.54%, ^{100}Mo 99.05%), and the 86.4% enriched Zr-96, supplied by CHEMOTRADE company (^{90}Zr 5.00%, ^{91}Zr 1.88%, ^{92}Zr 2.69%, ^{94}Zr 4.03%, ^{96}Zr 86.40%), were considered. Density values of enriched materials were calculated by rescaling density and mass number of naturally occurring elements, considering isotopic composition and isotope atomic weight (100% ^{100}Mo ρ=10.71 g/cm^3, 100% ^{96}Zr ρ=6.82 g/cm^3, 99.05% ^{100}Mo ρ=10.70 g/cm^3, 86.4% ^{96}Zr ρ=6.78 g/cm^3). Production yield calculations were performed for all possible ^{xx}Mo(p,x)^{xx}Mo and ^{xx}Zr(α,x)^{xx}Mo open reactions, by using theoretical excitation functions higher than 1 mb in the energy windows of interest [31].

Two estimations were carried out in case of the ^{96}Zr(α,n)^{99}Mo reaction, respectively for 25-12 MeV and 20-10 MeV, due to the discrepancy in the optimized energy ranges for experimental [27] and theoretical [31] cross sections. Regarding the p-based route, the energy windows of 40-10 MeV and 70-10 MeV have been chosen, since both theoretical [31] and experimental [32] excitation functions are negligible for Ep<10MeV (threshold energy E=8.4 MeV). Since ^{99}Mo cannot be chemically separated from ^{100}Mo targets, the SA of resulting ^{99}Mo is driven by the mass of the sample This was calculated by considering area, thickness (relative to each energy range) and density of irradiated material. ^{99}Mo yields and target thicknesses were calculated for the energy ranges of interest, in case of both ^{100}Mo(p,x)^{99}Mo and ^{96}Zr(α,n)^{99}Mo reactions, by using experimental and theoretical cross sections. Yields resulting from the p-based route are much higher (a factor 10^2) than the ones produced with the α-induced reaction, whose ^{99}Mo yield is about 1 MBq/μAh. The advantage of using the ^{96}Zr(α,n)^{99}Mo reaction is the resulting high SA, that is even higher than the one required for large-sized generator systems.

In order to have a more realistic evaluation of ^{99}Mo SA in case of p- and α-induced reactions, the isotopic composition of commercially available enriched materials has been considered and the production of all ^{xx}Mo-isotopes has been estimated, as shown in Table 6 and 7. It has to be noted that ^{93m}Mo (half-life 6.85 h) is the only radioactive Mo-isotope produced, and that the main radioactive nuclides, i.e. ^{95m}Nb (half-life 3.61 d), ^{95g}Nb (half-life 35 d), ^{96}Nb (half-life 23.35 h), ^{95}Zr (half-life 64 d) and ^{97}Zr (half-life 16.75 h), can be chemically separated from ^{99}Mo.

TABLE 6. THEORETICAL ESTIMATIONS OF ^{99}Mo ACTIVITY AND SA AT EOB FOR 99.05% ENRICHED ^{100}Mo, A MEAN POWER AREAL DENSITY 500 W/cm^2 AND IP = 500 mA.

	E_P = 40-10 MeV		E_P = 70-10 MeV	
Irradiation Time	Activity [TBq]	SA [GBq/g]	Activity [TBq]	SA [GBq/g]
12h	0.6	6.7	2.2	4.7
24h	1.2	12.6	4.2	8.8
72h	2.9	30.1	9.9	21.0
120h	3.9	40.1	13.4	28.4
21d	5.4	56.6	18.7	38.5

TABLE 7. THEORETICAL ESTIMATIONS OF ^{99}Mo ACTIVITY AND SA AT EOB FOR 86.4% ENRICHED ^{96}Zr.

	Eα = 25-12 MeV			Eα = 20-10 MeV		
Irradiation Time [h]	Act. [GBq] I=35μA	Act. [GBq] I=100μA	SA [TBq/g]	Act. [GBq] I=35μA	Act. [GBq] I=100μA	SA [TBq/g]
12	0.4	1.3	$5.9 \cdot 10^6$	0.2	0.6	$7.0 \cdot 10^6$
24	0.8	2.4	$5.6 \cdot 10^6$	0.4	1.2	$6.6 \cdot 10^6$
72	2.0	5.6	$4.4 \cdot 10^6$	1.0	2.9	$5.2 \cdot 10^6$
120	2.7	7.6	$3.6 \cdot 10^6$	1.4	3.9	$4.2 \cdot 10^6$
21d	3.7	10.5	$1.2 \cdot 10^6$	1.9	5.4	$1.4 \cdot 10^6$

Table 6 shows that ^{99}Mo activity at EOB resulting from the p-based route seems to be adequate for the manufacture of small and/or medium sized generator systems, but the associated SA is much lower than the one currently adopted (i.e. by a factor 10^2-10^5), forcing certain changes in the existing ^{99}Mo/^{99m}Tc generator production chain. Results obtained via the α-induced reactions on ^{96}Zr are opposite (Table 7): the SA values are a factor 10^4 higher than the one used in the largest commercial generator systems (i.e. 370 TBq/g). However, the ^{99}Mo activities produced at EOB are too low to be used in the construction of few small-sized generator systems, making this route having poor practical interest for commercial cyclotrons. Considering that in this case the limiting factor is the intensity of the particle flux and that dedicated sources and accelerating techniques are under development, the production of high SA ^{99}Mo may be accomplished in the near future by using 10-100 mA α-beam [33, 34].

The direct ^{99m}Tc production in small cyclotrons via the ^{100}Mo(p,2n) reaction has been investigated by many authors and under this Coordinated Research Project on Accelerator Based Alternatives to Non-HEU Production of ^{99}Mo/^{99m}Tc. Considering the short half-life of ^{99m}Tc, this alternative seems to be an excellent solution only for local needs. Anyway, it requires a distributed network of cyclotron-based facilities and good logistic. Another issue related to this route is the co-production of other Tc-isotopes that remain in the final Tc-labelled radiopharmaceuticals, increasing patient dose and, in case of γ-emitters, affecting image quality. The production of Tc-isotopes may occur via open reaction channels on both ^{100}Mo (Ep>20MeV) and ^{xx}Mo-isotopes contained in the target. For this reason, the use of highly enriched ^{100}Mo is mandatory and, in order to keep competitive production costs, the recovery and reuse of irradiated ^{100}Mo-enriched moly, affected by an increasing amount of ^{xx}Mo-isotopes, should be also considered. Even if final limits for radionuclidic impurities in cyclotron-produced ^{99m}Tc have still to be set by currently non-existing specific Pharmacopoeia, the scientific community recommended short irradiation (3-6 hours) and cooling times (12 hours). However, different optimal proton beam energies have been proposed (see Paragraph 2) [1, 4, 35, 36]. Detailed results have been reported in the paper by G. Pupillo et al. [29] and Manenti et al. [4].

References

[1] ESPOSITO, J., G. VECCHI, G. PUPILLO, A. TAIBI, L. UCCELLI, A. BOSCHI, M. GAMBACCINI, Evaluation of ^{99}Mo and ^{99m}Tc productions based on a high-performance cyclotron, Science and Technology of Nuclear Installation (2013) 972381.

[2] INTERNATIONAL ATOMIC ENERGY AGENCY, 2nd RCM report on “Accelerator-based Alternatives to Non-HEU Production of ^{99}Mo/^{99m}Tc”, 7-11 October 2013, Legnaro, Italy, http://www-naweb.iaea.org/napc/iachem/working_materials/TR-RCM2-Final-Report-Draft-oct-22nd.pdf.

[3] ISOFLEX-USA 2012 Batch, Certificate of Analyses Mo-100 enriched molybdenum metallic material.

[4] MANENTI, S., HOLZWART, U., LORIGGIOLA, M., GINI, L., ESPOSITO, J., GROPPI, F., SIMONELLI, F., The excitation functions of Mo-100(p,x)Mo-99 and Mo-100(p,2n)Tc-99m, Applied Radiation and Isotopes **94** (2014) 344.

[5] MORLEY, THOMAS J., et al., An automated module for the separation and purification of cyclotron-produced $^{99m}TcO_4^-$, Nuclear Medicine and Biology **39** (2012) 551-559.

[6] MARTINI, P., et al., Extraction Techniques of ^{99m}Tc from ^{100}Mo Metal Target”, LNL INFN Annual Report (2013) 162, ISSN 1828-8561.

[7] MARTINI, P., et al., Development of an automatic separation/extraction module for the accelerator ^{99m}Tc production from 100Mo-enriched molybdenum metal targets, LNL INFN Annual Report (2014).

[8] DEL GUERRA, A., et al., IEEE Trans.Nucl.Science (2004).

[9] DI DOMENICO G. et al., Nucl Instrum Meth A **571** (2007) 110–113.

[10] NUDAT 2.6 DATABASE, http://www.nndc.bnl.gov/nudat2.

[11] BRODA, R., A review of the triple-to-double coincidence ratio (TDCR) method for standardizing radionuclides, Appl. Radiat. Isotopes. **58** (2003) 585–594.

[12] BRODA, R. et al., Study of the influence of the LS-cocktail composition for the standardisation of radionuclides using the TDCR model, Appl Radiat. Isotopes **56** (2002) 285–289.

[13] TDCR-07 software http://www.nucleide.org.

[14] NEMA STANDARD PUBLICATION NU 1-2001, Performance Measurements Of Scintillation Cameras, USA, Rosslyn: National Electrical Manufacturers Association, (2001).

[15] UZUNOV, N.M., et al., Characterization of Scintillation Imaging Camera for Evaluation the Imaging Properties of Isotopes Produced in APOTEMA Experiments, INFN-LNL Report **239** (2013) ISSN 1828-8561.

[16] KRASSAS, G.E., et al., Thyroid function and human reproductive, Health Endocrine Reviews, **31(5)** (2010) 702-755.

[17] UNDERWOOD, S.R., et al., Myocardial perfusion scintigraphy: the evidence - A consensus conference organised by the British Cardiac Society, the British Nuclear Cardiology Society and the British Nuclear Medicine Society, endorsed by the Royal College of Physicians of London and the Royal College of Radiologists, European Journal of Nuclear Medicine and Molecular Imaging **31(2)** (2004)261-291.

[18] WYPER, D.J., Functional neuroimaging with single-photon emission computed-tomography (SPECT), Cerebrovascular and Brain Metabolism Reviews **5(3)** (1993) 199-217.

[19] LAM, M., et al., Bone seeking radiopharmaceuticals for palliation of pain in cancer patients with osseous metastases, Anti-Cancer Agents in Medicinal Chemistry **7(4)** (2007) 381-397.

[20] INTERNATIONAL COMMISSION OF RADIOLOGICAL PROTECTION (ICRP) 1988, Radiation Dose to Patients from Radiopharmaceuticals. ICRP Publication **53**, Ann. ICRP 18 (1-4).

[21] INTERNATIONAL COMMISSION OF RADIOLOGICAL PROTECTION (ICRP), 1998, Radiation Dose To Patients From Radiopharmaceuticals (Addendum to ICRP Publication 53), ICRP Publication **80**, Ann. ICRP 28 (3).

[22] INTERNATIONAL COMMISSION OF RADIOLOGICAL PROTECTION (ICRP), 2008, Radiation Dose To Patients From Radiopharmaceuticals - Addendum 3 to ICRP Publication **53**, ICRP Publication **106,** Ann. ICRP **38** (1-2).

[23] STABIN, M.G., SPARKS R.B., CROWE E., OLINDA/EXM: The second-generation personal computer software for internal dose assessment in nuclear medicine. Journal of Nuclear Medicine, **46(6)** (2005) 1023-1027.

[24] SKLIAROVA, H., AZZOLINI, O., CHERENKOVA-DOUSSET, O., JOHNSON, R.R., PALMIERI, V., Niobium-based sputtered thin films for corrosion protection of proton-irradiated liquid water targets for [18F] production, J. Phys. D: Appl. Phys., **47** (2014) 045306.

[25] SKLIAROVA, H., RENZELLI, M., AZZOLINI, O., DE FELICIS, D., BEMPORAD, E., JOHNSON, R.R., PALMIERI, V., Niobium-niobium oxide multilayered coatings for corrosion protection of proton-irradiated liquid water targets for [18F] production, Thin Solid Films (2015).

[26] SKLIAROVA, H., AZZOLINI, O., JOHNSON, R.R., PALMIERI, V., Co-sputtered amorphous Nb–Ta, Nb–Zr and Ta–Zr coatings for corrosion protection of cyclotron targets for [18F] production, J. Alloys Compd., **639** (2015) 488-495.

[27] PUPILLO, G., ESPOSITO, J., GAMBACCINI, M., HADDAD, F., MICHEL, N., Experimental cross section evaluation for innovative Mo-99 production via the (alpha,n) reaction on Zr-96 target., Journal of Radioanalytical and Nuclear Chemistry (2014) DOI: 10.1007/s10967-014-3321-9,

[28] HADDAD, F., et al., Eur. J. Nucl. Med. Mol. Imaging **35** (2008) 1377-1387.

[29] PUPILLO, G., ESPOSITO, J., GAMBACCINI, M., HADDAD, F., MICHEL, N., Accelerator-based production of ^{99}Mo: A comparison between the ^{100}Mo(p,x) and ^{96}Zr(α,n) reactions, Journal of Radioanalytical and Nuclear Chemistry (2015) DOI 10.1007/s10967-015-4091-8.

[30] WOLTERBEEK, B., et al., What is wise in the production of ^{99}Mo? A comparison of eight possible production routes, Journal of Radioanalytical and Nuclear Chemistry (2014) DOI: 10.1007/s10967-014-3188-9.

[31] KONING, A.J., et al., TENDL-2013: TALYS-based evaluated nuclear data library, www.talys.eu/tendl-2013.html.

[32] Qaim, S.A., et al., Evaluation of excitation functions of ^{100}Mo(p,d+pn)^{99}Mo and ^{100}Mo (p,2n)^{99m}Tc reactions: Estimation of long-lived Tc-impurity and its implication on the specific activity of cyclotron-produced ^{99m}Tc, Appl Radiat Isotopes **85** (2014) 101-113.

[33] ROSENTHAL, G.B., Patent No. US 8,624,502 B2 (2014).

[34] ROSENTHAL, G.B., et al., (2014) http://mo99.ne.anl.gov/2014/pdfs/.

[35] CELLER, A., et al., Phys. Med. Biol. **56** (2011) 5469–5484.

[36] LEBEDA, O., et al., Nucl. Med. Biol. **39** (2012) 1286–1291.

^{99m}Tc PRODUCTION BY 18 MeV PROTONS ON ^{100}Mo TARGET: RESULTS AND CONSIDERATIONS

M. CLEMENZA[CD], F. GROPPI[f], S. MANENTI[f], M. ODDONE[b,e], A. SALVINI[a,e], L. STRADA[a,e]

a) Laboratorio Energia Nucleare Applicata (L.E.N.A.) of the University of Pavia, Via Aselli 41, 27100, Italy
b) Chemistry Department, University of Pavia, Via Taramelli 12, 27100, Pavia, Italy
c) Physics Department "G. Occhialini" of the University of Milano-Bicocca, P.zza della Scienza 3, 20126 Milano, Italy
d) INFN Section of Milano-Bicocca, P.zza della Scienza 3, 20126, Italy
e) INFN sez Pavia Via Bassi, 6 27100 Pavia – Italy
f) Laboratorio Acceleratori e Superconduttività Applicata - L.A.S.A., INFN and Physics Dept. of University of Milano, Via F.lli Cervi 201, 20090 Segrate (MI), Italy

Abstract

The University of Pavia, with Laboratory of Nuclear Energy Applied (LENA) and Radiochemistry Area, tested the ^{99m}Tc production using enriched ^{100}Mo as target in a protons accelerator. The research involves the radiochemical purity of the ^{99m}Tc product adopting different techniques, the evaluation of ^{99g}Tc production and studies on recycling of the enriched Molybdenum after separation.

1. FACILITIES

The facilities adopted are the Laboratories of the University of Pavia and protons irradiation are performed at the Cyclotron of the European Commission Joint Research Centre. The accelerator is a Scanditronix MC40 Fig.1. It is a highly versatile accelerator with variable particle energy and the capability of accelerating protons and alpha particles (8 – 40 MeV) as well as deuterons (4 – 20 MeV) and helium-3 nuclei (13 - 53 MeV). The University of Pavia used the Research Reactor Fig.1 to produce tracers used in the separation process and for NAA for purity measures of Mo recovered. The Reactor is a TRIGA type 250 kW in stable state with the following fluxes Table 1 and 2:

TABLE 1. MEAN VALUES AND STANDARD DEVIATIONS OF THE INTEGRAL NEUTRON FLUX RESULTS IN THE FOUR IRRADIATION FACILITIES. [1,2,3]

Irradiation facility	Measured Flux	RELATIVE ERROR
CENTRAL THIMBLE	$(1.72 \pm 0.17)\ 10^{13}$	10 %
RABBIT CHANNEL	$(7.40 \pm 0.95)\ 10^{12}$	13 %
LAZY SUSAN	$(2.40 \pm 0.24)\ 10^{12}$	10 %
THERMAL CHANNEL	$(2.52 \pm 0.36)\ 10^{11}$	14 %
THERMAL COLUMN [27]	$(1.19 \pm 0.08)\ 10^{10}$	------

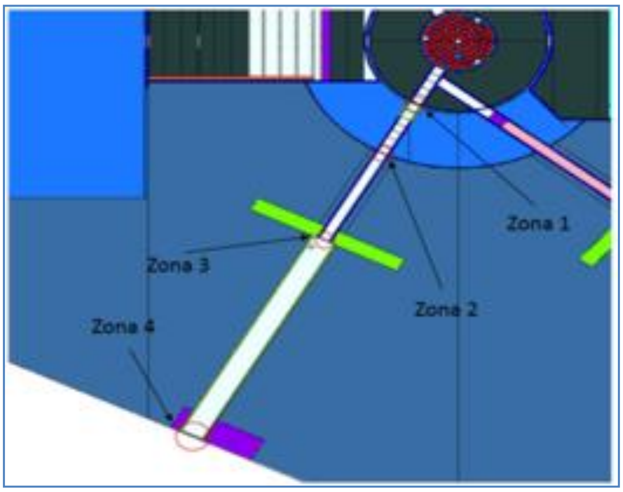

FIG. 1. Graphical output of MCNP simulation of the piercing channel D.

TABLE 2. THE INTEGRAL NEUTRON FLUX IN THE PIERCING CHANNEL D [1,2,3]

	ZONE 1	ZONE 2	ZONE 3	ZONE 4
NEUTRON FLUX $[n/(cm^2 s)]$	$1.14 \cdot 10^{12}$	$1.12 \cdot 10^{11}$	$9.07 \cdot 10^{9}$	$1.1 \cdot 10^{9}$

Targets preparations are made in collaboration with the laboratory of Accelerator and Applied Superconductivity Laboratory – L.A.S.A. (associated to INFN sez. Mi), INFN - LNL (Legnaro National Laboratories) and the University of Ferrara (INFN sez. Fe). Measures of ^{99g}Tc were performed with ICP-MS in University of Milan (Bicocca) Laboratory. Table 4. shows facilities and their applications.

TABLE 3. FACILITIES AND THEIR APPLICATIONS

Facilities	**application**
INFN - LNL (Legnaro National Laboratories)	Foils preparation
Laboratory of Accelerator and Applied Superconductivity Laboratory – L.A.S.A. (associated to INFN sez. Mi),	Irradiations
University of Pavia and Ferrara (INFN sez. Pv e Fe)	Separations
University of Pavia (INFN sez. Pv	Recovery and dosimetry
University Milan Bicocca	^{99g}Tc analysis

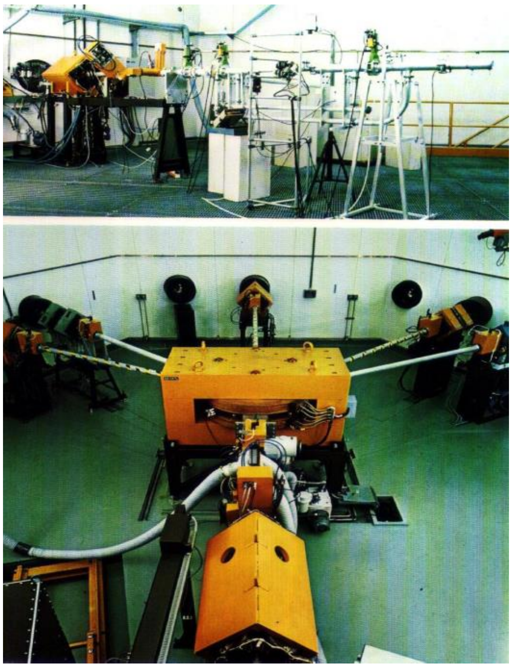

FIG.2. Scanditronix MC40.

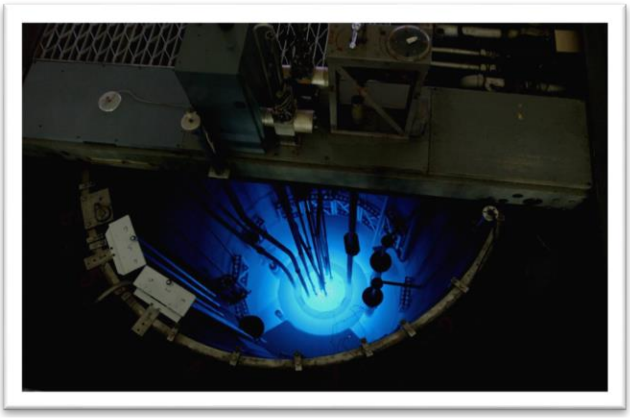

FIG.3. Research Reactor TRIGA type.

2. TARGETS PREPARATION

Targets are few foils ^{100}Mo enriched of 20-25 micron stick together and separated by aluminum foils prepared at Legnaro Laboratory. Fig.4.

FIG.4. Mo-100 Target.

3. IRRADIATION

The irradiations made at the JRC of Ispra were fixed with 18 MeV of Protons with a constant current of about 110 nA for a duration of 1 h. This energy was chosen considering the references, with the production yields on energy of both ^{99m}Tc and impurity, and the consideration that many cyclotrons installed inside hospitals, in Italy, are 18 MeV accelerators. If we consider the half life of the isotope we point that a local production could be convenient in case of world production lacks.

The final activity expected was about 2.5 MBq of ^{99m}Tc for each foil. This activity allowed the manipulation of the radioactive materials after the decay due to the time necessary to transfer the target to Pavia Laboratory, indeed the residual activity is enough to measure all parameter of interest. Fig. 5 show the irradiation setup and Tabble 4 the irradiation parameters.

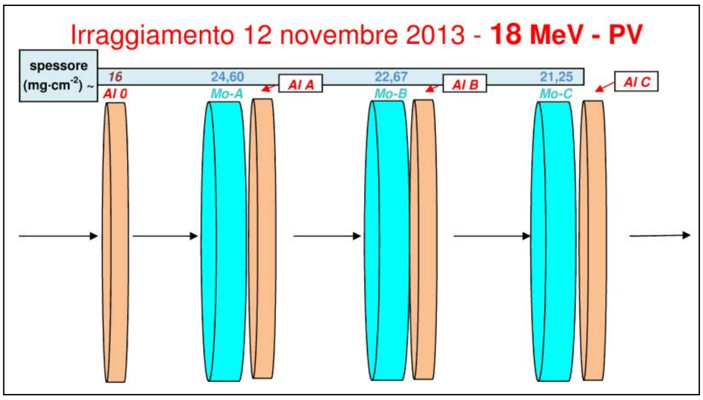

FIG. 5. Irradiation setup.

TABLE 4. IRRADIATION PARAMETERS

Start Energy	18.0 ± 0.2 MeV
Corrent	~110 nA
Time	60 min
Irradiation start time	8:55
End irradiation	9:55
Total Charge	$3862 \cdot 10^{-7}$ C

Energy lost trought target:

- MoA: from 17.91 MeV to 17.53 MeV
- MoB: from 17.44 MeV to 17.09 MeV
- MoC: from 16.99 MeV to 16.65 MeV

We can consider targets as “thin” targets. In table 5 are reported targets features.

TABLE 5. TARGETS FEATURES

Target	**Thikness [mg/cm^2]**	**weight [mg]**	**Measure time**	**Attivity [MBq]**
MoA	24.60	31	13:39	2.9
MoB	22.67	31.4	13:47	2.6
MoC	21.25	26.9	14:00	2.3

4. TARGET DISSOLUTION

^{99m}Tc should be separated by the bulk and we tested different approaches. Mo foils were dissolved in acid (different acids and concentrations), basic (NaOH in different concentrations with or without H_2O_2 and finally with only H_2O_2 and heat. In order to have the best yield is important to have the dissolution as fast as possible and in the final form useful for direct separation. After several tests we consider the use of heated H_2O_2 the best choice. Table 6 shows results.

TABLE 6. DISSOLUTION RESULTS

Dissolution approach	**Results**
HNO_3 at different concentrations	Fast reaction
HCl at different concentrations	medium
NaOH 6N	No reaction
NaOH 6N with H_2O_2 at different concentration	Passivation
H_2O_2 30% cold	No reaction
H_2O_2 30% and heating	Fast reaction

5. SEPARATION

Tests were performed using well known Methyl ethyl ketone (MEK) separation, Acetone and exchange resins as AG 1X8 and in connection with alumina column Fig6. We have used Waters Sep Pak Alumina A Plus Cartridge, 1710 mg sorbent, 50-330 µm (Activated with H_2O deionized). The column was rinsed 5 mL of H_2O. 1% of starting activity was retained on the column. At this stage the aim is to retain Mo and elute ^{99m} Tc. The solution was again passed through Sep-Pack Water Plus QMA in order to concentrate $^{99m}TcO_4^-$ on the column and subsequently elute it with saline. Only 10% of Tc-99m is retained. Finally we obtain best results with the separation using Methyl ethyl ketone (MEK) Fig.6 and solvent extraction technique result economical convenient. Tests were carried out in our laboratory for the separation of ^{99m}Tc dissolving Mo oxide or metallic with H_2O_2. At this step all Mo present is oxidized. After the addition of NaOH 6N solution and heating to eliminate all peroxide, the separations were made using Methyl-ethyl ketone (MEK) in three times in a separation funnel. ^{99m}Tc present in organic fractions were evaporated and recovered with sterile isotonic solution at the desired specific activity.

Table 7 Shows results. The final products were in compliant with pharmacopeia protocol (radionuclide purity) Fig6-7. Both methods have contamination by isotopes of ^{95}Nb, ^{96}Nb and ^{99}Mo with ratio less than 10^{-5}. These values are at level of detection limits.

TABLE 7. SEPARATION RESULTS

Separation technique	**Results**
MEK	Fast with good separation
Resin	Presence of interference like Mo isotope in the final products

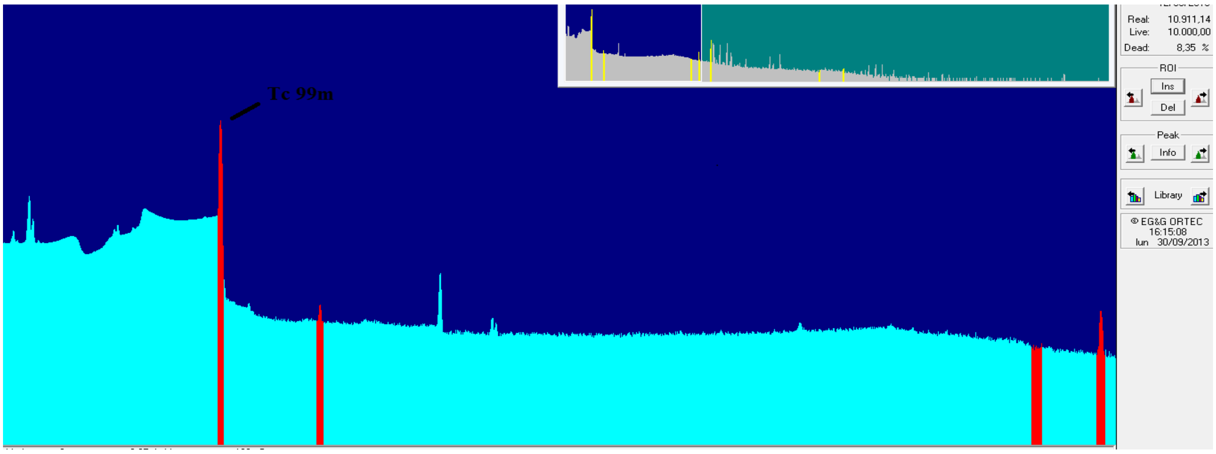

Real: 10.911,14
Live: 10.000,00
Dead: 8,35 %
16:15:08
lun 30/09/2013

FIG.6. Spectrum acquired after MEK separation.

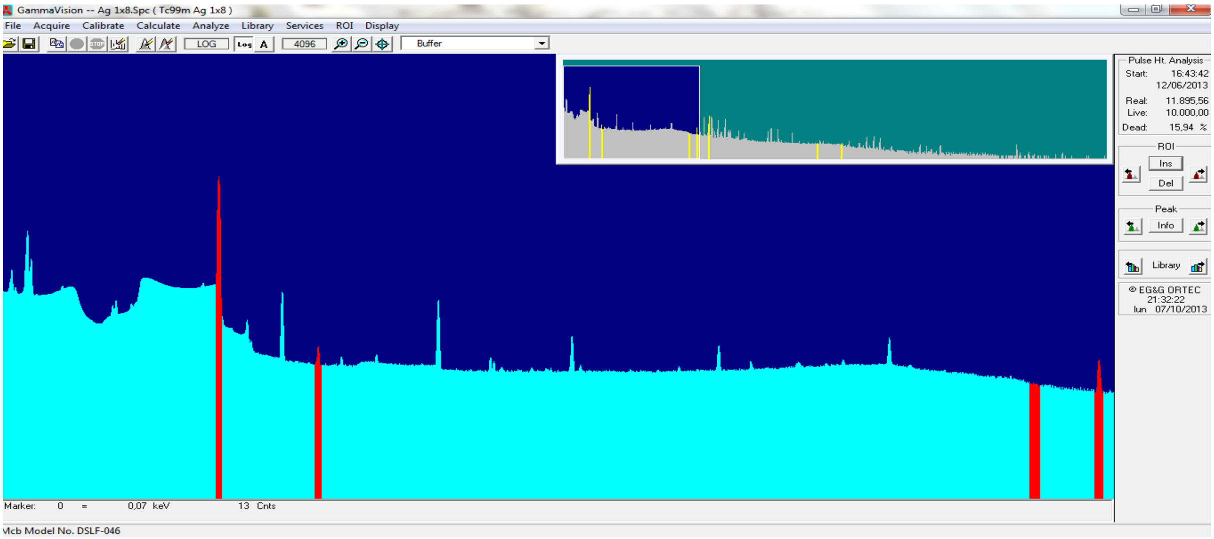

Pulse Ht. Analysis
Start: 16:43:42 12/06/2013
Real: 11.895,56
Live: 10.000,00
Dead: 15,94 %
21:32:22
lun 07/10/2013
Marker: 0 = 0,07 keV 13 Cnts
Mcb Model No. DSLF-046

FIG.7. Spectrum acquired after AG1X8 separation.

Detector features:

Resolution (FWHM) at 1.33 MeV ^{60}Co	1.70 KeV
Peek to Compton Ratio ^{60}Co	58:1
Relative Efficiency at 1.33 MeV ^{60}Co	33.1
Peak Shape (FWTM/FWHM) ^{60}Co	1.84
Peak Shape (FWFM/FWHM) ^{60}Co	2.45
Resolution (FWHM) at 122KeV ^{57}Co	731 eV

The detector is connected to a digital signal processing data acquisition system, DSPEC, PC-controlled by GammaVision™ software.

As shown, the separation with MEK gives better results. Typical radionuclidic purity values are reported in table 8.

TABLE 8. EXAMPLE OF RADIONUCLIDIC PURITY VALUES FOR A SAMPLE

$A_{Mo\text{-}99}/A_{Tc\text{-}99m}$	0,03 ± 0,01 %
$A_{Nb\text{-}97g}/A_{Tc\text{-}99m}$	< 0,004 %
$A_{Tc\text{-}93g}/A_{Tc\text{-}99m}$	0,11 ± 0,01 %
$A_{Tc\text{-}93g}/A_{Tc\text{-}99m}$	0,16 ± 0,01 %

In particular it is important to stress that the general ratio $A_{Tc\text{-}93g}/A_{Tc\text{-}99m}$ value is about 0,10 – 0,15 % and the ratio $A_{Tc\text{-}94g}/A_{Tc\text{-}99m}$ value is about 0,15 – 0,20 %.
Results are improved in the automatic productions with purification on alumina removing all impurity except Tc isotopes.

6. RECYCLING

We tested different approaches for the recovery of Mo oxide enriched after Methyl ethyl ketone (MEK) separation.

The one that showed best results was the precipitation of ammonium isopolymolibdate at pH 2-4. We used different acids to bring the pH to about 2. In particular we used sulfuric acid, concentrated hydrochloric acid and nitric acid 8 M which is what showed the best result for our needs. Then we reported the pH to a value close to 4 with a 1M solution of NH4OH. The solution was reduced in volume by half using a mild eating. After filtration of the ammonium salt with no ashes filter the product was calcinated at about 500°C obtaining Mo oxide Figures 8 and 9.

FIG. 8. Starting stage of recycling.

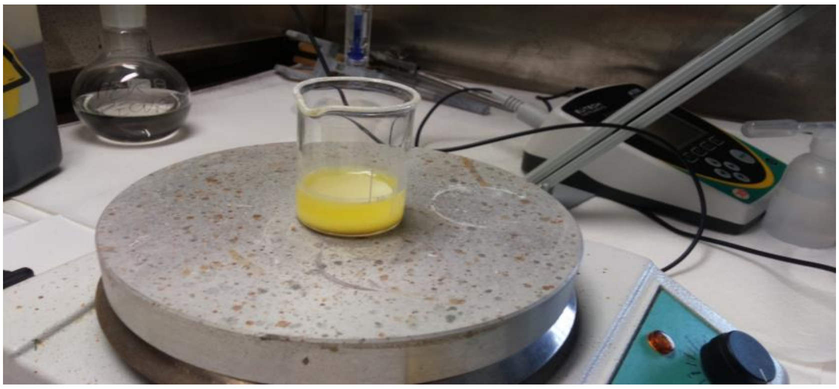

FIG.9. Precipitation stage of recycling.

Future testing of other recovery methods foreseen the precipitation with 8-ossichinolina addition that has the advantage to be quantitative and the final product is $MoO_2(Ox)_2$.

7. EVALUATION OF ^{99g}Tc PRODUCTION

We have tested two methods for the determination of ^{99g}Tc. We have used activation analysis and ICP/MS.

By activation we used the ^{100}Tc isotope with 15,8 sec half-life. The detection limit is higher than ICP/MS (ppm), it can be used only as reference of other techniques (Fig. 10). Sensitivity could be increased adopting cycle analysis system. Tested were performed with 5 x 10^{-2}g/g.

Starting from standard solution Eckert & Ziegler containing 5,84 x 10^{-05} g/g of ^{99}Tc (activity: 185.1 kBq mass: 5.01365 g) it was prepared the solutions for calibration. Determination limits result between 1 and 5 x 10^{-12} g/g .
This measure will be used to determine cross section of ^{99g}Tc productions (table 9).

TABLE 9. CALIBRATION CURVE SAMPLES ICP/MS TECHNIQUE

ID	Fattore di diluizione	g/g
Tc7	1/100 Sol Madre	5,84E-07
Tc6_5	1/2 Tc7	2,92E-07
Tc6	1/5 Tc7	1,17E-07
Tc5	1/10 Tc7	5,84E-08
Tc4	1/4 Tc6	2,92E-08
Tc3	1/5 Tc4	5,84E-09
Tc2	1/2 Tc3	2,92E-09
Tc1_5	1/2 Tc2	1,46E-09
Tc1	1/7 Tc2	4,17E-10
Tc0_5	1/5 Tc1	8,34E-11
Z1	H2O 3% di HNO3	Blank
Z2	H2O 3% di HNO3	Blank

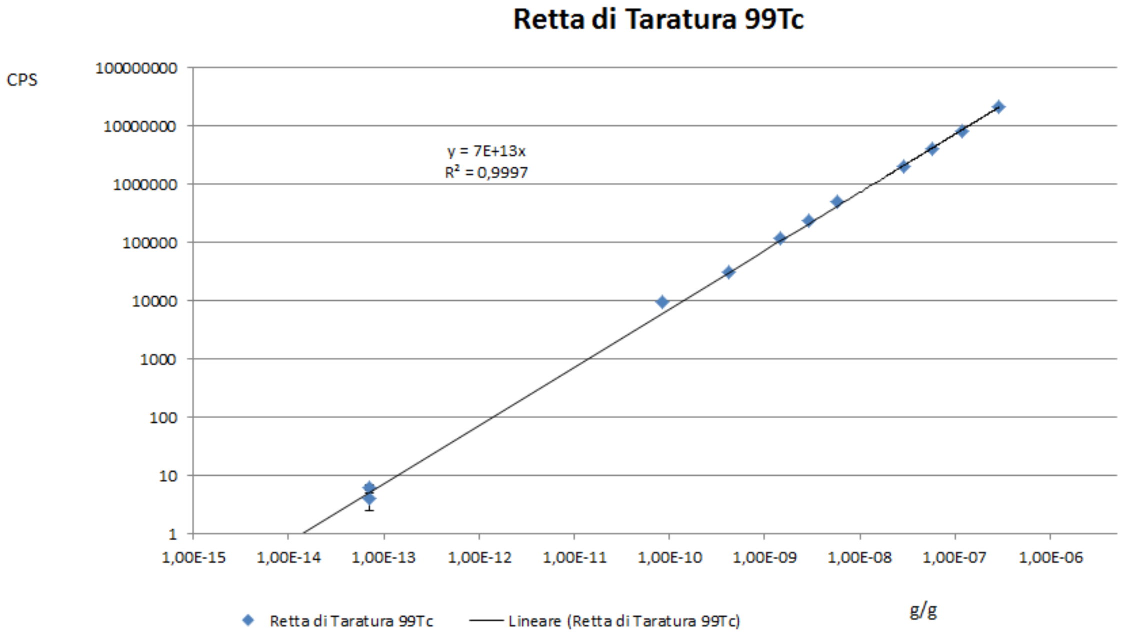

FIG. 10. Calibration curve ICP/MS Technique.

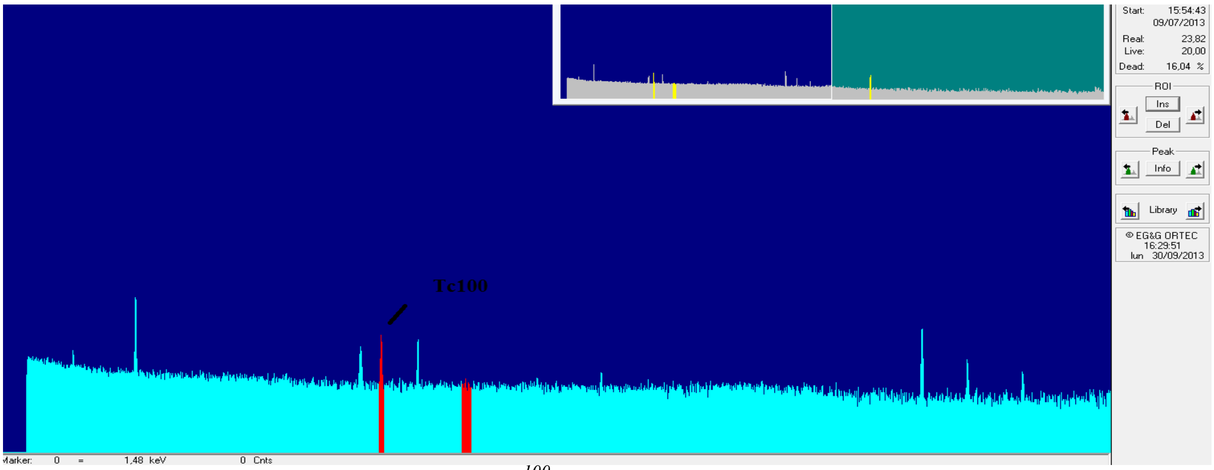

FIG. 11. ^{100}*Tc isotope spectrum.*

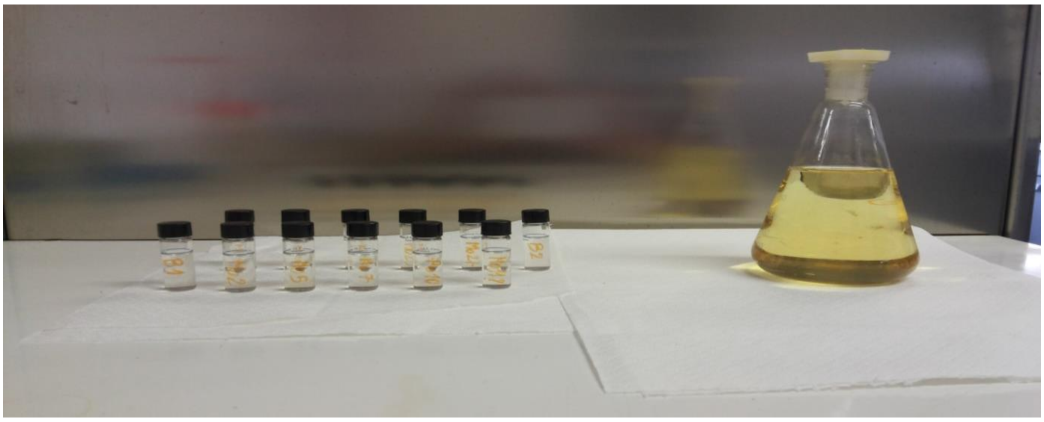

FIG. 12. Samples.

The excitation functions were measured using the stacked-foil technique covering the proton energy range from 8 MeV to 21 MeV.

All irradiations were carried out with the cyclotron (Scanditronix MC40) of the JRC-Ispra (VA) at different incident energies with a constant current of about 100 nA for a duration of 1 h. The excitation functions were obtained from seven foil stacks irradiated in seven different irradiation experiments. After the irradiations the targets were transported to LASA in Segrate (MI) to be measured. We utilized ICP-MS for evaluating the ^{99g}Tc content and, ultimately, the excitation function: the direct ^{99g}Tc excitation function was thus determined using ICP-MS in combination with γ-ray spectrometry to correct for the indirect ^{99g}Tc contributions produced by the complete decay of ^{99m}Tc and ^{99}Mo [4a] (figures 10-13).

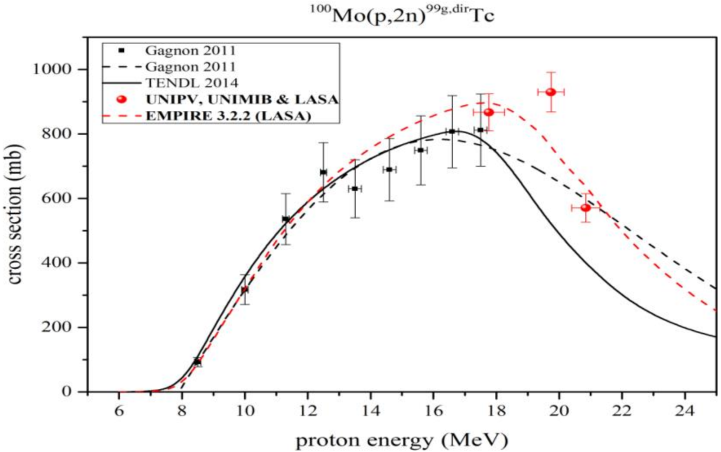

FIG. 13. Excitation functions for ^{100}*Mo(p,x)*^{99g,dir}*Tc nuclear reactions.*

8. RECOVERY

The precipitate is analyzed by Nuclear Activation Analysis (NAA) to verify the purity of the recovered oxide. Samples were irradiated at 250 kW in the Reactor rotary specimen rack for 40 minutes and then analyzed using the gamma lines at 140,5 keV and 739,5 keV in 5 cm geometry after one day (figure 14).

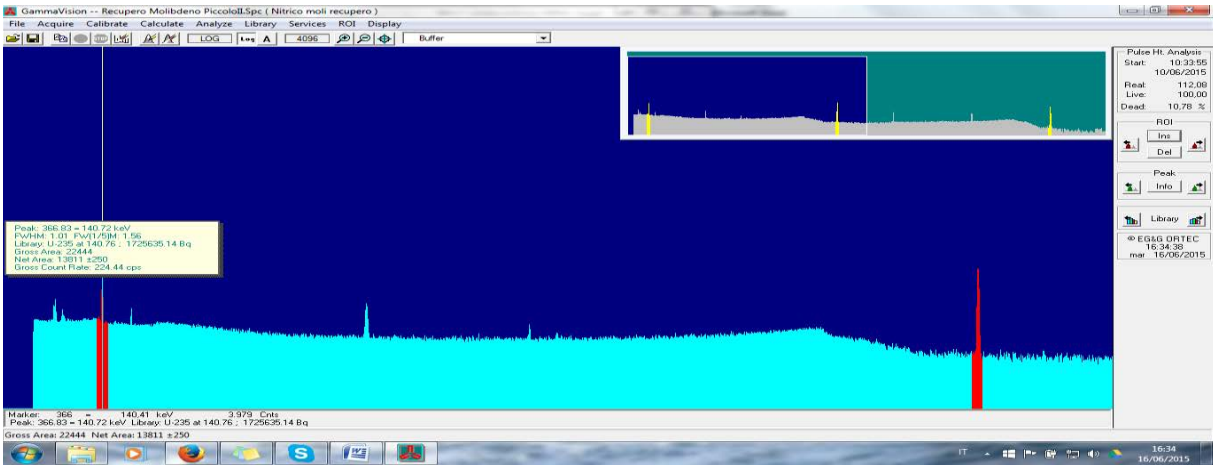

```
Peak: 366.83 = 140.72 keV
FWHM: 1.01  FW(1/5)M: 1.56
Library: U-235 at 140.76 ;  1725635.14 Bq
Gross Area: 22444
Net Area: 13811 ±250
Gross Count Rate: 224.44 cps
```

```
Pulse Ht. Analysis
Start:      10:33:55
          10/06/2015
Real:         112,08
Live:         100,00
Dead:        10,78 %
```

```
16:34:38
mar   16/06/2015
```

```
Marker:    366    =       140,41  keV              3.979  Cnts
Peak: 366,83 = 140,72 keV  Library: U-235 at 140,76 ;  1725635,14 Bq
Gross Area: 22444  Net Area: 13811 ±250
```

FIG. 14. NAA on recovered MoO_3.

The recovered MoO_3 was contaminated with Na but the final quality can be increased washing with deionized water. In order to reuse the enriched Mo with spattering technique we have to reduce MoO_3 to Mo metallic. There are many references [4,5,6,7]. In general we should consider that Molybdenum is a refractory metal mainly used as an alloying agent for manufacturing steels. In general, the reaction between MoO_2 and $H_2(g)$ in the hydrogen reduction process to produce molybdenum powders can be represented by $MoO_2 + 2H_2(g) = Mo + 2H_2O(g)$.

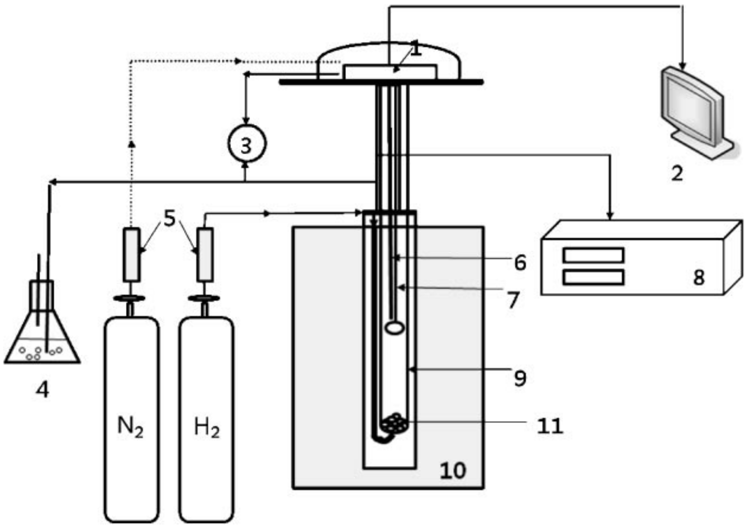

FIG. 15. Schematic diagram of the experimental apparatus for TGA thermal analysis; 1) Micro balance, 2) Data collector, 3) Pressure display, 4) Exhaust gases, 5) Mass flow controller, 6) Thermocouple, 7) Sample tray, 8) Temperature controller, 9) Reactor tube, 10) Furnace, 11) Ceramic ball.

The hydrogen reduction of MoO_2 will become to be fast at around over 900 K.
This activity will tack place after the Hydrogenate system setup.

9. RESULTS AND CONCLUSIONS

The production of the ^{99m}Tc using ^{100}Mo targets with 18 MeV protons gives good results. The best separation methods used is the dissolution with hot H_2O_2 than in NaOH 6N and finally separated with MEK. Other separation methods tested should be optimize because of the presence of Mo isotope in the final products. The solution obtained is really free from radiochemistry point of view apart the presence of other Tc isotopes like 97, 96, ground and ^{95}Nb, ^{96}Nb.

It is easy recover the Mo target in oxide form, than a new preparation of the target is needed considering also the redox reaction to metallic Mo.

An automatable extraction module was tested in Ferrara laboratory [8]. Components of the module were: two manual three-way valves, a silica column (Waters SEP-PAK CARTRIDGE), an acidic alumina column (Waters SEP-PAK CARTRIDGE), a vortex, syringes and vials. The solution was transferred from dissolution Mo vial to separation vial, containing 5 ml of MEK. The aqueous solution and the organic solvent were mixed by a vortex. After the phases separation (2 min), the organic solution, containing the ^{99m}Tc-pertechnetate and placed at the top of the vial, was transferred through silica and alumina columns to the *Waste* vial; on the contrary, in the bottom of B_{MEK} vial remained the aqueous phase. The silica column was washed with 1 ml of MEK and the alumina column with 10 ml of H_2O milliQ. The $^{99m}TcO_4^-$ adsorbed on the alumina column was eluted with 6 ml saline and collected in *FINAL* vial. An automatic and remote controlled prototype was than assembled. A detailed quality control (QC) analysis of the final pertechnetate solution was performed, in order to determine isotopes and impurity amounts, Mo breakthrough, percentage of organic solution etc. results are: MEK<0,0004% (v/v), Mo and Al < 5ppm, PH 4,5/5, Tc-99m <99%. The module recovery the ^{99m}Tc within 70 minutes [9]. In vivo multimodality imaging studies (SPECT-CT) were performed by using both the generator- and accelerator-produced ^{99m}Tc pertechnetate and the labeled within APOTEMA- TECHN_OSP INFN research activities.

Reference

[1] REVERSI, LUCA, Studio Computazionale per la Realizzazione di un Fascio di Difrattometria Neutronica Presso il Reattore TRIGA di Pavia, Master Degree Thesis – University of Pavia (2013).

[2] BORIO DI TIGLIOLE, A., et al., TRIGA reactor absolute neutron flux measurement using activated isotopes, Prog. Nucl. Ener. **70** (2014) 249–255.

[3] PROTTI, N., et al., Neutron Spectrometry for the University of Pavia TRIGA Thermal Neutron Source Facility, Transactions of the American Nuclear Society, **107**, San Diego, California, November 11–15, 2012.

[4a] MANENTI, S., HOLZWART, U., LORIGGIOLA, M., GINI, L., ESPOSITO, J., GROPPI, F., SIMONELLI, F., The excitation functions of ^{100}Mo(p,x)^{99}Mo and ^{100}Mo(p,2n)^{99m}Tc, Applied Radiation and Isotopes, **94** (2014) 344.

[4] IVANOVA, N.D., Electrodeposition of metal molybdenum from electrolytes containing hydrofluoric acid, Vernadskii Institute of General and Inorganic Chemistry, ISSN 0033-1732, Protection of Metals, Vol. **42**, No. 4, (2006) 354–358.

[5] BYUNG-SU KIM, Study on the reduction of molybdenum dioxide by hydrogen, Korea Institute of Geoscience & Mineral Resources, Daejeon, Korea Materials Transactions, Vol. **49**, No. 9 (2008) 2147 to 2152.

[6] ZHIQUAN, JIANG, Adsorption and decomposition of $Mo(CO)_6$ on thin Al_2O_3 films: fabrication of metallic molybdenum model catalyst, State Key Laboratory of Catalysis, Dalian Institute of Chemical Physics - Applied Surface Science **229** (2004) 43–50.

[7] YUANZHI, LI, A novel route to the synthesis of nanosized metallic molybdenum at moderate temperature and its catalytic properties, Department of Chemistry, Three Gorges University, Hubei, Yichang 44300, PR China - Materials Research Bulletin **39** (2004) 195–203.

[8] MARTINI, P., Extraction techniques of ^{99m}Tc from ^{100}Mo metal target , Annual report, Laboratori Nazionali di Legnaro.

[9] MARTINI, P., et al., Development of an Automatic Separation/Extraction Module for the Accelerator ^{99m}Tc Production from ^{100}Mo-Enriched Molybdenum Metal Targets, LNL INFN Annual Report (2014).

EVALUATION OF THE ^{99m}Tc REMOTE PRODUCTION BY PROTON BOMBARDMENT ON ^{100}Mo TARGET

KOTARO NAGATSU[A], KEIKO TAGAMI[B], TOSHIMITSU FUKUMURA[A], SHIGEO UCHIDA[B], YASUHISA FUJIBAYASHI[A]

[a] Molecular Imaging Centre,
National Institute of Radiological Sciences,
Anagawa, Inage, Chiba, Japan
[b] Research Centre for Radiation Protection,
National Institute of Radiological Sciences,
Anagawa, Inage, Chiba, Japan

Abstract

To combat the ^{99}Mo/^{99m}Tc crisis in Japan, we are proposing a concept for small-scall direct ^{99m}Tc production at multiple facilities. Because approximately 150 medical cyclotrons are in operation for routine PET diagnostics/studies in Japan, these cyclotrons present significant potential for contribution to the domestic ^{99m}Tc supply, namely through 'in-house' production or a 'micro-factory' network.

The automated production was evaluated by using ^{100}Mo oxide ($^{100}MoO_3$) or elemental ^{100}Mo powder as a target material, respectively. Briefly, ^{100}Mo oxide target was remotely prepared by a spray-dry method, where ^{100}Mo dissolved in H_2O_2 was sprayed onto a heated target vessel. In case of ^{99m}Tc productions from an elemental target, a weighed ^{100}Mo powder as purchased was prepared into a target vessel that was designed for a vertical irradiation system. In the recovery step following irradiation, both of the target was dissolved in H_2O_2 + NH_3 aq by directly loading of the solution into respective target vessel. The liquefied crude target solution was roughly purified and then transferred to a hot cell through a tube without using any robotic devices.

The recovered ^{99m}Tc crude using commercially available chelating-resin on an automated apparatus finely purified solution developed in this study. Approximately 3.7 GBq/6.3 GBq (100 mCi/170 mCi, decay uncorrected) of Na^{99m}TcO$_4$ with high radionuclidic- and radiochemical-purity was obtained from oxide/ elemental target, respectively, within 2 h of processing via irradiation with 18 MeV protons at 10 μA for 3 h.

Owing to the low stress involved in this production method, regional/in-house production could be performed with less effort. Moreover, if 100 or more cyclotrons in a sophisticated logistical network are available, the 'micro-factory' concept would work successfully at the level of 370 GBq (10 kCi) per day throughout the country.

1. INTRODUCTION

1.1. Background

The Japanese Society of Nuclear Medicine (JSNM), radiopharmaceutical companies, and all related organizations, including government ministries, were shocked by the ^{99}Mo/^{99m}Tc crisis in 2009–2010. Although Japan is the second largest ^{99m}Tc consumer in the world [1], there is no domestic production of ^{99}Mo. All the ^{99}Mo used in Japan has been imported every week from only a few countries; thus, the halting of production at both the reactors in Canada (NRU) and the Netherlands (HFR) was critical at that time. Several months later, a volcanic eruption in Iceland (spring in 2010) once again prevented the ^{99}Mo supply from reaching Japan owing to the malfunction of aerial transportation over Europe. Because of geographical location, Japan has a great risk for logistical isolation.

Hence, a reliable and sustainable supply of ^{99}Mo/^{99m}Tc, as well as the need for domestic production of these radionuclides, must be considered. An official consultation, organized in the end of 2009[1], discussed an action plan for the prevention of any such future crisis and the establishment of a method for independent, domestic production that was to be implemented by July 2011. The summary is as follows:

(1) Short-term actions (within 5 years: 2011–2016)

1. Identifying new/alternative ^{99}Mo suppliers (current import pathways remain alive)
2. Identifying alternative transportation routes
3. Pilot production in a research reactor of a quantity of ^{99}Mo that is approx. 1/3 of domestic demand
4. Commercializing a method for domestic production
5. Continuation of the R&D of alternatives, such as protons or neutrons on ^{100}Mo
6. Reviewing alternative methods/drugs instead of ^{99m}Tc, such as PET or other modalities in nuclear medicine

(2) Long-term actions (over 5 years or permanent: 2016–)

1. Cultivate a ^{98}Mo activation process that is competitive in the global marketplace
2. Investigate ^{99}Mo production by nuclear power plants

In the short-term action plan, briefly, radiopharmaceutical companies are responsible for identifying alternative ^{99}Mo imports; the Japan Atomic Energy Agency (JAEA) is responsible for developing an alternative reactor-based production method; and the National Institute of Radiological Sciences (NIRS, our group) is responsible for developing an accelerator (charged particle) method. Owing to the Nuclear Non-Proliferation Treaty (NPT), likely many other countries, Japan cannot use highly enriched ^{235}U; therefore, the neutron activation method for ^{98}Mo using a research reactor is the process selected as the primary plan for domestic production.

A research reactor, the Japan Material Testing Reactor (JMTR)[2] at the JAEA, has been modified since 2010 to produce ^{99}Mo. The planned amount of supply will be 8.51 TBq (230 Ci), which will be referred to as '6-days Ci/week;' the yield during shipping will then decay to about 1/4 of the initial value, or 60 Ci/week, which is approximately 10 Ci/day, and is potentially a practical amount. However, the any projects on reactor productions, including a long-term parallel plan in power plant, are completely halted because of the Great East Japan Earthquake. Actually, no commercial plant nor research reactor is in operation currently, therefore, the neutron activation schemes are now up in the air.

On the other hand, the accelerator alternative using a channel of the ^{100}Mo(p,2n)^{99m}Tc, which was proposed by our group (NIRS), is regrettably regarded as the second or lower priority option, yet. Although NIRS is not responsible for supplying any ^{99m}Tc products for practical consumption, we have continued our research and development efforts.

To summarize the current situation and prospects in near future, Japan will continue to import ^{99}Mo from many countries (including new supplier(s) and via new route(s)) as the main source of domestic supply. The plan for domestic production of ^{99}Mo by using a research reactor would be severely delayed, or as a worst-case scenario, discontinued. Since the Fukushima Dai-ichi nuclear accident, the social situation surrounding the nuclear energy, including research reactors, has been considerably worsened; in contrast, although accelerator

---

[1] The group of consultants included: The Cabinet Office; The Ministry of Health, Labour and Welfare (MHLW); The Ministry of Education, Culture, Sports, Science and Technology (MEXT) – 3 governmental groups

The Japan Atomic Energy Agency (JAEA); The National Institute of Radiological Sciences (NIRS); The Japan Radioisotope Association (JRIA) – 3 research institutes

Nihon Medi-Physics; Fujifilm RI-Pharma; Chiyoda Technol; Hitachi-GE Nuclear Energy; and Kaken – 5 commercial groups

[2] Located in Ibaraki Prefecture approximately 150 km northeast of Tokyo. The first critical event was performed in 1968. Its power is 50 MW_{TH} (4×10^{14} n/cm^2·s), and its operating rate (machine time) is expected to be approximately 60% (~ 200 days/year).

production methods are currently regarded as the secondary option, accelerators are not plagued with nuclear concerns; therefore, they might play an important role in the domestic supply of ^{99}Mo/^{99m}Tc in the future.

1.2. Records and estimated demand of ^{99m}Tc

In Japanese nuclear medicine, ^{99m}Tc and its parent ^{99}Mo are the most used radionuclides. Typically, their annual supply as radiopharmaceuticals is approximately 370 TBq (10 kCi) and 111 TBq (3 kCi), respectively (as of 2007–2013, [2]). Because the trends in demand for both nuclides seem to be stable or slightly decreasing, the demand for ^{99}Mo/^{99m}Tc in the near future is not expected to change significantly.

There are 1,256 nuclear medicine facilities in Japan that can perform common clinical diagnoses (as of 2012, [2]). An approximate estimation of the average daily demand for ^{99m}Tc at each facility can be given as about 1.11 GBq (30 mCi)[3]. According to a single dose of ^{99m}Tc, 370–740 MBq (10–20 mCi), 1–3 diagnoses are carried out in every clinic every day in Japan.

In addition, in a response to a boom in PET diagnoses using ‘in-house’ produced [^{18}F]-fludeoxyglucose (^{18}F-FDG), the number of cyclotrons installed in Japan now totals 212 (as of 2013, [2]). They are widespread in research institutes, university hospitals, clinical PET centres, and commercial ^{18}F-FDG production industries. Considering its relatively narrow national territory (378,000 km^2), Japan has a large number of ‘radionuclide production equipment’ in highly crowded conditions. In other words, one cyclotron exists in a circle with a radius of nearly 25 km, or a cyclotron can probably be found within one hour’s drive in Japan. Most of these cyclotrons are dedicated to the production of PET nuclides for daily use, i.e., ^{11}C, ^{18}F. However, the beam times of these cyclotrons are, generally speaking, only a few hours per day, because no other purpose in nuclear medicine has been proposed at present.

1.3. ^{99m}Tc micro-factory for small-scale production and local distribution (Our proposal)

As mentioned above, fortunately, we have many cyclotrons with applicable beam time. It is possible that these medical cyclotrons can be applied to domestic ^{99m}Tc production, namely through ‘micro-factory’ production. Sholten et al. [3] showed that approximately 370 MBq/μAh (10 mCi/μAh) of ^{99m}Tc would be expected using nominal 20 MeV protons on a ^{100}Mo target (cf. 100% enriched). Based on this reference, 4–10 GBq (several hundred mCi) of ^{99m}Tc could be obtained in each medical cyclotron facility by using 20–30 μA protons and several hours of irradiation as a practically tolerable estimation.

To establish a firm and reasonable alternative, such small-scale production is favourable, because it could be achieved using present technologies with few challenging issues. First, typical in-house production of PET nuclides is practically performed at a beam intensity of about 10–30 μA. For example, 37 GBq (1 Ci) of ^{18}F, sufficient radioactivity for daily demand, is easily obtained by 18 MeV protons at 20 μA for 1 h of irradiation. Because such beam intensity will not place severe stress on the production system, the service life of both the target foil and the target vessel can be prolonged. In other words, the typical cooling system in use today is presumably applicable for small-scale ^{99m}Tc production without the need for any improvements/developments. Second, the radiation doses for the laboratory staff

---

[3] An estimated demand, 30 mCi/day at each facility, was calculated by the following:
Simply, [sum of both of the annual supplied activities (^{99m}Tc + ^{99}Mo)] divided by [number of facilities × 365 days] = 13.5 kCi / (1256 × 365) = 29 mCi/(day·facility)

that provide daily maintenance and inspection of the systems would be maintained at an acceptable level. These benefits would be seen only in small-scale production. In addition, because there are more than 100 cyclotrons in Japan, there are basically 100 micro-factories that can produce 100 mCi/day of ^{99m}Tc. By multiplying this value, the total yield of ^{99m}Tc in Japan could reach up to 10 Ci/day, which is very close to the expected value of the reactor production at 60 Ci/week of ^{99}Mo. As a result and this point is the key to our proposal, the very small production rate at each facility can be overcome and may be beneficial in some respects.

On the other hand, a large quantity, one-shot production of ^{99m}Tc, i.e., 370 TBq (10 Ci) or more, requires high power irradiation. To routinely carry out such scale of production, a significant amount of development and/or assessment would be needed, i.e., target preparation methods, target tolerance for high power irradiation, system durability, remotely operable equipment, production/maintenance schedules. We recognise that these R&D efforts are very important for promoting cyclotron technologies; however, it is difficult to carry out such a big project without governmental support, which we currently do not have. Therefore, we have chosen a small-scale production scheme.

We also have to consider the fact that direct ^{99m}Tc production has a disadvantage because of its short half-life (6 h) compared to its parent ^{99}Mo (66 h). This difference means that every process, from separation to shipping, must be completed as quickly as possible. Hence, a typical method applied for ^{99}Mo products might be insufficient for direct ^{99m}Tc production, particularly for shipping to distant clinical sites. However, because the existing cyclotron facilities, including PET centres, are almost evenly located from the north to the south of Japan, the situation is very favourable if they are considered as widely deployed factories. Namely, most ^{99m}Tc recipients would be expected to be within a distance of a few hours of driving from the nearest supplier.

Thus, the micro-factory concept and our development goals are summarized as

- A scale of production at less than 10 GBq (several hundred mCi) for 'in-house' uses or local supplies by pre-existing medical cyclotrons
- A shipping distance from each production site of nearly 1 h or 30 km
- Operator-friendly production by fully automated equipment with lower costs
- Compilation of evidence for regulatory requirements

The following section describes our developed system with several scientific results.

2. AUTOMATED PRODUCTION METHODS AND EXPERIMENTAL RESULTS

2.1. ^{100}Mo-oxide ($^{100}MoO_3$) target method

Accelerator production of ^{99m}Tc requires isotopically enriched ^{100}Mo or its appropriate derivatives as a solid target material. Generally, robotic devices are installed to handle solid targets for remote operation. The hot cell also requires remotely controlled devices, i.e., a manipulator or a specialised device for target disassembly, to reduce radiation exposure. However, such large-scale heavy systems increase the costs of installation and maintenance, and occupy a sizable working space; therefore, only a few institutes are able to accommodate these systems. This figure is completely the opposite of our concept. Because the scheme requires that a large number of facilities should be involved to be able to expect a certain amount of ^{99m}Tc, a low-cost method that is easy to operate is favourable and necessary. Moreover, the production of ^{99m}Tc, which would be carried out in parallel with daily PET pharmaceuticals production, should be operated automatically to reduce staff workloads. Therefore, we developed an automated production method that involves remote target preparation and recovery (Fig. 1), as well as separation and purification of the ^{99m}Tc. As mentioned above, the solid target is difficult to handle remotely because of its immobility; thus, in this method, we selected an oxide target that can be readily dissolved in appropriate solvents.

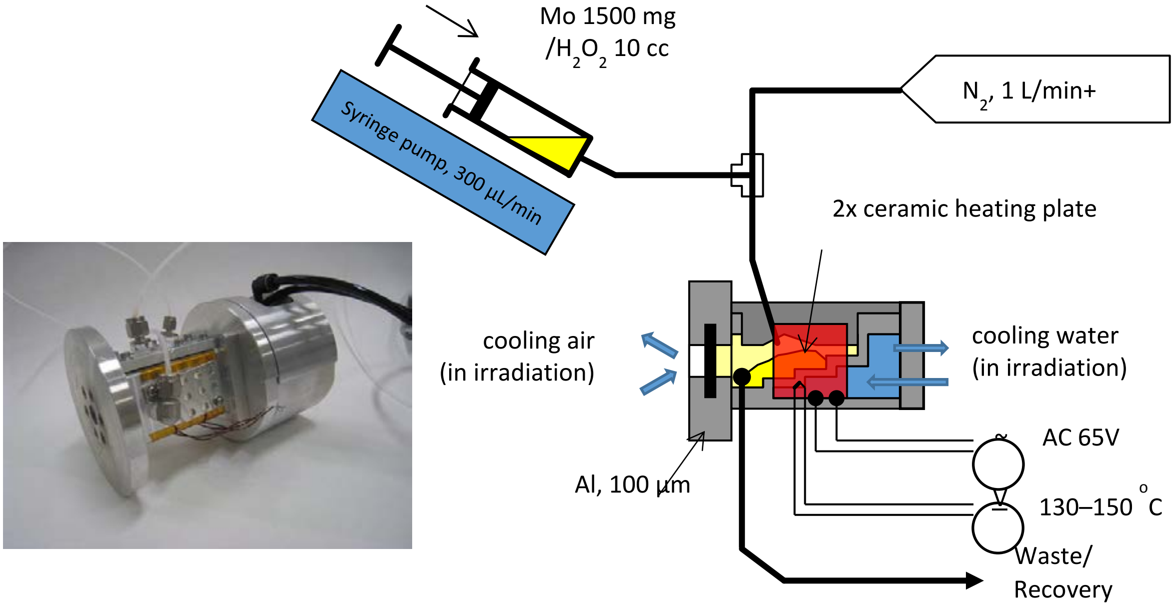

FIG. 1. Developed target vessel for $^{100}MoO_3$
The vessel has a stair-style structure where remotely introduced $^{100}MoO_3$ solution precipitates on under the condition of heating with high flow of N_2.

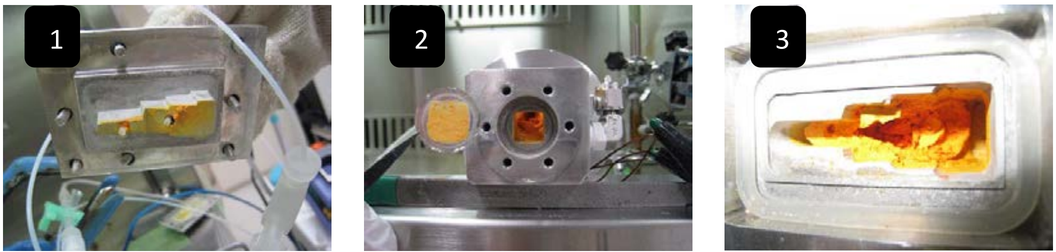

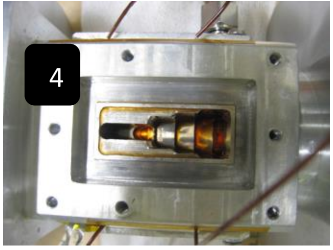

FIG. 2. Prepared target and post-processed vessel inside(decapped figures) [1] Top cover; [2] Front foil (Nb, 25 µm) as beam entrance; [3] Stair-style body (beam enters from right side); [4] After target solution discharged.

Briefly, the target material $^{100}MoO_4^{2-}$/ H_2O_2 solution was loaded into a target vessel at a speed of 300 µL/min by means of a syringe pump. On the way to the target vessel, the loaded solution was mixed with a relatively large amount of N_2 flow (1 L+/min) in an ordinal PEEK tubing (0.75 mm i.d.). Consequently, the ^{100}Mo solution splashed into the target vessel as a painting airbrush. The spread mist of ^{100}Mo solution was immediately dried and precipitated on an appropriate place inside target vessel, which was heated at 130–150 °C by an electric heater; and gave a 3–5 mm thick ^{100}Mo oxide layer on a stair-style vessel (Fig. 2). In this study, we used 1500 mg of ^{100}Mo (as elemental weight) in 10 mL of H_2O_2, and it took about 1.5 h to finish the preparation.

2.2. Elemental ^{100}Mo target method

In a direct ^{99m}Tc production, ^{100}Mo is the first choice as a target material. However, molybdenum is one of the highest melting point elements in the periodic table that sometime causes a laborious process to prepare a proper target by a method of hot-pressing or melting-formulation. A conventional method of electric deposition as an alternative, insofar as we know, gives a poor target unfortunately, i.e., very thin or easily peeled-off layer. Meanwhile, absolute composition of ^{100}Mo target can give a rich ^{99m}Tc yield; we thus attempted to use an unsolidified ^{100}Mo powdery target as purchased by employing a vertical irradiation technique. Fig. 3 shows a developed target vessel based on our previous study [4] for vertical irradiation method that can properly hold almost any forms of target material, including powders or low-melting-point materials, on the beam trajectory. The target vessel was made of a ceramic, silicon carbide (SiC), which has favourable properties, i.e., practically never melts, fair thermal conductivity, and excellent chemical resistance. In this study, a 500 mg of ^{100}Mo powder was prepared in the SiC target vessel, and sealed with a 25 μm Nb foil. The target was set to the beam port and ready to be irradiated.

FIG. 3. Developed target vessel made of SiC and its holder for vertical irradiation system
The SiC vessel has two connectors where the solution/pressure gas/exhaust can go through freely, thus the target ^{100}Mo was dissolved in-situ, and the dissolved ^{100}Mo solution was transferred to the hot cell by means of gas pressure without using any robotic devices.

2.3. Irradiation

Both targets, namely ^{100}Mo oxide and elemental ^{100}Mo, were irradiated by using a NIRS AVF-930 cyclotron at approximately 5–17 μA for 1–3 h with 18 MeV protons projected horizontally or vertically, respectively. The ^{100}Mo oxide target was cooled by compressed air (r.t., 90 L/min) and water (10 ^{o}C, 3 L/min); or chilled He (–10 ^{o}C, 400 L/min) and water (10 ^{o}C, 1.8 L/min) for the elemental ^{100}Mo target, respectively.

2.4. Recovery of irradiated target as a crude ^{99m}Tc solution

In both cases after irradiation, the recovery process was initiated by dissolving the target material inside the target vessel. Specifically, 30%-H_2O_2 (5 mL) was introduced into the target vessel and allowed to dissolve the target material for 10 min. Subsequently, 15%-H_2O_2 (10 mL) and 2 x 6.3%-NH_3 aq were introduced in series to complete dissolving reaction (10 min, each). The liquefied target was then collected into an interim reservoir (Fig. 4).

The collected ^{99m}Tc/^{100}Mo in about 30 mL of H_2O_2/NH_3 media was transferred to a Tc-selective disposable column (TEVA, Eichrom Technologies LLC, IL) to isolate ^{99m}Tc (specifically, TcO_4^-) from not only ^{100}Mo target but also H_2O_2[4]. After washing of TEVA by a

---

[4] In a case of long-distance-transfer of solution containing H_2O_2 in a narrow tubing, H_2O_2 generates considerable bubbles that absorb applying pressure as the force of recovery. Consequently, recovery of target solution will be unstable, likely clogging, that should be avoided. Therefore, elimination of H_2O_2 before transfer is essential.

series of solutions (0.1N-NH_3 aq (12 mL), 1.5N-HNO_3 (12 mL)), ^{99m}Tc trapped onto TEVA column was stripped off by 8N-HNO_3 (6 mL), and the eluted solution was led to a mixing vessel containing 2N-NaOH (24 mL). The two solutions were well mixed by bubbling of N_2 for 5 min, and the solution was then remotely transferred to the hot cell through a Teflon tubing (~15 m) similar to a typical liquid target. Hence, a low-cost, solid target remote production was achieved without using any robotic devices by this method.

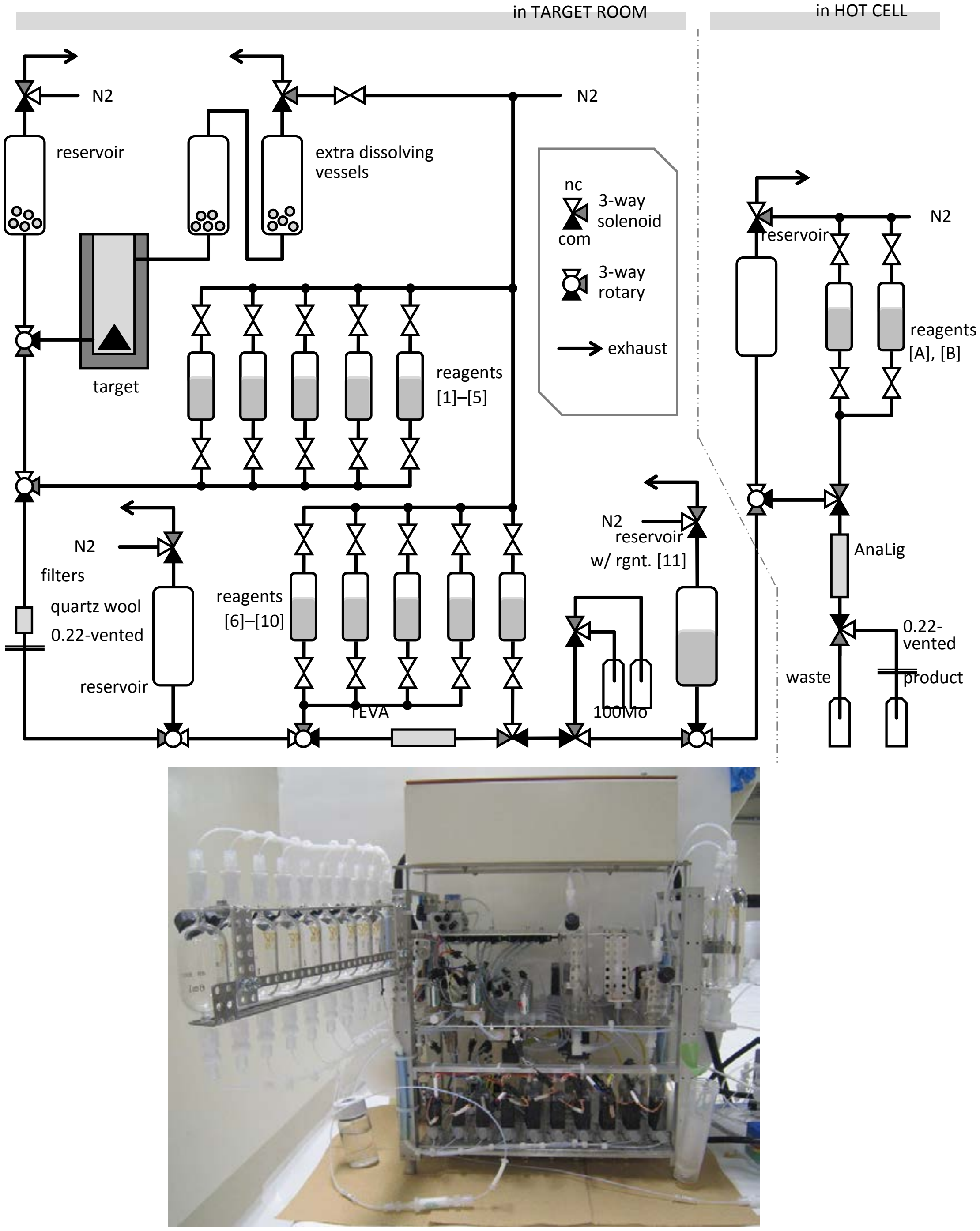

FIG. 4. Diagram and actual device of the ^{99m}Tc remote production system developed in this study. Reagents are 1) 30%-H_2O_2, 5 mL; 2), 15%-H_2O_2, 10 mL; 3) 6.3%-NH_3aq, 5 mL, 4) 6.3%-NH_3aq, 10 mL; 5) (reserved); 6) 0.1N-NH_3aq, 12 mL; 7) 1.5N-HNO_3, 12 mL; 8) 8N-HNO_3, 6 mL; 9) (reserved);10) pure water, 5 mL; 11) 2N-NaOH, 24 mL; (A) saline, 10 mL; (B) pure water, 10 mL.

2.5. Separation and Preparation of ^{99m}Tc

The fine separation and preparation steps were carried out by using another Tc-selective disposable column (AnaLig Tc-02, GL Sciences, Tokyo, Japan) in the hot cell. The ^{99m}Tc dissolved in nearly 1.4N-$NaNO_3$ (35 mL) solution delivered from the target room was loaded into the AnaLig column to trap ^{99m}Tc at a speed of 1 mL/min and isolate from impurities. The AnaLig column used in this process has a unique property that traps TcO_4^- quantitatively where Na^+ ionic strength of passing media is 0.1M or higher[5]. Therefore, after loading of crude ^{99m}Tc solution, the column was washed with saline (10 mL), and ^{99m}Tc as loading 10 mL of pure water stripped off the final product.

3. EXPERIMENTAL RESULTS

3.1. ^{99m}Tc yield by using $^{100}MoO_3$ target

The target yield of ^{99m}Tc from a $^{100}MoO_3$-precipitated target was 207 MBq/μAh (5.6 mCi/μA h) at the end of bombardment. These results showed good agreement with that obtained in reference [5], particularly considering the oxide target used, and was nearly stable (±9%) up to 17 μA irradiation. The efficiency of the liquefied-remote recovery of ^{99m}Tc was found to be 95–98%. Approximately 3.7 GBq (100 mCi) of ^{99m}Tc-pertechnatate solution was successfully obtained after irradiating the target with 10 μA, 18 MeV protons for 3 h (122 MBq/μAh or 3.3 mCi/μAh, without decay correction). The total processing time for the production was within about 2 h, where 45–50 min for target dissolving and 60 min for purification and preparation.

3.2. ^{99m}Tc yield by using elemental ^{100}Mo target

The target yield of ^{99m}Tc from elemental ^{100}Mo powdery target was 296 MBq/μAh (8.0 mCi/μAh) given from a condition of 18 MeV protons, 10 μA for 3 h maximum irradiation. The result also showed good agreement with the reference [5], and the maximum product yield at the end of separation reached to 170–190 mCi/(10 μA·3 h). The process completed within 75–90 min, including ^{100}Mo dissolving similar to those of oxide targets and chemical processing.

In the process of target dissolving, particularly at the first contact of elemental Mo and peroxide, or adding NH_3 aq into Mo/H_2O_2 solution, the reaction proceeds vigorously, and evolves considerable gas/bubbles that may cause severe malfunction on targetry system. Therefore, two empty vessels connected in series were placed near as possible from the target vessel that help to dissolve ^{100}Mo safely and effectively, also that acts as a void for pressure relief.

---

[5] According to an information about the eluents, solutions at temperature between 50–70 °C will strip the trapped Tc from the column. Meanwhile, mixing both solutions of ^{99m}Tc/HNO_3 and NaOH generates heat of neutralization, it may cause unstable performance on trapping efficiency. Therefore, we transferred the mixed solution via a long tubing, from target room to hot cell, to cool them down simultaneously that can be effective for reliable trapping without intended cooling period.

3.4. Impurities in the direct ^{99m}Tc from ^{100}Mo target

Due to relatively high yield of ^{99m}Tc and precise estimation can be expected, ^{99m}Tc used in the following studies were produced from an elemental ^{100}Mo target. Table 1 shows the observed radionuclides found in a crude solution just recovered from the target vessel and their estimated yields. Although several by-produced Tc isotopes, which were likely produced from small amounts of their respective Mo isotopes, were observed, their influence on the radionuclidic purity of ^{99m}Tc was maintained to a negligible level. Although ^{99}Mo was also found, the yield was too low to use for practical purpose, as expected.

Both ^{99}Mo and ^{97}Nb were eliminated with the purification procedure; thus, ^{99m}Tc of greater than 99% radionuclidic purity was obtained as the final product (Fig. 5).

TABLE 1. PRACTICAL THICK TARGET YIELDS FOR 18 MEV PROTONS ON AN ELEMENTAL ^{100}Mo TARGET*

Nuclide	$T_{1/2}$	Yield at EOB (activity% according to ^{99m}Tc)
^{99m}Tc	6.0 h	8.0 mCi/µAh
^{99}Mo	66 h	2.6 µCi/µAh
^{94}Tc	4.9 h	0.033% of ^{99m}Tc
^{95}Tc	20 h	0.036%
^{96}Tc	4.3 d	0.012%
^{97}Nb	1.2 h	5.2%

* Isotopic analysis of ^{100}Mo (>99.6 atom%) used in this study was ^{92}Mo (<0.004%), ^{94}Mo (<0.0018%), ^{95}Mo (<0.0014%), ^{96}Mo (<0.0013%), ^{97}Mo (<0.0015%), and ^{98}Mo (<0.39%): taken from the Certificate of Analysis provided by the supplier (Trace Science International, Inc.)

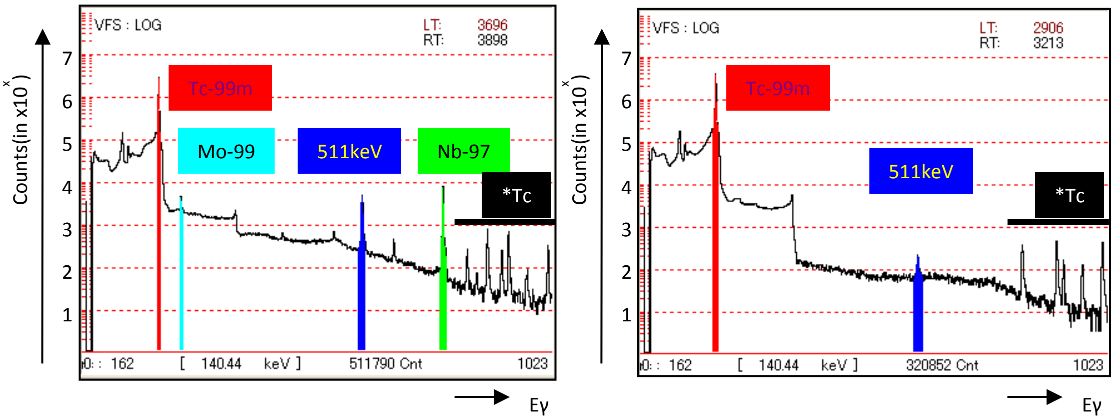

*FIG. 5. Gamma spectra of the ^{99m}Tc samples obtained via the ^{100}Mo(p,2n) reaction (left) crude sample of the target solution at 2.5 h from EOB(right) purified, final product at 4.5 h from EOB [*Tc] means other Tc isotopes except ^{99m}Tc, some of which decay by beta^{+}/EC.*

A purified, three-months-decayed ^{99m}Tc sample was subjected to ICP-MS to evaluate the amount of ^{99g}Tc ($T_{1/2} = 2.14 \times 10^5$ y). The sample was prepared by 1 h irradiation with 10 µA, 18 MeV protons and then purifying by the above method (585 MBq, corrected to EOB). For convenience, this yield was regarded as the target yield in this estimation (it contained a purification loss). Therefore, the values presented here are not the actual target yields; however, the ^{99g}Tc/^{99m}Tc ratio in the final product can be estimated using these values.

The quantitative evaluation of ^{99g}Tc was carried out by referring to the peak at m/z = 99, where each peak was well separated after the appropriate dilution. The calibration for ^{99g}Tc was achieved using an authentic standard solution (TCZ44, Amersham). The activity of ^{99g}Tc in sample was found to be 5.0 Bq (4.87×10^{13} atoms), which was sum of the followings: decayed ^{99m}Tc product (585 MBq at EOB, 1.83×10^{13} atoms), directly produced ^{99g}Tc via the ^{100}Mo(p,2n)-channel, and the decayed ^{99m}Tc produced during irradiation. Although an approximate estimation could be made using the above data, a much more precise estimation can be achieved if the ^{99m}Tc saturation rate is considered (Fig. 6). The amount of directly produced ^{99g}Tc in the final product was calculated to be approximately 2.94×10^{13} (atoms) in this system, approximately 1.6-fold that of ^{99m}Tc.

Table 2 lists estimation of the ^{99g}Tc/^{99m}Tc ratios in the final product under various likely, practical conditions. As seen the table, the ^{99g}Tc/^{99m}Tc ratios after 3 h of purification would be 3–4 within 6 h irradiation conditions. For evaluations of the labelling efficiency, most of commercially available ^{99m}Tc-labelling kits were successfully prepared followed by the instruction with a ^{99g}Tc/^{99m}Tc ratio of greater than 4.5 of the 'direct-^{99m}Tc' produced in this study (see below).

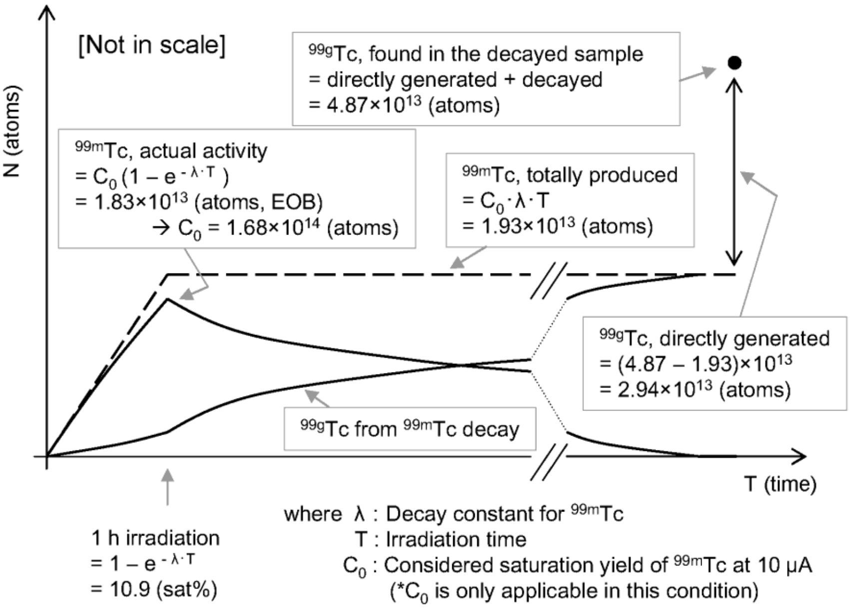

Fig. 6 Schematic relationship of ^{99m}Tc and ^{99g}Tc.

TABLE 2. ESTIMATED RATIOS OF ^{99g}Tc/^{99m}Tc IN THE FINAL PRODUCT UNDER LIKELY, PRACTICAL CONDITIONS

Irradiation period [h] (saturation% for ^{99m}Tc)	Ratio of ^{99g}Tc/^{99m}Tc at EOB (*1)	Ratio of ^{99g}Tc/^{99m}Tc at 3 h from EOB (*2)
1 (11%)	1.67	2.77
2 (21%)	1.82	2.99
3 (29%)	1.98	3.21
6 (50%)	2.49	3.92
12 (75%)	3.65	5.56

(*1) ^{99g}Tc = (directly produced) + (decayed during irradiation)
(*2) ^{99g}Tc = (directly produced) + (decayed during irradiation) + (decay during purification)

3.5. A typical QC evaluation

The quality of the sodium pertechnetate (Na^{99m}TcO$_4$) prepared by the above method was evaluated by applying the Standards for Radiopharmaceuticals, a domestic regulation defined by the Pharmaceutical Affairs Act (Table 3). However, the criteria for the Standards assume that all the ^{99m}Tc products, including Na^{99m}TcO$_4$, are daughter products of ^{99}Mo, strictly[6]. Therefore, while applying these quality control (QC) standards to the accelerator product is insufficient or less meaning, it is still rewarding to note that the sample met all the criteria.

TABLE 3. QC-REQUIREMENTS FOR RADIOPHARM-GRADE NA^{99m}TcO$_4$ AND RESULTS FOR THE ACCELERATOR PRODUCT

Items	Criteria	Result (method)
Radiochemical impurities	<5%	99%+ (Radio-TLC)
Radionuclide identity*	0.140 MeV photopeak	Found (HPGe)
pH	4.5–7.0	5.78 (pH meter)
Chemical purity	Al^{3+}, <10 µg/mL (10 ppm)	<1 ppm (test strip)
Relative osmolality (vs saline)	0.9–1.1	1.01 (osmometer)

* There is no description on the radionuclidic purity, probably due to its limited origin (^{99}Mo)

3.6. Labelling efficacy of the direct ^{99m}Tc for commercial kits

Fig. 7 shows the radio-TLC chromatograms of the ^{99m}TcO$_4^-$ and ^{99m}Tc-labelled compounds obtained by commercial kits available in Japan. Following the respective instruction carried out preparation of each compound with its QC evaluation.

According to the respective radio-chromatogram, we found that all compounds except the entry 3 were labelled successfully with 96% or higher radiochemical purity. It should be noted that the labelling of compound 3, exametazime, requires ^{99m}Tc with high specific activity to accomplish its labelling; specifically, the prescribed ^{99m}Tc for this compound should be a fresh batch eluted from ^{99}Mo, which is not exceeded 2 h from the last milking, nearly carrier-free ^{99m}Tc. Therefore, the insufficient labelling of this compound can be explained by the above reason, and this case is a typical example for the limitation of the direct ^{99m}Tc applicability. However, we should focus on many other successful results on the labelling, and we concluded that the applicability of the direct ^{99m}Tc as an alternative source is still feasible with considering proper ways of application.

4. CONCLUSION

We evaluated the feasibility of ^{99m}Tc direct production in this study. A yield of ^{99m}Tc, which was remotely produced from a relatively simple system, can be regarded as practical amount in terms of small-scale/ in-house production. That means ^{99m}Tc can be obtained at the level of daily doses, similar to those of major PET radiopharmaceuticals, by using own compact cyclotron and radiochemical apparatus. Although detailed clinical studies are further needed to assure the quality and applicability of the 'direct ^{99m}Tc', most of ^{99m}Tc-labelled compounds were successfully prepared by using commercial kits and that met the conventional QC criteria.

According to the above results, we are convinced that the direct ^{99m}Tc production is the best viable alternative among other possible methods.

---

[6] ^{99m}TcO$_4^-$ should be prepared by either (1) elution from ^{99}Mo deposited on alumina by an appropriate volume of saline, or (2) extraction from a ^{99}Mo solution using methyl ethyl ketone (2-butanone) as an extraction solvent, and then purification on an alumina column.

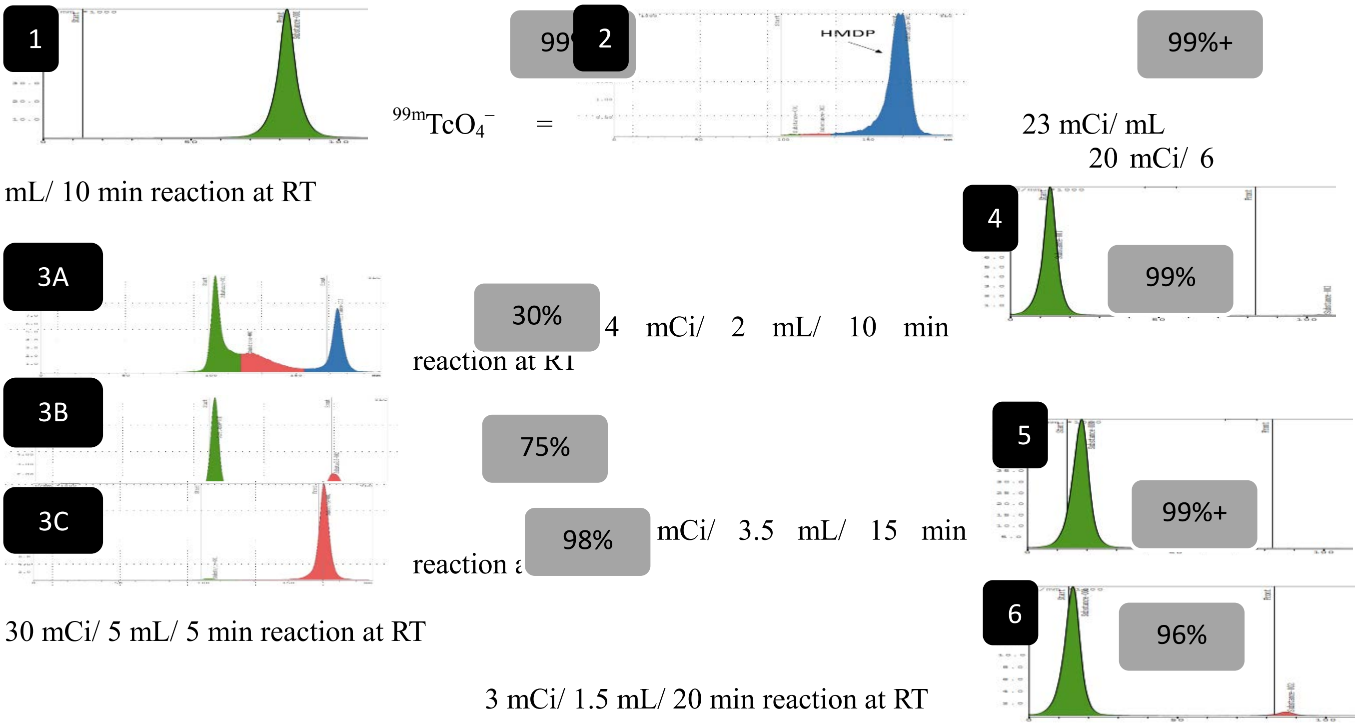

Fig. 7. Radio-TLC chromatograms of ^{99m}Tc compounds prepared by using 'direct-^{99m}Tc. (1) $^{99m}TcO_4^-$ (pertechnetate) at Rf = 0.9–1.0 on MEK/ silica gel; (2) a bone scintigram probe, Clearbone®, hydroxymethylene diphosphonate (^{99m}Tc-HMDP) at Rf = 0.9–1.0 on NH_4Cl+urea+Na_2SO_3+poly-phospholic acid/ silica gel; (3A–3C) a brain function probe, Cerebrotech®, ^{99m}Tc-exametazime at (A) Rf = 0.9–1.0 on MEK/ silica gel, (B) Rf = 0.0–0.1 on saline/ silica gel, (C) Rf = 0.9–1.0 on 50% CH_3CN/ paper; (4) a kidney function probe, Kidneyscinti®, ^{99m}Tc-dimercapto-succinic acid at Rf = 0.0–0.1 on acetone/ alumina; (5) a heart scintigram probe, Myoview®, ^{99m}Tc-tetrofosmin at Rf = 0.1–0.2 on CH_2Cl_2+acetone/ silica gel; (6) a liver/spleen scintigram probe, ^{99m}Tc-stannous colloid at Rf = 0.0–0.1 on MEK/ silica gel.

Acknowledgement

The authors are grateful to Mr. K. Minegishi, Mr. M. Fukada, and Mr. H. Suzuki, for fully technical support, including to assemble all chemical devices and to design the target boxes for vertical irradiation. We are also expressing our gratitude to NIRS cyclotron crew for providing excellent beam. Finally, we gratefully acknowledge the IAEA coordinators and all of the related staff. A part of this work was supported by JSPS KAKENHI Grant Number 24791355 (K.N.)

References

[1] BALLINGER, J.R., ^{99}Mo shortage in nuclear medicine: crisis or challenge, J. Labelled Compd. Radiopharm **53** (2010) 167–168.

[2] JRIA, Statistics on the distribution of radioisotopes in Japan – 2013. Available on the web site at http://www.jrias.or.jp/report/ritoke2013.pdf (in Japanese with English summary).

[3] Japanese Council of PET Imaging, a special-interest group of the Japanese Society of Nuclear Medicine. Available on the web site at http://www.jcpet.jp/1-3-4-1 (in Japanese).

[4] NAGATSU, K., et al., An alumina ceramic target vessel for the remote production of metallic radionuclides by in situ target dissolution, Nucl. Med. Biol. **39** (2012) 1281–1285.

[5] SCHOLTEN, B., et al., Excitation functions for the cyclotron production of ^{99m}Tc and^{99}Mo, Appl. Radiat. Isot. **51** (1999) 69–80.

CYCLOTRON PRODUCTION OF ^{99m}Tc - COLLABORATIVE PROJECT IN POLAND

R. MIKOŁAJCZAK[A], J.L. PARUS[A], D. PAWLAK[A], T. JANIAK[A], W. WOJDOWSKA[A], I. CIESZYKOWSKA[A], K. JERZYK[A], P. GARNUSZEK[A], M. MIELCARSKI[A], J. CHOIŃSKI[B], J. JASTRZĘBSKI[B], A. STOLARZ[B], A. TRZCIŃSKA[B], A. BILEWICZ[C], M. GUMIELA[C], E. GNIAZDOWSKA[C], P. KOŹMIŃSKI[C], K. SZKLINIARZ[D], W. ZIPPER[D]

[a]National Centre for Nuclear Research,
Radioisotope Centre POLATOM
Otwock, Poland

[b]Heavy Ion Laboratory, University of Warsaw
Warsaw, Poland

[c]Institute of Nuclear Chemistry and Technology,
Warsaw, Poland

[d] University of Silesia, Department of Nuclear Physics,
Katowice, Poland

Abstract

Technetium-99m is the most often used radionuclide in nuclear medicine. Current global crisis of ^{99}Mo supply, aging nuclear reactors and staggering costs force the search for alternative sources of ^{99m}Tc. The goal of the project is the development of ^{99m}Tc production method using the reaction of proton with ^{100}Mo in a cyclotron. Experimental program covered: determination of parameters for reaction ^{100}Mo(p,xn)^{99m}Tc in relation to beam energy and time of reaction, construction of robust ^{100}Mo target allowing high yield of ^{99m}Tc, rapid, simple and efficient methods for target dissolution and isolation of ^{99m}Tc from Mo targets, assessment of quality of ^{99m}Tc and its suitability for medical use, development of methods of the ^{100}Mo recovery and assessment of the effects of isotopic composition of ^{100}Mo on the quality of ^{99m}Tc. The planned outcome of the project is the development of a method for ^{99m}Tc production in Polish present and possibly future cyclotrons which could overcome the shortages of ^{99}Mo.

This project was supported by the grant ALTECH PBS1/A9/2/2012 awarded by the National Centre for Research and Development in Poland.

1. INTRODUCTION

Technetium-99m with the half-life of 6.02 h is the most often used radionuclide for diagnostic imaging due to its favorable physical characteristics. It is estimated that around 25 million of diagnostic procedures are performed yearly in the world, which is close to 80% of all applications in this field. At present the common route of production of ^{99m}Tc is from decay of mother radionuclide ^{99}Mo ($T_{1/2}$ = 65.94 h), which is separated from the fission products of ^{235}U after its irradiation in nuclear reactor.

Current global interruptions of ^{99}Mo supply caused by the unexpected prolonged shutdowns of the Chalk River (Canada) and Petten (The Netherlands) reactors, aging other nuclear reactors and the staggering costs of their maintenance have accelerated the search for alternative sources of ^{99m}Tc. One such alternative is the direct formation of ^{99m}Tc by proton bombardment of isotopically enriched ^{100}Mo, which can be carried out in conventional medical cyclotrons.

The goal of our project was the adaptation of ^{99m}Tc production technology using the reaction of proton bombardment of enriched molybdenum-100 in a cyclotron. The agreement holder in the current CRP is the National Centre for Nuclear Research Radioisotope Centre POLATOM located in Otwock. The research program was carried out with the Heavy Ion Laboratory, University of Warsaw and The Institute of Nuclear Chemistry and Technology in Warsaw. These three partners offered their unique experience and specialized facilities for the realization of the project. All three institutions are members of the scientific network "Radiopharmacy and Nuclear Medicine" established in 2008. The aim of this scientific networking is the advancement of radiopharmacy as a branch of nuclear medicine providing innovative products and technologies, among the others by promoting the use of accelerator based production of radionuclides useful for preparation of diagnostic radiopharmaceuticals. They are also participants of the Warsaw Pet Consortium.

2. PROTON IRRADIATIONS OF THE Mo SELF-SUPPORTING TARGETS

The ^{100}Mo samples of various enrichment were irradiated with proton beam. The natural Mo sample was irradiated with protons of 23 MeV energy delivered by cyclotron at National Centre of Nuclear Research, Świerk. A stack of two targets with the energy range 21.3 –19.8 and 19.8—11.0 MeV was used. The beam intensity was monitored with 10 µm Cu foil. Using the specially designed and home constructed external irradiation station (see description at chapter 4) the 16 MeV proton beam from the PETtrace cyclotron was employed to produce ^{99m}Tc with 100Mo samples of 99.05% and 99.815% enrichment. The beam energy range was 16—8 MeV.

The gamma-ray energies and intensities of irradiated samples were measured during a few months after irradiation and the radionuclidic purity of the produced ^{99m}Tc was deduced as a function of time and sample enrichment. The experimentally determined Thick Target Yield (TTY) was compared with calculated values using the published reaction cross sections and the theoretically calculated ones (EMPIRE evaporation code). Similar measurements at proton energy of 25 MeV are in preparation.

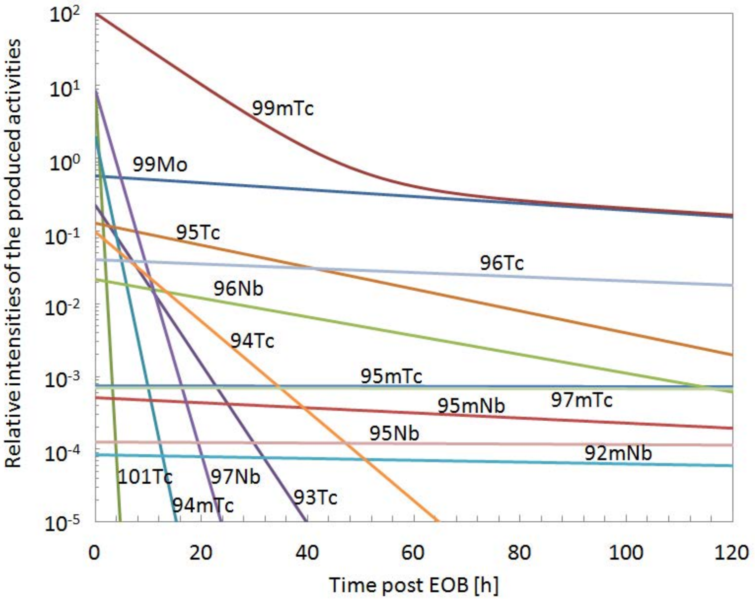

FIG. 1. Activity balance as a function of time for ^{100}Mo(99.05%) target irradiated from 16 to 8 MeV during 0.05 h.

3. SELF-SUPPORTING TARGET PREPARATION

3.1. Molybdenum foils produced by mechanical reshaping

Targets for determination of the parameters of the ^{100}Mo(p,xn)^{99m}Tc reaction, subject of studies within the ALTECH project, and estimation of the ^{99m}Tc production yield were prepared starting with powder material as isotopically enriched molybdenum is available in powder form only.

Since enriched isotopic material (^{100}Mo) is available in the powder form it was necessary to develop procedure allowing preparation of the foils with minimal loss of the expensive isotopic material.

In the developed procedure [1] the powdered material in the amount corresponding to the target thickness and its size was pelletized with use of the hydraulic press.
The obtained pellet was melted into a droplet in the vacuum of ~10^{-6} mbar with electrons provided by the e-beam gun. The total material loss during melting process was of about 15 - 18%.

Droplet produced by powder melting was placed between stainless steel sheets (rolling pack) to pass through the rolling mill. To remove stresses from the rolled foils, after reduction of the foil thickness by ~30-40 %, they were annealed in vacuum for ~10-15 minutes at temperature of ~1200 ºC. Described procedure allows production of thin (10 μm) foils.

Annealing useful at preparation of thin foils (below 100 μm) was not significantly helpful in production of thick ones (400-600 μm). The amount of cracks was lower but when appearing they propagated through the foil/disc area preventing production of the foil of the required size (Fig. 2).

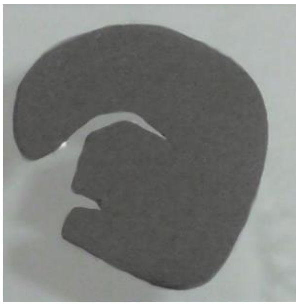

FIG. 2. Example of the crack passing through the disc of ~1 mm thick.

Expecting improvement of the purity of the melted material, and thus its malleability, the Mo powder was heated in the reducing atmosphere (1 h at 1600 ºC at H_2 atmosphere) for removing the oxide residues before pellet forming. At other approach the pellet was sintered under mentioned condition but in both cases no improvement of the molybdenum malleability was observed.

3.2. Hot reshaping of the droplet and subsequent cold rolling

To produce thick foils the relatively big droplets (6-7 mm diameter) were flattened at a high temperature before rolling. Molybdenum, oxygen resistant metal at ambient temperature, oxidises easily at temperature above 600 ºC. To protect molybdenum from oxidation at elevated temperature droplet was packed into the stainless steel packet (envelope) under argon atmosphere.

The packed droplets were heated at temperature of 1100 ºC for 3-5 minutes and when hot were flattened with use of hydraulic press as quickly as possible to preserve the high temperature. When cold, discs were removed from the envelope and rolled down to the required thickness of few hundreds µm.

The thinnest foil produced in this way was of ~250 nm (thickness measured by alpha particle energy loss method). Below this thickness material starts sticking to the rolling pack and attempts to reduce the foil thickness further were not undertaken.

3.3. Construction of the external, well cooled, target holder for the PETtrace cyclotron

In 2014 the fulfillment of the objective no 3 of the grant "ALTECH", agreement no PBS1/A9/2/2012 awarded to a consortium and financed by the National Centre for Research and Development, was continued. As a result a molybdenum target station was designed, manufactured and assembled as a standalone external target system. It consists of:

A) a drift tube with its 100 cm and two correction magnets (steering) made of permanent magnets;
B) a vacuum chamber equipped with a diagnostic system consisting of a graphite collimator and a Faraday cup, and with its complete, autonomous vacuum system; the graphite collimator consists of two independent electrodes;
C) a target chamber of the target station;
D) an autonomous control system;
E) a helium cooling system of the vacuum window;
F) a water cooling system of the Faraday cup;
G) a water cooling system of the target chamber;
H) a compressed air system.

All mentioned above mechanical subsystems were tested on a temporary prepared test stand. The autonomous control system of the molybdenum target station consists of two subsystems. The subsystem I is based on a programmable logic controller (PLC). This is the main control unit. Its objective is to control all processes of the target station on an autonomous basis. It also communicates with the subsystem II. The subsystem II is based on a PC computer equipped with the Windows 7 operating system. A window of Graphical User Interface displays on a monitor all important information for the operator about the current status of the target station, respectively, before, during and after irradiation. It allows an operator to control the target station remotely.

When all tests were passed successfully the target station has been transported from the test stand to a PETtrace cyclotron vault and connected to the cyclotron, Fig. 3. On the final place we have done several tests with a proton beam to check functionality of all subsystems in real terms. Currently, the station provides irradiated targets of ^{100}Mo or $^{nat.}$Mo for further investigations according to the objectives of the "ALTECH" grant.

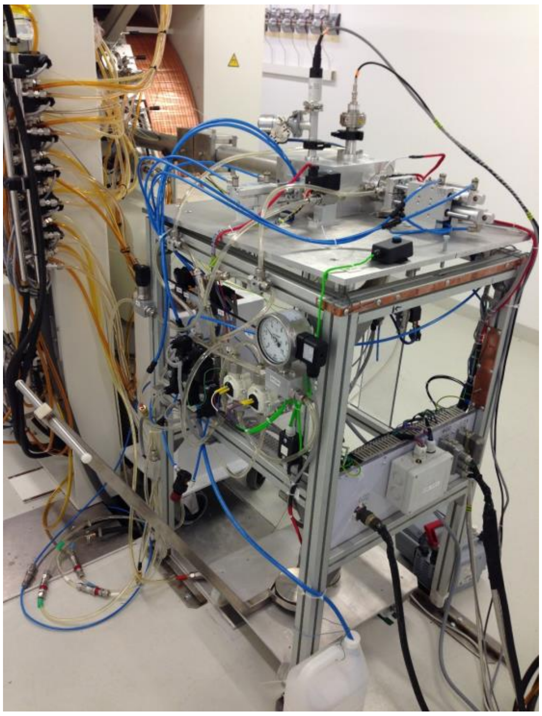

FIG. 3. The external irradiation station with target holder for the PETtrace cyclotron.

3.4. Preparation of molybdenum target material

In order to prepare a molybdenum target material for its irradiation with protons, molybdenum powder was pressed into pellets followed by its sintering. For pressing, hardened, stainless steel matrix was used. The powdered molybdenum was pressed for 60-90 minutes by the use of hydraulic press PLH-25, with the pressure of 800 MPa inside the matrix. In order to improve mechanical strength, pressed molybdenum pellets were sintered in hydrogen flow at temperature of 1600°C for 60 minutes. For this purpose, the tube furnace [Carbolite model CTF 300/1800] was used. For developing parameters of pressing and sintering, dozens pellets using natural molybdenum powder with particles size of 2 µm in diameter was used. Optimized parameters were then applied for preparation of pellets from metallic powder molybdenum enriched in 99.815 % in ^{100}Mo (Isoflex, USA). The cross section of pressed and sintered pellets was visualized by the use of a metallographic microscope. For determination of nanohardness of sintered molybdenum pellets, nanoindentation measurements were performed using NanoTest Vantage, Micro Materials Ltd. with Berkovich type indender. Measurements were conducted in ambient temperature, with the maximum load of 50 mN.

Performed calculation shown, that the mass of powdered molybdenum required for manufacture pellet 14 mm in diameter and about 0.700 mm in thickness is 730 mg [2].

The experimental observations shown, that after pressing pellets did not adhere to the stainless steel plates and they conducted electricity very well. Pellets pressed in longer time were more mechanically resistant, however even at the longest time satisfactory stability was not achieved. This was due to the low density of pressed pellets of only 6.4 g/cm^2 and a large air space in the structure of pressed pellets (Fig.4).

In order to improve mechanical strength, pressed molybdenum pellets were sintered in hydrogen atmosphere at the temperature of 1600°C. In result of this process the dimensions of Mo pellets decreased: diameter by 13%, thickness by 12%, weight by 1.5%, volume by 34% while density increased by 50%. The difference in the dimensions of pellet before and after sintering is shown in Fig.5.

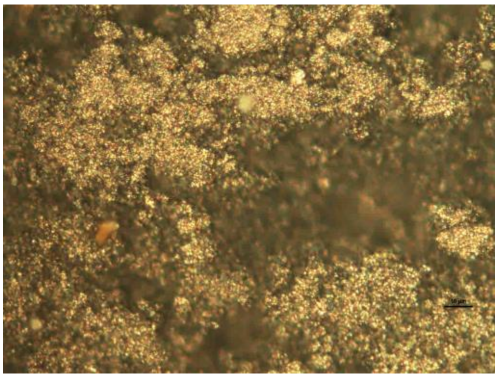

FIG. 4. Cross section of pellet prepared by 60 min. pressing. Photo with 500 times enlargement.

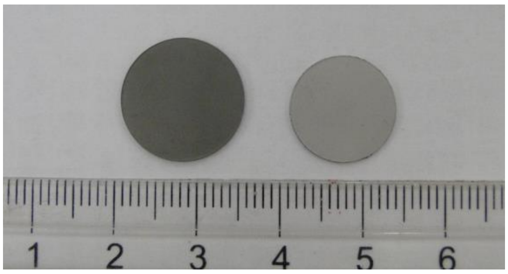

FIG. 5. Mo pellets before and after sintering.

The changes of mentioned parameters are associated with reduction of molybdenum oxide and removal of oxygen from intermetallic space. It was confirmed by photos of microscopic cross section of pellets before and after sintering (Fig.6).

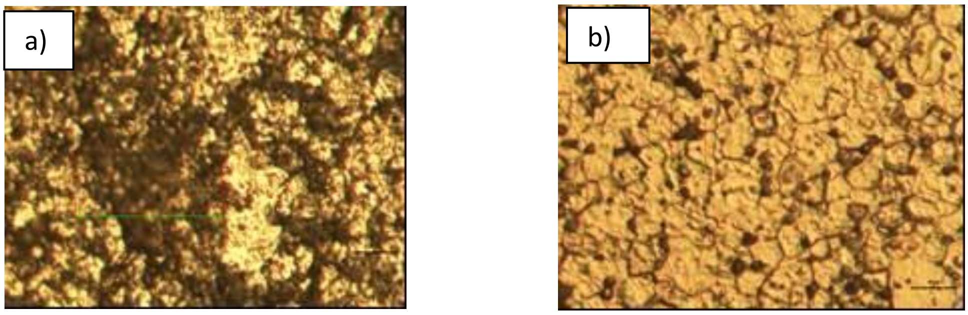

FIG. 6. Cross sectional view of molybdenum pellets, a) before sintering, b) after sintering.

The results of nanohardness of sintered natural molybenum pellet are shown in Fig.7. Hardness of pellet is not changing across the pellet. This confirms, that parmaters of molybdenum pellet sintering ensure its hardening in the entire cross-section. The measured hardness of sintered molybdenum pellets manufactured in these conditions was 5.02 GPa and significantly exceeded the value for similar sinters described in the literature (3.44 GPa) [3].

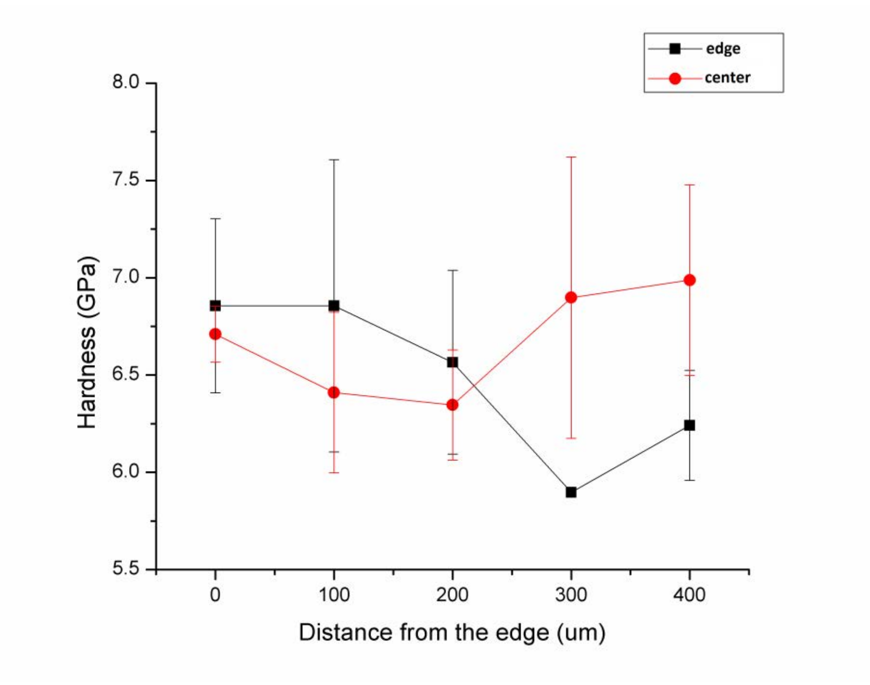

FIG. 7. Hardness distribution of molybdenum pellets.

Parameters optimized for pressing and sintering natural molybdenum were applied for manufacturing of pellets with enriched ^{100}Mo. The SEM/EDS investigations shown, that enriched molybdenum (99.815 % ^{100}Mo, Isoflex, USA) consists of heterogeneous particles with the size in the range 2-200 µm. In consequence the ^{100}Mo pellets obtained from the same as quantity of powder as in case of natural molybdenum had different thickness. For example, as result of pressing of 730 mg molybdenum powder for 60 min. under 28 MPa in order to prepare pellets with diameter of 14 mm, the thickness for ^{100}Mo pellets was 0.604 mm, whereas for natural molybdenum pellet it was 0.720 mm. This difference could be attributed to the better packing of particles with different size, however the mechanical strength of both pellet types was similar. In result of sintering of pressed ^{100}Mo pellet, the density of target material increased from 7.8 to 9.6 g/cm^3. Having in mind that the density of metallic molybdenum is 10.22 g/cm^3 [2], the obtained result can be considered as impressive. After irradiation the ^{100}Mo pellets remained unchanged, neither any visible discolouration nor distortion were observed.

4. DISSOLUTION OF MOLYBDENUM METAL

4.1. Chemical dissolution

In alkaline medium the dissolution obeys the following reactions:

$$Mo + H_2O_2 \rightarrow MoO_3 + 3\ H_2O$$
$$MoO_3 + 2\ NaOH \rightarrow Na_2MoO_4 + H_2O$$

The Mo metal used for dissolution was in the form of either powder (100 µm) or foil of 1 mm thickness. Mo powder dissolves in 1 M NaOH using twofold excess of the basic solution and 25% excess of H_2O_2 at the temperature of 70^{o}C after 30 minutes. Mo as a foil does not dissolve in these conditions. To achieve complete dissolution within 30 minutes it was necessary to use sevenfold excess of H_2O_2.

4.2. Electrochemical dissolution

For electrochemical dissolution of metallic molybdenum, galvanostatic method was used. In order to optimize parameters of molybdenum dissolution, two electrode system was used. As the anode small pieces (1-5 cm^2) of molybdenum foil or pressed and sintered molybdenum pellets of the surface around 2.6 cm^2 were used. The mass of each cathode was adjusted to the real mass of molybdenum target used for irradiation and was around 700 mg. Platinum foil (21 cm^2) or gauze (21cm^2) served as cathode. Electrolyte solutions contained 1-5 M KOH with the volume of 13-20 ml. The effect of addition of 30% H_2O_2 on the rate and efficiency of molybdenum dissolution was investigated. Dissolution was carried out at a constant current with current density of 80-755 mA/cm^2 for molybdenum pellets and of 14-280 mA/cm^2 for molybdenum foil. Process was carried out at ambient and elevated temperature (50°C). The efficiency of molybdenum dissolution was determined as the change of molybdenum weight before and after electrolysis, after its drying.

Due to the short half-life of technetium-99m, the recovery of this product after target irradiation must be rapid. Therefore it was assumed that the parameters of electrochemical dissolution allow complete dissolution of metallic molybdenum target in no more than 60 minutes.

The mass of molybdenum used in the experiments appeared to be the most essential parameter influencing the rate and effectiveness of dissolution. When using the current of 100 mA, molybdenum anode with mass of 60 mg was dissolved completely in 3M KOH after 1 h. In the same conditions the efficiency of dissolving 702 mg of molybdenum was only 23 %. Moreover, the effects of current density and electrolyte concentration on molybdenum electrochemical dissolution was observed. It was found, that the rate of electrochemical dissolution is increased by addition of 30% H_2O_2 and this effect is greater for more concentrated solutions of KOH. Efficiency of described process was improved with increasing the temperature of electrolyte solution from 25 to 50°C. However higher temperature could not be applied for electrochemical dissolution of molybdenum in mixtures of KOH and 30% H_2O_2 due to the violent chemical reaction, foaming of the solution, causing in consequence rapid leaps of voltage between electrodes. The highest yield of 80% was achieved by electrochemical dissolution of molybdenum in 5M KOH at temperature of 50°C, whereas the yield of 72% was reached for mixture of 5M KOH and 30% H_2O_2 at ambient temperature. For complete dissolution of target material 70 minutes were needed.

5. SEPARATION OF ^{99m}Tc FROM ^{99}Mo EXCESS

Following 3 methods have been evaluated for ^{99m}Tc separation from large molybdenum excess:

1. anion exchange on Dowex-1x8 [4-5]
2. adsorption on AnaLig® Tc-02 resin [6]
3. modified ABEC procedure [5,7]

5.1. Dowex-1x8

After soaking of 100 to 140 mg of resin in 5 mL of 0.5M NaOH the suspension was introduced in a column of 1 mL capacity with a glass frit filter in lower part of it. Before depositing the solution onto bed the column was washed with 5 mL of 0.5M NaOH. Ten mL of Na_2MoO_4 80 mg/mL solution containing 10 MBq of ^{99m}Tc had been introduced onto the column with a flow rate in the range from 1 to 0.6 mL/min. Eluat from column was collected in portions of 1 mL volume. Activity of ^{99m}Tc in collected aliquots was measured in a scintillation counter. Before the ^{99m}Tc elution the column was rinsed using 10 mL of 0.9% NaCl. As an eluent 5 mL of TBAB (tetrabutyloammonium bromide) solution of 0.2 mg/mL in CH_2Cl_2 was used. The eluat was collected as 1 mL aliquots and measured in scintillation counter. The yield of adsorption and desorption processes was calculated as a ratio of measured activities of ^{99m}Tc in collected aliquots to the total activity of ^{99m}Tc loaded onto the column. Diagram of the process is shown in Fig.8.

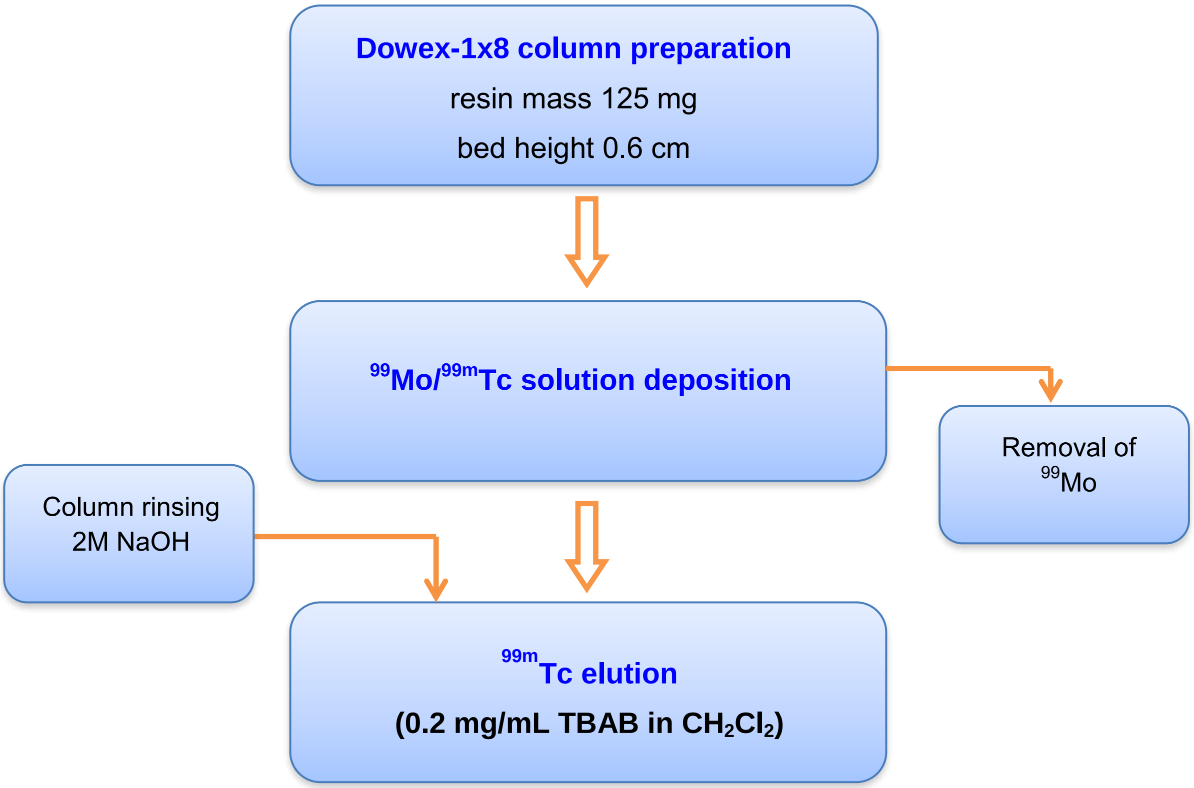

Dowex-1x8 column preparation

resin mass 125 mg

bed height 0.6 cm

^{99}Mo/^{99m}Tc solution deposition

Removal of ^{99}Mo

Column rinsing 2M NaOH

^{99m}Tc elution

(0.2 mg/mL TBAB in CH_2Cl_2)

FIG. 8. Diagram of sorption and elution process on Dowex-1x8.

In four experimental runs the ^{99m}Tc yield was 77.5, 78.6, 78.5 and 79.1%, respectively. Almost total retention of ^{99m}Tc was achieved for the flow rate of 0.6 mL/min. Increasing flow rate to 2 mL/min during column loading and elution resulted in decreasing the elution yield for more than 10%. The elution is fastest at the beginning and is more than 90% of ^{99m}Tc in the first 5 mL of TBAB solution. Maximum value of ^{99m}Tc yield was obtained after about 10 minutes of TBAB solution contact with Dowex resin.

5.2. AnaLig resin

Columns Empty Bond Reservoir of Varian with glass frits filters below and above a resin layer were used. The columns were filled with about 100 mg of resin suspension. To 10 mL of Na_2MoO_4 solution of 120 mg/mL in 2M NaOH the tracers of ^{99}Mo (80 to 100 kBq) or $^{99m}TcO_4^{-1}$ (170 to 240 MBq) were added. The solution was delivered on the column using a peristaltic pump with the flow rate of 0.2 mL/min. To the column outlet a flexible tube was connected enabling the collection of eluate to vials for gamma spectrometry measurements of ^{99}Mo with the use of HPGe detector. At the end, the column was rinsed with 3 mL of 2M NaOH. It was found that optimal flow rate was 0.2 mL/min.

Before recovery of ^{99m}Tc from the column it was rinsed with 5 ml of 2M NaOH. As eluent 5 to 10 mL of water was used and the eluate was collected in 1 mL portions to penicylin vials. Due to high activities of ^{99m}Tc the vials were measured in CAPINTEC dose calibrator. The flow rate was 0.5 mL/min.

The ^{99m}Tc retention yield on the column was determined based on ^{99m}Tc activity measured in solution leaving the column. The recovery of ^{99m}Tc amounted to 85%. The diagram of the separation and desorption processes is shown in Fig.9.

The layout of ^{99m}Tc separation process is shown in Fig.10.

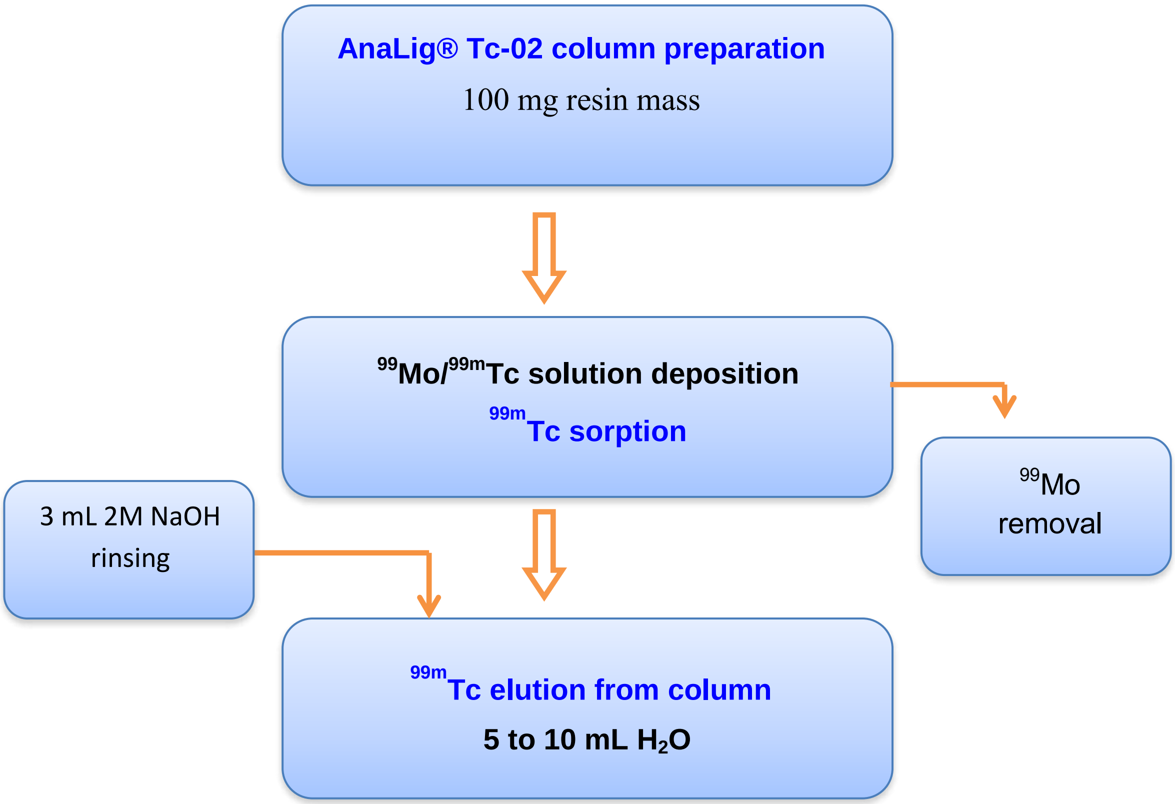

FIG. 9. Diagram of separation process using AnaLig® resin.

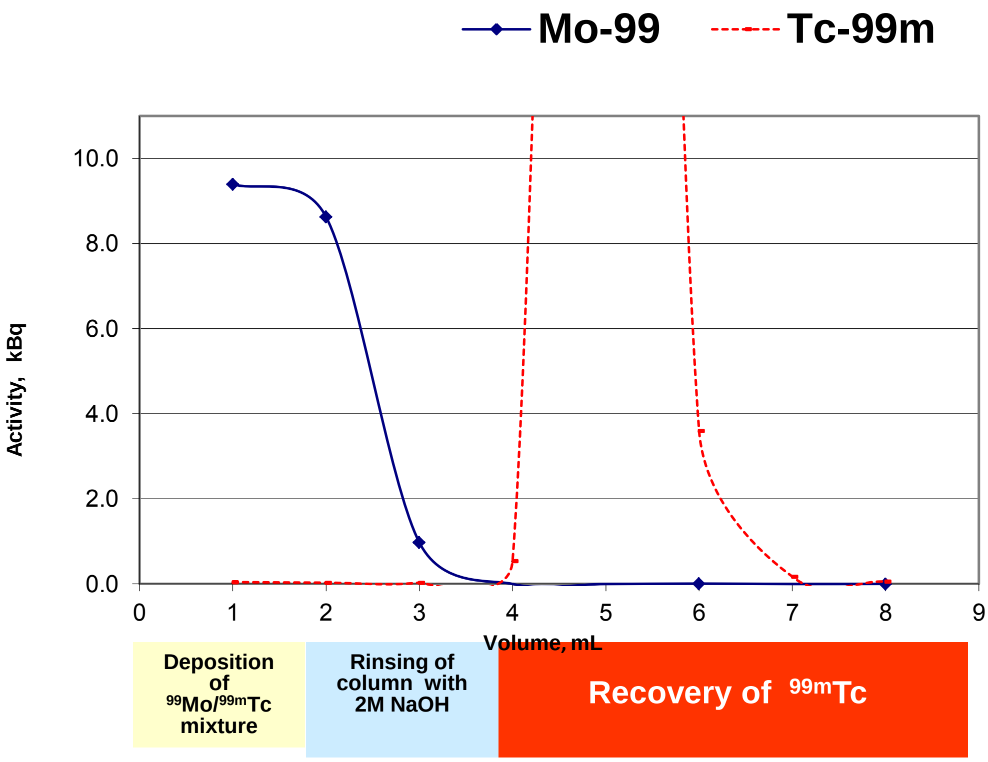

FIG. 10. ^{99m}Tc separation process on AnaLig® resin.

5.3. Modified ABEC

The aqueous biphasic extraction chromatography with C18 (OASIS HB) column coated with polyethylene glycol as extractant was used. Around tenfold excess of polyethylene glycol (PEG, Fluka AG) with molecular weight in the range from 2000 to 6000 was loaded on the column containing 0.1 g of C18 resin in water. The excess of PEG unbound with resin was washed with water. The solution of ammonium molybdate (0.05 g of Mo) with about 2 MBq of ^{99}Mo in 10 mL of 3M ammonium carbonate solution was loaded on the column. The column was washed with 10 mL 3M ammonium carbonate and then ^{99m}Tc was eluted with around 50 mL of water. Elution yield and content of ^{99}Mo in technetium fraction was determined by gamma spectrometry with HPGe detector. The content of polyethylene glycol in ^{99m}Tc fraction was measured by TOC (Total Organic Carbon) method.

Typical elution profile of ^{99}Mo and ^{99m}Tc from C-18 column coated with PEG is presented in Fig.11. Blue line represents the ^{99}Mo eluted during solution loading on the column while the red line represents ^{99m}Tc eluted from the column with water after successful ^{99}Mo loading.

The ^{99m}Tc elution profile improves with decrease of PEG molecular weight. Using the C-18 column in-house modified with polyethylene glycol allowed to separate ^{99m}Tc from excess of Mo with over 80% yield. The highest elution yield of ^{99m}Tc > 80% were obtained for polyethylene glycol with low molecular weight (PEG-2000 and PEG-3000). With increasing a molecular weight of PEG, elution yields of ^{99m}Tc drops to around 70% for PEG-6000. Assuming the TOC method quantifies the level of PEG residue in ^{99m}Tc solution, the PEG contamination was lower than 0.005% and significantly decreased with increasing PEG molecular weight. The contamination of ^{99m}Tc with ^{99}Mo was lower than 0.01% for all experiments. Despite the high separation yield, the volume of ^{99m}Tc eluate is rather high and further post-elution concentration might be required.

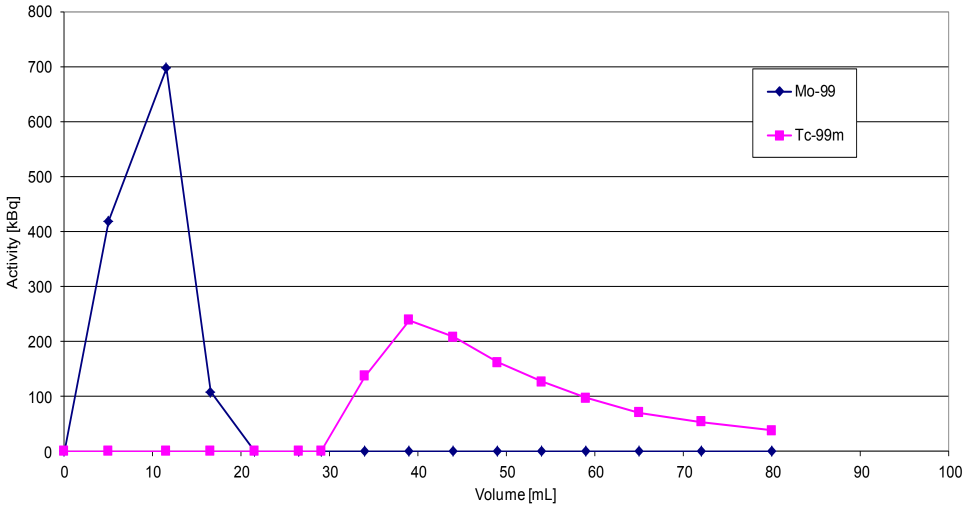

FIG. 11. Typical elution profile of ^{99}*Mo and* ^{99m}*Tc from OASIS HLB Plus column coated with PEG.*

6. CYCLOTRON PRODUCTION OF ^{99m}Tc FROM HIGHLY ENRICHED ^{100}Mo

Molybdenum target was prepared by pressing metal powder containing 99.815% of ^{100}Mo into pellet of 12 mm in diameter and mass of 0.723 g. After sintering in hydrogen atmosphere at 1600^{0}C for 60 min, the pellet was loaded into aluminum holder which was mounted in GE PETtrace 840 cyclotron (at HIL, University of Warsaw) proton beam and irradiated for 2 h at 2 µA current to total activity of 1.6 GBq at the EOB. The target was automatically disassembled into transportation container.

After releasing from holder the target was dissolved in 30% H_2O_2 and alkalized with 10M NaOH (both reagents added in about 2 mL portions) to total volume of 19 mL. ^{99m}Tc was separated in 3 columns connected in series containing AnaLig, Dionex and alumina beds. The ^{99m}Tc recovery yields amounted to 76.3% and losses were 8.2%, 13.2% and 2.3% at each column respectively. The ^{99m}Tc solution was free of molybdenum. Method is further optimized to increase separation yield.

7. QUALITY ASSESSMENT OF ^{99m}Tc AND KIT RADIOLABELING

A critical challenge in the development of cyclotron-produced ^{99m}Tc is to ensure that the final pertechnetate is equivalent to that obtained from ^{99}Mo/^{99m}Tc generator. QC analysis of the final pertechnetate was performed to determine impurity levels and to compare these data against the pertechnetate from the generator.

Using gamma spectrometry the radionuclidic purity of pertechnetate and radionuclidic identification were determined. ICP-OES was used to assess the chemical impurity. Radio-TLC was used to determine the radiochemical purity.

Two batches of cyclotron-produced ^{99m}Tc–pertechnetate revealed that the separation procedure enable to recover over 80% of ^{99m}Tc and the product – pertechnetate eluate is free from the parent ^{99}Mo. The radiochemical purity of ^{99m}Tc –pertechnetate was 99.5%.

Poltech HMPaO kit for radiopharmaceutical preparation was chosen to asses radiolabelling efficiency of cyclotron-produced ^{99m}Tc-pertechnetate. This model freeze-dried containing 0.5 mg of d,l-HMPO and 3 µg of SnCl2 was reconstituted with 0.9% of NaCl and then 600-700 MBq of $^{99m}TcO_4^-$ was added. The reaction mixture was stirred at RT for 5 minutes. The radiochemical purity of the labelled complex was determined using HPLC and TLC.

8. NEW METHOD OF ^{99m}Tc SEPARATION FROM MACRO AMOUNTS OF MOLYBDENUM BY PRECIPITATION

Several methods for technetium separation from irradiated molybdenum target are available in the literature. Few of them are based on the high volatility of technetium heptaoxide, Tc_2O_7, others on the wet chemistry [8]. We decided to develop and use a different method, due to the concern on very high specific activity of Tc radiotracers and the necessity to have a radiochemical separation as fast as possible.

Besides the ^{99m}Tc and ^{99g}Tc radionuclides, irradiation of enriched ^{100}Mo target with protons induces direct production of Mo, Nb radionuclides (Fig.1). In the gamma spectra also Y radionuclides, obtained from decay of ^{88}Zr and ^{89}Zr, were identified. For separation of ^{99m}Tc from irradiated Mo target we tested two precipitation methods. First was elaborated by Bonardi [9] and based on precipitation of MoO_3 hydrate, whereas the second one was elaborated in our laboratory. In the first method the metallic Mo (25 mg) irradiated in thermal neutron flux was dissolved in 1 ml of nitric acid (from 1 M to 7 M). The bulk of poorly soluble precipitated molybdic acid (MoO_3 hydrate) was filtered off and the activity of ^{99}Mo and ^{99m}Tc was measured in the filtrate. We found that in 7 M HNO_3 only 75 % of molybdenum is present in a solid form and coprecipitation of ^{99m}Tc is negligible (less than 6%).

Therefore we elaborated second method based on precipitation of insoluble heteropolyacid salt - ammonium molybdenum phosphate hydrate (AMP) and obtained results were more promising. The schematic diagram of proposed method is presented on Fig.12.

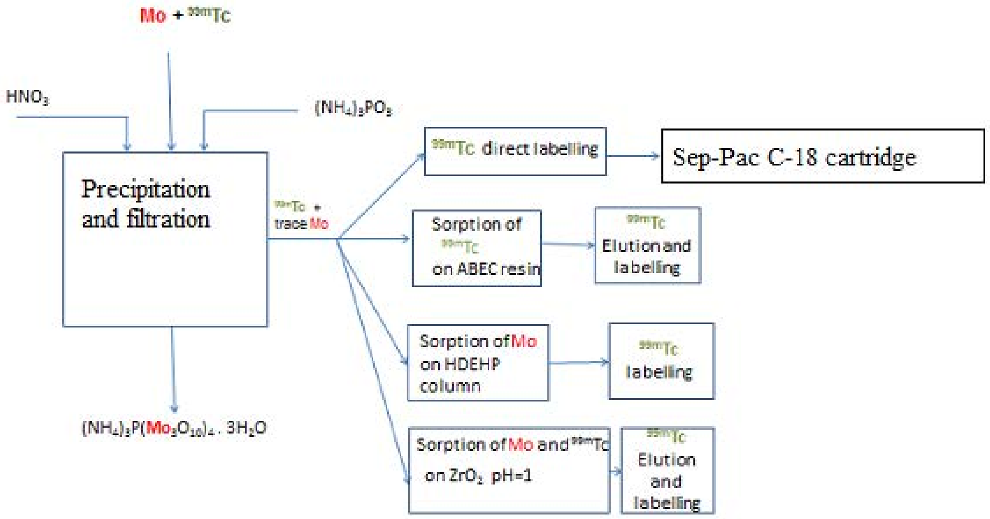

FIG. 12. Separation scheme of the process elaborated in the Institute of Nuclear Chemistry and Technology.

In the first step metallic molybdenum target was dissolved in 3,5 M HNO_3. Next, triammonium phosphate was added and Mo was precipitated from the solution according to the reaction:

$$(NH_4)_3PO_4*3H_2O + 12MoO_4^{2-} + 24H^+ \rightarrow (NH_4)_3P(Mo_3O_{10})_4\downarrow + 15H_2O$$

Different Mo:P substrate ratios were tested to find the optimum separation conditions. The results are presented in Table I.

TABLE 1. INFLUENCE OF TRIAMMONIUM PHOSPHATE CONCENTRATION ON EFFICIENCY OF AMP PRECIPITATION

triammonium phosphate (M)	% stoichiometry	concentration of Mo in solution (mg/ml)	% Mo in precipitate
0.06	100	4.04	84.0
0.075	125	1.46	94.1
0.15	250	1.57	94.0

As shown in Table 1 to effectively precipitate of molybdenum only 25% excess of triammonium phosphate is sufficient. To improve the efficiency of the process we examined the effect of the ammonium nitrate addition on the yield of AMP precipitation.

TABLE 2. INFLUENCE OF NH_4NO_3 ADDITION ON MO SEPARATION FROM SOLUTION

Ammonium nitrate (M)	Concentration of Mo in solution (mg/ml)	% Mo in precipitate
0	1.6	93.6
0.16	0.64	97.4
1.56	0.54	97.8
3.12	0.50	98.0

As can be seen in Table 2 only small addition of ammonium nitrate significantly increased precipitation of AMP. Based on the performed experiments the following parameters of AMP precipitation are proposed: for 25 mg of metallic Mo target dissolved in 1 ml 3,5 M HNO_3 exactly 0.3 mmol of $(NH_4)_3PO_4$ and 0.16 mmol of NH_4NO_3 should be added. The precipitate can be separated by filtration or centrifugation after 15 minutes. We studied also possible cooprecipitation of ^{99m}Tc with AMP. After separation process in conditions presented above we found in the filtrate solution 99.6% of total ^{99m}Tc activity.
From performed studies it can be concluded that the proposed process is promising and allows fast separation of macroamounts of Mo from the solution without co-precipitation of ^{99m}Tc.

9. PURIFICATION OF THE SOLUTION AFTER AMP PRECIPITATION

After the precipitation of AMP 98.8 % of molybdenum is separated from solution. After filtration the solution contains about 0.3 mg/ml molybdenum. Because the accepted value for Mo in ^{99m}Tc cannot exceeds 10 ppm additional process for purification is needed. In order to remove residue of Mo following methods were proposed:

9.1. Separation on ZrO_2 nanoparticles

The conventional inorganic sorbents like alumina have very low sorption capacity due to the limited number of active sites and relatively low accessible surface area and cannot be used in our process. To increase accessible surface area and active sites of the sorbents we propose to use nanosorbents where surface atoms of nanoparticles metal oxides are unsaturated and exhibit intrinsic surface reactivity. On the basis of the publications from Bhabha Atomic Research Centre [10-11] we selected ZrO_2 nanoparticles which exhibits in neutral solutions high affinity for molybdate anions (K_d=270 ml/g) and very low for TcO_4^- anions (K_d=0.2 ml/g).

Nano-ZrO_2 was synthesized according [9] by controlled hydrolysis of zirconium. Ammonia solution was added drop-wise to zirconium oxychloride with vigorous stirring. The ammonia solution was added until complete formation of the white precipitate at pH around 12. The precipitate was subsequently refluxed for 12 hours at 96 ^oC. The precipitate obtained was washed with distilled water, dried at 100 ^oC and calcined at 600 ^oC for 2 h. The scheme of synthesis of ZrO_2 nanoparticles is presented in Fig.13.

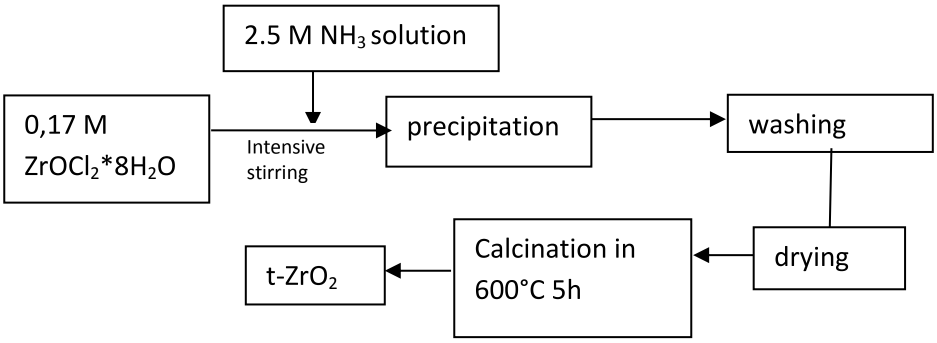

FIG. 13. Scheme of t-ZrO_2 synthesis.

In order to find the optimum conditions for Mo-Tc separations the weight distribution coefficients (K_d) of molybdate and pertechnetate anions were determined as a function of pH. Experiments were performed using $^{99m}TcO_4^-$ from a generator produced by Polatom and natural molybdenum from Sigma-Aldrich. The distribution coeficients for $^{99m}TcO_4^-$ and $P(Mo_3O_{10})_4^{3-}$ anions determined in static condition is presented in Table 3.

TABLE 3. DISTRIBUTION COEFICIENTS OF $^{99m}TcO_4^-$ AND $P(Mo_3O_{10})_4^{3-}$ ANIONS ON t-ZrO_2 IN FUNCTION OF pH.

pH	Kd (ml/g)	
	$^{99m}TcO_4^-$	$P(Mo_3O_{10})_4^{3-}$
1	0.96	10
3	1.70	32
5	2.6	-
7	2.7	25
10	0.85	12

The obtained results suggest that it is possible to separate these two species in neutral solution. In the column process ^{99m}Tc should elute in the first fraction while Mo retains on the column. Unfortunately, due to the nanometer particle size of t-ZrO_2 it was not possible to form a column bed and nanoparticles with adsorbed Mo passed trough the column frit On the other hand, application of nanofiltration module requires a multistage process.

9.2. Separation on the porous teflon coated with HDEHP

Another system that we examined was based on extraction of Mo using HDEHP acid (bis (2-ethylhexyl) phosphoric acid), which was proposed by Bonardi et al [9]. We prepared extraction bed by adsorption of HDEHP on porous teflon grains. The separation of Mo-Tc was performed in small column with elution by 1 M HNO_3. We observed co-elution of both Mo and Tc ions. In our system Mo occurs in the form P $(Mo_3O_{10})_4^{3-}$ hence a completely different process was observed than suggested by literature data [9].

9.3. Separation on C18 sorbent modified by PEG-2000

Due to the unsuccessful attempts to apply nano ZrO_2 and HDEHP bed, our works were focused on application of PEG-2000 modified sorbents, where molybdate and pertechnetate anions are adsorbed from highly saline solutions (2.5 M NH_4NO_3 or 4 M NaOH) and TcO_4^- anions are selectively eluted using pure water.
C18 cartridges (Oasis HLB Plus 225 mg) were coated by 5 ml PEG-2000 solution (0,25 M), through the cartridge and then washing with 50 ml deionized water (D.I. H_2O). Initial separation experiment was performed using generator eluted $^{99m}TcO_4^-$ and solution containing 300 mg/l Mo (after separation of AMP) with 8 M NaOH (1:1, volume). After loading, the column was washed with 5 ml NaOH (4 M). The $^{99m}TcO_4^-$ was eluted using 50 ml water. Recovery of ^{99m}Tc was greater than 99%. Due to the relatively high volume of solution it was necessary to pass this solution through an alumina column in order to concentrate $^{99m}TcO_4^-$.

10. LABELING OF HYNIC-SUBSTANCE P WITH ^{99m}Tc IN PRESENCE OF MOLYBDENIUM IN SOLUTION

The second objective of our studies was the elaboration of conditions for labeling of biomolecules with ^{99m}Tc in presence of small amount of ^{100}Mo target. As mentioned in previous point, after dissolution of metallic Mo in concentrated HNO_3 and addition of triammonium phosphate the insoluble ammonium molybdenum phosphate hydrate (AMP) is formed. After separation of AMP by filtration the concentration of Mo in solution is around 0.3 mg/ml.

In the first step we studied labeling of Hynic-Substance P(1-11), HYNIC-SP. **SP**, is an undecapeptide from the family of neurokinins termed tachykinins (**NKs**) (Fig.14). It is a mediator responsible for the neural-immune/hematopoietic cross-talk. SP is the preferential endogenous ligand for the neurokinin type 1 receptors (NK-1), which are overexpressed in malignant gliomas [12].

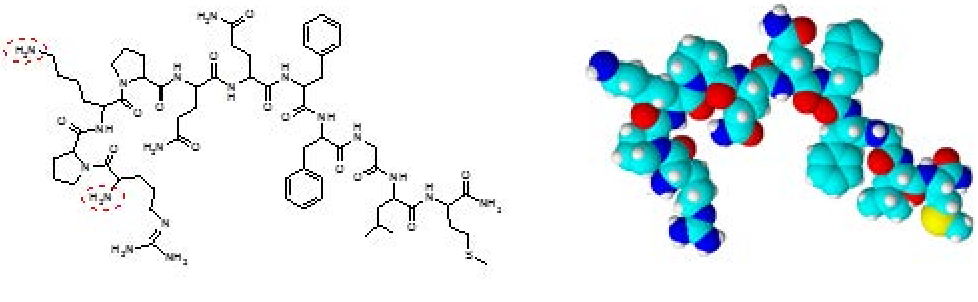

FIG. 14. The peptide: Substance P, $Arg^1Pro^2Lys^3Pro^4Gln^5Gln^6Phe^7Phe^8Gly^9Leu^{10}Met^{11}$.

Substance P is also known as neurokinin NK1, it is widely distributed in the peripheral and central nervous system, along with other neurotransmitters, such as serotonin and dopamine, and acts as neuromodulator.

For the synthesis ^{99m}Tc (HYNIC-SP) $(Tricine)_2$ radiobioconjugate a commercially available ligand HYNIC conjugated to substance P(1-11) was used. Studies were performed in two stages: Stage I - synthesis of ^{99m}Tc(HYNIC-SP)$(Tricine)_2$ with ^{99m}Tc from ^{99}Mo/^{99m}Tc generator and Stage II - synthesis and studies of bioconjugate ^{99m}Tc(HYNIC-SP)$(Tricine)_2$ using solution containing ^{99m}Tc and Mo after precipitation of AMP.

In the first step (HYNIC-SP)(Tricine)$_2$ was labeled with ^{99m}Tc in solution without addition of Mo: To a solution of 10 µg (6.7×10^{-3} µmol) HYNIC-SP, 20 mg (0.11 mmol) of tricine and 5 mg of EDDA (2.8×10^{-2} mmol) in 500 µl of 0.1 M PBS were added slowly 500 µl Na^{99m}TcO$_4$ eluted from ^{99}Mo/^{99m}Tc, 50 - 100 MBq) and 5 µL SnCl$_2$ (5.3×10^{-3} M in 0.1 M HCl). The reaction mixture was incubated for 20 min at 90° C, and the progress of the reaction was monitored by HPLC. The radiochemical yield of the synthesis ^{99m}Tc(HYNIC-SP)(Tricine)$_2$ bioconjugate was 98% (Fig.15).

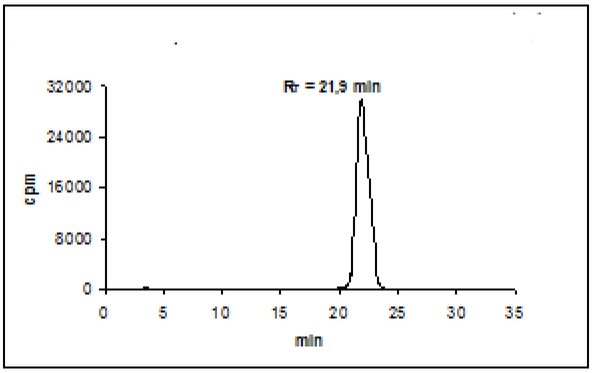

FIG. 15. The radiochromatogram of the reaction products of synthesis ^{99m}Tc(HYNIC-SP) (Tricine)$_2$. Process without addition of Mo.

The same procedure was used for labeling HYNIC-SP from solution containing small amount of Mo. To the solution after separation of AMP 100 MBq of ^{99m}Tc from generator was added. The concentration of Mo in solution was 0.3 mg/ml. The processes of labeling were performed in pH<1, pH 4 and pH 7 (Fig.16 a, b, c).

FIG. 16. The radiochromatogram of the reaction products of synthesis ^{99m}Tc(HYNIC-SP) (Tricine)$_2$ in presence of 0.3 mg/ml Mo. a, pH<1, b, pH 4 and c, pH 7.

As shown in Fig.16, the synthesis of ^{99m}Tc(HYNIC-SP)(Tricine)$_2$ radiobioconjugate performed in the presence of 0.3 mg/ml molybdenum proceeds with very good yield only at pH higher than 4. This demonstrates that after partial separation of Mo by precipitation of AMP it is possible to synthesize radiopharmaceuticals based on a HYNIC chelator. Because the initial solution is highly acidic (pH<1) before labeling it must be neutralized (possibly with a small volume of NaOH to a pH of about 7.

11. LABELING OF NS$_3$-CN-SUBSTANCE P WITH ^{99m}Tc IN PRESENCE OF MOLYBDENIUM IN SOLUTION

The NS$_3$-CN strategy of labeling biomolecules was elaborated by Pietzsch and Spies from Forschungszentrum Rossendorf [13]. The Tc(III) chelate formed by the tripodal 2,2',2''-nitrilotris(ethanethiol) and a monodentate isocyanide fulfill the requirements for a lipophilic, nonpolar building block stable against ligand exchange reaction in vivo (Fig.17). Such precursor was conjugated to various biomolecules, like octreotide, bombesine, ghrelin and substance P.

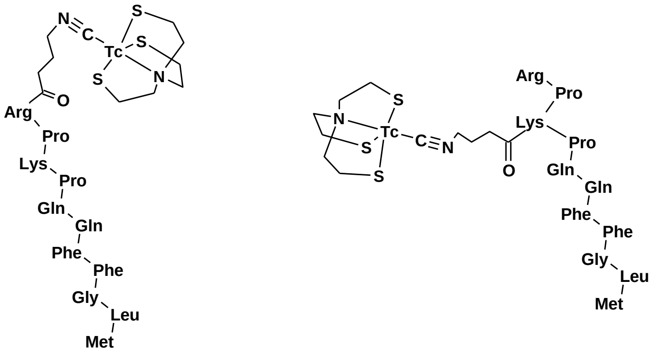

Fig. 17. Two forms of ^{99m}Tc-NS$_3$-CN-SP(1-11).

Similarly like in the case of (HYNIC-SP)(Tricine)$_2$ the labeling experiments were performed in solution without addition of Mo and in presence of 0.3 mg/ml Mo. The labeling procedure was following: for the synthesis of technetium complexes (III) "4 + 1" type , tridentate ligand tris (2-mercaptoethyl) amine, N(CH$_2$CH$_2$SH)$_3$, (NS3), and monodentate izonitryl substance P (1-11), conjugate (CN-SP) were used. The synthesis of the complexes was performed in two steps (Fig.18). The first step is the reduction of Tc(VII) to Tc (III) by SnCl$_2$ in the presence of EDTA and mannitol. In the second stage, resulting in a ligand exchange reaction, the complex intermediate ^{99m}Tc-EDTA/mannitol is converted into a complex ^{99m}Tc-NS$_3$-CN-SP(1-11).

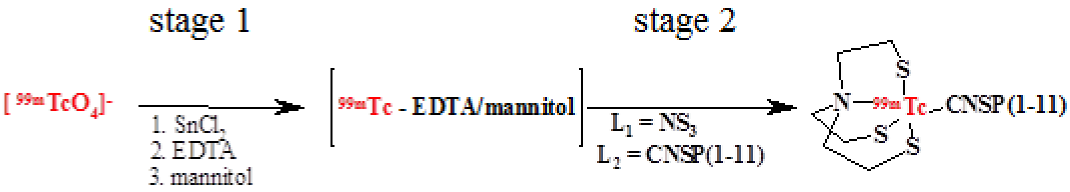

FIG. 18. Scheme of the synthesis of "4+1" Tc(III) complexes.

We compared labeling eficiency in two systems: first, using ^{99m}TcO$_4^-$ from ^{99}Mo/^{99m}Tc generator and second, in simulating solution after Mo precipitation containing ^{99m}Tc (concentration of Mo – 0.3 mg/ml). The radiochroatograms of labeling solution are presented in Fig. 19.

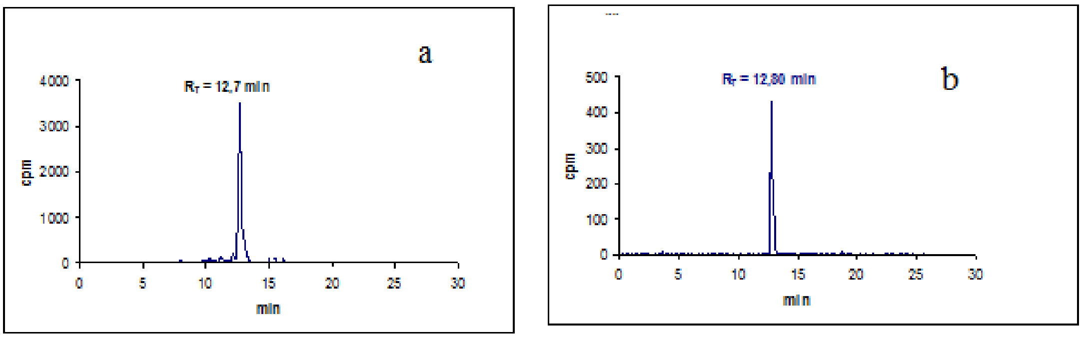

Fig. 19. The radiochromatogram of the reaction products of synthesis ^{99m}*Tc-NS*$_3$*-CN-SP(1-11) in solutions without Mo (a) and in presence of 0.3 mg/ml Mo (b).*

As shown in Fig.19, the synthesis of ^{99m}Tc-NS$_3$-CN-SP(1-11) radiobioconjugate in the presence of 0.3 mg/ml molybdenum occurs with the same efficiency as in solutions without Mo. We did not observe any influenece of Mo on labeling process.

12. CONCLUSIONS

- Technology of Mo metallic foil of required thickness have been developed.
- Pressed and sintered ^{100}Mo pellets with sufficient hardness, density and mechanical strength adequate for irradiation in cyclotrons have been reproducibly produced.
- Chemical and electrochemical dissolution of target in 15 to 20 mL of 30% H_2O_2 and 19 mL of 5M KOH has been achieved in 45 and 70 minutes, respectively.
- About 90 % recovery of ^{99m}Tc in less than 100 minutes with 99.6% radiochemical purity has been achieved using AnaLig resin for separation. It was superior to ion exchange and PEG and gave the product of sufficient radiochemical purity [14].
- The proposed method of molybdenum separation in the form of a solid AMP was fast and efficient. In this method low co-precipitation of $^{99m}TcO_4^-$ and good recovery of Mo was achieved. To obtain pure $^{99m}TcO_4^-$ product in the next step, pertechnetate anions were separated from the excess of molybdate ions on a C18 column coated with PEG-2000 and finally $^{99m}TcO_4^-$ was concentrated on alumina column.
- Labelling Hynic-Substance P and NS$_3$-CN-Substance P conjugates with ^{99m}Tc in presence of molybdenum in solution were performed with a high yield. The separation and labeling processes will be confirmed on real solutions obtained from dissolution of irradiated ^{100}Mo target.

Acknowledgements

This scientific work was funded by the National Centre for Research and Development within the PBS I project, contract No. PBS1/A9/2/2012
Authors are thankfull to Dr. Łukasz Kurpaska from Department of Materials Physics (NCBJ) for testing of nanohardness and to Dr. Marek Barlak from the Department of Technology Plasma and Ion (NCBJ) for performing SEM/EDS investigations.

References

[1] STOLARZ, A., et al., Molybdenum targets produced by mechanical reshaping J. Radioanal. Nucl. Chem. DOI 10.1007/s10967-015-3956-1.

[2] RUTKOWSKI, W., Design of the properties of products sintered from powders and fibres, PWN, Warszawa 1977 (in polish).

[3] SRIVATSAN, T.S., The microstructure and hardness of molybdenum powders consolidated by plasma pressure compaction, Powder Technology **114** (2001) 136-144.

[4] CHATTOPADHYAY, S., et al., Recovery of Tc-99m from Na_2[Mo-99]MoO_4 solution obtained from reactor-produced (n,gamma) Mo-99 using a tiny Dowex-1 column in tandem with a small alumina column, Appl. Radiat. Isotopes **66** (2009) 1814-1817.

[5] MORLEY, T., et al., An automated module for the separation and purification of cyclotron-produced ^{99m}TcO4$^-$, Nucl. Med. Biol. **39** (2012) 551-559.

[6] BENARD, F., et al., Implementation of multi-curie production of ^{99m}Tc by conventional medical cyclotrons, J. Nucl. Med. **55 (**2014) 1017-1022.

[7] ANDERSSON, J., et. al., Separation of TcO_4^- and MoO_4^{2-} using PEG coated C18 SPE cartridge, J. Nucl. Med. **54** (Supplement 2) (2013) 1001.

[8] DASH. A., et al., ^{99}Mo/^{99m}Tc separation: An assessment of technology options, Nucl. Med. Biol. **40** (2013) 167–176.

[9] BONARDI, M., et. al., Thin-target excitation functions, cross-sections and optimised thick-target yields for Mo-nat(p,xn) Tc-94g, Tc-95m, Tc-95g, Tc-96(m+g) nuclear reactions induced by protons from threshold up to 44 MeV, No carrier added radiochemical separation and quality control, Appl. Radiat. Isotop. **57** (2002) 617-635.

[10] CHAKRAVARTY, R., et al., Nano crystalline zirconia: a new sorbent for the preparation of ^{99}Mo-^{99m}Tc generators, J. Labell. Cpm. Radiopharm. **52** (2009) S500-S500.

[11] CHAKRAVARTY, R., et al., Practicality of tetragonal nano-zirconia as a prospective sorbent in the preparation of ^{99}Mo-^{99m}Tc generator for biomedical applications, Chromatographia **72** (2010) 875-884.

[12] PALMA, C., Tachykinins and their receptors in human malignancies, Curr. Drug. Targets **7** (2006) 1043–1052.

[13] PIETZSCH, H., et al., Mixed-ligand technetium(III) complexes with tetradendate/monodendate NS_3/isocyanide coordination: A new nonpolar technetium chelate system for the design of neutral and lipophilic complexes stable in vivo, Bioconjugate Chem. **12** (2001) 538-554.

[14] WOJDOWSKA, W., et al., Studies on the separation of ^{99m}Tc from large excess of molybdenum. Nucl. Med. Rev. Cent. East. Eur. (2015).

PRODUCTION OF Tc-99m AT KING FAISAL SPECIALIST HOSPITAL AND RESEARCH CENTRE (KFSHRC)

I. AL-JAMMAZ, F. AL-RUMAYAN, S. AL-YANBAWI, AND A. AL-RABIHA

Cyclotron and radiopharmaceuticals department
King Faisal Specialist Hospital and Research Centre
Riyadh, Saudi Arabia

Abstract

The production of technetium radioisotope is reported in this study including production via natural and enriched Molybdenum (^{100}Mo). In this study the Mo target was bombard with different beam current in order to study the stability of the pressed target. A maximum total activity of ^{99m}Tc was 1100 mCi was obtained when the target was bombarded with 15 uA. Moreover, radiolabeling of Pertechnetate with MDP was successfully performed.

1. INTRODUCTION

Nuclear medicine applications of the cyclotron produced radiopharmaceuticals are being increasingly utilized for both research and routine clinical diagnosis and therapy of an extensive variety of diseases. Numbers of medium energy cyclotrons world-wide have rapidly increased specially after the introduction of Positron Emission Tomography (PET) and this number is expected to grow in the future. Due to the major shortage supply of the molybdenum-99 (^{99}Mo) caused by the prolonged shutdown of various reactors, the need to explore alternative methods of producing technetium-99m (^{99m}Tc) isotope using medium energy cyclotron is well justified to allow continued use of all existing radiopharmaceuticals designed for ^{99m}Tc in nuclear medicine [1-5].

Recently, numbers of member states have embarked on research programs to investigate the use of accelerators for the production of ^{99}Mo or ^{99m}Tc directly. These approaches make use of the ^{100}Mo(γ,n)^{99}Mo and ^{100}Mo(p,2n)^{99m}Tc reactions, respectively. Early indications have shown that the cyclotron approach holds promise for at least being able to supplement generator availability with production rate of 17 mCi/μAh. At this rate it is possible for the existing cyclotrons with proton energies of 16-19 MeV and beam current ranging from 60-100 μA to produce significant amounts of ^{99m}Tc for local use on a daily basis.

2. DESIGN OF SOLID TARGETS SYSTEM

The crucial part of designing a solid target is associated with heat transfer problem that need to be removed continuously as the beam bombarding the target surface. Because the density of solids is typically higher than that of liquids or gases, the path length of the beam is shorter, and the target somewhat smaller. The energy lost when charged particles pass through the target medium is dissipated in the form of heat. The following items were found to play role in affecting yield:

- Target inclination (Beam to target angle)
- Sufficient cooling system (water and helium)
- Beam current

- Beam energy and
- Beam sweeping method

Therefore, the target is designed to be cooled by both water and helium channels and the beam aligned to be perpendicular to the target (90°). Figure 1 displays the developed solid target for ^{100}Mo and its control system which remotely controls the target from the cyclotron room. This target is a modified target of the recently developed solid target for I-124 and Cu-64.

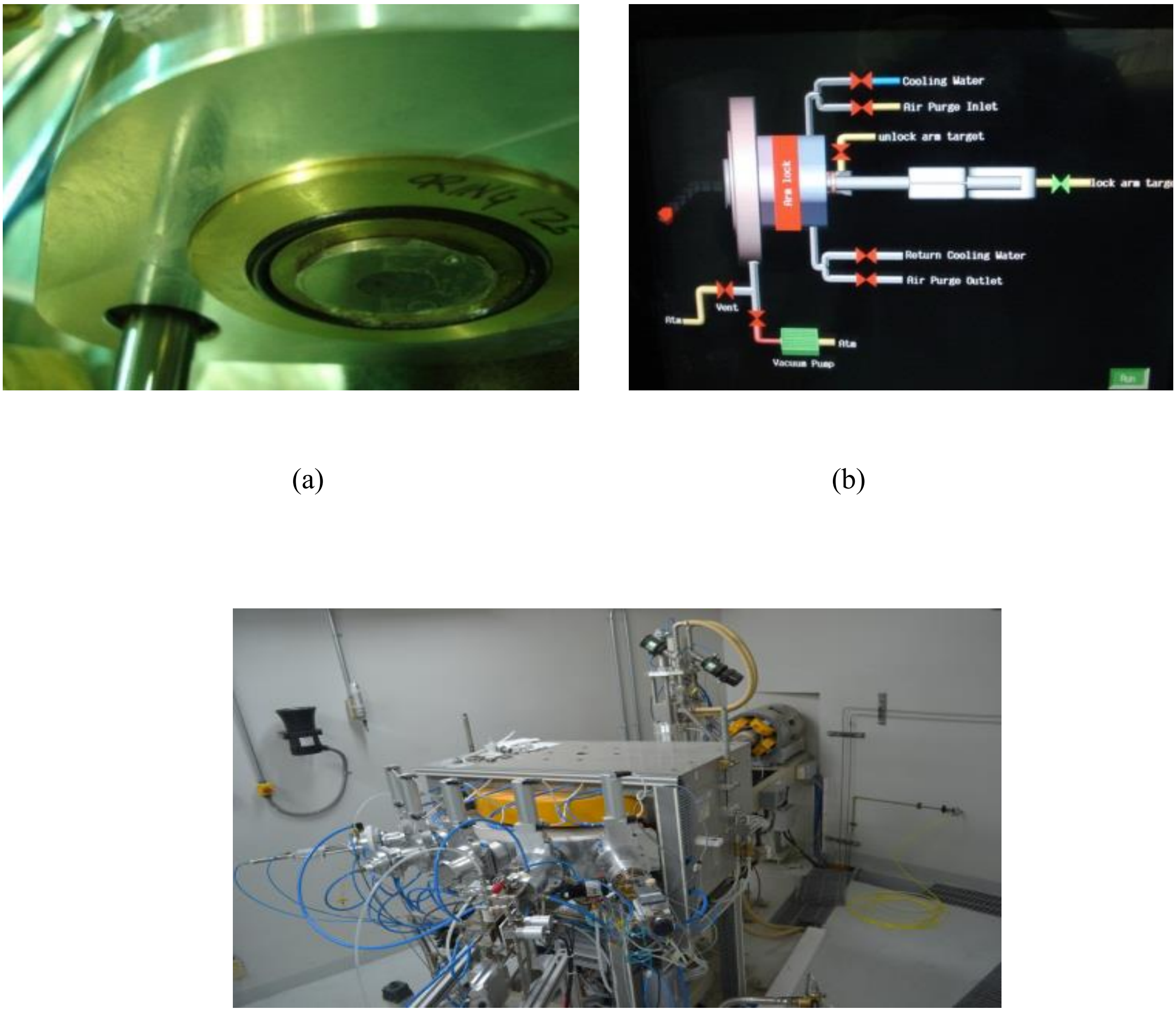

(a) (b)

(C)

FIG. 1. Solid target system (a) Solid target assembly, (b) control system (c) target being installed in one of the C-30 ports (first to left).

3. BEAM MONITORING AND CONTROL SYSTEMS

In order to ensure that the beam is spread over the target area; beam diagnostic tool such as collimator system can be used. Collimators are usually designed to be slightly smaller than the target opening or window. This ensures the size of the beam is limited to the size of the target opening and, therefore, the beam current that is read on the target is an accurate indication of the beam hitting the target. Moreover, it prevents the front flange of the target from becoming activated and therefore lowers the radiation dose to the operator when maintenance is required. Figure 2 elucidates the developed four fingers collimator system at the research centre in King Faisal Specialist Hospital (FSHRC). In such a system beam current is adjusted until measured on the four figures indicating that the beam is wide enough and covering the whole area. For beam to be spreaded, other tools are used to defocus it on the collimator: a magnetic focusing element (quadruples) and steering magnet.

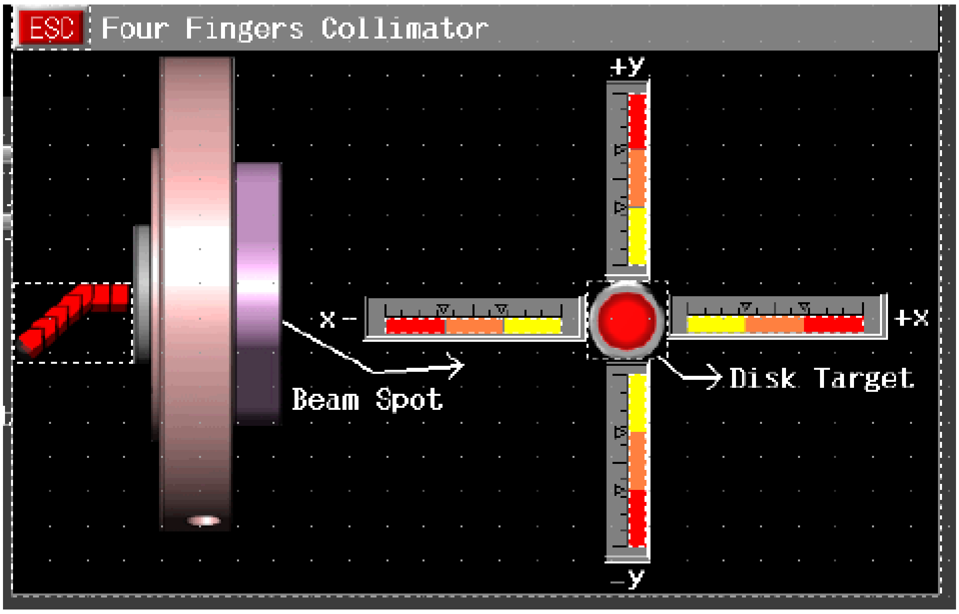

FIG. 2. Four fingers collimator designed and fabricated at the research centre of KFSHRC.

4. TARGET PREPARATION

While the use of ^{nat}Mo foil is the simplest target design employed for ^{94m}Tc production, thick foils of enriched ^{100}Mo are not readily available. Therefore, several alternative strategies for target preparation using different forms of ^{100}Mo metal and oxide have been investigated previously to overcome this limitation. In addition, our initial attempt to electroplate enriched ^{100}Mo (99.8%) on aluminum target plate did not proceed well. Since one of the most common methods for thick target preparation is the pressing of an enriched MoO_3 pellet into copper or platinum cavity target, circular copper and aluminum target plates to fit the remotely controlled target were fabricated utilizing our well-equipped precision machine shop. The diameter of target plate is 25 mm, thickness is 2 mm and the cavity depth in the center of the target is 1.25 mm with diameter of 10 mm (Figure 3).

FIG. 3. Circular copper and aluminum target plates.

4.1. Old Method

Initially the enriched (^{100}Mo) targets in oxide form were prepared by hydraulically pressing ^{100}Mo metallic powder (300-400 mg) into the circular cavity aluminum target plates at 5000 psi, this was followed by heating in a furnace at 450°C for four hours. For quality control, each target was examined microscopically to ensure its smoothness and homogeneity.

In initial experiments, when hydraulically pressing was 5000 psi and temperature was increased to insure the rigidity and homogeneity of Mo-oxide to the aluminum plate, however, cracks and ununiformed shape was observed and target material flakes during irradiation (Figure 4).

a) virgin sample

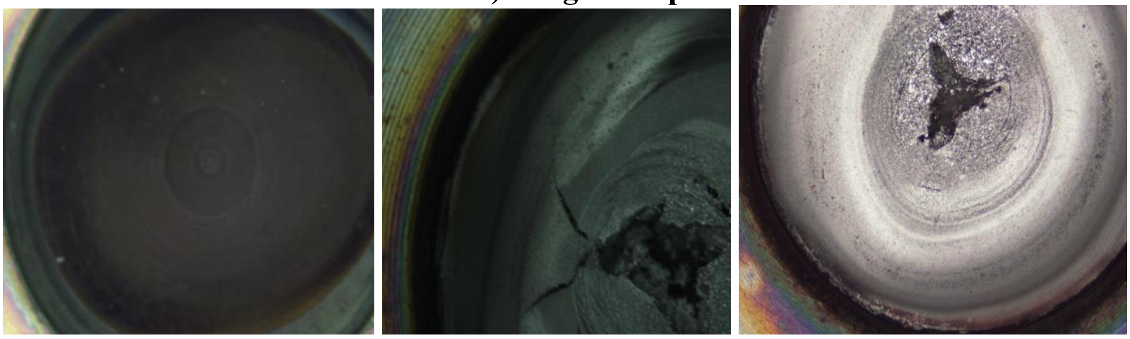

e)15 uA **c) 22uA** **d) 30 uA**

FIG. 4. Effect of high beam current on ^{nat}Mo targets.

4.2. New Method

In order to improve the method of target pressing, a new technique was developed and explained as follow. The enriched MoO_3 pellet is pressed at 5000 psi using the pressing assembly shown in in figure 5. The pellet, then, removed from the assembly and insert into the furnace where it backed at 1000°C for 4 hrs. The pellet then pressed again into an aluminum disk at 250 psi. The target is again inserted into furnace and heated up at 450°C for 4 hrs. Figure 5 shows tools used in the new method.

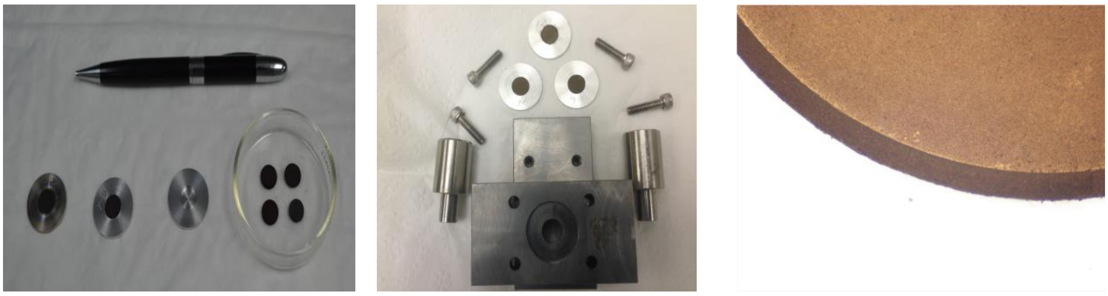

FIG. 5. Pressing assembly with some ready-made targets.

5. RESULTS AND DISCUSSIONS

5.1. Target Irradiation

Several experiments were conducted on both natural and enriched Molybdenum. Beam current was increased gradually on target as shown in runs 1, 2, 3, and 4. Due to the use of ^{nat}Mo several technetium radioisotopes were seen during MCA analysis, in addition to ^{99m}Tc. Results are tabulated in table 1. The percentage of each of whcihc may differ with beam current. Attention should be drawn to run# 4 where high current was bombarding the target. Results reveal high yield but with low ^{99m}Tc purity.

TABLE 1. EXPERIMENT PERFORMED ON NATURAL MO

Run	**Energy (MeV)**	**T (hr)**	**I (uA)**	**Wt (mg)**	**Produced Isotopes (%)**			
					Tc-94	**Tc-95**	**Tc-96**	**Tc-99m**
1	19	1	15	454	42.6	29.7	7.5	20.13
2	19	2	15	342	45.8	32	8	14.2
3	19	0.5	30	292	20	48	12	40
4	19	0.5	40	317.7	44.9	27.7	6.73	21.24

However, the attention shold be drawn to the Tc-99 percentage when beam was bombarding pure ^{100}Mo. The percentage was reaching >99%.

In order to qunatify the activity of very long experiment, the enriched Mo was bombard with 15 uA for 6 hrs. The total activity collected was 1170 mCi. The Tc-99 percentage was 99.97 and only Tc96(104.4 h) was measured.Moreover, in order to study the impact of energy on Tc-99m purity, we have increased the energy up to26 MeV, and yet purity reached 99.6 as shown in Table 2. One important finding in our study that the yield produced from irradiating enriched was giving high yeild as seen below.

TABLE 2. EXPERIMENT PERFORMED ON ^{100}Mo

Run	**Energy**	**T**	**I**	**Wt**	**Produced Isotopes**			
	(MeV)	**(hr)**	**(uA)**	**(mg)**	**(%)**			
					Tc-94	**Tc-95**	**Tc-96**	**Tc-99m**
1	19	1	15	353	0	0	0.03	99.97
2	22	1	15	296	0	0	0.4	99.6
3	22	6	15	354	0	0	0.025	99.7
4	26	1	15	325	0	0	0.4	99.6

5.2. Preparation and Radiolabelling of Pertechnetate “TcO4$^-$ with MDP

The produced Tc-99 was extracted as follow. Hydrogen Byroxide H_2O_2 (30% concentration) is added to the target. Then 10M of NaoH is added to ensure the PH is >7.5. Extraction of Pertechnetate TcO4- is done using Methane ethyl ketone (MEK). Compound was washed with 5M of NaOH and then sodium sulfate was added and filtrated. Compound was Evaporate to Dryness. 0.9% of NaCL (to dissolve Pertechnetate) was added. Purification of Pertechnetate performed using alumina column.

The MDP (Methylene-diphosphonate) is a medical product for diagnostic purposes. And field of indication is isotopes diagnostic bone Scintigraphy. In many case, it can be used of the following diseases:

- Primer bone tumour
- Bone metastases of other tumours. (e.g. prostate, breast and lung cancer).
- Osteomyelities
- Metabolic diseases of the bone.

After extraction of $TcO4^-$ in normal saline for kit radiolabeling, we prepared [Tc]-MDP as model radiolabeled kit. We place the glass vial containing the freeze-dried material in a small lead pot of 3 mm wall thickness. In aseptic conditions the required activity of sterile Tc-99m Pertechnetate injected into the vial through the rubber cap with sterile syringe. Initial radiolabeling results using the TLC showed less efficiency as shown in figure 6. Efficiency was reached 90%.

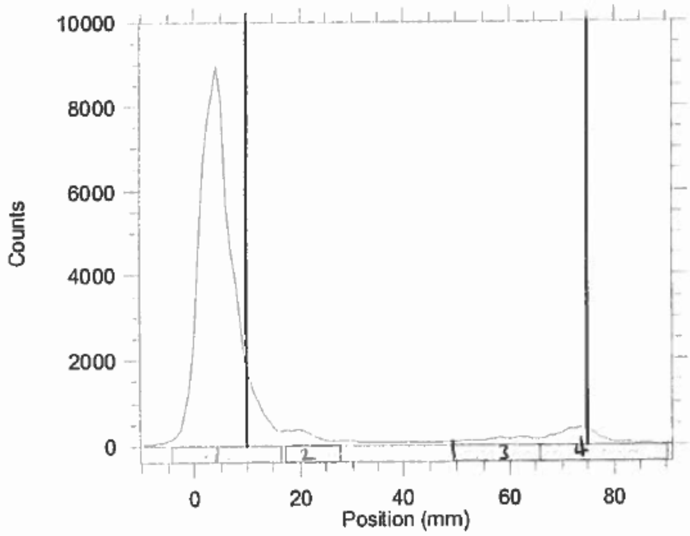

FIG. 6. Radiolabeling of ^{99m}Tc with MDP.

6. CONCLUSION

The production of technetium radioisotope is reported in this study including production via natural and enriched Mo. In this study the Mo target was bombard with different beam current in order to study the stability of the pressed target. A maximum total activity of ^{99m}Tc was 1100 mCi was obtained when the target was bombarded with 15 uA.

Moreover, radiolabeling of pertechnetate with MDP was performing with efficiency being 90 %.

Acknowledgment

The research team would like to acknowledge the International Atomic Energy Agency (IAEA) and King Faisal Specialist Hospital and Research Center (KFSH&RC) for their support.

References

[1] GAGNON, K., BENARD, F., KOVACS M., RUTH, T.J., SCHAFFER, P., WILSON, J.S., MCQUARRIE, S.A., Cyclotron production of 99mTc: experimental measurement of the ^{100}Mo(p,x)^{99}Mo, ^{99m}Tc and ^{99g}Tc excitation functions from 8 to 18 MeV, Nucl. Med. Biol. **38** (2011) 907-916.

[2] ESPOSITO, J., Feasibility Study Report on Alternative ^{99}Mo/^{99m}Tc Production Routes using Particle Accelerators at LNL (2011 version), INFN-LNL-235 (2011).

[3] ALFASSI, Z., GROPPI, F., BONARDI, M., GOEIJ, J., On the artificial nature of Tc and the carrier-free nature of ^{99m}Tc from ^{99}Mo/^{99m}Tc generators, Appl. Radiat. Isot. (2002) 6337-6340.

[4] ZOLLE, I., Technetium-99m Pharmaceuticals: preparation and quality control in nuclear medicine, Springer, Berlin (Germany), (2007), ISBN 978-3-540-33989-2.

[5] UCCELLI, L., BOSCHI, A., PASQUALI, M., DUATTI, A., DI DOMENICO, G., PUPILLO, G., ESPOSITO, J., GIGANTI, M., TAIBI, A., GAMBACCINI, M., Influence of the Generator in- Growth Time on the Final Radiochemical Purity and Stability of Radiopharmaceuticals, Sci. Tech. Nuc. Inst., Article ID 379283, Vol. **2013**, 7 pages, (2013), doi: 10.1155/2013/.

[6] ISOFLEX 2012 Batch, Certificate of Analyses Mo-100 enriched molybdenum metallic material (ISOFLEX-USA).

HIGH ACTIVITY CYCLOTRON PRODUCED Tc-99m FOR MEDICAL APPLICATIONS

A. H. AL-RAYYES

Atomic Energy Commission of Syria, Radioisotopes Department, Cyclotron Division.

Abstract

Multiple methods and experiences have been carried out to perform a suitable target for high current proton beam for ^{99m}Tc production.

Different electroplating bathes have been used for target support electroplating.

The quality of the different electroplated Mo layer on copper substrate was not suitable for high current proton beam and high activity Tc-99m production.

The thickness obtained by different electroplating procedure do not exceed 2-3 micrometer having a total surface of 10 cm^2.

After these non-satisfied electroplating experiences, testes on pressed then sintered of molybdenum oxide method in order to prepare a molybdenum target had been achieved. An experiment on molybdenum oxide sintering has been performed, but again with no success due to the appearance of crystals on the surface of the prepared pellets.

Another method for the production of ^{99m}Tc based on liquid target has been explored.

A related method for the separation of ^{99m}Tc and recovery of enriched molybdenum has been tested.

At the final period of the project a new production method of ^{99m}Tc was tested using a high current solid target. This method can meet cost-effective production and quality of the produced ^{99m}Tc criteria. The separation and purification setup was elaborated to produce high quantity and high specific activity of $^{99m}TcO4^-$ suitable for labeling different ligands in order to be used in nuclear medicine imaging. A semi-automated target dissolution and separation system has been developed and achieved for $^{99m}TcO4^-$ production. The separation chemistry is based on a chromatographic column system. Chemical and radiochemical purity was found to be in accordance with the USP and EP specifications. 99% of radioisotopes in the final product were attributed to the presence of ^{99m}Tc. The labeling efficiency results of the produced $Na^{99m}TcO_4$ show that less than 1% of ^{99m}Tc activity was not labeled with MDP kit. Biodistribution of labeled kits results and their application for in vivo SPECT images demonstrate that the quality of the produced ^{99m}Tc-pertechnetate is identical to that produced from ^{99}Mo/^{99m}Tc generators.

1. INTRODUCTION

The global shortage of Mo-99 production and the increasing demands on Tc-99m in nuclear medicine, have led to look for other routes for production of Tc-99m. Several reactions were investigated for the production of Tc-99m directly or indirectly via production of Mo-99. In this study we will focus our research on the direct production of Tc-99m by proton bombardment of enriched molybdenum. High activity of Tc-99m will be produced based on $^{100}Mo(p,2n)^{99m}Tc$ reaction. To make this production route feasible using 30MeV cyclotron, proton energy will be adjusted on different energies between 18 and 24 MeV. Targets irradiated on different energies, at the same irradiation time, (18, 20, 22, 24 MeV) will be treated in order to determined the impurities and results will be compared with theoretical calculations.

The successful key of this work is to prepare a robust target which can resist to more than 150 micro ampere of proton beam. This step will take more time than the other step of production.

Method for separation and purification will be investigated. The ion exchange chromatography technique will be applied for Tc-99m separation to meet the requirement of high specific activity and purity.

Quality control of the cyclotron-produced pertechnetate will be investigated. Voltamprommetric method will be use to measure the presence of any contaminant.

Radionuclidic impurities will be determined by gamma spectrometry.

Labelling efficiency of different kits and image quality of Tc-radiopharmaceuticals using cyclotron-produced ^{99m}Tc will be investigated.

Possible parameters of consideration with regards to target design include the molybdenum deposition technique, the selection of target support plate material (e.g. with regards to thermal properties, machinability, mechanical strength, chemical inertness, cost, activation products, etc.), the beam power density, and the target cooling system.

While several strategies for metallic molybdenum deposition have been tested, further development into these and/or other methods is warranted. Examples of molybdenum deposition strategies which have been tested for this application include both sintering and electroplating. Sintering has been used to prepare dense (100 μm) metallic molybdenum targets. The conditions for sintering, the lower-limit of thickness that can be achieved, and the development of a simple technique for bonding of the enriched molybdenum pellet to a suitable backing plate require further evaluation. Electroplating molybdenum directly from a molybdate solution onto a suitable target plate can be achieved to make thin (<5 μm) metallic coatings, however accelerator targets need to be substantially thicker. Research into the plating conditions and electrolyte composition can be carried out to develop a technique that promotes thick, adherent, metallic molybdenum deposits for irradiation.

We think that improving pressed then sintered metal powder target will be the suitable method that can be used for preparation from new metallic and recovered material of Mo metallic powder.

A new method for the production of ^{99m}Tc has been explored based on liquid target.

The activity production yield should be studied in more details. As well as the quality of the separated and purified pertechnetate need confirmation for direct medical uses.

The chemical properties and suitable half life of ^{99m}Tc (6.01 h) make it very suitable for Labeling of many diagnostic radiopharmaceuticals used for imaging via Single Photon Emission Computed Tomography (SPECT) or planar scintigraphy. It is by far the most widespread medical radionuclide used in more than 70% of all nuclear medicine procedures worldwide [1-3]

The majority of the used ^{99m}Tc is produced from the decay of ^{99}Mo, a fission product of ^{235}U. Nuclear fission of ^{235}U occurs in nuclear reactors after highly enriched uranium (HEU) undergoes neutron bombardment.

Given the current worldwide shortage of reactor-produced ^{99}Mo/^{99m}Tc, it became necessary to explore an alternative Method for producing ^{99m}Tc, which would allow continued use of its all existing radiopharmaceuticals [4-6].

Actually there is a growing interest in exploring the large-scale cyclotron production of ^{99m}Tc using the ^{100}Mo(p,2n)^{99m}Tc reaction. The measured yields of this reaction suggest that ^{99m}Tc can be produced in quantities sufficient for supplying regional radiopharmacies and may supplement or in some instances even replace ^{99}Mo generators [7-9].

Today the direct production of ^{99m}Tc using the ^{100}Mo(p,2n)-reaction on highly enriched ^{100}Mo as the target material appears to be the most promising. The best proton energy giving less radioactive impurities was calculated to be about 22MeV [10-11].

This work focuses on several technical aspects related to the large-scale direct cyclotron production of ^{99m}Tc using the ^{100}Mo(p,2n)^{99m}Tc reaction.

2. RESULTS AND DISCUSSION

2.1. Target support electroplating method

The electrolyte bath for electroplating consists of 100 grams of potassium fluoride dehydrate, KF_2H_2O: 10 to 15 cc. of 48% aqueous hydrofluoric acid , HF: 50 to 130 cc. of water: and 5 grams of molybdic anhydride, MoO_2.

The current density used is from 0.25 to 0.35 ampere per square centimeter. The temperature is preferably maintained between 30°C and 50°C.
When the temperature rises above than 65°C, dark non-adherent deposits are obtained.

With our process as above described, we have been able to obtain smooth, bright, adherent deposits of molybdenum in five minutes. The deposited metal is resistant to acid such as cold hydrochloric and sulfuric and resistant to strong alkailes, but is soluble in nitric acid.
The accent used process in our laboratory as following:
5 g molybdic anhydride
100 g. KF_2H_2O
13.5 cc. HF (48%)
50 ml water

The optimum conditions for obtaining deposition of molybdenum from this bath are cathode current density 0.3 ampere per square centimeter (the used current is about : 240 mA); temperature 30°C to 50° C (used temperature is about : 45° C) dark, non-adherent deposits are obtained in five minutes, The weight of the average deposit (two targets) is 0.0075 g. on an area of 10 square centimeters of cathode surface, the used anode is a conducting material which not be attacked by the reaction products such as carbon.
Figure 1 shows the electroplated target and target surface.

FIG. 1. Copper target support electroplated with Mo.

2.2. Pressing and sintering of molybdenum oxide method

Natural molybdenum oxide has been pressed in a disc form. Then this disc is sintered at 650°C for the duration of 24 hours air atmosphere. The disc became harder and more resistant to chocks. When the surface has been analyzed by Scanning Electron Microscopy (SEM), the particle consisting the disc appeared to be not well bounded. This means the heat conductance of sintered material will be not good.

Figure 2 and 3 shows the surface by SEM before and after pressing and sintering experiments.

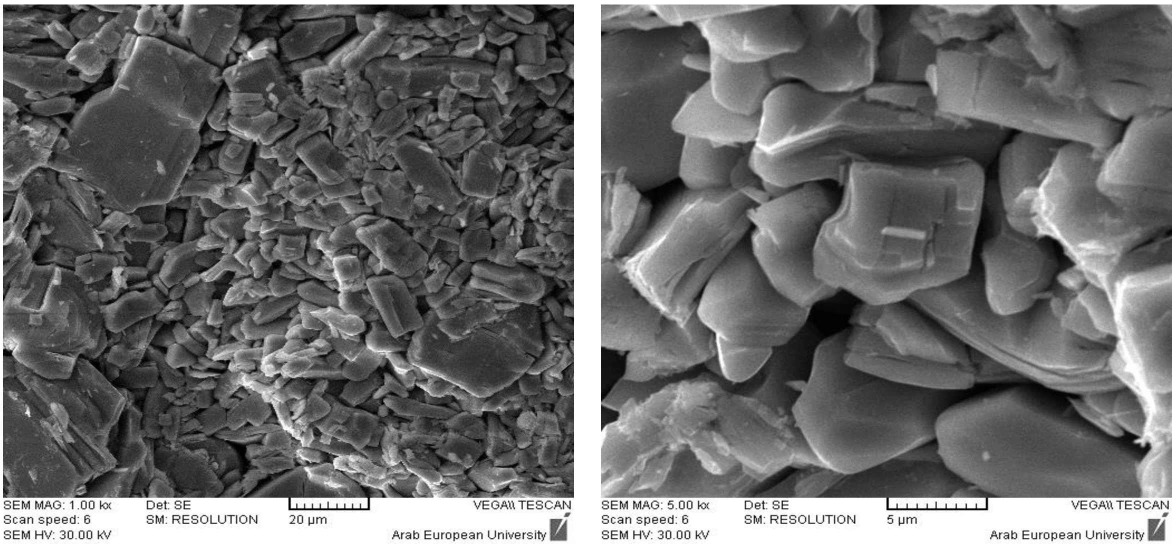

FIG. 2. Scanning electron microscopy (SEM) of the pressed non-sintered MoO_3.

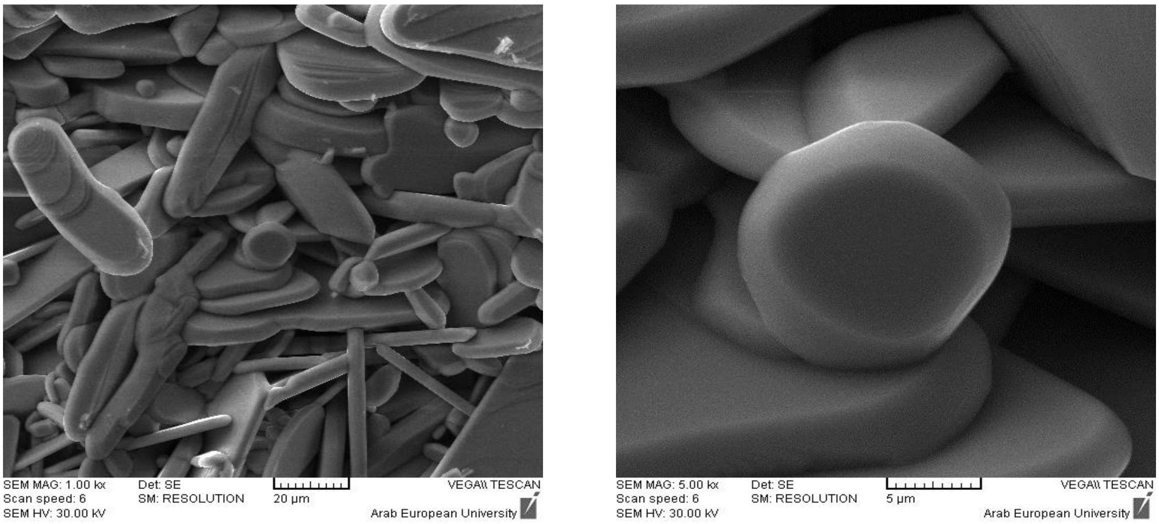

FIG. 3. Scanning electron microscopy (SEM) of the pressed and sintered MoO_3 (650^{o}C, 24h).

Another experiment has been carried out in order to see the effect of the temperature on the sintered materials. We found that at 750^{o}C crystals of sintered molybdenum oxide is formed on the surface of the disc. Figure 4 shows the surface of the sintered MO_3 at 750^{o}C and 650^{o}C.

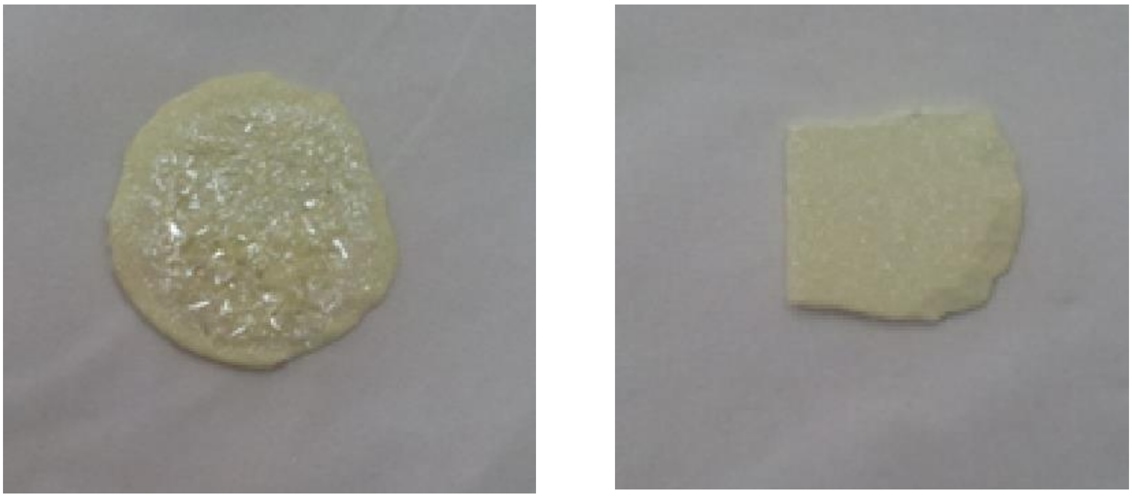

Pressed and Sintered MoO_3 *(750* ^{o}*C, 24h)* *Pressed and Sintered* MoO_3 *(650* ^{o}*C, 24h)*

FIG. 4. Surface of the sintered MO_3 *at 750*^{o}*C and 650*^{o}*C.*

At this time a sintering condition for molybdenum powder metal (temperature and heating atmosphere will be optimized. We hope that this target can resist to more than 150 µA proton beam current.

For our future work we can enlarge engraved central area (may be can be an oval shape) where we can put more Mo metal powder.

2.3. Irradiation of Molybdenum in liquid target

Sodium molybdate solution has been prepared by the dissolution of 0.5 g of $Na_2MoO_4.2H_2O$/1 ml deionized water (solubility 0.56 g/ml, 0^{o}C)

Irradiation conditions:

Irradiated Liquid Volume: 0.85 ml
Niobium target used for ^{18}F production
Target Window: Havar
Irradiation current: 30 Micro Amperes
Target pressure: 35 Bars
Irradiation time: 30 min
Irradiated Mo weight: 0.16 g

After the bombardment, the irradiated liquid has been loaded on the separation column containing Acidic Alumina resin which has been preconditioned by HNO_3 3M.
The column has been rinsed by 2ml of HNO_3 3M (Figure 5).
Then radioactive molybdenum is eluted by 5ml of 0.9% NaCl.
Then the recovery of molybdenum was performed by passing 30 ml of NH_4OH 1M.
All these solutions were analyzed by gamma spectrometry (Figures 6-12).

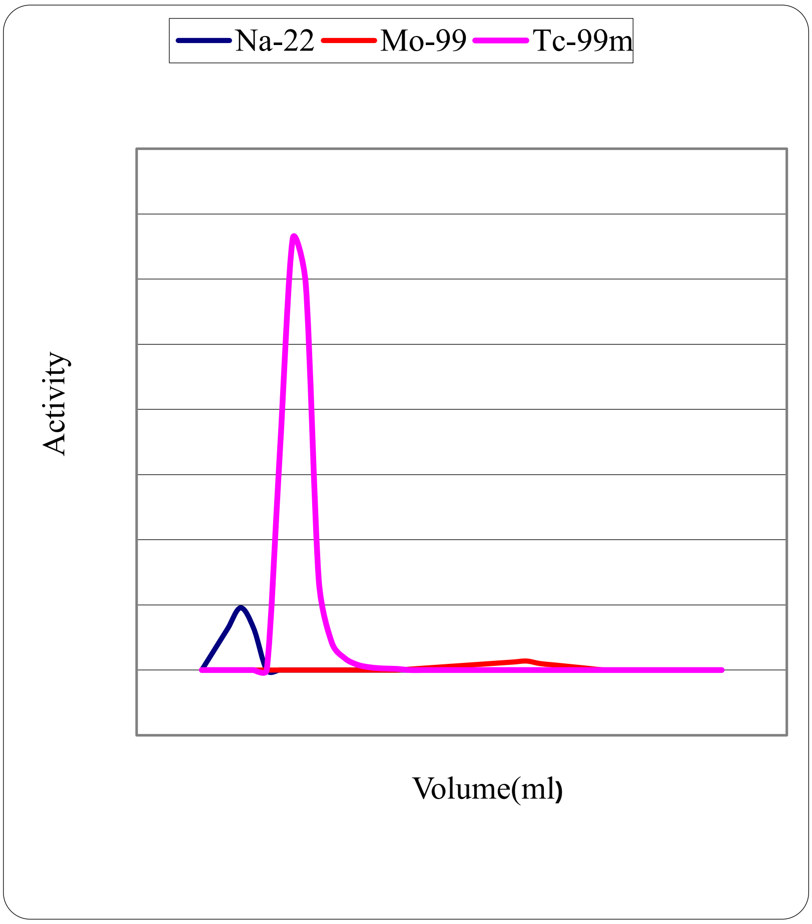

FIG. 5. Column elution profile.

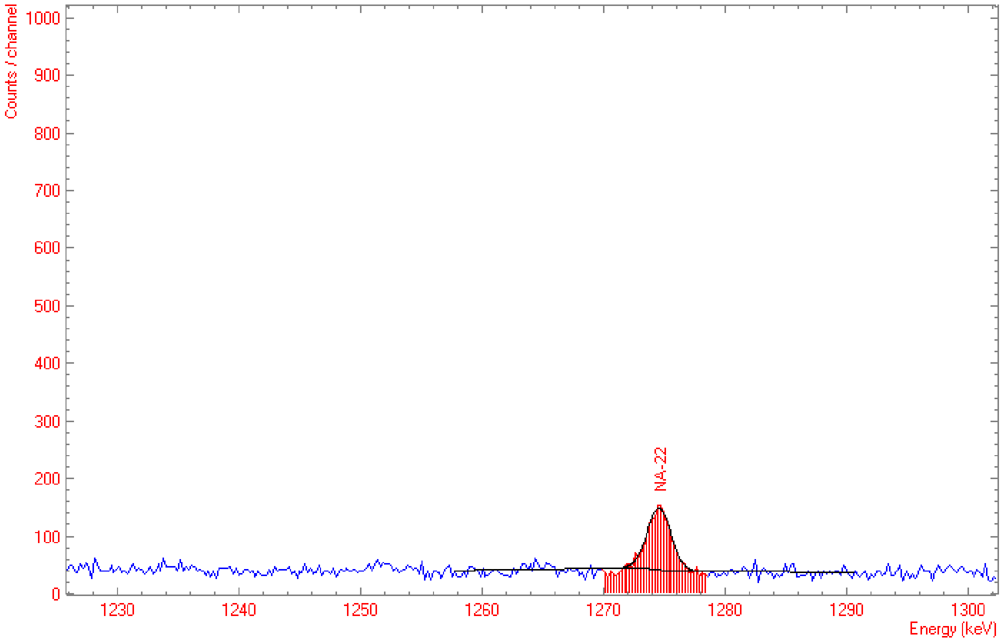

FIG. 6. Gamma ray spectra of the first rinsed solution by HNO_3.

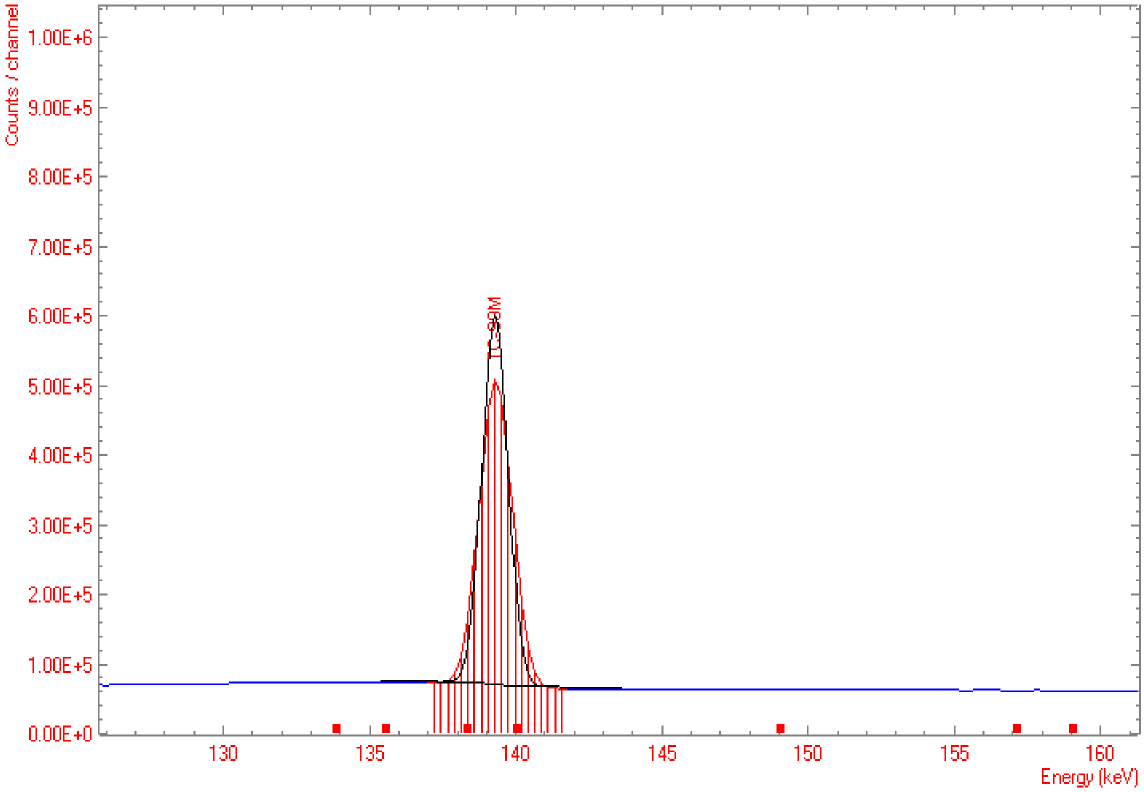

FIG. 7. Gamma ray spectra of the eluted radioactive technetium.

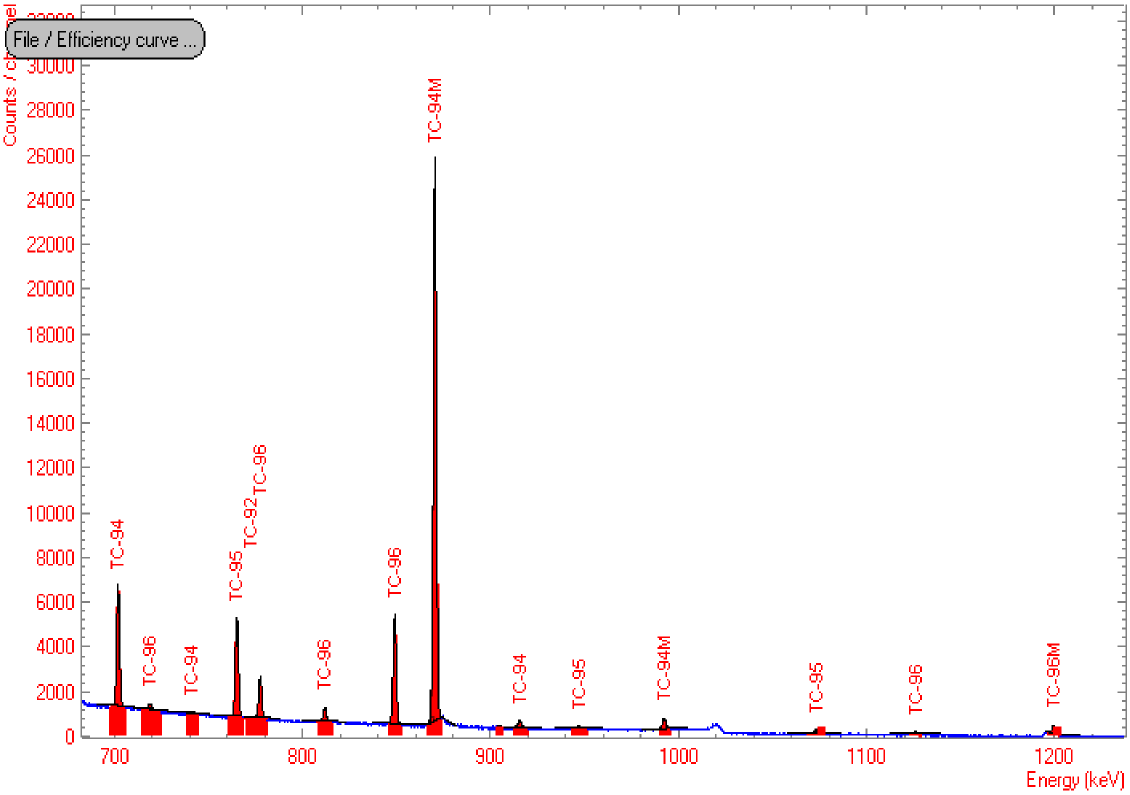

FIG. 8. Gamma ray spectra of the eluted radioactive technetium.

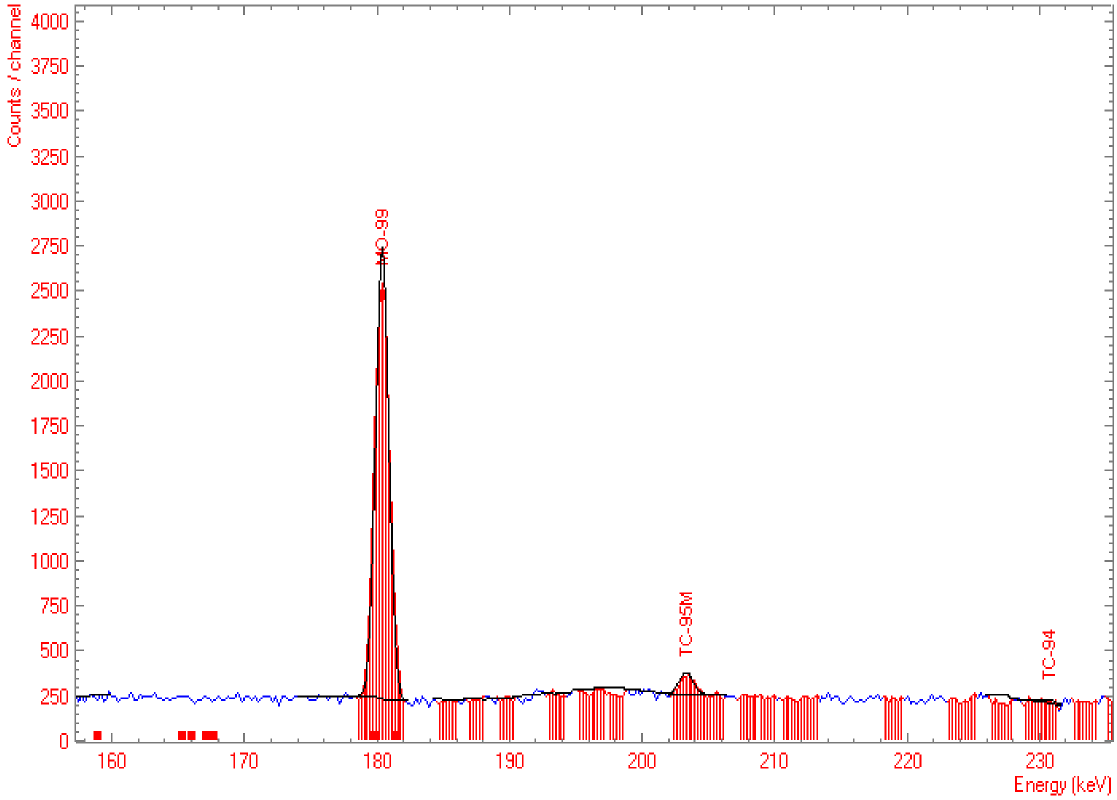

FIG. 9. Gamma ray spectra of the recovered Molybdenum.

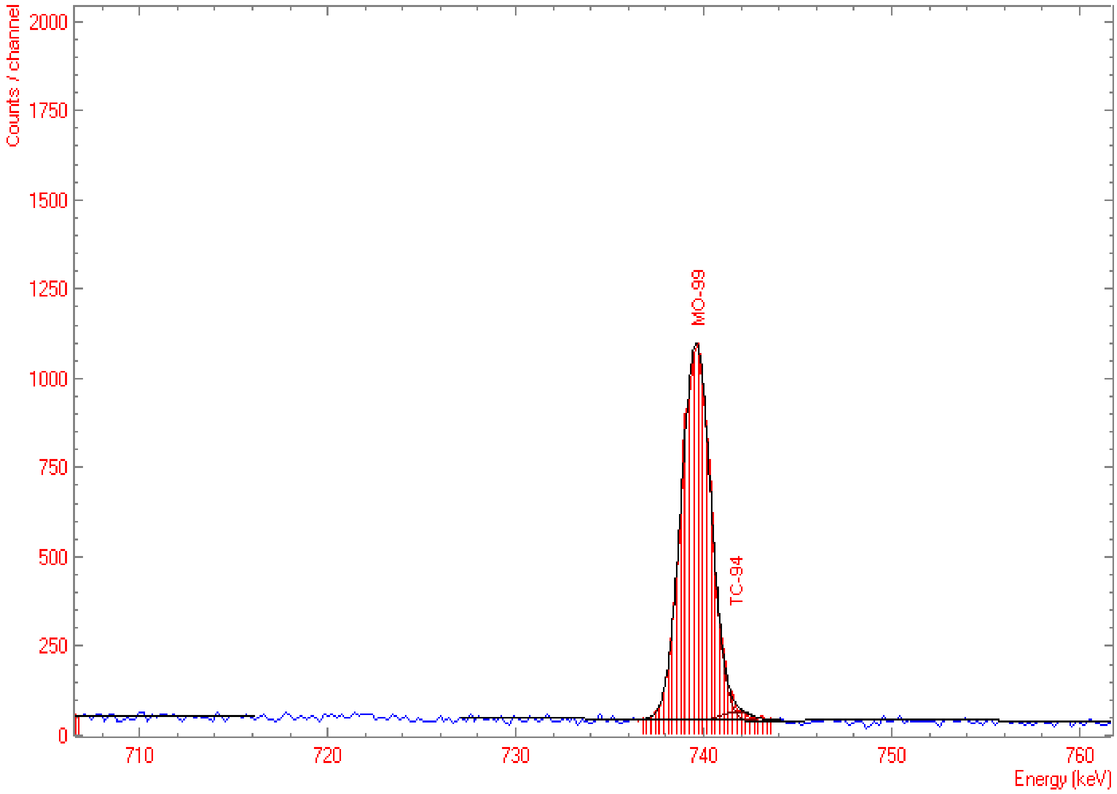

FIG. 10. Gamma ray spectra of the recovered Molybdenum.

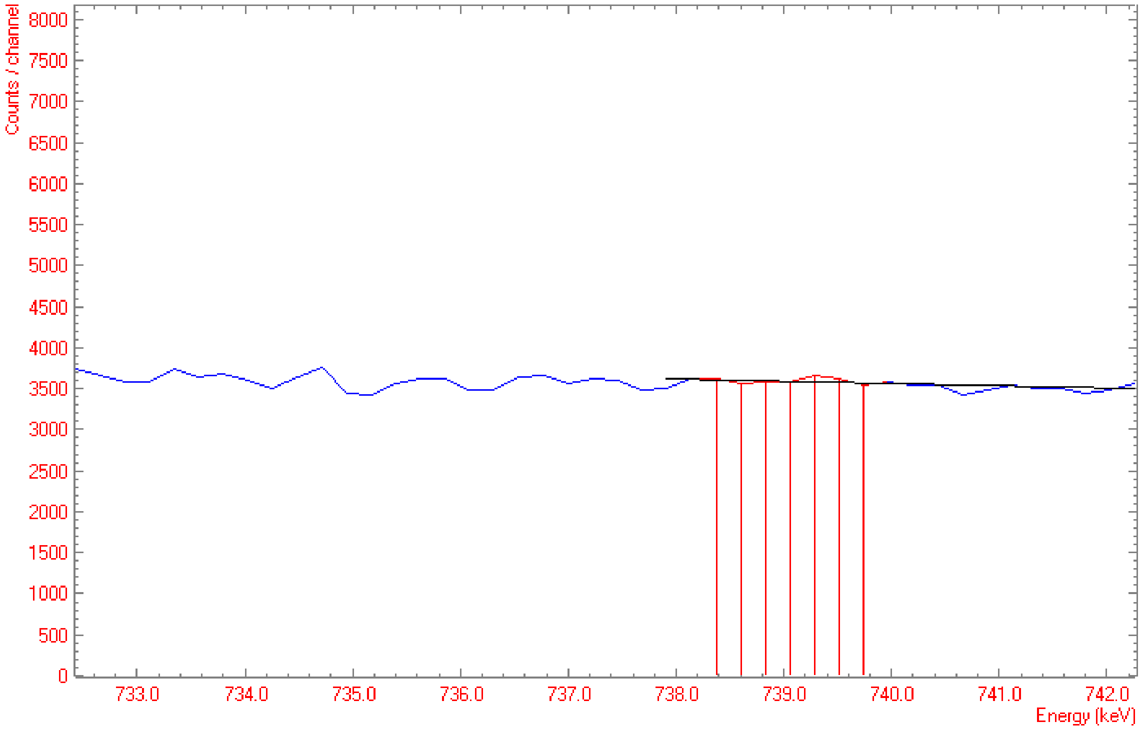

FIG. 11. Gamma ray spectra of the separation column confirm no molybdenum, good recovery.

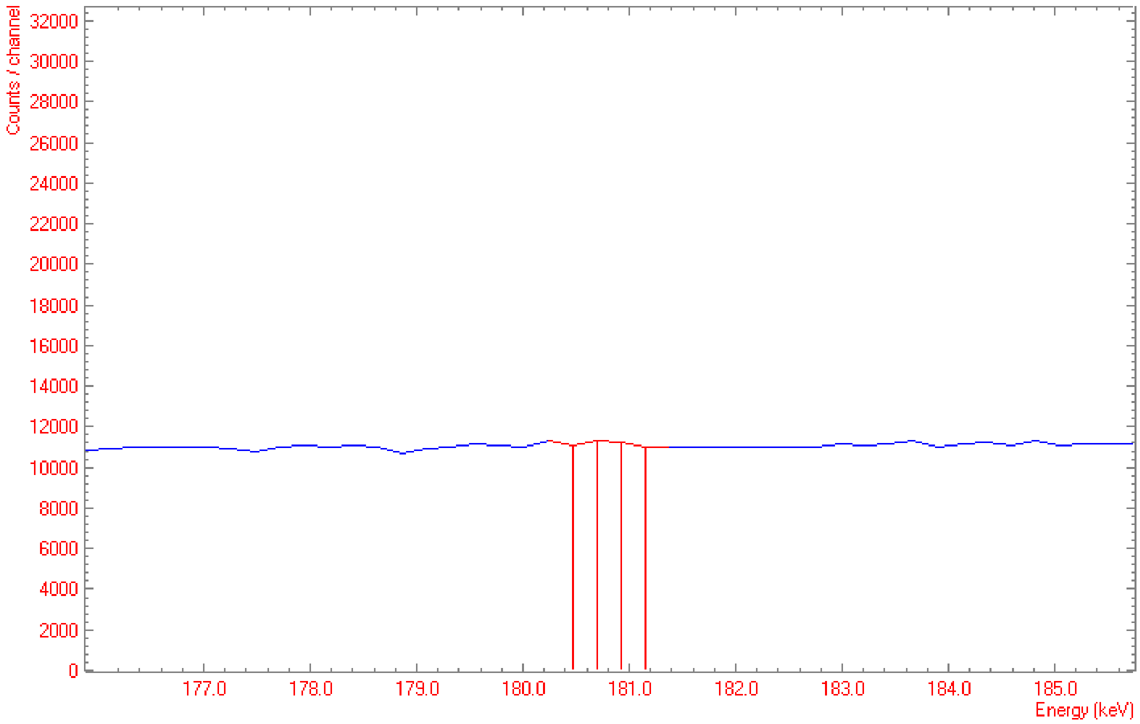

FIG. 12. Gamma ray spectra of the separation column confirm no molybdenum, good recovery.

2.4. Production and Quality Control of ^{99m}Tc using high current solid target

On the other side we use a modified IBA solid target, which we think can be an ideal effective system for cooling point of view.

We used a modified IBA blank target before pressing Mo inside the engraved central region of this support.

Then on the engraved area we pressed Mo metal powder on the center of the target (surface 1 cm$^{2)}$.

FIG. 13. Pressed target before irradiation.

Figure 13 and 14 shows the prepared target before and after irradiation. The thickness of the pressed material is about 50 µm.

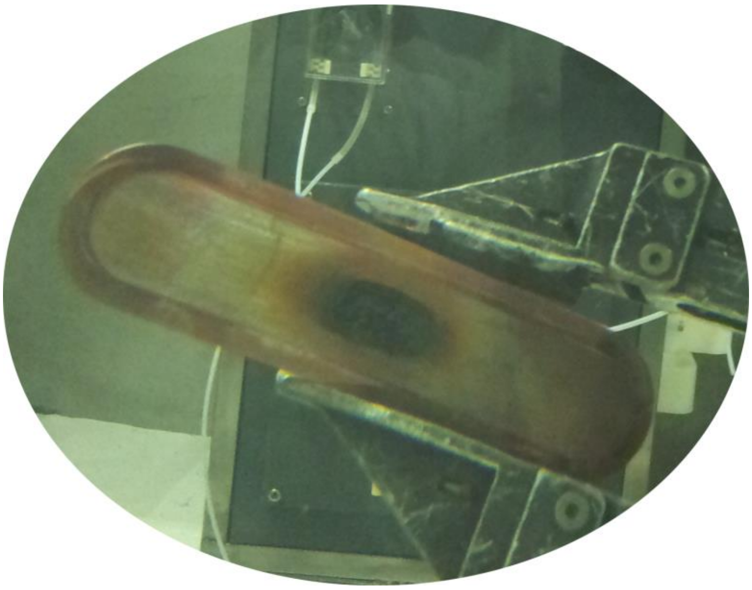

FIG. 14. Target after irradiation.

The irradiated target has been dissolved by hydrogen peroxide 30% using special homemade system [12]. The resulting solution was evaporated to dryness then the residue containing ^{100}Mo, ^{nat}Cu, ^{99m}Tc and ^{65}Zn was re-dissolved by nitric acid 0.1 N. This solution was loaded on the preconditioned TEVA cartridge. All ^{99m}Tc and trace of enriched molybdenum were retained by TEVA cartridge after rinsing by nitric acid 1 N. The solution containing ^{100}Mo, ^{nat}Cu and ^{65}Zn was stored to recover high costly enriched molybdenum. ^{99m}Tc was eluted from TEVA cartridge by HNO_3 8 N. The resulting solution was evaporated to dryness then sodium chloride 0.9% for injection and 2 drops of hydrogen peroxide 30% were added. This solution passed on the preconditioned alumina column to remove any trace of enriched molybdenum from the final produced bulk. Figure 1 shows the diagram of ^{99m} Tc-pertechnetate production process.

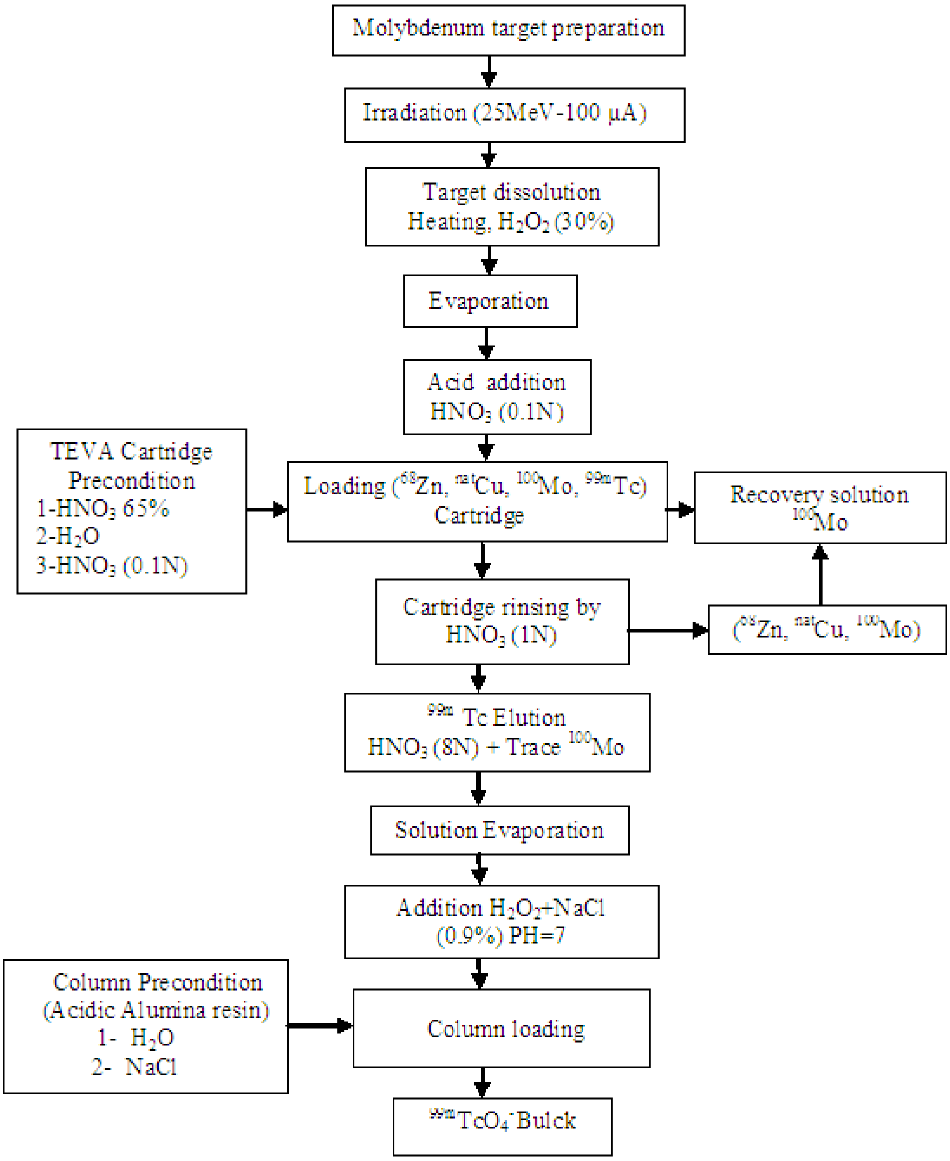

FIG. 15. Block diagram of ^{99m}Tc-pertechnetate production process.

2.5. Quality control of the produced ^{99m}TcO4$^-$

2.5.1. Chemical purity

Developed anodic stripping voltammetry system purchased from Metrohm (746 VA trace analyzer with 747 VA stand) was used for trace metals analysis in the produced ^{99m}Tc bulk. This system uses a working electrode (Static Mercury Dropped Electrode (SMDE)), a reference electrode Ag/AgCl/KCl (3 mol) and an auxiliary electrode from platinum.

The results show that trace metals concentration in final product was found to be 0.5±0.1µg/ml for ^{100}Mo and 0.2±0.01µg/ml for copper originating from target support.

2.5.2. Radionuclidic Purity

Radioisotopes were identified by gamma spectrometry using a high purity germanium (HPGe) detector with 25% efficiency, where the amplifier output of the detector was processed by a 4096 channels multi-channel analyzer (MCA) system. The fitting program (INTER WINER) was used for spectral data processing.
The results show that more than 99% of the total activity in the final product is due to ^{99m}Tc. Other radionuclidic impurities contribute to less than 1%. Figure 16 shows the gamma-ray spectrum of the produced Na^{99m}TcO$_4$ with the characteristic 140 keV peak for ^{99m}Tc.

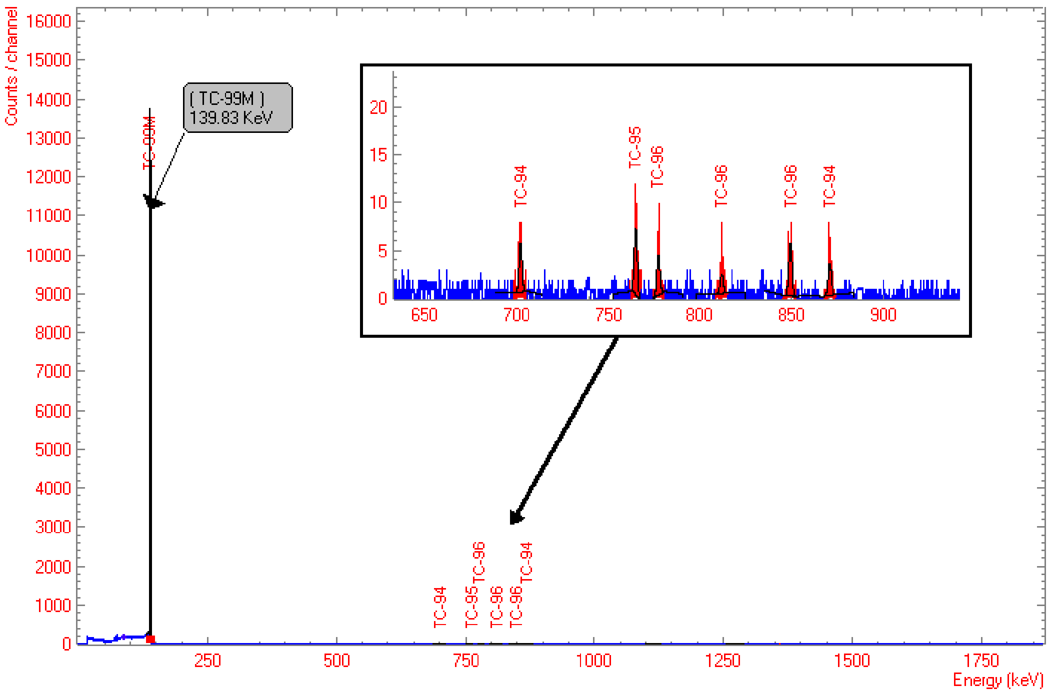

FIG. 16. Gamma Spectra of the produced Na^{99m}TcO$_4$.

2.5.3. Radiochemical purity

ITLC (instant thin-layer chromatography) was carried out using Whatman No. 3 strips (Sigma Chemical Company, USA) and counted by a gamma scanner (Raytest minigita, Model: BGO-V-detector) equipped with NaI (Tl) detector and single channel analyzer. Methylene diphosphonate (MDP) and ethylene dicysteine (EC) kits were obtained from the commercial available kits produced by Atomic Energy Commission of Syria. The European Pharmacopeia describes descending paper chromatography using methanol/water (85:15 v/v) as solvent. The ^{99m}Tc-pertechnetate anion migrates with an Rf value of 0.6. More than 99% of the measured radioactivity corresponds to an Rf of 0.6, less than 1% was detected at the start. Figure 17 shows the obtained results. ^{99m}Tc-pertechnetate migrates with the solvent (saline) front; reduced, hydrolyzed activity remains at the start. The results of radiochemical purity generally exceed 99%.

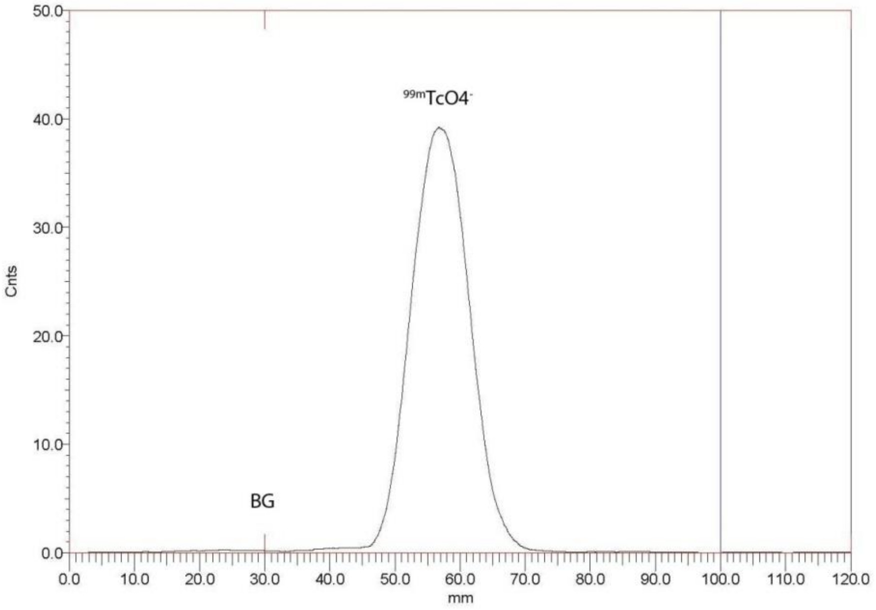

FIG. 17. Elution profile of the produced $^{99m}TcO_4^-$using methanol/water (85:15 v/v).

2.6. Radiolabelling and purification of ^{99m}Tc-MDP

Radiolabelling of the kit was carried out by initial warming up of the vial to the room temperature followed by the addition of 10 mCi of $^{99m}TcO_4^-$ in maximum 1-2 ml of normal saline and incubation of the vial for 15 min at room temperature. Radiochemical purity was determined by (ITLC). Tow mobile phases are used acetone and saline solution. By using Acetone as the mobile phase, reduced ^{99m}Tc and ^{99m}Tc-Compounds remained at the point of spotting, while free $^{99m}TcO_4^-$ moved towards the front of the solvent, see Figure 18. By using saline solution mobile phase, ^{99m}Tc Compounds and $^{99m}TcO_4^-$ moved to the front, while reduced ^{99m}Tc remained at the point of spotting, see Figure 19.

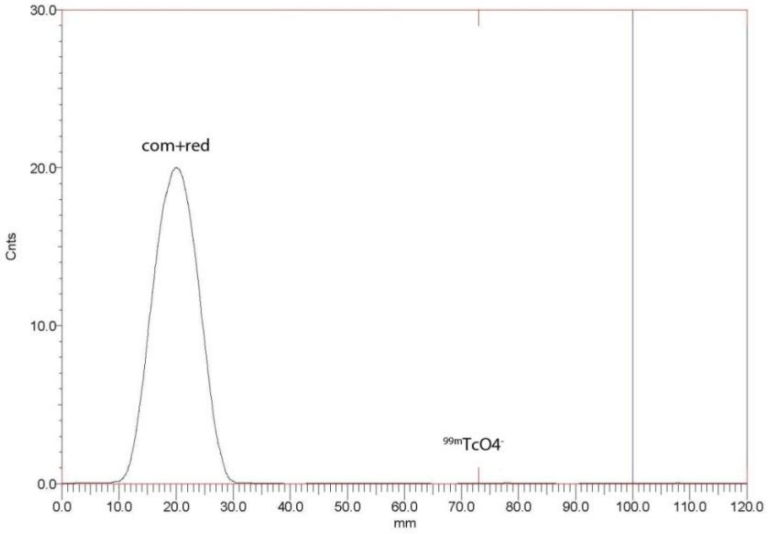

FIG. 18. Elution profile with acetone of the labeled MDP kit.

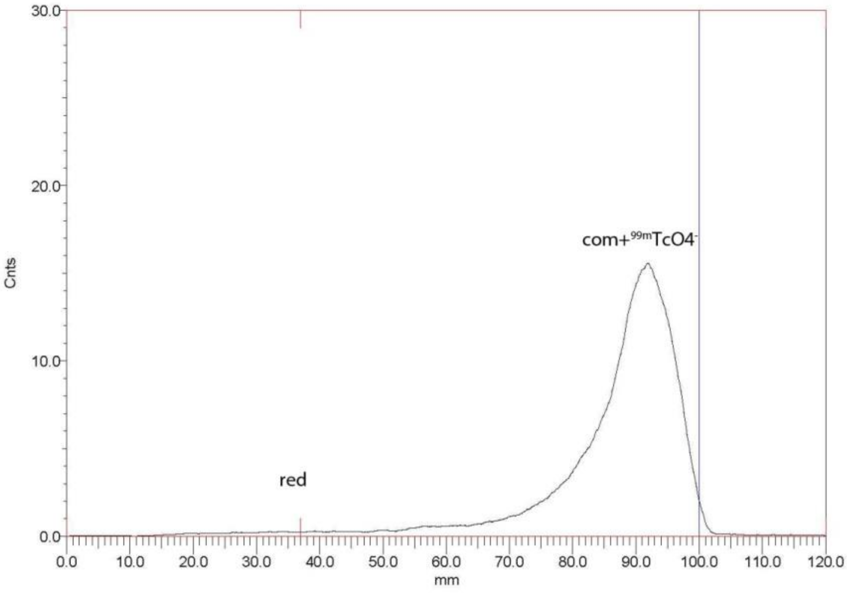

FIG. 19. Elution profile with 0.9% NaCl of the labeled MDP kit.

2.7. Biodistribution studies in rats

2.7.1 ^{99m}Tc-MDP Biodistribution studies

Experiments in rats were carried out in compliance with appropriate European Community directive guidelines (86/609/EEC). Bio distribution studies were performed in healthy Wistarhan rats (male, 160–220 g). Amounts of 0.3 ml of ^{99m}Tc-MDP or ^{99m}Tc-pertechnetate (2.2–3.7 MBq) in saline was administered to rats intravenously via the tail vein. The animals were anaesthetized and sacrificed, routinely 1 h post-intravenous injection (p.i.v.), and selected tissues were taken out. The radioactivity of samples of femur, Liver, Kidneys, and Blood were measured using a Gamma Counter CE/SN: 03L 504. The uptakes in the different organs expressed as %ID of ^{99m}TC-MDP are shown in Figure 20.

The results of the biodistribution studies for both ^{99m}TC-MDP prepared from cyclotron produced ^{99m}Tc, and ^{99m}TC-MDP from commercially available ^{99}Mo/^{99m}Tc generator-produced ^{99m}Tc, were similar and revealed significant bone uptake within 1 h post injection. Femur was taken as a representative of the skeleton and observed uptake in femur were 1.22 % and 1.18 % for ^{99m}TC-MDP (^{99}Mo/^{99m}Tc generator-produced ^{99m}Tc) and ^{99m}TC-MDP (cyclotron produced ^{99m}Tc) respectively. Some radioactivity is also seen in the liver and Kidney. Most radioactivities (54 %) are excreted through the bladder.

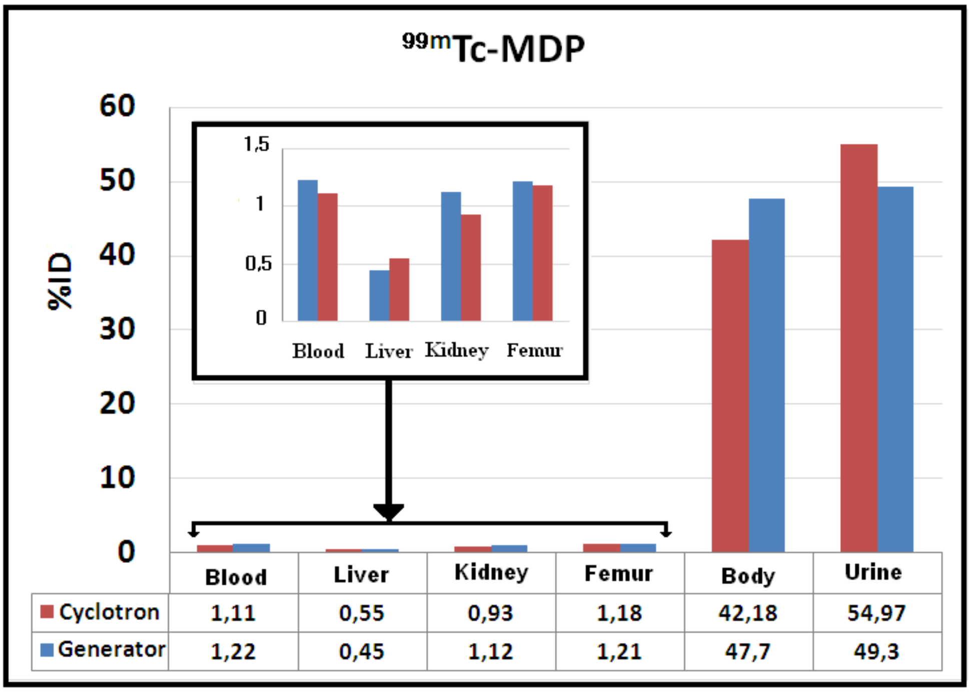

	Blood	Liver	Kidney	Femur	Body	Urine
🟥 Cyclotron	1,11	0,55	0,93	1,18	42,18	54,97
🟦 Generator	1,22	0,45	1,12	1,21	47,7	49,3

FIG. 20. Biodistribution pattern of ^{99m}TC-MDP complex in Wistar rats.

2.8. Application in human

^{99m}Tc-Ethylen Dicysteine (^{99m}TC-EC) was prepared by adding the ^{99m}Tc-pertechnetate produced by the cyclotron to the EC kit. The prepared radiopharmaceutical was injected to the patient 15 min post preparation. A dynamic imaging carried out for 20 min post injection. Figure 21 shows the images of renal scan study of 5 years old male child.

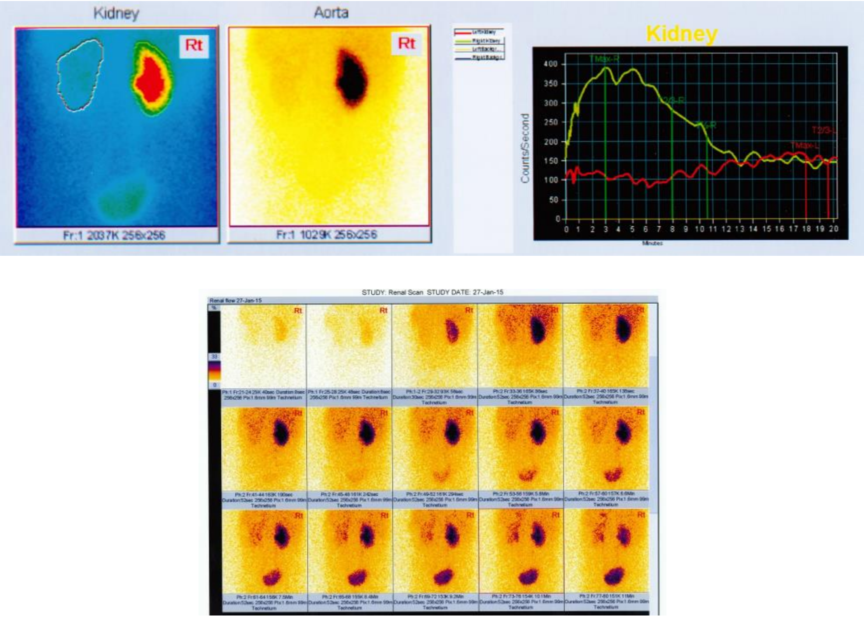

FIG. 21. ^{99m}Tc-EC image showing uniform biodistribution in the right kidney and the evidence failure in the left kidney.

References

[1] ARANO, Y., Recent advances in ^{99m}Tc radiopharmaceuticals, Annals of Nuclear Medicine **16(2)** (2002) 79–93.

[2] BANDOLI, G., TISATO, F., DOLMELLA, A., AGOSTINI, S., Structural overview of technetium compounds (2000-2004), Coordination Chemistry Review **250** (2006) 561-573.

[3] LIU, S., Bifunctional coupling agents for radiolabeling of biomolecules and target-specific delivery of metallic radionuclides, Advanced Drug Delivery Reviews **60 (12)** (2008) 1347–1370, DOI: 10.1016/j.addr.2008.04.006.

[4] PILLAI, M.R., DASH, A., KNAPP, JR. F.F., Sustained availability of ^{99m}Tc: possible paths forward, Journal of Nuclear Medicine **54(2)** (2013)313-323, DOI: 10.2967/jnumed.112.110338.

[5] BALLINGER, J.R., ^{99}Mo shortage in nuclear medicine: crisis or challenge, Journal of Labelled Compounds and Radiopharmaceuticals **53** (2010) 167–168.

[6] VON HIPPEL FRANK, N., KAHN, LAURA H., Feasibility of eliminating the use of highly enriched uranium in the production of medical radioisotopes, Sciences and Global Security **14** (2006) 151–162, DOI: 10.1080/08929880600993071.

[7] SCHOLTEN, B., LAMBRECHT, R.M., COGNEAU, M., VERA RUIZ, H., QAIM., S.M., Excitation functions for the cyclotron production of ^{99m}Tc and ^{99}Mo, Applied Radiation and Isotopes **51** (1999) 69–80, DOI:10.1016/S0969-8043(98)00153-5.

[8] TAKÁCS, S., SZŰCS, Z., TÁRKÁNYI, F., HERMANNE, A., SONCK, M., Evaluation of proton induced reactions on ^{100}Mo, New cross sections for production of ^{99m}Tc and ^{99}Mo, Journal of Radioanalytical and Nuclear Chemistry **257(1)** (2003) 195-201, DOI:10.1023/A:1024790520036.

[9] LEBEDA, O., PRUSZYNSKI, M., New measurement of excitation functions for (p,x) reactions on ^{nat}Mo with special regard to the formation of ^{95m}Tc, $^{96m+g}$Tc, ^{99m}Tc and ^{99}Mo, Applied Radiation and Isotopes **68(12)** (2010) 2355–2365, DOI:10.1016/j.apradiso.2010.05.011.

[10] QAIM, S.M., SUDÁRA, S., SCHOLTEN, B., KONING, A.J., & COENEN, H.H., Evaluation of excitation functions of ^{100}Mo(p,d^{+}pn)^{99}Mo and ^{100}Mo (p,2n)^{99m}Tc reactions: Estimation of long-lived Tc-impurity and its implication on the specific activity of cyclotron-produced ^{99m}Tc, Applied Radiation and Isotopes **85** (2014) 101–113, DOI: 10.1016/j.apradiso.2013.10.004.

[11] GAGNON, K., BÉNARD, F., KOVACS, M., RUTH, T.J., SCHAFFER, P., WILSON, J.S., MC QUARRIE, S.A., Cyclotron production of ^{99m}Tc: experimental measurement of the ^{100}Mo(p,x)^{99}Mo, ^{99m}Tc and ^{99g}Tc excitation functions from 8 to 18 MeV, Nuclear Medicine and Biology **38(6)** (2011) 907-916 DOI: 10.1016/j.nucmedbio.2011.02.010.

[12] AL RAYYES, A.H., AILOUTI, Y., Production and Quality Control of ^{64}Cu from High Current Ni Target, World Journal of Nuclear Science and Technology **3** (2013) 72-77, DOI:10.4236/wjnst.2013.32012.

CYCLOTRON PRODUCTION OF ^{99m}Tc AND ^{186}Re AT WASHINGTON UNIVERSITY

VERNAL RICHARDS AND SUZANNE E. LAPI

Mallinckrodt Institute of Radiology
Washington University School of Medicine,
510 South Kingshighway Boulevard
St. Louis, MO, 63110, USA

Abstract

^{99m}Tc is the most commonly used isotope in diagnostic nuclear medicine with over 16 million scans using this isotope performed annually in the United States and over 40 million scans performed annually worldwide. Common procedures using this isotope include bone scans, heart studies and more recently, targeted molecular imaging in oncology using agents such as ^{99m}Tc octreotide analogues. This project aims to address the current urgent problem of availability of ^{99m}Tc. Currently ^{99m}Tc is mainly produced via nuclear fission using highly enriched uranium (HEU), which is a concern due to nuclear proliferation risks.

During the course of the CRP, we have conducted studies of the ^{100}Mo(p,2n)^{99m}Tc reaction on a medical cyclotron using $^{100}Mo_2C$ and ^{100}Mo metal targets. This was the first report of $^{100}Mo_2C$ being used as a target for this reaction. $^{100}Mo_2C$, refractory carbide with high thermal conductivity, properties which underscore its use on a cyclotron, was synthesized using $^{100}MoO_3$. Its ease of oxidation back to $^{100}MoO_3$ under air at elevated temperatures facilitates the use of thermo-chromatography, a high temperature gas phase separation technique for the separation and isolation of ^{99m}Tc. Using a similar technique, we also conducted experiments using enriched ^{100}Mo metal targets. These experiments illustrated that Mo metal was also amenable to the thermo-chromatographic method of separation and that Mo metal can be efficiently recycled under low reducing conditions. Tc was recovered by rinsing the glassware with 0.1mM NaOH. Radio-ITLC analysis of the recovered ^{99m}Tc revealed that a small amount of $^{99m}TcO_3$ (5%) was present along with $^{99m}TcO_4^-$. Purification of the wash with Sep-Pak light alumina N cartridge conditioned by acidified Millipore water (pH 2) resulted in only the TcO_4^- species. Activity yields for ^{99m}Tc averaged 84% of the calculated theoretical yields. Additionally, the percent recovery of MoO_3, the precursor for both Mo metal and Mo_2C, was consistently high at 85% ensuring a good life cycle for this target material

1. INTRODUCTION

^{99m}Tc is the most commonly used isotope in diagnostic nuclear medicine with over 16 million scans using this isotope performed annually in the United States[1] and over 40 million scans performed annually worldwide[2]. Common procedures using this isotope include bone scans, heart studies and more recently, targeted molecular imaging in oncology using agents such as ^{99m}Tc octreotide analogues[3].

^{99m}Tc is commonly available in a generator form. In this system, the parent radionuclide ^{99}Mo ($t_{1/2}$ = 2.75 d) is bound to a solid phase column and the daughter isotope, ^{99m}Tc, is continuously 'milked' off the column with a saline eluant and incorporated into an appropriate radiopharmaceutical. In this manner hospital nuclear medicine departments can have a generator delivered approximately once a week for ongoing maintenance of ^{99m}Tc supplies for diagnostic patient procedures. Presently, Canadian reactors generate the majority of the United States supply of ^{99}Mo. These reactors are ageing and have become unreliable with several recent unexpected shutdowns. Over the last few years the ^{99m}Tc isotope supply has been reduced several times due to issues with the Canadian reactors and with other suppliers in the world.

In addition to this vulnerability in supply due to the reactors' age, these reactors run using highly enriched (weapons grade) uranium fuel (HEU) for the production of ^{99}Mo, HEU is a proliferation risk and thus there are significant security issues associated with the current route of production. The American Medical Isotopes Production Act [2] (introduced in 2009) would also halt United States export of highly enriched uranium in seven to ten years thus making fuel availability for these reactors uncertain. AECL currently runs the (130 MW) NRU reactor with low enriched uranium (LEU) fuel and HEU targets. Substantial radioactive waste (also classified as HEU) is also generated in processing. HEU (> 19.7% ^{235}U) is currently supplied to Canada by the US. As HEU has significant security issues, the future of ^{99}Mo/^{99m}Tc production will require alternative routes of production.

1.1. Direct production of ^{99m}Tc

The direct production of ^{99m}Tc using lower energy medical accelerators via the ^{100}Mo(p,2n) reaction has several advantages, few of which are listed below:

- Cyclotrons already in operation could be used to produce ^{99m}Tc, thus alleviating the problem without having to invest in new infrastructure.
- The ability to produce these isotopes onsite at hospitals will result in less shipping, thus reducing costs and loss of the radionuclide due to decay.
- This method is an alternative to using HEU and thus solves the proliferation risk associated with current methods of production

Overall this is a straightforward solution to the current isotope crisis which also addresses the proliferation issues associated with the current method of production. The sharing of this technology with institutes in developing nations will enhance the supply, utilization and hence the reliability of these important radiotracers.

2. RESEARCH PLAN

2.1. Progress over the course of the CRP

This progress period we have focused on production of ^{99m}Tc via the ^{100}Mo (p,2n)^{99m}Tc reaction, using a ^{100}Mo target material of Mo_2C [4]. Previous work at Washington University used $^{94}MoO_3$ to produce ^{94m}Tc via the ^{94}Mo(p,n)^{94m}Tc reaction and the highly efficient thermo-chromatographic method to separate the ^{94m}Tc from the ^{94}Mo target material [5]. MoO_3 has a lower melting point and low thermal conductivity. Thus we chose to initially use $^{100}Mo_2C$ as an alternative target material. This compound has been synthesized from $^{100}MoO_3$ and has ideal properties that make it suitable for use on a cyclotron. Its melting point is 50 °C below that of Molybdenum metal, and being an interstitial carbide it maintains metal-metal bonds [6], which along with other factors gives it a high degree of thermal conductivity. Pressing into well compacted powdered targets can be achieved at room temperature. In addition, it lends itself to be processed by the well-established and efficient thermo-chromatographic technique, as it re- oxidizes to the oxide at temperatures above 500 °C facilitating easy separation of the ^{99m}Tc and collection of the $^{100}MoO_3$ starting material. Additional experiments illustrated that $^{100}Mo_2C$ could be converted to elemental Mo under a reducing atmosphere and sintered targets from this material were also prepared.

3. MATERIALS AND METHODS

3.1. Synthesis of Ammonium heptamolybdate [7]

Enriched $^{100}MoO_3$ was used as the molybdenum source for the synthesis of ammonium molybdate. The full isotopic composition of the material as given by the supplier was ^{92}Mo (0.09%), ^{94}Mo (0.06%), ^{95}Mo (0.10%), ^{96}Mo (0.11%), ^{97}Mo (0.08%), ^{98}Mo (0.55%) and ^{100}Mo (99.01%). 1.00 g of ^{100} MoO_3 was dissolved in 10 ml of 28% aqueous ammonia ($NH_3.H_2O$) solution while stirring. The resulting clear solution was evaporated slowly to dryness at 40 °C.

3.1.1. Synthesis of Ammonium heptamolybdate –HMT complex and Molybdenum carbide [8]

$$(NH_4)_6Mo_7O_{24}\cdot 4H_2O + \text{excess } (CH_2)_6N_4 \rightarrow (NH_4)_4(HMT)_2Mo_7O_{24}\cdot 4H_2O$$

0.800 g of ammonium molybdate and 0.900 g of hexamethyltetramine (HMT) were dissolved in 20 ml of 28% NH_3 solution while stirring. The solution was allowed to evaporate to dryness under air at room temperature after which the resulting solid was subjected to drying under vacuum at 40 °C for 3 hours. The solid obtained (1.550 g) was crushed to a fine powder using a mortar and pestle, after which it was loaded in a quartz boat and placed inside a quartz tube of a horizontal furnace. Heating was carried out under argon flow.

$$(NH_4)_4(HMT)_2Mo_7O_{24} \rightarrow 7/2\ Mo_2C_{(s)} + 17/2\ CO_{(g)} + 7/2\ H_2O_{(g)} + 3NH_{3(g)} + 9/2N_{2(g)}$$

The temperature of the furnace was increased by step by step heating at a rate of 10 °C per minute until a temperature of 700°C was reached. Heating was maintained at this temperature for 2 hours after which it was increased to 900°C and heating continued for an additional 2 hours. On cooling the powder was removed, ground with a mortar pestle and stored in air at room temperature for further use.

3.2. Target preparation and irradiation

A platinum disc target holder was used for the cyclotron bombardment of $^{100}Mo_2C$. Approximately 50 mg of $^{100}Mo_2C$ was transferred to the cylindrical dimple located in the center of the platinum disc. The powder was pressed at 5000 psi for 30 seconds to secure it in place, after which the target was mounted into the cyclotron for bombardment. Proton irradiations were carried out using the CS-15 at Washington University. Production runs were conducted in the 15→ 10 MeV energy window determined by SRIM software [9, 10], and at 3, 4 and 5 μA currents. For each μA, the total μAhr was varied from 1 to 3 in successive runs.

3.3. Target Processing

After bombardment, the target was allowed to decay for two hours before being processed in order to allow short lived isotopes (^{100}Tc, ^{96m}Tc) to decay. To extract the ^{99m}Tc from the irradiated target material, a sublimation method described by Vleck *et al.* [11, 12] was employed. Custom quartz glassware based on the design put forward by Roesch *et al.* [13] was used for the separation. The individual pieces and the complete arrangement of the apparatus are shown in Figure 1. The assembled glassware with the target in the location was inserted into a preheated furnace at 850°C. Moist air was pumped into the apparatus, via the spout- like opening on tube B. Moist air was obtained by pumping air through a water-filled bubbling tube. Heating under these conditions continued for 20 minutes and the ^{99m}Tc and ^{100} Mo compounds were deposited in tubes D (~ 250 °C) and C respectively. The deposition is temperature dependent, thus ^{100} Mo deposits lower down in tube C at a higher temperature zone (~500 ºC). Heating under these conditions converts the $^{100}Mo_2C$ to $^{100}MoO_3$. After the processing, Tube D was washed with 8 ml of hot 1.0 x 10^{-4} M NaOH.

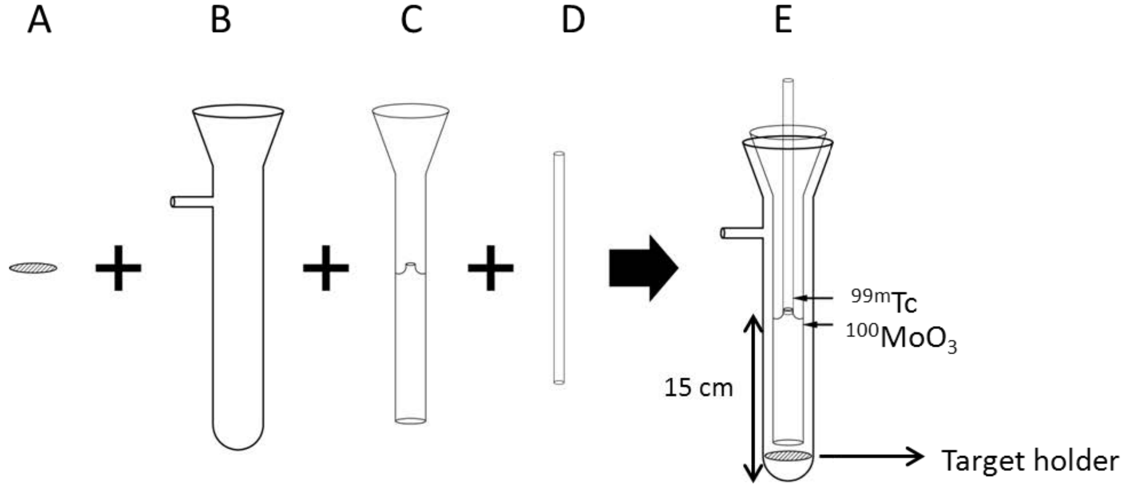

FIG. 1. Apparatus used for target processing. Platinum target holder (A), outer (B), middle (C) and inner (D) quartz tubes, along with the assembled apparatus (E).

3.4. Radionuclidic and Radiochemical purity analysis

10 µL of the resulting solution was diluted to 1000 µL using Millipore water and analyzed on a high purity Ge gamma spectrometer 5 minutes after obtaining the NaOH solution. Using the peak areas and peak efficiencies, radioactivity quantities were subsequently determined and back calculated to end of bombardment (EOB). To determine the identities and quantities of long lived radionuclidic impurities, the solution was allowed to decay for a minimum of 72 hours after which the analysis was repeated where peak data was collected for 6 h.

Radiochemical purity of the $^{99m}TcO_4^-$ in NaOH was determined by instant radio-thin layer chromatography (ITLC) using Alumina oxide TLC plates and acetone as the developing solvent.

Sep-Pak Light alumina N cartridges were used to purify and concentrate the $^{99m}TcO_4^-$ for radiochemistry. The column was first conditioned with 8 ml of acidified Millipore water (pH 2). The water was acidified with 2 M HCl by drop wise addition until the desired pH was reached. After conditioning, 8 ml of NaOH containing $^{99m}TcO_4^-$ was then slowly passed through the column, followed by elution with 400 µL of saline solution resulting in the final purified product. Radiochemical purity of the final product was also determined by radio-ITLC.

In order to examine the efficiency of recovery of ^{99m}Tc through the sublimation process, a separate target was bombarded under identical conditions as those processed and entirely dissolved in 10 ml of 30% H_2O_2 . 10 µL of this raw target peroxide solution was then subjected to the same dilution and Ge gamma spectrometer analysis as performed above.

4. RESULTS

4.1. Target Synthesis

Enriched $^{100}Mo_2C$ was synthesized from enriched $^{100}MoO_3$ using a 3 step thermal carburization method. The initial step involved the conversion of $^{100}MoO_3$ to ammonium heptamolybdate tetrahydrate ($(NH_4)_6Mo_7O_{24}.4H_2O$) with 28% NH_3(aq). $(NH_4)_6Mo_7O_{24}.4H_2O$ yield was consistently averaged at 99% ± 0.7%. The second step involved the conversion of $(NH_4)_6Mo_7O_{24}.4H_2O$ to a HMT-molybdate complex ($(NH_4)_4(HMT)_2Mo_7O_{24}.4H_2O$) by its reaction in 28% NH_3(aq) with hexamethyltetramine (HMT). The third step involved heating the dried HMT-molybdate complex in argon atmosphere to give $^{100}Mo_2C$ with an average yield of 96% for this step. The process was repeated starting with recycled $^{100}MoO_3$ (from previous irradiation and sublimation separation) resulting in a yield of 93. Elemental analysis showed the following composition Mo – 87%, C – 7.2%. Theoretical composition was calculated to yield, Mo – 93%, C – 6.2%. The X-ray diffraction (XRD) pattern is shown in Figure 2. The major component is Mo_2C, and matched ICDD card 04-008-1889.

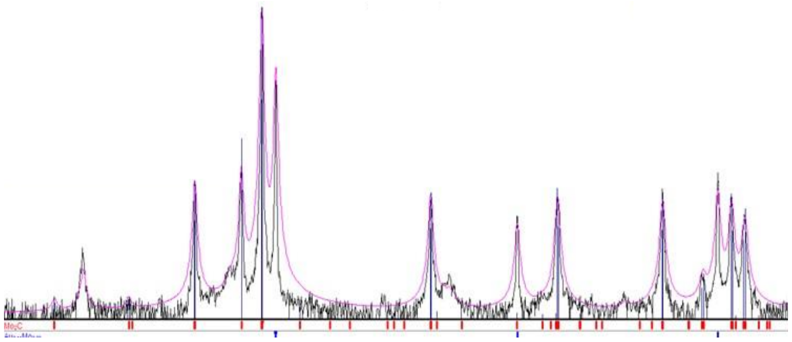

FIG. 2. XRD pattern for Mo_2C sample: overlay of purple spectra indicates Mo_2C reference standard.

4.2. Target preparation, bombardment and processing

Using Pt as the target holder, $^{100}Mo_2C$ powder targets were pressed at 5000 psi for bombardment. The integrity of the powder was preserved during bombardment period. While processing the target by thermal chromatography using moist air, hot $^{100}MoO_3$ (yellowish) is deposited below the constriction in tube C, and ^{99m}Tc as pertechnetate ($^{99m}TcO_4^-$) was deposited in tube D. Confirmation of the yield of ^{99m}Tc deposited in tube D was confirmed post thermo-chromatography by using a dose calibrator. The depth to which the thermo-chromatography apparatus was lowered into the vertical furnace was 15 cm as indicated in Figure 1. This ensured maximum deposition of ^{99m}Tc in tube D and washing tube D with hot (~ 100 °C) NaOH resulted in near quantitative recovery of ^{99m}Tc. The total processing time typically less than 45 minutes, with 20 minutes required for the thermal chromatography process. Complete dissolution of targets irradiated under identical conditions using 30% H_2O_2 after bombardment was employed and the activities obtained were compared to recovered values obtained *via* thermo-chromatography, in order to evaluate the recovery efficiency of the chromatography process. Calculated activities for H_2O_2 processed targets show good agreement with activities for thermal chromatography processed targets indicating near quantitative recovery.

4.3. Purification

Radio-ITLC analysis performed on the recovered ^{99m}Tc revealed that a small amount of $^{99m}TcO_3$ (5%)was present along with $^{99m}TcO_4$ -. Purification of the wash with a Sep-Pak light alumina N cartridge conditioned by acidified Millipore water (pH 2) resulted in only pertechnetate. Eluting this cartridge with 400µL saline solution was effective in releasing the pertechnetate with a 71% to 75% activity recovery.

4.4. Analysis of radionuclidic impurities

The gamma–ray spectrum in Figure 3A shows the characteristic 140 keV peak for ^{99m}Tc. Table 1 lists the calculated activities corrected to EOB along with the percent recovery for the various parameter settings employed. Radionuclidic impurities were identified following a 6 hour scan on samples where ^{99m}Tc was allowed to decay for 72 hours post irradiation. A gamma-ray spectrum of an analysis for long-lived impurities is shown in Figure 3B. In addition to the peak at 140 keV other peaks at various energies became more conspicuous. Based on their energies peaks were assigned to ^{95}Tc and ^{96}Tc. Those associated with ^{95}Tc occurred at the following energies, 204 keV and 765 keV, with branching ratios of 63% and 94% respectively. Peaks at 778 keV, 812 keV, 850 keV and 1127 keV were assigned to ^{96}Tc, with branching ratios of 99%, 82%, 97% and 15% respectively. The percentages of these impurities expressed relative to ^{99m}Tc are shown in Table 1.

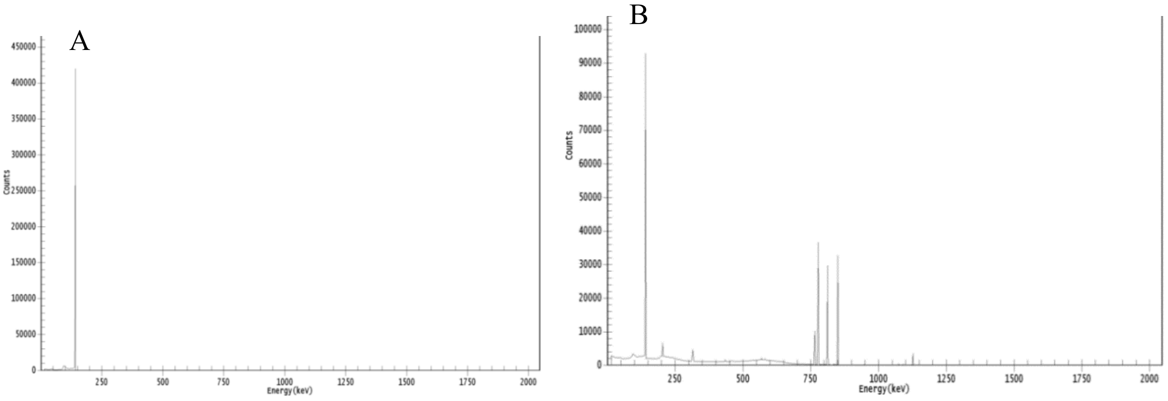

FIG. 3. ***A.*** *Gamma Spectroscopy plot for ^{99m}Tc sample at 4 hours post EOB.* ***B.****Gamma Spectrometer plot of ^{99m}Tc, ^{96}Tc and ^{95}Tc at 85 hours post EOB. Scan time was 6 hours.*

TABLE 1. AVERAGE ISOTOPIC IMPURITIES AT EOB. VALUES EXPRESSED AS A PERCENTAGE RELATIVE TO ^{99m}Tc

^{99m}Tc	^{96}Tc	^{95}Tc
100%	0.08 %	$8.6*10^{-6}$ %

4.5. Target Recycling

As the thermal chromatography process results in a conversion of the $^{100}Mo_2C$ target material to $^{100}MoO_3$ we aimed to develop a life cycle recycling process. This is illustrated in Figure 4. Tube B was washed with 28% $NH_3(aq)$ to dissolve the material and this ammonia solution was stored for further use in the synthesis of $(NH_4)_6Mo_7O_{24}.4H_2O$. MoO_3 was converted to Mo_2C as described above with an average efficiency of 85%. In the synthesis of $(NH_4)_6Mo_7O_{24}.4H_2O$ using recovered $^{100}MoO_3$, Heating to 50 °C was necessary for complete dissolution. On using $^{100}Mo_2C$ obtained from recycled $^{100}MoO_3$, activities were identical to those obtained using fresh $^{100}MoO_3$.

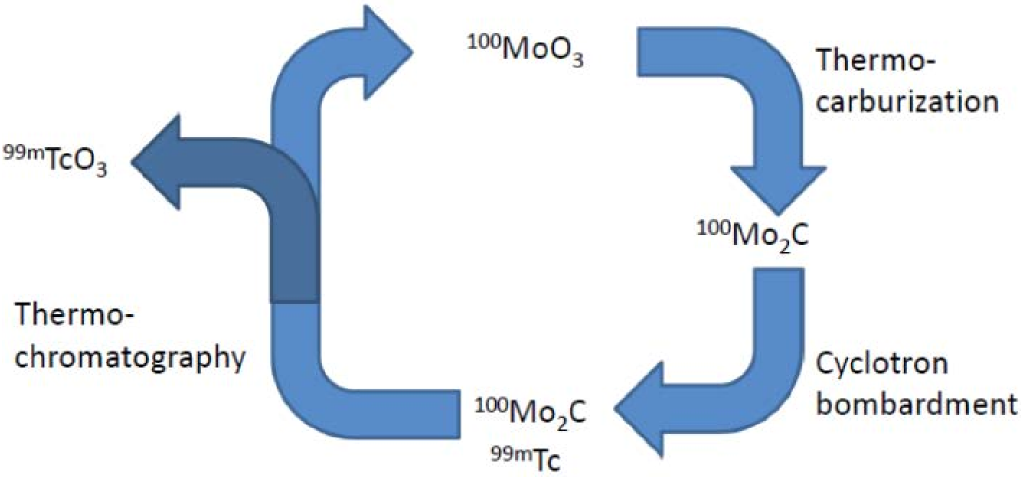

FIG. 4. Life cycle of MoO_3 *in the* $^{100}Mo(p,2n)^{99m}Tc$ *reaction production method.*

4.6. Experiments conducted using Mo metal targets

Using a similar technique, we also conducted experiments using Mo metal targets. Targets were pressed and sintered under vacuum at 900 degrees C for four hours before use. Yields were in agreement with previously published data and the ^{99m}Tc was obtained as $^{99m}TcO_4^-$ via the same process as described above. These experiments illustrated that Mo metal was also amenable to the thermo-chromatographic method of separation and that Mo metal can be efficiently recycled under low reducing conditions (4% H_2 in Argon).

1- Thermochromatography

$Mo + 1.5O_2 \rightarrow MoO_3$

2- Complex formation

$(NH_4)_4((CH_2)_6N_4)_2Mo_7O_{24}$

3- Thermocarburization

Mo_2C

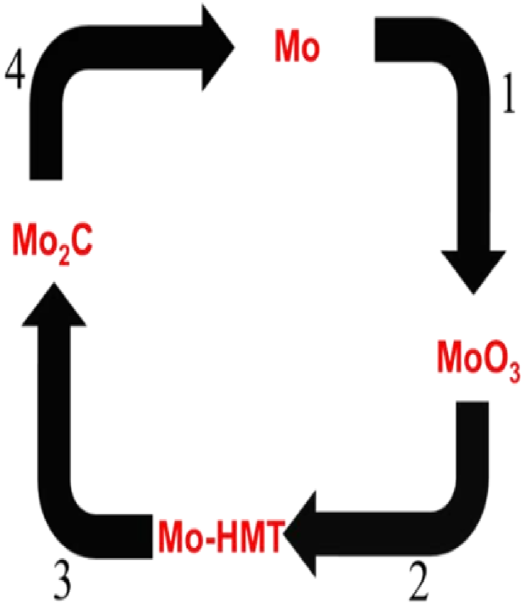

FIG. 5. Life cycle of Mo metal targets in the $^{100}Mo(p,2n)^{99m}Tc$ *reaction production method with thermochromatography purification.*

4.7. Application to ^{186}Re production

While outside the scope of this CRP, additional work was also conducted to assess the use of tungsten carbide for the production of ^{186}Re, a therapeutic analogue of ^{99m}Tc. A proof of concept study was undertaken where no-carrier added ^{186g}Re was produced from the cyclotron bombardment of ^{186}WC. ^{186}WC was carbo-thermally generated from a novel precursor synthesized from $^{186}WO_3$, aqueous ammonia and hexamethyltetramine. The inherent high electrical and thermal conductivity of this material, coupled with its high melting point, made it an ideal candidate for proton bombardment for production of ^{186}Re. An18 µA irradiation for three hours and processing via thermo-chromatography, ^{186}WC yielded 0.93 mCi of ^{186g}Re which corresponds to 89% of the calculated theoretical yields. The radiochemical purity of the desired ^{186g}Re species was found to be between 95 and 97% with small contaminants of $^{186}ReO_2$. The radiochemistry utility of the product was investigated using S-benzoyl-MAG3 and 100% complexation was achieved with stability being maintained for 96 hours. The re-oxidation of ^{186}WC back to$^{186}WO_3$ by oxygen in the thermo-chromatography method of processing, ensured that the starting material was regenerated and recovered from the process in 94-98% yield.

5. DISCUSSION

Use of the material $^{100}MoO_3$ for the sustainable cyclotron production of ^{99m}Tc was not considered ideal for a number of reasons. The first and foremost issue is that the low thermal conductivity of MoO_3 means that heat dissipation upon bombardment would be low. At room temperature MoO_3 is an insulator due to its fixed ions in its ionic lattice. As temperature rises, thermal conductivity in insulators fall leading to local thermal hotspots, which in the case of MoO_3 would facilitate sublimation of the oxide. Additionally, if the target holder being used is not sufficiently inert, such hotspots could possibly be the starting points for a chemical reaction between the MoO_3 and the target holder. The third and perhaps most important issue is one of stoichiometry. Each unit of MoO_3 has one in every four atoms being ^{100}Mo, thus the percentage of target atoms is considerable lower than that of other materials.

Ideally, one would want to use elemental metal ^{100}Mo as the target material for the cyclotron production of ^{99m}Tc. ^{100}Mo has a high melting point of 2850 °C and has a high thermal conductivity. Additionally this target material contains 100% ^{100}Mo nuclei. Whereas one can readily obtain ^{100}Mo powder for cyclotron bombardment, pretreatment of this starting material by sintering and melting are necessary for maximum adherence to a metallic backing and also for a sufficiently dense structure [14, 15]. The wet chemical processing techniques that are used are multi-chemical, multi-step [14, 15] and at times multi-column operations to a purified pertechnetate. Similarly, the recovery of the target material entails a multi-step high temperature hydrogen reduction [14]. The production of $^{94m}TcO_4^-$ using $^{94}MoO_3$ piqued our interest because of its simplicity in arriving at the purified pertechnetate solution and recovery of the starting material [5].

Mo_2C was seen as a viable alternative to MoO_3 because of its unique properties. These include its high melting point of 2800 °C, which compares favorably with elemental Mo. Also the high degree of chemical stability of Mo_2C means that handling at ambient conditions is possible. The high thermal conductivity also aid with heat dissipation during bombardment. Unlike insulators where thermal conductivity decreases with temperature, Mo_2C as an interstitial carbide experiences an increase in thermal conductivity caused by strong scattering of electrons and phonons by the carbon vacancies [16]. Unlike MoO_3 where only 25% of the nuclei are Mo, Mo_2C has a much higher percentage of Mo nuclei, 66.66%.

Thermo-chromatographic separation has proven itself as an efficient method for the separation of Mo and Tc species [5, 11-13, 17]. Dash *et al.* list the high radio-nuclidic purity of ^{99m}Tc attained, the repeated use of the same set up and the ready recycling of target material as some of the strengths of using this separation method [17]. Under these conditions, Mo_2C undergoes oxidation to MoO_3 which then readily sublimes at a lower temperature than Mo_2C would, thus enhancing the feasibility of this process. It should be noted that under these processing conditions platinum was an ideal target holder material due to its inert nature and high melting point.

Tc was recovered by rinsing the glassware with 0.1mM NaOH. Radio-ITLC analysis of the recovered ^{99m}Tc revealed that a small amount of $^{99m}TcO_3$ (5%) [13, 18] was present along with $^{99m}TcO_4^-$. Purification of the wash with Sep-Pak light alumina N cartridge conditioned by acidified Millipore water (pH 2) resulted in only the TcO_4^- species.

The cross section values for, Sholten [19], Takas [20] and Khandaker [21] were used in the determination of the theoretical yields. Actual yields for this study were determined to be an average of 84% for the various currents employed. These high yields indicate that Mo_2C is an effective target material for the ^{100} Mo (p, 2n) ^{99m}Tc reaction. In addition to the high yields, the radionuclidic impurities produced in this reaction, ^{95}Tc and ^{96}Tc were relatively low.

6. PROJECT SUMMARY

The overarching goal of this project was for Washington University to develop the in house capability to routinely produce ^{99m}Tc for nuclear medicine patient procedures and to translate this capability to other nuclear medicine departments. Overall the proposal introduces a straightforward solution to the current crisis while also addressing the proliferation issues associated with the current method of production This project has the potential to substantially alleviate the current major problem of the diagnostic SPECT isotope, ^{99m}Tc, availability in the United States.

References

[1] ORENSTEIN, B., Caution - Lack of Imaging Isotopes may be Hazardous to Patients, Radiology Today **10(14)** (2009) 14.

[2] ECKELMAN, W., Unparalleled Contributions of Technetium-99m to Medicine over 5 Deacades, Journal of American College of Cardiology Imaging **2** (2009) 364-368.

[3] CWIKLA, J.B., et al., Initial direct comparison of 99mTc-TOC and 99mTc-TATE in identifying sites of disease in patients with proven GEP NETs, J. Nucl. Med. (2008) **49(7)** 1060-1065.

[4] RICHARDS, V.N., et al., Cyclotron Production of (99m)Tc using (100)Mo2C targets, Nucl. Med. Biol. **40(7)** (2013) 939-945.

[5] BIGOTT, H.M., et al., Advances in the production, processing and microPET image quality of technetium-94m, Nuclear medicine and biology **33(7)** (2006) 923-933.

[6] YAMASAKI, S., BAHADESHIA, H.K.D.H., Modelling and characterisation of Mo2C precipitation and cementite Dissolution during the tempering of Fe-C-Mo martensitic steel, Materials Science and Technology **19** (2003) 723-731.

[7] LEOPOLD GMELIN, R.J.M., Gmelin's Handbuch für Anorganische Chemie (Verlag Chemie) (1935).

[8] WANG, H-M., et al., Synthesis of bulk and supported molybdenum carbide by a single-step thermal carburization method, Chemistry of Materials **19(7)** (2007) 1801-1807.

[9] BIERSACK, J.P. H.L., A Monte Carlo computer program for the transport of energetic ions in amorphous targets, Nucl.Instr. and Meth. **174** (1980) 257.

[10] ZIEGLER, J.F. BP, ZIEGLER, M.D., *SRIM:*The Stopping Range of Ions in Matter (Lulu Press Co) (2008).

[11] RUSEK, V., et al., Thermal separation of /sup 99m/Tc from molybdenum trioxide. I. Separation of /sup 99m/Tc from molybdenum trioxide at temperatures below 650$sup 0$C, Journal Name: Radiochem. Radioanal. Lett., **20**, no. 1, (1974) 15-22; Other Information: Orig. Receipt Date: 30-JUN-75:Medium: X.

[12] VLCEK, J., et al., Thermal separation of /sup 99m/Tc from molybdenum trioxide. II. Separation of /sup 99m/Tc from molybdenum trioxide at temperatures above 650$sup 0$C, Journal Name: Radiochem. Radioanal. Lett., **20**, no. 1, (1974) 23-31; Other Information: Orig. Receipt Date: 30-JUN-75:Medium: X.

[13] RÖSCH, F. AFN, QAIM, S.M., Thermochromatographic separation of ^{94m}Tc from enriched molybdenum targets and its large scale production for nuclear medical application, Radiochim Acta **64** (1994) 113-120.

[14] GAGNON, K., et al., Cyclotron production of< sup> 99m</sup> Tc: Recycling of enriched< sup> 100</sup> Mo metal targets, Applied radiation and isotopes (2012).

[15] GUÉRIN, B., et al., Cyclotron production of ^{99m}Tc: an approach to the medical isotope crisis, Journal of Nuclear Medicine **51(4)** (2010) 13N-16N.

[16] WILLIAMS, W.S., High-Temperature Thermal Conductivity of Transition Metal Carbides and Nitrides, Journal of the American Ceramic Society **49(3)** (1966)156-159.

[17] DASH, A., et al., ^{99}Mo/^{99m}Tc separation: An assessment of technology options, Nuclear medicine and biology **40(2)** (2013) 167-176.

[18] GIBSON, J., High temperature oxide and hydroxide vapor species of technetium, Radiochim. acta **60** (1993) 121-126.

[19] SCHOLTEN, B., et al., Excitation functions for the cyclotron production of< sup> 99m</sup> Tc and< sup> 99</sup> Mo, Applied radiation and isotopes **51(1)** (1999) 69-80.

[20] TAKÁCS, S., *et* al., Evaluation of proton induced reactions on <sup>100</sup>Mo: New cross sections for production of <sup>99</sup><sup>m</sup>Tc and <sup>99</sup>Mo, Journal of Radioanalytical and Nuclear Chemistry **257(1)** (2003) 195-201.

[21] KHANDAKER, M., et al., Measurement of cross-sections for the (p, xn) reactions in natural molybdenum, Nuclear Instruments and Methods in Physics Research Section B: Beam Interactions with Materials and Atoms **262(2)** (2007) 171-181.

LIST OF CRP PARTICIPANTS

Al-Jammaz, I	Cyclotron & Radiopharmaceuticals Research Centre, King Faisal Specialist Hospital & Research Centre, Riyadh, **Kingdom of Saudi Arabia**
Al Rayyes, A.H.	Atomic Energy Commission of Syria (AECS) Damascus, **Syrian Arab Republic**
Avetisyan, A.	National Science Laboratory Foundation, Yerevan, **Armenia**
Das, Malay Kanti	Board of Radiation and Isotope Technology (BRIT), Variable Energy Cyclotron Centre (VECC), Kolkata, **India**
Esposito, J.	Legnaro National Laboratories, INFN, Legnaro (Padua), **Italy**
Fujibayashi ,Y.	Molecular Imaging Center National Institute of Radiological Sciences Chiba, **Japan**
Lapi, S.	Mallinckrodt Institute of RadiologyWashington University School of Medicine, St. Louis, MO **USA**
McQuarrie, S.A.	University of Alberta, Faculty of Medicine and Dentistry, Edmonton, Alberta, **Canada**
Mikołajczak, R.	National Centre for Nuclear Research, Radioisotope Centre POLATOM, Otwock, **Poland**
Ruth, Thomas J.	TRIUMF and the British Columbia Cancer Agency, Vancouver, **Canada**
Salvini. A.	Laboratorio Energia Nucleare Applicata (L.E.N.A.) of the University of Pavia, Pavia, **Italy**
Takacs, S.	Institute for Nuclear Research, Hungarian Academy of Sciences, Debrecen, **Hungary**

Scientific Secretary

Haji Saeid, M.	International Atomic Energy Agency Wargramerstrasse Vienna, **Austria**